DEPARTAMENT DE FISIOLOGIA

THE IMPORTANCE OF THE NUCLEAR GLUTATHIONE IN THE CELL PROLIFERATION.

JELENA MARKOVIC

UNIVERSITAT DE VALÈNCIA
Servei de Publicacions
2009

Aquesta Tesi Doctoral va ser presentada a València el dia 18 de febrer de 2009 davant un tribunal format per:

- Dr. Juan Viña Ribes
- Dr. Giovanni Mann
- Dr. Richard Siow
- Dra. Mónica de la Fuente del Rey
- Dr. Juan Sastre Belloch

Va ser dirigida per:
Dr. Federico Vicente Pallardó Calatayud
Dr. José Viña Ribes

Dipòsit legal: V-4149-2010
I.S.B.N.: 978-84-370-7636-2
Edita: Universitat de València
Servei de Publicacions
C/ Arts Gràfiques, 13 baix
46010 València
Spain
Telèfon:(0034)963864115

UNIVERSIDAD DE VALENCIA
Facultad de Medicina y Odontología
Departamento de Fisiología

TESIS DOCTORAL

THE IMPORTANCE OF NUCLEAR GLUTATHIONE IN CELL PROLIFERATION

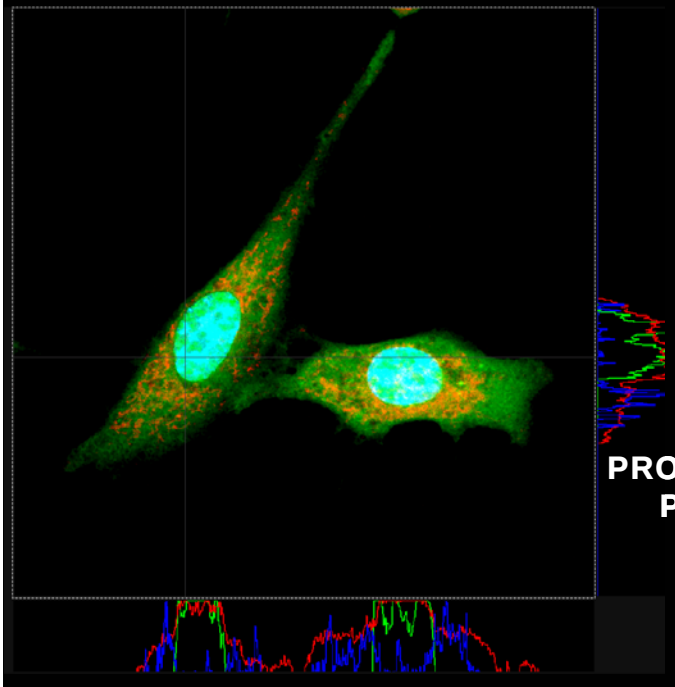

PRESENTADA POR:

JELENA MARKOVIC

DIRIGIDA POR:

PROF. D FEDERICO V. PALLARDO
PROF. D. JOSÉ VIÑA RIBES

Valencia, 2009

VNIVERSITAT DE VALÈNCIA

FACULTAD DE MEDICINA Y ODONTOLOGIA
DEPARTAMENTO DE FISIOLOGÍA

TESIS DOCTORAL

THE IMPORTANCE OF NUCLEAR GLUTATHIONE IN CELL PROLIFERATION

PRESENTADA POR:

JELENA MARKOVIC

DIRIGIDA POR:

PROF. D FEDERICO V. PALLARDO
PROF. D. JOSÉ VIÑA RIBES

Valencia, 2009

Facultad de Medicina y Odontología
Departamento de Fisiología

Prof. D. Federico V. Pallardo, Catedrático del Departamento de Fisiología de la Facultad de Medicina y Odontología de la Universidad de Valencia.

Prof. D. José Viña Ribes, Catedrático del Departamento de Fisiología de la Facultad de Medicina y Odontología de la Universidad de Valencia.

CERTIFICAN:

Que Dña. Jelena Markovic, Licenciada en Biología Molecular y Fisiología, por la Universidad de Belgrado, Serbia, ha realizado bajo su dirección la presente tesis titulada:

THE IMPORTANCE OF NUCLEAR GLUTATHIONE IN CELL PROLIFERATION

para la obtención del título de Doctora

Y para que conste a los efectos oportunos, firman la presente certificación.

Valencia, a 12 de Enero de 2009

Prof. D. Federico V. Pallardo Prof. D. José Viña Ribes

Za Zoe, moju zvezdu, pravog druga u avanturi

Za Alisu, moju sreću, ciji osmeh mi greje srce

Za moje roditelje, kojima sve dugujem

A Tito

HVALA, GRACIAS AND THANKS

Quiero expresar mi más profundo agradecimiento a las siguientes personas:

Al Dr. D. Federico Pallardó, porque han sido muchos años de colaboración científica y también personal. Por ser un amigo antes que un jefe. Por entender mi rol de mujer y madre investigadora. Muchas gracias, Fede.

Al Dr. D. José Viña, por darme la oportunidad de incorporarme a su grupo, por sus consejos científicos y su trato amable.

Al Dr. D. Juan Viña, por confiar en mi profesionalidad en todo momento, por sus ideas y su apoyo, por su elegancia personal y su sentido del humor.

Al Dr. D. Juan Sastre, por estar siempre dispuesto a ayudar cuando se le necesita y por su calidez.

A las secretarias, las que están: a Mari, Teresa, Vicen, Elena, y a las que ya se han librado de nosotros, Eva y Elena Cavero, les doy las gracias por resolver con sonrisa y competencia todos los complicados trámites que conlleva la realización de una tesis.

Al Dr. Ángel Ortega debo mi gratitud tanto por su excelente asistencia en la microscopía confocal, como por su compañerismo y simpatía.

A la Dra. Amparo Ruiz, le agradezco sus valiosos consejos y su buena predisposición en todo momento.

Al equipo de bioquímica, Concha, Elena y Rosa, de verdad estoy encantada de haber podido trabajar con vosotras.

I would like to express my gratitude to the wonderful people from King's College, London. It was a pleasure and a privilege to work with them.
To Professor Giovanni Mann, for being so kind and supportive; being a part of his team was a challenging and fulfilling experience.
To Dr. Richard Siow, for supervising thoroughly and with interest my work in the lab, for excellent advices, and above all, for all the thoughtfulness and attention he gave to my family and me.
To Dr. Patricia de Winter, for her rare passion for science and true friendship.

To René Fischer and Hilvert's group, from ETH Zurich, and Galeotti's group from Universitá Cattolica del "Sacro Cuore", Roma, for everything they taught me.

Durante 2 años he disfrutado de la beca de la Agencia Española de Cooperación Internacional, por lo que me gustaría expresar mi gratitud, así como a la UNESCO MCBN por su financiación de mi estancia en Universitá Cattolica del "Sacro Cuore".

Tampoco puedo dejar de agradecer a mis compañeros de laboratorio por haber compartido el día a día de esta poco comprendida ilusión: Mª Carmen y Chelo, Juan, Javi, Marco y Alessandro, Javi y Pain, Soraya y

Pablo, Consuelo, Lele, Noelia, Raúl y Rubén. A los "raritos": Amparito, José Luís, Gema, Carmen, Ana, Isabel y Paco, muchas gracias.
A Juamba, cuya amistad ha sido un refugio
A Ana Lucía, su dulce sonrisa, su optimismo.
A Ana Broseta, futura brillante doctora, y espero, investigadora. Su inteligencia, ilusión y simpatía han sido una verdadera inspiración.
A Ana Lloret, le agradezco su vocación y su admirable inquietud científica, y sobre todo, con mucho cariño, su "un poco de azúcar".
A Nancy Mora, por su tremenda capacidad de trabajo que tanto admiro, por su entusiasmo por aprender y crecer, por su fina diplomacia y por una verdadera amistad que me ha regalado día tras día.

Slavene, sve se ovo ne bi dogodilo da je Pera na vreme otiš'o u policiju. A možda i bi, ko to zna? Hvala, Miko, za sve.

Gospodine Dragane Živkoviću, bez Vaše pomoći na teškom početku sve bi bilo mnogo komplikovanije, ako ne i nemoguće. Sećam Vas se sa najdubljom zahvalnošću.

Y sobre todo quiero que mi familia este tan presente en mis agradecimientos como lo ha estado todos estos años.
Mama i tata, evo poklanjam vam vašu drugu doktorsku disertaciju. Vaša je koliko i moja, a ako je suditi po želji i veri u njeno ostvarenje, i više. 2500 km nije ništa, uvek ste bili uz mene.
A mis suegros, que nos han ofrecido siempre una "red de seguridad" para los malabarismos que impone la vida de estudiantes y a la vez, padres. Muchísimas gracias.

A mi marido, por demostrar que amar es trabajar en los potenciales de la persona que quieres. Gracias, Titin.

Mojim divnim devojčicama: Zoe koja je u svemu pomogla, svojim veselim karakterom, neumornom radoznalošću i ponekad neocekivanom ozbiljnošću, pretvarala je nemoguće u dostižno i Alisa koja je donela novu inspiraciju i osmehom obnovila energiju.

Vi ste moje najveće blago, ovo je za vas.

THE TABLE OF CONTENTS

THE TABLE OF CONTENTS

I INTRODUCTION

I INTRODUCTION

1. The phenomenon of cell proliferation

1.1 Biological importance of cell proliferation

In a normal adult organism many varied cell types die by programmed cell death every day in order to provide the homeostasis. All organs have remarkable capacity for regeneration and repair, even those traditionally thought to be postmitotic, like pancreas or brain. Lost cells must be constantly replaced by new ones and the rate of cell loss must be matched with the rate of renewal. If in an organ the cells are dying off with accelerated pace comparing to the proliferation level a decline in organ function is inevitable and it could result in a chronic degenerative disease. But if this imbalance is generalized to the whole organism, then it could lead to accelerated aging and death.

The maintenance of normal cell function and tissue homeostasis requires the precise regulation of multiple signalling pathways that define cell commitment to proliferation, differentiation, growth arrest or programmed cell death. Proper duplication, maintenance, and repair of

the genome are necessary to guarantee the genomic stability.

1.2. Cell cycle

*…Double or nothing. With few exceptions a living cell either reproduces or dies; the principle is so simple that no one has bothered to call it a principle. A cell is born in the division of a parent cell. It then doubles in every respect: in every part, in every kind of molecule, even in the amount of water it contains. Thereafter it divides with such equal justice that each new daughter cell is an identical copy of the parent. This doubling and halving, the cycle of growth and division, is known generally as the cell cycle…*Daniel Mazia, 1974 [1]

During the evolution of the cell, the size of the genome increased and multiple origins of the replication and the chromatin compactation into chromosomes became necessary. During eukaryotic cell cycle the enormous amount of DNA is accurately duplicated and segregated within chromosomes into two daughter cells. The inevitable separation of S phase and mitosis required the development of new controls to ensure that S phase can be initiated only when mitosis is completed and that mitosis proceeds only when the replication of DNA is finished.

1.2.1 Phases of the cell cycle

The eukaryotic cell cycle has been divided into 4 phases that make possible the correct formation of two fully functional daughter cells. Mitosis (M phase) was first to be described more than hundred years ago thanks to distinctive morphological stages, but it was not until 1951 and the work of Alma Howard and Steve Pelc when the very concept of cell cycle emerged [2]. Mitosis was followed by a long interval before the DNA was synthesized again, and after DNA synthesis was completed there was short interval before the mitosis occurred. These intervals or brakes were called gap1 (G1) and gap2 (G2), respectively, and the period of DNA synthesis is called S phase. The time when the cell is not dividing, namely G1, S and G2 phase are denominated interphase, the phase between two mitosis. In a normal tissue, not all cells are cycling; the concept of growth fraction was introduced by Mendelsohn et al [3], who laid the bases of the delineation between temporarily inactive cells, in G0 phase, which upon adequate stimulation could re-enter cell cycle, and terminally differentiated cells, which are dying by apoptosis without ever dividing again. The work of Lieberman et al. in 1963 [4] suggested that the interval of cell cycle defined as G0, G1 and G2 phases which, comparing to dramatic mitosis seemed uneventful was actually hiding the sophisticated

biochemical machinery. It is now generally accepted that G1 cells are biochemically different from G0 cells, although the dilemma weather the Go phase is just a long G1 phase has puzzled the researchers for many years.

1.2.2 The duration of the cell cycle

The length of each phase was determined in various cell lines by different methodologies. For example, Essers et al. [5] used GFP-hPCNA translocation during cell cycle followed by the time-lapse imaging to measure the time spans of the cell cycle phases in CHO9 cells. They found that G1 phase lasted 380±250min, early S phase 266±26min, mid-S phase 323±53min, the late S phase 141±39min, and the G2 phase 77±19min. It is apparent that the time individual cell needs to pass trough one cell cycle is variable and that the largest variations exist in the duration of G1 phase. This is true not only when individual cells of the same type are compared, but also in the case of the cells originating from different tissues. Proliferation rates in the adult body differ in the time that cells pass between G1 checkpoint and mitosis or in G0 phase; neuronal cells almost never divide, liver cells normally divide once in every year or two, although stimulated by an acute liver damage could reduce their cycle time to a day or two, and some epithelial cells of

small intestine divide twice a day. On the contrary, the period from the beginning of S phase to the end of mitosis is usually brief, from 12 to 24h in mammals, and constant, regardless of the period between two divisions.

1.2.3 The control of the cell cycle.

1.2.3.1 Cyclins, Cyclin dependent kinases and checkpoints

The sequence of cell cycle events is strictly controlled by successive activation of different types of complexes of cyclin and cyclin dependent kinase. Several checkpoint mechanisms have been identified that insures the proper timing and order of various processes fundamental for cell duplication.

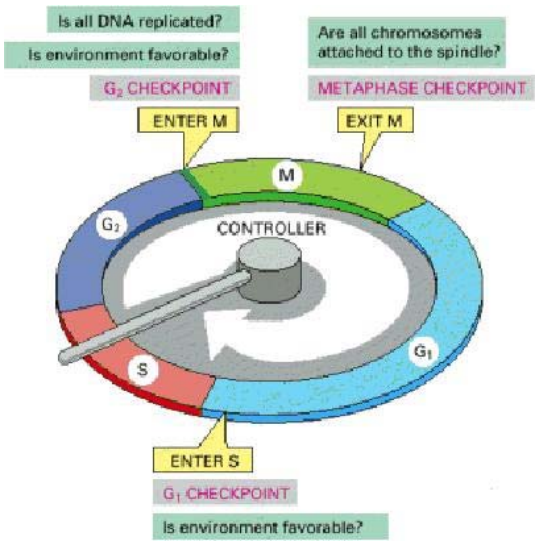

Figure I 1. **Checkpoints and inputs of regulatory information to the cell cycle control system**. Alberts, B. Molecular Biology of the Cell

Each step in the cell cycle is conditioned by the correct development of the previous one, and it could not be initiated until the previous event is completed. This dependence is not the consequence of the characteristics of the process itself, but of the function of the check point mechanisms (Fig I 1.).

According to Hartwell, LH, Weinert, TA [6], ordering of the cell cycle events may be accomplished by two alternative mechanisms: firstly, the product of an early event is a substrate for a later event (the so-called substrate-product relationship) and secondly, regulatory mechanisms, termed checkpoints, may delay later events until earlier events are complete. Thus, *checkpoints are biochemical pathways that ensure dependence of one process on another process that is otherwise biochemically unrelated* [6]. For example, G1/S check point prevents the premature entry into S phase [7, 8]. Mitosis can not begin until the DNA replication is completed, which is confirmed at the G2/M check point. DNA has to be replicated only once per cell cycle and there are mechanisms that prevent re-replication until the cell has passed mitosis. However, if re-replication is initiated, checkpoint proteins would cause G2/M arrest. Several cell cycle transitions rely on the activity of cyclin-dependent kinases (CDKs) and they are inhibited by some check point pathways in cell cycle arrest involving cyclin dependent kinase inhibitors (CKIs) [9]. These enzymes are composed of a serine-threonine kinase

subunit, the CDK, and an activating subunite, the cyclin [10], which have to reach a critical concentration to be able to activate CDKs. The concentration of CDKs is relatively stable, while the concentrationc of different cyclins oscillate throughout the cell cycle. The CDKs once activated, phopshorylate other proteins, enabling them to carry out their particular role in the correct moment of the cell cycle.

1.2.3.2 At the crossroad between initiation of cell proliferation and differentiation

The start of cell proliferation is often dependent on the stimulation by specific growth factors or hormones, which bound to the receptor present on the cell surface and initiates the signal for replication. This process affects the concentration of G1 cyclins: cyclin D and cyclin E. These cyclins form a complex with CDKs, enabling them to phoshorylate retinoblastoma gene product, pRb. This protein is present in early G1 phase in hypophosphorilated form and binds to E2F transcription factors inhibiting them in their role of preparing the nucleus for the DNA replication. The phosporylation of pRb causes release of E2F and subsequent onset of DNA replication [11]. The concentration of cyclin A increases gradually during G1 phase and its binding to CDK2 is necessary for the progress to S phase. A-CDK2 complex contributes to the maintainance of the DNA replication by activating the proteins at the DNA replication origins

[12]. On the other hand, towards the end of S phase A-CDK1 complex prevails which is a signal for G2 phase. During this interval that precedes mitosis cell cycle could be stopped if the DNA replication had not been complete and accurate. The mitosis is initiated and controlled by the cyclin B-CDK1 complex. The B cyclins take over form cyclin A as activators of CDK1. The proper activation of this kinase is controlled at various steps of phosphorylation and dephosphorylation [10], which guarantees that mitotic division does not occur until the DNA has been replicated. The complex that activates mitosis is also called M-phase-promoting factor, MPF. Its activation is followed by a strong positive feedback which causes the concentration of MPF to increase "at an accelerating pace until the critical flashpoint is reached, whereupon a flood of active MPF triggers downstream events that propel the cell into mitosis" [13]. When activated, CDK1 phosphorylates structural nuclear proteins, nucleolin and lamins which makes possible the progress through mitosis and finally cell division.

Weather the cell is going to continue to divide and enter the cell cycle or undergo differentiation and cell cycle exit is decided by a member of Id protein family, Id2. This protein coordinates inhibition of differentiation and stimulation of proliferation by the capacity to disrupt the antiproliferative effect of Rb family, thus allowing the cell cycle progression [14]. The Id2 expression rapidly increases following mitogenic stimulation, and shows

another peak as cell advances into the S phase, which indicates a possible dual role of this protein in the cell cycle progression [15]. Firstly, it could influence the activity of p140/E2F4/5 complexes which have inhibitory effect on cell proliferation during G0 phase [16], and secondly, during late G1 phase where it releases the E2F1-3 from the inhibitory complex with pRb/p107 and thus facilitate the gene expression required for the onset of S phase [17]. It has been shown that the loss of Id2 siginifcantly reduces the rate of proliferation of primary and immortalized embryonic fibroblasts, and that Id2 expression determines the rate of proliferation in primary, immortalized and tumour cell lines [18]. In general, expression level of Id genes is high in proliferating cells, and is low or absent in differentiated cells [19].

1.2.3.3 The inhibition of the cell cycle

The cell in G0 or early G1 phase is characterized by a high concentration of cyclin kinase inhibitors, CKIs divided in two families: p21 family, which includes p21, p27 and p57 and INK4 family which consists of p15, p16, p18, and p19. P27 is one of the most important inhibitors of the CDKs phosphorilation and consequently, the cell cycle progression. Upon the mitogenic stimuli, the concentration of p27 decreases, CDKs are activated and pRb could be phosphorilated. pRb itself is an inhibitor of the cell cycle and it has been termed "gateway" for the

proliferation, because its inactivation is necessary for the cell cycle to begin [11]. If mitogenic stimulation is stopped, the p27 concentration increases and the cell is halted in G1. However, if the mitogenic stimuli are removed some time in late G1 phase, the cell will already be committed to proliferation and would be immune to external factors. This means that the cell has passed the "restriction point". Both p15 ad p16 have been identified as tumor suppressors under the control of pRb. P21 is a cell cycle inhibitor that contributes to the cell cycle arrest in G1 or early S phase if the DNA damage has been detected. P53 protein, also called "the guardian of human genome" recognizes the damage in the DNA and induces the transcription of p21 [20] which then inhibits the activation of CDK2. This delay in the cell cycle progression permits the DNA repair, or if the damage is too extensive, the initiation of apoptosis.

This mechanism also operates in G2 to M transition, just before the beginning of mitosis. In this case, p21expression, induced by p53, leads to the inhibition of the CDK1 activation by cyclin B.

The different stages of mitosis are also under rigorous control which assures the correct and timely development of each cell division phase.

2. The Implication of Cellular Redox Balance in Cell Proliferation.

The oxidizing environment, shared by all aerobic organisms and crucial for their survival, poses a continuous treat to cellular structures all the living beings are made of. Structural proteins and lipids, and cellular membranes they compose, nucleic acids and enzymes that govern vital cellular processes are all susceptible to oxidative damage. Dealing with this inevitable and constant danger is one of the greatest challenges the living being with aerobic metabolism has to meet.

2.1 Reactive Oxidative Species in Cell Proliferation

Classical work of Kelvin Davies [21], almost ten years ago, showed that the cells show a whole range of responses to oxidative stress that depends on the intensity of the stress. Low level of hydrogen peroxide induced mitogenic responses and growth stimulation; this observation was firstly reported by Oberly et al [22] who have described that oxidative stimuli, such as superoxide and hydrogen peroxide, could activate signalling pathways that lead to proliferation. Davies et al. further assert that considerable increase in the oxidant concentrations caused temporary growth arrest which became permanent with a progressive increase. When high H_2O_2 concentrations were used, apoptosis took place and at very high oxidant levels the cells

were killed by necrosis. A year later, Pani et al [23] demonstrate a causal link between redox changes and growth control by cell density: they show that low level of oxygen species in the environment of proliferating cells was not only stimulating but necessary for the correct mitogenic signalling. This study was immediately followed by the work of Menon et al [24] who suggested that an oxidation event early in G1 phase may be a critical regulatory step in the progression of the cells into S phase. This lead to the development of the model of the "redox cycle within a cell cycle" proposed by the same group several years later [25].

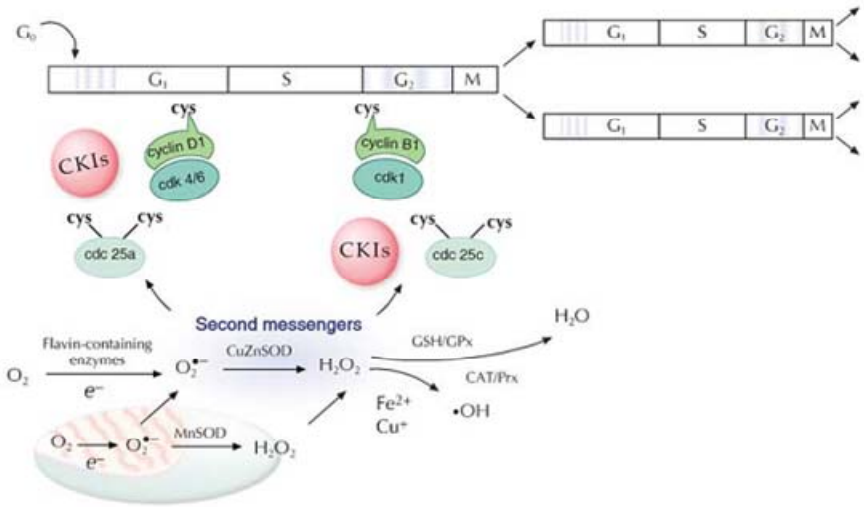

Menon, SG and Goswami, PC, 2007

According to this model, the transient change in ROS could modify the redox state of cell cycle regulatory proteins, at their critical cysteine residues, and thus determine progression or arrest in the proliferation.

Antioxidant mechanism could scavenge ROS and reverse the process. In accordance to these reports, Barry Halliwell [26] draw a complete view of the present knowledge of the role of oxidative stress in promoting cancer, its damaging effects to DNA, and its action on cell proliferation and apoptosis. Malignant cells produce more radical species and, although antioxidant defence could also be induced in these cells, they display a pro-oxidant state. However, apparently the oxidative stress generated in these high proliferative cells does not exceed the level where oxidative damage becomes so severe that cell function is impaired. This finding is in line with previously cited and many others that support the role of reactive oxidative species mediated signalling in the promotion of cell growth.

Thus, a clear picture emerges where oxidative stress is able to modulate cell growth suggesting its importance in cancer therapy. However, little information has been provided on the active role of glutathione and other powerful antioxidant cellular defence mechanisms during the cell cycle.

2.2 The bridge between the oxidative stress and cell proliferation. Glutathione

Glutathione (GSH) is the most abundant non-protein thiol in mammalian cells [27]. It is considered essential for survival in mammalian cells [28] and yeast [27, 29], but not in

prokaryotic cells. The exact nature of this important difference has not been elucidated.

Glutathione was discovered in 1888 by Rey Pailhade as "organic hydrogenate of sulphur" [30] and "rediscovered" and fully described by Sir Frederic Gowland Hopkins in the 1920s [31] ([30] and [31] quoted in [32])

Glutathione has attracted the scientific interest with variable intensity along the century since its discovery and many important cellular functions of this tripeptide were revealed along the years.

Glutathione shows a widespread localization within cells and considerably high concentration in cells and tissues (up to 10 mM) [33]. Examples of normal physiological functions of glutathione known for a long time include regulation of the transport of certain amino acids [34] control of cytoskeleton assembly [35] and regulation of enzymatic activity [36, 37]. During 1960s, GSH was demonstrated to be a co-substrate for a number of important enzymatic reactions: GSH-S-transferase was described (Booth 1961) and its role in a first–line defence against electrophilic insult, obviously dependent on glutathione, was suggested (Boyland, E 1969). These pioneer works became the bases for many studies that lead to the development of concepts such as drug and foreign compound detoxification, and multidrug resistance (Smith, 1977) of crucial importance in the modern cancer therapy. Glutathione, as it lacks toxicity linked to cysteine [38], is considered perfect as a cellular thiol "redox buffer" with a

purpose to maintain a given thiol/disulfide redox potential [32]. Therefore, the redox properties and abundance that characterise this molecule grant it a major role in protecting the cell against oxidants and electrophiles, and during 1980s this particular role of glutathione is central in many research efforts.

Association of redox regulation with toxicity events lead to the introduction of the concept of "oxidative stress" at biochemical and cellular level [39]. Oxidative stress is generally defined as an imbalance between prooxidants and antioxidants with a considerable effect on other cellular components, including redox sensitive functional groups of proteins. Nowadays, with the increasing awareness of the importance of ROS and glutathione in cellular signalling, and the cellular redox environment in fundamental physiological processes, a new definition of oxidative stress is proposed. Acording to Jones, DP [40], oxidative stress may be better defined as a disruption of redox signaling and control.

Interestingly, more than 10 years ago, searching for a molecular link between oxidative stress and cell proliferation, Cotgrave IA and Gerdes RG recommended similar term: "oxidant mediated regulation" [41].

2.3 Glutathione in cell proliferation

It seems that, traditionally, the attempts to elucidate the behaviour of highly proliferating cells in the light of its redox

status relayed mainly on the increased production of ROS, while little insight was devoted to the potential role of the antioxidant system.

Several studies from more than 20 years ago have suggested that changes in low molecular weight thiols are associated with regulation of cell growth. Harris and Patt published in 1969 [42] that nonproliferating mouse tumour cells contained less LMWT than proliferating cells and in early eighties various authors report similar results: human lung and ovarian tumour cells during the exponential growth demonstrate higher GSH levels than during nondividing state [42-44]). In accordance to these findings, Kosower and Kosower [45] have demonstrated that decrease of GSH biosynthesis in vivo inhibits tumour growth rate. Moreover, it was suggested that cellular GSH may have to reach certain critical levels before proliferation can be initiated and that variations in the protein sulfhydril redox status may directly relate to regulation of cell growth [46].

Defining the intrinsic cellular redox environment by estimation of glutathione (GSH)/glutathione disulfide (GSSG) redox state, the group of Dean P. Jones [47] concluded that each phase in the life of the cell is characterized by the certain redox state.

Proliferating cells are in the most reduced state, with the values of Eh between -260mV and -230mV [48]. Upon a growth arrest caused by differentiation [47] or contact inhibition [48] cells are 40 mV more oxidised (-220mV to -

190mV) while the apoptotic process is accompanied by further oxidation up to -165mV [49].

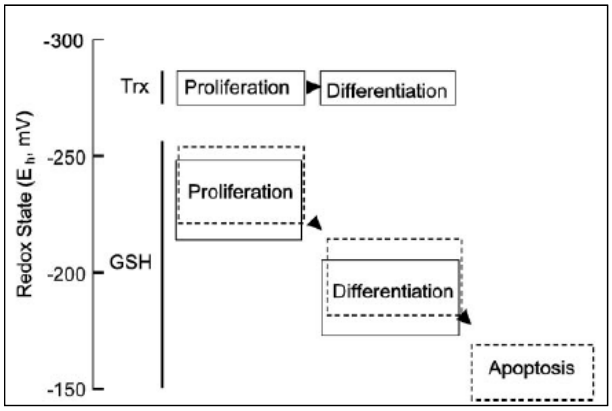

Cellular redox changes in assotiation with the growth state.
Nkabio, YS et al. 2002

Therefore, while the cell progresses from proliferation, through contact inhibition, differentiation, and finally apoptosis, there is an intrinsic and natural progression from more reduced to more oxidised cellular redox environment.
The universality of this model which applies to various cells from different organisms (reviewed in [48]) inspired a daring hypothesis of Schafer and Buettner on the implication and function of thiols and disulfides as nano-switches.

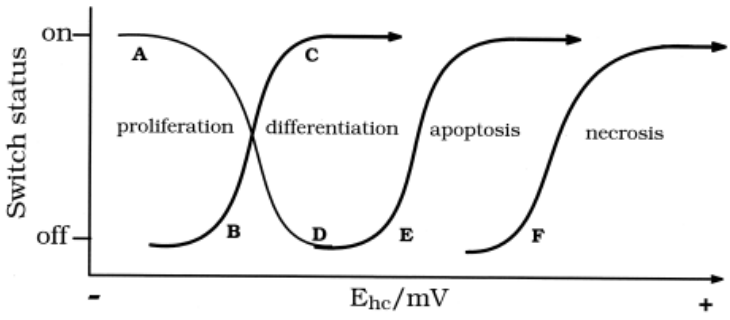

Schafer, FQ and Buettner, GR, 2001

The GSSG/2GSH couple is imagined as a switchboard that move the cell from proliferation through differentiation towards programmed cell death, if the redox environment could not be maintained, or necrosis when the oxidative insult is to severe.

2.4 Glutathiolation of regulatory proteins as a link between a stimulating oxidative event and reduced cell environment in cell proliferation

During last two decades the increasing body of evidence reveals that several transcription factors undergo oxidant modification necessary for their activation. For instance, the property of binding DNA and thus regulate gene expression of AP1, Nfkb, p53, and SP1 depends on the redox status of cysteinyl thiols in their structures [49].

Thus, the idea of protein glutathionation as a regulatory mechanism of importance in cell proliferation came into sight.

Glutathiolation is a protein modification which consists in the covalent union of the tripeptide glutathione to the SH group of the cysteine residue. For a long time this reaction was considered to be a consequence of the equilibrium between protein thiols and GSSG inevitably related to oxidative stress. From this point of view, glutathiolation flufills two important functions. Firstly, its reversibility enables the preservation of glutathione in the cell and serve

as a buffer for the reduction potential; otherwise, GSSG efflux would cause the loss of GSH from the cell, decreasing the reducing capacity which could be recovered only by the synthesis of new GSH [48]. Secondly, it provides protection for protein-SH against irreversible modifications and protein damage in response to higher levels of oxidative stress [50]. Interestingly, it was demonstrated that glutathiolation as a posttranslational modification occurs not only during oxidative stress, but also under basal conditions and is involved in regulating distinct transcription factors, such as NF-kB [51], its inhibitor factor IKK [52] and c-Jun [53]. Apparently, the binding capacity of these proteins for DNA or other proteins is modulated by glutathiolation. This relatively recent focus on the implication of glutathiolation modulatory effects on protein function yielded important breakthrough in elucidation of the implication of this modification in various physiological and pathological situations [54] and raises interesting questions about its possible implications in cell proliferation.

2.3.1 The Role of Glutathione in DNA Synthesis

Among the important roles that GSH plays in cellular physiology, and among the first to be described, was its role in DNA synthesis.

The pentose phosphate pathway is a cellular source of NADPH that is involved in reductive biosynthesis. In this

process, ribose-5-phosphate is formed and subsequently used for the synthesis of RNA, DNA and nucleotide coenzymes. Apart from the synthesis of nucleotides, NADPH is also required for the formation of amino acids, fatty acids, cholesterol, neurotransmitters and nitric oxide (NO). Furthermore, NADPH is the source of electrons in the process of reduction of ribonucleotides to deoxyribonucleotides catalyzed by the ribonucleotide reductase [55].

The rout is initialized by two distinct but complemented systems, the thioredoxin system and the glutaredoxin system. Thioredoxin operates by transferring the electrons to ribonucleotide reductase, and they are supplied by the thioredoxin reductase and NADPH. The glutaredoxin system is initialised by the glutathione reductase, which reduces the GSSG to GSH using the NADPH as source of electrons. GSH is used by the glutaredoxin to provide the reducing power to the ribonucleotide reductase.

The crucial role of glutathione in DNA synthesis has been extensively documented [55, 56]. For instance, Dethlefsen and co-workers [57] showed that glutathione depletion inhibits DNA synthesis in mammary carcinoma cells. In addition, the vital importance of GSH in this process has also been demonstrated in human T lymphocytes [58]. As mentioned above GSH is an indispensable requirement in eukaryotes. In contrast, it does not demonstrate the same importance in prokariotes. It has been shown that E. Coli lacking gshA, the rate limiting enzyme in the synthesis of

GSH, can grow without GSH supplementation [59, 60]. On the contrary, in yeast, the depletion of GSH does affect cell proliferation on the level different from DNA synthesis: mutants deficient in GCS after GSH withdrawal arrest cells in G1, whereas a strain with a defect in ribonucleotide reduction arrest cells in S phase [61]. Since other possible explanations, such as protection against oxidative stress or protection against non-native protein disulfides, have been discarded [62], it appears that the essential function of GSH in yeast is related to the redox properties of its thiol group. Consequently, glutathione can be replaced by dithiothreitol, but not with a GSH analog where a thiol group has been substituted by a methyl group [63]. Since GSH is the reductant for glutaredoxin as explained previously, and glutaredoxin is also essential [64] presumably their vital importance may be interdependent.

2.3.2 Regulation of Telomerase Activity by Glutathione

The eukaryotic chromosomes are capped by telomeres, which consist of telomeric DNA repeated in tandem, associated with several proteins. These structures play an important role in the stability and the complete replication of the chromosomes. Conventional DNA polymerases cannot fully replicate the 3'-end of the lagging strand of linear molecules, and therefore in every cell division telomeric sequences are lost [65]. Telomerase is an important enzyme that ensures the maintenance of normal

telomere length. This activity is high in human cancers [66], but virtually absent in normal human tissues, except germinal cells [67]. Telomerase regulation is not completely understood, but its changes are related to both cancer and aging [68]. Studies carried out by Jady et al. show that human telomeres are more accessible during the S-phase [69] and that the telomerase assembly with telomeres takes place at this specific moment of the cell cycle [69, 70]. Telomerase plays a key role in cellular homeostasis, because it maintains the length of the telomeres. This especially important in germinal cells in which it is necessary to keep a normal telomeric length after many cellular divisions. Recently, Maria Blasco has suggested that telomeres are under epigenetic control [71]. Mammalian telomeres and subtelomeric regions are enriched in epigenetic markers that are characteristic of heterochromatin.

There are evidence that point to a role of redox environment in a short term regulation of the activity of this important enzyme. Minamino *et al.* [72] using vascular smooth muscle cells, reported that hypoxia up-regulates telomerase activity. Hypoxia is known to lower oxidative stress and thus to increase levels of glutathione. A specific inhibitor of telomerase, 2-[3-(trifluoromethyl) phenyl]isothiazolin-3-one, reacts with a key cysteine residue, which is essential for telomerase activity and must be kept reduced. Consequently, it has been reported that dithiothreitol reverses this inhibition [73]. Furthermore, antioxidants have been shown to inhibit nuclear export of

telomerase reverse transcriptase and thus delay replicative senescence of endothelial cells [74]. In conclusion, a critical cysteine residue must be kept reduced in order to maintain full telomerase activity. It is likely that the glutathione redox potential may be important in this process.

Previous findings of our group demonstrated that telomerase is regulated by the shift in glutathione redox potential within values similar to those found *in* vivo and alterations in telomerase activity are coordinated with changes in critical cell cycle proteins, particularly Id2 and E2F4 [75]. Thus, physiological variations in glutathione level induce changes in telomerase activities that are in concordance with changes in cell cycle regulatory proteins. A number of reports have shown similar results. Brown et al. [76] demonstrated for the first time *in vivo* that high hepatic glutathione levels correlate with increased telomerase activity. Also, the importance of glutathione regulation in telomerase activity has been proved in endothelial progenitor cells (EPC): impairment of antioxidant defences in EPC promoted oxidant mediated apoptosis and telomerase inactivation which subsequently lead to development and/or progression of atherothrombosis [77].

Recent data suggest that telomerase activity is regulated and ordered by telomere structure and telomerase assembly. Although not proven, the telomere structure may change in a cell cycle-dependent manner to restrict telomerase activity to S phase [78]. For this to happen, the precise control of the changes not only in telomerase

conformation, but in chromatin structure (i.e. in its compactation level) as well, is of vital importance. This finding that telomere length, and, therefore, telomere structure, is tightly regulated in telomerase proficient cells invokes a connection between cell cycle, telomerase and telomere structure [79]. In other words, the mechanism that lies beneath telomerase regulation might be related with the mechanism that control cell proliferation. This opens a highly significant area for exploratory study and the diversity of processes and control mechanisms that could be involved in this phenomenon remain to be elucidated.

3. Compartmentalization of Glutathione

3.1. The physiological importance of compartmentalization of glutathione

Pioneer work from Alton [27] correlated GSH synthesis and its degradation throughout the so-called γ-glutamyl cycle, and defined it as a cytosolic processes. The importance of cellular compartmentalization of GSH is two fold, first because it plays an important role in fighting against radical oxygen species (ROS). It is well known that these molecules have a very short half life and exert their action close to the place they were produced. Thus, the presence or absence of GSH could determine the development of localized oxidative damage for the cell

structure or metabolic function developed in the vicinity. Secondly, GSH compartmentalization is of vital importance because of its role as a cellular detoxifying agent; it is known that tumours that have high glutathione levels are more resistant to chemotherapy, and the importance of nuclear [80] and mitochondrial [81] compartimentalization of GSH has been pointed out.

The overview of compartmentalization of glutathione in mammal cells is a complicated matter. This is due to the presence in the literature of a number of contradictory reports. The reason for the controversy is mainly methodological. Until very recently most reports were mainly based on cell-fractionation techniques. Those techniques appear to be reliable for mitochondrial studies; however their usefulness in nuclear or even endoplasmic reticulum measurements is at least controversial.

However, although knowledge on cellular GSH distribution is not completely established, a considerable number of studies describe a reliable picture, which we present in the continuation.

3.2. Glutathione content in cells

3.2.1 Whole cells

Glutathione concentration in some cells could be as high as 10 mM. Cellular glutathione status suffer significant changes

under both physiological and pathological conditions. Lowering the concentration of the reduced form of glutathione (GSH) may or may not be accompanied by an increase in the levels of the oxidized form (GSSG), depending on whether it is caused by oxidative stress or by eflux. Accurate determination of glutathione in biological samples is of critical importance and is largely dependent on a proper sample treatment. The GSSG concentration is usually very low compared to the GSH concentration [29, 82]. Pioneer work by Tateishi and co-workers and Akerboom and Sies [82, 83] showed that rat liver GSH ranges from 2.0 to 7.0 μmols/g of tissue and GSSG from 0.007 to 0.084 μmols/g of tissue. In isolated rat hepatocytes GSH concentration is 4 μmoles/g of wet weight [29].

Most of the glutathione is maintained in its reduced form by glutathione reductase. As mentioned above, glutathione synthesis and its degradation are linked by the γ-glutamyl cycle which involves cytosolic steps and one membrane bound enzyme, γ-glutamyl transferase.

The main cellular localizations that have been described for glutathione are the cytosol, mitochondria, the endoplasmic reticulum (ER), and the cell nucleus.

3.2.2. Cytosol

As pointed out above, GSH synthesis occurs by two sequential, ATP-dependent reactions in the cytoplasm, catalyzed by glutamate cysteine ligase (formerly known as γ-

glutamylcysteine synthase) and GSH synthetase. Almost all cellular GSH is synthesized in the cytosol with little if any production in other organelles, including mitochondria [84, 85]. The capacity for GSH synthesis is present in almost all mammalians cells. Degradation of GSH is mediated by a different pathway. However, not all mammalian cell types can degrade GSH [86]. Cleavage of the γ-glutamyl-peptide bond by γ-glutamyl transferase (γ-GT) takes place mainly in epithelial cells but its expression is very low in parenchymal cells. The cytosolic concentration of GSH depends not only on the rate of synthesis and degradation but also its efflux through the plasma membrane. Recently a number of plasma membrane proteins capable of exporting GSH out of the cell have been described in tumour cells. These are ATP-binding cassette C1 (ABCC1) and cystic fibrosis transmembrane conductance regulator (CFTR) [87, 88]. ABCC1 is a member of the ABC transmembrane proteins that function as efflux pumps with diverse substrate specificity. It is involved in the extrusion of several endogenous cell metabolites, including leukotriene C4 (LTC4) and GSH. CFTR forms an ion channel that is permeable both to Cl^- and to larger organic anions, among them GSH. In airway epithelial cells CFTR exports GSH to the airway surface fluid. Thus, a new direction of research on the regulation of cytosolic GSH has been opened by different families of membrane transporters.

3.2.3 Mitochondria

Mitochondria are major sources of ROS, thus it is a cellular priority to maintain high glutathione levels within mitochondria. In fact, their function is closely linked to maintenance of the redox balance since mitochondria are the main consumers of oxygen within the cell. The generation of ROS as a by-product of mitochondrial physiological metabolism is due to the partial reduction reactions that take place during the four-electron reduction of molecular oxygen (O_2) to water.

Increased ROS production by mitochondria could induce a chronic oxidative stress, impaired mitochondrial function, and further production of ROS. This inevitably leads to mitochondrial damage and even to lesions in other cellular structures [89-91]. Not only oxygen-derived free radicals, but also reactive nitrogen species (RNS) like nitric oxide (NO) and peroxynitrite (ONOO) are produced inside mitochondria. Thus, formations of S-nitrosoglutathione (GSNO) takes place during normal mitochondrial metabolism. The formation of GSNO has been reported to play a regulatory role in mitochondrial homeostasis.

In hepatocytes, 15 % of all cellular glutathione is in mitochondria [92].

Initial studies on mitochondrial GSH transport were performed by Kurosawa et al [93] in the early nineties. These authors found higher GSH levels in mitochondria than in the cytosol and described the presence of mitochondrial

transport activity that was dependent on the respiratory state of mitochondria. The highest transport activity was found under state 4 conditions. Martensson [94] and co-workers found a two-kinetic component when studying isolated mitochondria form rat liver. Similar results, using different approaches, where reported by Garcia-Ruiz et al. in 1995 [95] and Schnellman et al. [96].

Nowadays a clear picture emerges, where at least two anion carrier proteins, the dicarboxylate carrier (DIC) and the 2-oxoglutarate carrier (OGC), play a major role in the transport of GSH to mitochondria (for a review see [89]). According to Lash and co-workers [97] approximately 60% of the total amount of GSH transport in renal cortical mitochondria is mediated by DIC and around 40% is mediated by OGC. The authors do not exclude the presence of other unidentified carriers. It is known that DIC is responsible for the transport of dicarboxilates from the cytoplasm to mitochondria, thereby supplying substrates for the Krebs cycle [98, 99]. Thus, GSH would compete for the carrier and could explain the reported correlation between GSH transport and the mitochondrial state.

3.2.4. Endoplasmic reticulum

The endoplasmic reticulum (ER) plays a major role in the folding of native proteins. By contrast to the cytosol the ER contains a relatively higher concentration of oxidized glutathione (GSSG) [100]. This allows the formation of

native disulphide-bonds in the ER. The folding of many proteins depends upon the formation of disulphide bonds. Despite the vital importance of redox regulation in the ER, we have little knowledge about the mechanisms responsible for the ER redox balance. This process is catalyzed by protein disulphide isomerases and GSSG is believed to be involved in the oxidation of protein disulphide isomerases [101]. It has also been shown, however, that ER flavoprotein Erol catalyses the oxidation of protein disulphide isomerases *in vivo* and *in vitro* [102, 103].

Recent advances in genetics and cell biology have outlined a core pathway for disulphide bond formation in the ER of eukaryotic cells. In this pathway, oxidizing equivalents flow from the recently identified ER membrane protein Ero1p to secretory proteins. The reaction is catalyzed by the protein disulphide isomerase (PDI) [104].

Furthermore, very little information is available on the effects of different pathological conditions on the thiol metabolism and redox folding in the ER. For instance, when Nardai et al. [105] were examining the role of molecular chaperones in the cellular pathology of diabetes mellitus, they found that the ER redox environment moved to a more reducing state. This could be of major importance in the pathophysiology of the late-onset complications of the disease.

3.2.5 Nucleus

Although the role of nuclear GSH in the synthesis of DNA [55] and in protection against oxidative damage or ionizing radiation [106] is well established, little is known about the concentration of GSH in the nucleus and its regulation. This is due to two main factors. The first is methodological: it is impossible to determine the nuclear concentration of GSH using standard cell fractionation and analytical approaches (for a review see Söderdahl *et al*. [107]) In view of this problem, in the present thesis we used confocal microscopy (see Material and Methods).

The second factor is that most, if not all, of the reports share the common view of nuclear GSH distribution in a static situation. Cells are usually studied under steady state conditions *i.e.* when they are confluent (G_0/G_1 phase of the cell cycle). The nuclear membrane dissolves during mitosis and is formed again around newly replicated DNA packed in chromosomes; this spectacular change involves a variety of regulatory mechanisms. Therefore, if the nuclear GSH distribution is studied, the cell cycle physiology should be carefully considered.

A number of reports underscore the important role that GSH plays in cell proliferation but it is not clear which is the exact nature of its intervention further from its contribution in DNA and protein synthesis.

The role of GSH in cell cycle regulation has been addressed mainly from the point of view of its overall cellular content.

This is surprising since it is in the nucleus where most cell cycle progression events take place. The nucleus changes dramatically during the different phases of cell cycle, and failing to consider the corresponding changes in its redox environment could confer an important disadvantage in elucidating the actual importance of glutathione in the control of cell proliferation.

To our knowledge there is a lack of information about the cellular distribution of glutathione during the different phases of the cell cycle and the possible correlation between cellular growth and nuclear GSH levels.

4. Bibliography

1. Sluder G, H.E., Rieder CL, *Mitosis: the Culmination of the Cell Cycle* in *The Molecular Basis of Cell Cycle and Growth Control*, B.R. Stein GS, Giordano A, Denhardt, DT, Editor. 1999, Wiley-Liss, Inc. p. 155-182.
2. Baserga, R., *Introduction to the Cell Cycle*, in *The Molecular Basis of Cell Cycle and Growth Control*, B.R. Stein GS, Giordano A, Denhardt, DT, Editor. 1999, Wiley-Liss, Inc.
3. Mendelsohn, M.L., *Autoradiographic analysis of cell proliferation in spontaneous breast cancer of C3H mouse. III. The growth fraction.* J Natl Cancer Inst, 1962. **28**: p. 1015-29.
4. Lieberman, I., R. Abrams, and P. Ove, *Changes in the metabolism of ribonucleic acid preceding the synthesis of deoxyribonucleic acid in mammalian cells cultured from the animal.* J Biol Chem, 1963. **238**: p. 2141-9.

5. Essers, J., et al., *Nuclear dynamics of PCNA in DNA replication and repair.* Mol Cell Biol, 2005. **25**(21): p. 9350-9.
6. Hartwell, L.H. and T.A. Weinert, *Checkpoints: controls that ensure the order of cell cycle events.* Science, 1989. **246**(4930): p. 629-34.
7. Machida, Y.J., J.K. Teer, and A. Dutta, *Acute reduction of an origin recognition complex (ORC) subunit in human cells reveals a requirement of ORC for Cdk2 activation.* J Biol Chem, 2005. **280**(30): p. 27624-30.
8. Machida, Y.J. and A. Dutta, *Cellular checkpoint mechanisms monitoring proper initiation of DNA replication.* J Biol Chem, 2005. **280**(8): p. 6253-6.
9. MacLachlan, T.K., N. Sang, and A. Giordano, *Cyclins, cyclin-dependent kinases and cdk inhibitors: implications in cell cycle control and cancer.* Crit Rev Eukaryot Gene Expr, 1995. **5**(2): p. 127-56.
10. Morgan, D.O., *Principles of CDK regulation.* Nature, 1995. **374**(6518): p. 131-4.
11. Weinberg, R.A., *The retinoblastoma protein and cell cycle control.* Cell, 1995. **81**(3): p. 323-30.
12. Stillman, B., *Cell cycle control of DNA replication.* Science, 1996. **274**(5293): p. 1659-64.
13. Alberts B, B.D., Lewis J, Raff M, Roberts K, Watson JD *The Cell -Division Cycle*, in *Molecular Biology of the Cell* 1994, Garland Publishing, Taylor & Francis group: New York. p. 863-906.
14. Lasorella, A., A. Iavarone, and M.A. Israel, *Id2 specifically alters regulation of the cell cycle by tumor suppressor proteins.* Mol Cell Biol, 1996. **16**(6): p. 2570-8.
15. Zebedee, Z. and E. Hara, *Id proteins in cell cycle control and cellular senescence.* Oncogene, 2001. **20**(58): p. 8317-25.
16. Hansen, K., et al., *Phosphorylation-dependent and -independent functions of p130 cooperate to evoke a sustained G1 block.* Embo J, 2001. **20**(3): p. 422-32.
17. Humbert, P.O., et al., *E2f3 is critical for normal cellular proliferation.* Genes Dev, 2000. **14**(6): p. 690-703.
18. Lasorella, A., et al., *Id2 is critical for cellular proliferation and is the oncogenic effector of N-myc in*

human neuroblastoma. Cancer Res, 2002. **62**(1): p. 301-6.
19. Norton, J.D., *ID helix-loop-helix proteins in cell growth, differentiation and tumorigenesis.* J Cell Sci, 2000. **113 (Pt 22)**: p. 3897-905.
20. el-Deiry, W.S., et al., *WAF1/CIP1 is induced in p53-mediated G1 arrest and apoptosis.* Cancer Res, 1994. **54**(5): p. 1169-74.
21. Davies, K.J., *The broad spectrum of responses to oxidants in proliferating cells: a new paradigm for oxidative stress.* IUBMB Life, 1999. **48**(1): p. 41-7.
22. Oberley, L.W., T.D. Oberley, and G.R. Buettner, *Cell division in normal and transformed cells: the possible role of superoxide and hydrogen peroxide.* Med Hypotheses, 1981. **7**(1): p. 21-42.
23. Pani, G., et al., *A redox signaling mechanism for density-dependent inhibition of cell growth.* J Biol Chem, 2000. **275**(49): p. 38891-9.
24. Menon, S.G., et al., *Redox regulation of the G1 to S phase transition in the mouse embryo fibroblast cell cycle.* Cancer Res, 2003. **63**(9): p. 2109-17.
25. Menon, S.G. and P.C. Goswami, *A redox cycle within the cell cycle: ring in the old with the new.* Oncogene, 2007. **26**(8): p. 1101-9.
26. Halliwell, B., *Oxidative stress and cancer: have we moved forward?* Biochem J, 2007. **401**(1): p. 1-11.
27. Meister, A. and M.E. Anderson, *Glutathione.* Annu Rev Biochem, 1983. **52**: p. 711-60.
28. Viña, J., *Glutathione: Metabolism and Physiological Function*. 1990: CRC Press Boston.
29. Vina, J., R. Hems, and H.A. Krebs, *Maintenance of glutathione content is isolated hepatocyctes.* Biochem J, 1978. **170**(3): p. 627-30.
30. De Rey Pailhade, M., *Sur un corps d'origine organique hydrogénant le soufre á froid.* C.R. Acad. Sci. , 1988. **106**: p. 1683-1684.
31. Hopkins, F., *On glutathione: a reinvestigation.* Journal of Biological Chemistry, 1929. **84**: p. 269-320.
32. Sies, H., *Glutathione and its role in cellular functions.* Free Radic Biol Med, 1999. **27**(9-10): p. 916-21.

33. Tateishi, N., et al., *Studies on the regulation of glutathione level in rat liver.* J Biochem, 1974. **75**(1): p. 93-103.
34. Vina, J.a.V., JR, *Role of gamma glutamil traspeptidase in the regulation of amino acid uptake by mammary gland of the lactating rat.*, in *Functions of glutathione. Biochemical, physiological, Toxicological and clinical aspects*, A.L.e. al, Editor. 1983, Raven press New York. p. 23-30.
35. Burchill, B.R., et al., *Microtubule dynamics and glutathione metabolism in phagocytizing human polymorphonuclear leukocytes.* J Cell Biol, 1978. **76**(2): p. 439-47.
36. Ziegler, D.M., *Role of reversible oxidation-reduction of enzyme thiols-disulfides in metabolic regulation.* Annu Rev Biochem, 1985. **54**: p. 305-29.
37. Ernst, V., D.H. Levin, and I.M. London, *Inhibition of protein synthesis initiation by oxidized glutathione: activation of a protein kinase that phosphorylates the alpha subunit of eukaryotic initiation factor 2.* Proc Natl Acad Sci U S A, 1978. **75**(9): p. 4110-4.
38. Vina, J., et al., *The effect of cysteine oxidation on isolated hepatocytes.* Biochem J, 1983. **212**(1): p. 39-44.
39. Sies, H. and E. Cadenas, *Oxidative stress: damage to intact cells and organs.* Philos Trans R Soc Lond B Biol Sci, 1985. **311**(1152): p. 617-31.
40. Jones, D.P., *Redefining oxidative stress.* Antioxid Redox Signal, 2006. **8**(9-10): p. 1865-79.
41. Cotgreave, I.A. and R.G. Gerdes, *Recent trends in glutathione biochemistry--glutathione-protein interactions: a molecular link between oxidative stress and cell proliferation?* Biochem Biophys Res Commun, 1998. **242**(1): p. 1-9.
42. Harris, J.W. and H.M. Patt, *Non-protein sulfhydryl content and cell-cycle dynamics of Ehrlich ascites tumor.* Exp Cell Res, 1969. **56**(1): p. 134-41.
43. Wolf, C.R., et al., *The role of glutathione in determining the response of normal and tumor cells to anticancer drugs.* Biochem Soc Trans, 1987. **15**(4): p. 728-30.

44. Post, G.B., et al., *Effects of culture conditions on glutathione content in A549 cells.* Biochem Biophys Res Commun, 1983. **114**(2): p. 737-42.
45. Kosower, N.S. and E.M. Kosower, *The glutathione status of cells.* Int Rev Cytol, 1978. **54**: p. 109-60.
46. Atzori, L., et al., *Growth-associated modifications of low-molecular-weight thiols and protein sulfhydryls in human bronchial fibroblasts.* J Cell Physiol, 1990. **143**(1): p. 165-71.
47. Nkabyo, Y.S., et al., *Glutathione and thioredoxin redox during differentiation in human colon epithelial (Caco-2) cells.* Am J Physiol Gastrointest Liver Physiol, 2002. **283**(6): p. G1352-9.
48. Schafer, F.Q. and G.R. Buettner, *Redox environment of the cell as viewed through the redox state of the glutathione disulfide/glutathione couple.* Free Radic Biol Med, 2001. **30**(11): p. 1191-212.
49. Sun, Y. and L.W. Oberley, *Redox regulation of transcriptional activators.* Free Radic Biol Med, 1996. **21**(3): p. 335-48.
50. Dalle-Donne, I., et al., *S-glutathionylation in protein redox regulation.* Free Radic Biol Med, 2007. **43**(6): p. 883-98.
51. Pineda-Molina, E., et al., *Glutathionylation of the p50 subunit of NF-kappaB: a mechanism for redox-induced inhibition of DNA binding.* Biochemistry, 2001. **40**(47): p. 14134-42.
52. Reynaert, N.L., et al., *Dynamic redox control of NF-kappaB through glutaredoxin-regulated S-glutathionylation of inhibitory kappaB kinase beta.* Proc Natl Acad Sci U S A, 2006. **103**(35): p. 13086-91.
53. Canela, A., et al., *High-throughput telomere length quantification by FISH and its application to human population studies.* Proc Natl Acad Sci U S A, 2007. **104**(13): p. 5300-5.
54. Giustarini, D., et al., *S-glutathionylation: from redox regulation of protein functions to human diseases.* J Cell Mol Med, 2004. **8**(2): p. 201-12.

55. Thelander, L. and P. Reichard, *Reduction of ribonucleotides.* Annu Rev Biochem, 1979. **48**: p. 133-58.
56. Holmgren, A., *Hydrogen donor system for Escherichia coli ribonucleoside-diphosphate reductase dependent upon glutathione.* Proc Natl Acad Sci U S A, 1976. **73**(7): p. 2275-9.
57. Dethlefsen, L.A., et al., *Toxic effects of acute glutathione depletion by buthionine sulfoximine and dimethylfumarate on murine mammary carcinoma cells.* Radiat Res, 1988. **114**(2): p. 215-24.
58. Suthanthiran, M., et al., *Glutathione regulates activation-dependent DNA synthesis in highly purified normal human T lymphocytes stimulated via the CD2 and CD3 antigens.* Proc Natl Acad Sci U S A, 1990. **87**(9): p. 3343-7.
59. Greenberg, J.T. and B. Demple, *Glutathione in Escherichia coli is dispensable for resistance to H2O2 and gamma radiation.* J Bacteriol, 1986. **168**(2): p. 1026-9.
60. Miranda-Vizuete, A., et al., *The levels of ribonucleotide reductase, thioredoxin, glutaredoxin 1, and GSH are balanced in Escherichia coli K12.* J Biol Chem, 1996. **271**(32): p. 19099-103.
61. Wang, P.J., et al., *Rnr4p, a novel ribonucleotide reductase small-subunit protein.* Mol Cell Biol, 1997. **17**(10): p. 6114-21.
62. Spector, D., J. Labarre, and M.B. Toledano, *A genetic investigation of the essential role of glutathione: mutations in the proline biosynthesis pathway are the only suppressors of glutathione auxotrophy in yeast.* J Biol Chem, 2001. **276**(10): p. 7011-6.
63. Grant, C.M., F.H. MacIver, and I.W. Dawes, *Glutathione is an essential metabolite required for resistance to oxidative stress in the yeast Saccharomyces cerevisiae.* Curr Genet, 1996. **29**(6): p. 511-5.
64. Rodriguez-Manzaneque, M.T., et al., *Grx5 glutaredoxin plays a central role in protection against protein oxidative damage in Saccharomyces cerevisiae.* Mol Cell Biol, 1999. **19**(12): p. 8180-90.

65. Kornberg, A., *Active center of DNA polymerase.* Science, 1969. **163**(874): p. 1410-8.
66. Kim, N.W., et al., *Specific association of human telomerase activity with immortal cells and cancer.* Science, 1994. **266**(5193): p. 2011-5.
67. Harley, C.B., A.B. Futcher, and C.W. Greider, *Telomeres shorten during ageing of human fibroblasts.* Nature, 1990. **345**(6274): p. 458-60.
68. Sharpless, N.E. and R.A. DePinho, *Telomeres, stem cells, senescence, and cancer.* J Clin Invest, 2004. **113**(2): p. 160-8.
69. Jady, B.E., et al., *Cell cycle-dependent recruitment of telomerase RNA and Cajal bodies to human telomeres.* Mol Biol Cell, 2006. **17**(2): p. 944-54.
70. Tomlinson, R.L., et al., *Cell cycle-regulated trafficking of human telomerase to telomeres.* Mol Biol Cell, 2006. **17**(2): p. 955-65.
71. Garcia-Cao, M., et al., *Epigenetic regulation of telomere length in mammalian cells by the Suv39h1 and Suv39h2 histone methyltransferases.* Nat Genet, 2004. **36**(1): p. 94-9.
72. Minamino, T., S.A. Mitsialis, and S. Kourembanas, *Hypoxia extends the life span of vascular smooth muscle cells through telomerase activation.* Mol Cell Biol, 2001. **21**(10): p. 3336-42.
73. Hayakawa, N., et al., *Isothiazolone derivatives selectively inhibit telomerase from human and rat cancer cells in vitro.* Biochemistry, 1999. **38**(35): p. 11501-7.
74. Haendeler, J., et al., *Antioxidants inhibit nuclear export of telomerase reverse transcriptase and delay replicative senescence of endothelial cells.* Circ Res, 2004. **94**(6): p. 768-75.
75. Borras, C., et al., *Glutathione regulates telomerase activity in 3T3 fibroblasts.* J Biol Chem, 2004. **279**(33): p. 34332-5.
76. Brown, K.E., et al., *Increased hepatic telomerase activity in a rat model of iron overload: a role for altered thiol redox state?* Free Radic Biol Med, 2007. **42**(2): p. 228-35.

77. Fujii, H., et al., *C-reactive protein alters antioxidant defenses and promotes apoptosis in endothelial progenitor cells.* Arterioscler Thromb Vasc Biol, 2006. **26**(11): p. 2476-82.
78. Hug, N. and J. Lingner, *Telomere length homeostasis.* Chromosoma, 2006. **115**(6): p. 413-25.
79. Blasco, M.A., *Telomerase beyond telomeres.* Nat Rev Cancer, 2002. **2**(8): p. 627-33.
80. Voehringer, D.W., et al., *Bcl-2 expression causes redistribution of glutathione to the nucleus.* Proc Natl Acad Sci U S A, 1998. **95**(6): p. 2956-60.
81. Benlloch, M., et al., *Acceleration of glutathione efflux and inhibition of gamma-glutamyltranspeptidase sensitize metastatic B16 melanoma cells to endothelium-induced cytotoxicity.* J Biol Chem, 2005. **280**(8): p. 6950-9.
82. Akerboom, T.P. and H. Sies, *Assay of glutathione, glutathione disulfide, and glutathione mixed disulfides in biological samples.* Methods Enzymol, 1981. **77**: p. 373-82.
83. Sies, H., et al., *Cellular redox changes and response to drugs and toxic agents.* Fundam Appl Toxicol, 1983. **3**(4): p. 200-8.
84. Griffith, O.W. and A. Meister, *Origin and turnover of mitochondrial glutathione.* Proc Natl Acad Sci U S A, 1985. **82**(14): p. 4668-72.
85. McKernan, T.B., E.B. Woods, and L.H. Lash, *Uptake of glutathione by renal cortical mitochondria.* Arch Biochem Biophys, 1991. **288**(2): p. 653-63.
86. Hinchman, C.A. and N. Ballatori, *Glutathione-degrading capacities of liver and kidney in different species.* Biochem Pharmacol, 1990. **40**(5): p. 1131-5.
87. Laberge, R.M., et al., *Modulation of GSH levels in ABCC1 expressing tumor cells triggers apoptosis through oxidative stress.* Biochem Pharmacol, 2007. **73**(11): p. 1727-37.
88. Linsdell, P. and J.W. Hanrahan, *Glutathione permeability of CFTR.* Am J Physiol, 1998. **275**(1 Pt 1): p. C323-6.
89. Passos, J.F. and T. Von Zglinicki, *Oxygen free radicals in cell senescence: are they signal transducers?* Free Radic Res, 2006. **40**(12): p. 1277-83.

90. Monsalve, M., et al., *Mitochondrial dysfunction in human pathologies.* Front Biosci, 2007. **12**: p. 1131-53.
91. Sastre, J., et al., *Mitochondrial function in liver disease.* Front Biosci, 2007. **12**: p. 1200-9.
92. Hansen, J.M., Y.M. Go, and D.P. Jones, *Nuclear and mitochondrial compartmentation of oxidative stress and redox signaling.* Annu Rev Pharmacol Toxicol, 2006. **46**: p. 215-34.
93. Kurosawa, K., et al., *Transport of glutathione across the mitochondrial membranes.* Biochem Biophys Res Commun, 1990. **167**(1): p. 367-72.
94. Martensson, J., J.C. Lai, and A. Meister, *High-affinity transport of glutathione is part of a multicomponent system essential for mitochondrial function.* Proc Natl Acad Sci U S A, 1990. **87**(18): p. 7185-9.
95. Garcia-Ruiz, C., et al., *Evidence that the rat hepatic mitochondrial carrier is distinct from the sinusoidal and canalicular transporters for reduced glutathione. Expression studies in Xenopus laevis oocytes.* J Biol Chem, 1995. **270**(27): p. 15946-9.
96. Schnellmann, R.G., *Renal mitochondrial glutathione transport.* Life Sci, 1991. **49**(5): p. 393-8.
97. Lash, L.H., *Mitochondrial glutathione transport: physiological, pathological and toxicological implications.* Chem Biol Interact, 2006. **163**(1-2): p. 54-67.
98. Klingenberg, M., *Overview of mitochondrial metabolite transport systems.* Methods Enzymol, 1979. **56**: p. 245-52.
99. Palmieri, F., *The mitochondrial transporter family (SLC25): physiological and pathological implications.* Pflugers Arch, 2004. **447**(5): p. 689-709.
100. Hwang, C., A.J. Sinskey, and H.F. Lodish, *Oxidized redox state of glutathione in the endoplasmic reticulum.* Science, 1992. **257**(5076): p. 1496-502.
101. Chakravarthi, S., C.E. Jessop, and N.J. Bulleid, *The role of glutathione in disulphide bond formation and endoplasmic-reticulum-generated oxidative stress.* EMBO Rep, 2006. **7**(3): p. 271-5.

102. Weissman, J.S. and P.S. Kim, *Efficient catalysis of disulphide bond rearrangements by protein disulphide isomerase.* Nature, 1993. **365**(6442): p. 185-8.
103. Tu, B.P. and J.S. Weissman, *The FAD- and O(2)-dependent reaction cycle of Ero1-mediated oxidative protein folding in the endoplasmic reticulum.* Mol Cell, 2002. **10**(5): p. 983-94.
104. Frand, A.R. and C.A. Kaiser, *Ero1p oxidizes protein disulfide isomerase in a pathway for disulfide bond formation in the endoplasmic reticulum.* Mol Cell, 1999. **4**(4): p. 469-77.
105. Nardai, G., et al., *Reduction of the endoplasmic reticulum accompanies the oxidative damage of diabetes mellitus.* Biofactors, 2003. **17**(1-4): p. 259-67.
106. Biaglow, J.E., et al., *The role of thiols in cellular response to radiation and drugs.* Radiat Res, 1983. **95**(3): p. 437-55.
107. Soderdahl, T., et al., *Visualization of the compartmentalization of glutathione and protein-glutathione mixed disulfides in cultured cells.* Faseb J, 2003. **17**(1): p. 124-6.

II OBJECTIVES

II OBJECTIVES

The main objective of the present thesis was to elucidate the importance of glutathione and its nuclear pool in the proliferation of cell lines with different inherent proliferative capacity, origin and differentiation level.

Specific goals:

1. Elucidation of the role of glutathione as a driving force for cell cycle progression., with an emphasis on the implication of the relationship between glutathione and telomerase activity
2. Revealing the changes in the cellular/nuclear distribution of the glutathione along the cell cycle
3. Disclosing the consequences of the depletion of the nuclear glutathione on the cell cycle progression.
4. Exploring the possible mechanism involved in the sequestration of the glutathione to the nucleus and the potential implication of the Bcl-2 in this process.

III MATERIALS AND METHODS

III MATERIALS AND METHODS

1. MATERIALS

1.1. Experimental model

This work was entirely performed in cellular model that included:

- established cell lines (a gift from Mr. Rene Fisher, ETH, Zurich, originally purchased from ATCC, USA)

1. 3T3 fibroblasts
2. MCF7 WT
3. MCF7 Bcl-2, transfected with Bcl-2 oncogene

- embryonic neural cell culture

3T3 fibroblasts were previously used by our group in the study of the relationship between cellular glutathione levels and telomerase activity [1], so it was the cell type of choice in this work.

Cancer cell line, MCF7 (bcl2 wild type), allowed us to study the implication of the GSH and its compartmentalization in the highly proliferating cellular model. In addition, it has been demonstrated that overexpression of Bcl-2 induces higher cellular levels of GSH and its nuclear compartmentalization [2-4]. Therefore, an analogue that over expresses Bcl-2, MCF7 (bcl2+/+), was included in this study.

Embryonic neural cell culture gave us the insight in the significance of our findings in non proliferative model. Moreover, this election of cellular models permitted us to challenge our hypothesis in three different species: mouse, human and rat.

1.1.1. 3T3 fibroblasts

The 3T3 Swiss is adherent cell line of embryonic fibroblasts. It was established by G. Todaro and H. Green in 1962 from disaggregated Swiss mouse embryos. The cells are contact inhibited.

3T3 fibroblasts were maintained and subcultured according to ATCC recommendations (available at www.atcc.com). Briefly, cells were maintained in Dulbecco's modified Eagle's medium (DMEM) (Gibco Invitrogen) supplemented with 10% foetal calf serum (Gibco Invitrogen) and antibiotics (25 U/ml penicillin, 25 µg/ml streptomycin), and 0.3 µg/ml amphotericin B (Sigma-Aldrich) in 5% CO2 in

air at 37°C. Cells were subcultured before they reach confluence in 1:5 ratio, and medium was changed 2 times per week. For experiments, cells were plated in 25 or 75 cm^2 flasks (Nunc, TPP), or, for confocal microscopy, in 2cm^2 LAB-TEK II chambered cover glass (Nunc) at the density of 20 000 cells/cm^2.

1.1.2. MCF7

MCF7 are adherent epithelial cells obtained by pleural effusion of mammary gland of a 69 year old caucasic female patient with metastatic adenocarcinoma. The MCF7 line retains several characteristics of differentiated mammary epithelium including ability to process estradiol via cytoplasmic estrogen receptors and the capability of forming domes.

Transfection of MCF7 with human oncogen Bcl-2 resulted in an analogue cell line over expressing Bcl-2: MCF7 bcl2.

MCF7 cell lines were maintained and subcultured according to ATCC recommendations (available at www.atcc.org). Briefly, cells were maintained in Iscove's modified Dulbeco's medium (IMDM) (Gibco Invitrogen) supplemented with 10% foetal calf serum (Gibco Invitrogen), antibiotics (25 U/ml penicillin, 25 µg/ml streptomycin) and in 5% CO2 in air at 37°C. Medium was renewed 2-3 times per week and cells were subcultured in

1:10 ratio. For experiments, cells were plated in 25 or 75 cm^2 flasks (Nunc, TPP), or, for confocal microscopy, in 2cm^2 LAB-TEK II chambered cover glass (Nunc) at the density of 10 000 cells/cm^2.

1.1.3. Embryonic neural cell cultures

The Wistar rats were sacrificed at 14th day of gestation, and foetal neurons were isolated as described by Valles et al. [5]

Briefly, the homogenate of the foetal brain obtained by the careful disagreggation in DMEM (Gibco Invitrogen) supplemented with 10% FBS (Gibco Invitrogen) and 1% penicillin-streptomycin (Sigma-Aldrich), was filtered through a nylon mesh (pore size of 90 μm). The suspension obtained was plated in poly-L-Lysine (Sigma-Aldrich) pre-coated flasks at a density of $5x10^4$ cells/mm^2, and cells were grown in a humidified atmosphere of 5% CO_2 and 95% air at 37ºC. The medium was changed after 1h to discard dead cells and tissue particles. To prevent non-neural proliferation cytosine-β-D-arabinofuranoside [5μM] was added on the 4th day of culture, and 24h afterwards half of the culture medium was changed. The level of glial contamination was defined by immunocitochemistry with anti-GFAP (glial fibrillary acidic protein) and anti-MAP2 (microtubule associated protein 2) and was less than 3%.

1.2. EQUIPMENT

Centrifuges

SORVALL, model GLC-1 and

HERAEUS, model Sepatech megafuge 1.0 R, for low speed centrifugations

HERAEUS, model Sepatech Biofuge 17RS for high speed centrifugations

Spectrophotometer: KONTRON, model Uvikon 810

Autoclave: SELECTA, model Autester-G. **Owen:** HERAEUS Instruments

Magnetic stirrer: SELECTA, model Agimatic-S

pH-meter: CRISON, model Microph 2001, electrode: INGLOD.

Fluorimeter: PERKIN ELMER, model LS 50B.

Precision scales: SALTER, model HA-120M, SARTORIUS, model PT 1200.

Water purification system: MILLIPORE, models Milli-Q and Milli-RO.

Tanks for electrophoresis: BIORAD, model Mini-PROTEAN 3 Cell

Tanks for electrotransference: BIORAD, model Mini Trans-Blot Cell.

Power supply for electrophoresis: SIGMA, model PS 250-2, BIORAD, model 200/2.0 Power Supply.

Image analysis system: FUJIFILM, modelo LAS-1000 plus.

H.P.L.C.

The device used includes:

-2 pumps: WATERS model 510.

-injector PHARMACIA LKB, model 2157.

- UV detector WATERS, model 441, at the constant wave length of 365 nm.

-Computer IBM XT model 286 with integrator –equipment control

-Chromatography column WATERS, model Spherisorb aminated, 20 X 0.46 cm and with particle diameter 5 µm

Microscopes: Zeiss, inverted microscope, Nikon SE

Hoods: Telstar AV-30/70, Cult*air* BC 100

Incubators: Napco 5415

Flow citometer: EPICS PROFILE II (Counter Electronics, Hialeah, FL, USA) with software E 11/94 version 4.0 EPICS, equipped with argon laser

Confocal microscope: Leica TCS-SP2 confocal laser scanning unit equipped with argon and helium-neon laser beams and attached to a Leica DM1RB inverted microscope.

Thermo cycler: i Cycler BIO-RAD

1.3. MATERIAL

1.3.1. Material and reagents for general use

Protein determinations

"Bradford Reagent" BIORAD

"Lowry" reagent, Sigma

Folin-Ciocalteu's phenol reagent, 2N, Sigma

Western Blotts developing

-"Protoblot Western Blot AP System", Promega, for the use of horse radish peroxidase (HRP) conjugated anti bodies.

-LumiGLOl® Reagent (Cell Signalling Technologies).

Enzymes

Glutathion-S-transferase (SIGMA).

Fluorochromes

-CellTracker green 5-chloromethylfluorescein diacetate (CMFDA) (Molecular probes)

-propidium iodide (PI) (Sigma)

-MitoTracker Red 580 (Molecular probes)

-Hoechst 33342 (Sigma)

-2',7'-dichlorodihydrofluorescein diacetate (2',7'-dichlorofluorescin diacetate; H_2DCFDA) (Molecular probes)

-Dihydroethidium (Hydroethidine, HE) (Molecular probes)

Kits

-Telomerase activity detection kit (Roche)

-Nuclear Extraction Kit (Active Motif North America)

-Oxy Blot protein Oxidation Detection Kit (Chemicon International)

Other chemicals

Perchloric acid 60% (PCA), sodium acetate, baptholphenanthrolinesulfonate (BPDS), *N*-ethylmaleimide (NEM), potasium hydroxide (KOH), 2-[*N*-cyclohexylamino]ethanesulfonic acid (CHES), iodoacetic acid, meta-cresol purple, 1-fluoro-2, 4-dinitrobenzene (FDNB), reduced glutathione (GSH), glutathione ester, glutathione disulfide-reduced glutathione (GSSG), γ-Glu-Glu, H2O2, potassium phosphate, 1-chloro-2,4-dinitrobenzene (CDNB), sodium chloride, ethylenediaminetetraacetic acid (EDTA), ethylene glycol tetraacetic acid (EGTA), 3-(N-morpholino)propanesulfonic acid (MOPS), (4-(2-hydroxyethyl)-1-piperazineethanesulfonic acid (HEPES), trishydroxymethylaminomethane (TRIS), glycine, acrylamide, bis-acrylamide, acetic acid, sucrose, hydrichloric acid (HCl),sodium dodecyl sulfate (SDS), bromophenol blue, coomassie brilliant blue (CBB), dimethyl sulfoxide (DMSO), 2-mercaptoethanol (β-mercaptoethanol), N,N,N',N'-tetramethylethylenediamine (TEMED), bovine serum albumin (BSA), ammonium persulfate (APS), dithiothreitol (DTT), phenylmethylsulphonyl fluoride (PMSF), ethanol, methanol, Tween 20, paraformaldehyde, protease inhibitor, phosphate buffered saline (PBS), diethil maleate (DEM), buthionine sulfoximine (BSO), Carbonyl cyanide m-chlorophenylhydrazone (CCCP), carbonyl cyanide p-trifluoromethoxy p henyl hydrazone (FCCP). Los reactivos se obtuvieron de las firmas: Sigma-Aldrich Química (Spain),

Boehringer Manheim S.A. (Germany), Panreac, Merck Biochemica (Germany).

1.3.2. Material and reagents for cell culture

The sterile material and reagents used in cell culture were the following:

TPP

Flasks 25cm^2, flasks 75cm^2, Flasks 150cm^2, Tube 15mL, Tube 50mL, Petri dish 60mm, Pipettes 10mL, Pipettes 25mL, 6 well plates, 12 well plates, 24 well plates, Cryotubes 2mL, Cell scrapers 24cm, Sterile filters 0,22 μm

Nalgene

Sterile filters 0,22 μm, cellulose, Sterile filters 0,22 μm, nylon

Corning

Cell Scrapers 25cm

Nunc

Cryotubes 1,8mL , LAB-TEK II chambered cover glass W/Cover#1,5 borosilicate sterile for confocal microscopy

Invitrogen

Iscove's modified Dulbecco's Medium (IMDM)+GlutaMAX (L-Alanyl-L-Glutamine), Dulbecco's Modified Eagle's Medium (4500 mg/L glucose, 4mM L-glutamine and 110 mg/L sodium pyruvate), (DMEM), Trypsin-EDTA (0.05% Trypsin with EDTA 4Na) 1X, Foetal Bovine Serum Origin: EU Approved (South American) , PBS sterile, liquid, PBS tablets, Fungizone (Amphotericin B)

Sigma

DMEM, Penicillin-Streptomycin, Trypsin-EDTA, Poli-L-lysine, Dimethyl sulfoxide (DMSO) 1L

2. METHODS

2.1. DETERMINATION OF THE PROTEIN CONTENT OF THE SAMPLES

2.1.1. Bradford method

Protocol

1. Prepare the BSA dilutions for standard curve. Use at least 5 known concentrations e.g. 5mg/ml, 2,5 mg/ml, 1,25 mg/ml, 0,5 mg/ml, 0,25 mg/ml, 0, 125 mg/ml. BSA dilutions can be stored at -20ºC for weeks.

2. Prepare 1:5 water dilution of Bradford reagent for all samples and standard curve (at least 5 points), 1 ml per sample.

3. Load microcuvettes with 998μl of Bradford dilution and read the absorbance at 595 nm. This value will be used as a blanc, and each sample has its own.

4. Add 2μl of the sample or the known concentration of BSA to the cuvette and read the absorbance again.

Calculations

Known concentrations of BSA and its ΔAbs (see below) are used to built the standard curve where the values of sample ΔAbs will be interpolated. The curve equation serves to calculate the protein concentration in the sample.

$$\Delta Abs = Abs_{sample} - Abs_{blanc}$$

2.1.2. Lowry method

Protocol

1. Reconstitute "Lowry" reagent

   1 vial + 40 ml $H_2O_{bidestilled}$

"Lowry" reagent can be stored diluted for weeks

2. Prepare Folin: 18 ml Folin (SIGMA) + 90 ml $H_2O_{bidestilled}$
3. Prepare the standard curve (see "Bradford" method) and the samples in the test tube:
4. 20 μl sample/BSA + 980 μl $H_2O_{bidestilled}$ = 1 ml
5. Add Lowry reagent:
6. 1 ml Lowry + 1 ml sample/BSA = 2 ml (V_{final})
7. Prepare the blanc: 1 ml of $H_2O_{bidestilled}$
8. Incubate in the dark for 20 minutes.

9. Add 500 μl of Folin per sample and vortex briefly

10. Incubate in the dark for another 30 minutes.

11. Load the sample in the macrocuvette and read the absorbance at 660 nm.

Calculations

The protein concentrations of the sample are calculated in the same way as for Bradford method.

2.2. DETERMINATION OF THE GLUTATHIONE LEVEL

The level of reduced glutathione (GSH) was measured spectrophotometrically using the glutathione-S-transferase assay, while the determination of total and glutathione disulfide-oxidized glutathione (GSSG) was carried out by high-performance liquid chromatography.

Preparation of the acid extract of the cells

For both techniques, the procedure of obtaining the extracts is similar:

1. Aspirate the cell culture medium.
2. Wash the cells with the cold PBS (2ml for 25cm^2 flasc) and aspirate.

3. Add directly to the cells:

- PCA 6%, EDTA 0.2mM for reduced GSH
- PCA 6%, BPDS 1mM for total glutathione
- PCA 6%, BPDS 1mM, NEM 20mM

Not more than 40μl/100000 cells.

4. Collect the extract with the cell scraper in an eppendorf.
5. Centrifuge the extracts at 13000 g, for 15 minutes at 4ºC.
6. Collect the supernatant – acid extract and measure its volume.
7. Add to the pellet the same volume of 1N (NaOH) and incubate the sample in water bath at 50ºC to dissolve the proteins.

Acid extract obtained was used for subsequent determination of the reduced GSH/total glutathione/GSSG depending on the acid used for the extraction.

Protein content was determined by Bradford or by Lowry method.

Preparation of the acid extract of the nuclei

For the determination of the nuclear GSH and GSSG level, cell nuclei were isolated and acid extract prepared as

described for total cellular extract starting from the step 3. Nuclei were isolated by the following procedure:

1. Aspirate the cell culture medium

2. Wash the cells with the cold PBS

3. Add directly to the cells the following buffer (200µl of the buffer/1X10^{6}cells)

10 mM Hepes pH 7,9, 10 mM KCl, 1,5 mM $MgCl_2$, 1 mM DTT, Protease Inhibitor cocktail

4. Collect into an eppendorf with a cell scraper and incubate on ice for 10 min.

5. Add IGEPAL (NP-40) and vortex

6. Centrifuge for 30 sec., at 4ºC and 14000 rpm

7. Discard the supernatant and proceed adding the corresponding acid buffers as described previously for the intact cells starting from the step 3.

2.2.1. Glutathione-S-transferase essay for the determination of reduced GSH by spectrophotometry

Preparation of the acid extract

The preparation of the sample for the determination of the reduced glutathione is as described previously.

Protocol

1. Prepare CDNB in ethanol at 2 mg/ml and isolate from light.

2. Put in a micro cuvette:

3. 80 μl acid extract (supernatant) + 10 μl CDNB + 770 μl buffer (KPI 0.2 mM + EDTA 2 mM ph=7, at room temperature)

4. Measure the blanc of the samples at 340 nm.

5. Add 10 μl of the glutathione-s-transferase (starts the enzymatic reaction) on the plastic stick and than to the cuvette and remove gently.

6. Incubate until the reaction reaches its final point (for 45 min. aprox) and read the absorbance again.

Calculations

- Level of GSH by the cell number:

$$\frac{\left(Abs_{GSH}\,sample - Abs_{GSH}\,blanc\right)}{9.6} + \frac{V_{cubette}}{V_{samplevolume}} * V_{acidextractvolume} = \mu molesGSH$$

-Level of GSH by protein content

$$\frac{\left(Abs_{GSH}\,sample - Abs_{GSH}\,blanc\right)}{9.6} + \frac{V_{cubette}}{V_{samplevolume}} = \frac{\mu molesGSH}{ml}$$

2.2.2. Determination of the total glutathione level by H.P.L.C.

The total glutathione level in the cell was measured by the H.P.L.C., according to the method of Reed et al. [6]

Preparation of the acid extract

The preparation of the sample for the determination of the total glutathione is as described previously.

Samples could be stored at -20º C until derivatization.

Derivatization of the sample

1. To 200 µL of the acid supernatant is added 20 µL of the internal standard (γ-glutamil-glutamato 1 mM in PCA at 0.3%) and 20 µL of iodoacetic acid 1 M dissolved in m-cresol purple 0.2 mM (pH indicator)
2. The sample pH is adjusted to 8.5–9 using KOH 3 M CHES 0.3M buffer and incubated 10 minutes at room temperature in the dark.
3. 400 µL of 1% 1-fluor dinitrobenzene in absolute ethanol is added to a sample and is maintained in the dark at 4ºC for at least 24h. At this point, samples are stable at 4ºC for weeks.
4. The samples are centrifuged at 15000g for 15 minutes at 4º C and the dilution that is going to be injected in the HPLC is prepared: 50 µL of the supernatant and 270 µL of the mixture methanol – water (800:200).

Chromatography

For the analysis of the total glutathione content, 80 µL of the sample containing solution is injected in the HPLC. Mobile phase contains 2 solvents:

- Solvent A: is 80% methanol in bi-distilled water.
- Solvent B: is acetic/acetate buffer 0.5 M in 64% methanol.

The procedure is performed at the constant flow of 1 ml/minute. The substances of interest are eluted using a gradient:

- The mobile phase is maintained for 5 minutes at 20% of solvent B and 80% of solvent A.

- After this period the solvent B concentration starts to increase linearly, to reach 99% after 15 minutes.

- This concentration of each solvent is maintained from 5-10 minutes depending on the elution time of the last substance.

- Once the last substance of interest is eluted, the column has to be re equilibrated. The initial condition of solvents has to be reached (20% of B and 80 % of A) and maintained for 15 minutes.

Calculations

GSH and GSSG concentrations are calculated from a chromatogram, on the basis of the known concentration of internal standard which has been added to each sample in the process of derivatization. The internal standard used is γ-glutamil-glutamate, previously calibrated against the standards of known concentrations of GSH and GSSG determined in the enzymatic reaction. The GSH is calibrated by the method based on glutathione s-transferase (see above) and for GSSG the enzymatic reaction used involved glutathione reductase.

Total cellular glutathione is calculated as the sum of the GSH concentration and double GSSG concentration.

[GSH]= Glutation total -(2X GSSG)

2.3. DETERMINATION OF THE LEVEL OF THE OXIDASED GLUTATHIONE (GSSG)

For GSSG determination the protocol described by Asensi and col. [7] was performed. It is based on separation of dinitrobenzene derivatives by H.P.L.C. and their detection at 365 nm.

Preparation of the acid extract

The samples for the determination of GSSG were obtained as described previously. The samples could be stored at -20ºC until analysis.

Derivatization

1. To 200 µL of the acid supernatant is added 20 µL of the internal standard (γ-glutamil-glutamato 1 mM in PCA at 0.3%) and 20 µL of m-cresol purple 0.2 mM (pH indicator)

2. The sample pH is adjusted to 8.5–9 using KOH 3 M CHES 0.3M buffer.

3. The samples are centrifuged at 15000g for 15 minutes at 4º C.

4. 25 µL of the supernatant is mixed with 50µL of 1-fluor dinitrobenzene at 1% in absolute ethanol.

5. The sample is incubated for 45 minutes in dark and is desiccated in the speed-vac.

6. Dried samples can be stored for months at –20ºC until its analysis by HPLC.

7. Just before the injection samples are resuspended in 200 µl of solvent A.

Calculations

Calculation of the GSSG concentration in the sample is done in the function of the calibration of the solutions of the standards of known GSSG concentrations against the internal standard concentration.

2.4. TELOMERASE ACTIVITY DETECTION

Sample preparation

1. Aspirate the cell culture medium.
2. Wash the cells with the PBS (2ml for 25cm^2 flasc) and aspirate.
3. Detach the cells by trypsinization.
4. Collect the cells with cold PBS to a corning tube.

Maintain on ice

5. Centrifuge at 425 g for 6 minutes at 4ºC
6. Discard the supernatant and resuspend the cells in 1ml of cold PBS.
7. Count the cells and pass an aliquot containing at least 200000 cells to an eppendorf.
8. Centrifuge at 425 g for 6 minutes at 4ºC.

9. Eliminate the supernatant and store the pellet at –80ºC until use.

The telomerase activity in this work was determined by *T*elo*TAGGG* Telomerase PCR ELISA^{PLUS} kit – a photometric enzyme immunoassay for quantitative determination of telomerase activity, utilizing the Telomeric Repeat Amplification Protocol. The test is performed in three steps: elongation, PCR, and ELISA. In the first step, telomerase from the sample adds telomeric repeats (TTAGGG) to the 3' –end of the biotin-labeled synthetic primers. This elongation products, together with the internal standard (IS-provided by the kit manufacturer) included in the same reaction vessel, are amplified by the PCR reaction. The positive control (known concentration of telomerase elongation product with 8 telomeric repeats) is included in the kit. The samples are split in two aliquots and they are denatured and hybridized separately to digoxigenin -labeled-detection probes, specific for the telomeric repeats or the internal standard, and immobilized via the biotin label to a streptavidin-coated microplate. The quantification of the amplicons is performed by the detection with an anti-digoxigenin antibody conjugated to horsradish-peroxidase and the sensitive peroxidase substrate. The absorbance is read at 450nm and the relative telomerase activity is obtained using the following formula:

$$RTA = \frac{(A_{sample} - A_{heattreatedsample}) / A_{sampleIS}}{(A_{controltemplate} - A_{lysisbuffer}) / A_{conroltemplateIS}} X100$$

2.5. ANALYSIS OF THE PROTEIN EXPRESSION BY WESTERN BLOTTING

2.5.1. Immunoblot analysis of the cell cycle proteins

Preparation of total cellular protein lysate for western blotting

Lyses buffer is prepared on the day and contains:

1. TRIS/SDS/Glicerol (3,766ml)
- 83ml of TRIS (0,927g in 100ml of H2O, ph 6,8)
- 2g of SDS
- 10ml of GLICEROL

(This buffer is kept in the fridge until use.)

2. Na Ortovanadate 200mM (optional) (40µl)
3. Protease inhibitor cocktail (Sigma) (40µl)

Protocol

1. Cells are washed twice with ice cold PBS, and the remains of PBS aspirated
2. Lysis buffer is added directly to the cells and left on ice for 30 min.

Time of culture	MCF7 + MCF7 -	3T3	Primary neurons
6 h	60	90	100
24 h	70	130	
48 h	225	230	200
72 h	300	230	
96 h	350		250
5-7 days	450	230	

Table II 1. Volumes of lyses buffer (µl) used for protein extraction

3. Lysates were collected with cell scraper to eppendorfs and incubated at 90ºC for 10 min.
4. Samples were kept at -20ºC until use

Protein concentration was determined by Lowry or Bradford method as described previously.

SDS/PAGE electrophoresis

Samples were separated by SDS/PAGE electrophoresis in polyacrylamide gels with 0,1% of SDS acording to the standard protocol. Stacking gel contained 4% polyacrylamide in a Tris buffer pH 6,8, while resolving gel was prepared as 10-12,5% polycacrylamide in Tris buffer pH 8,8. The gels were sumerged in the Tris-Glycine buffer (25 mM Tris, 200 mM Glicina, 0,1% SDS, pH 8,3), and an

electric current of the constant voltage (100V) was applied across the gel for at least 2h.

After electrophoresis, the proteins were electroblotted to 0.2-μm-pore-size nitrocellulose membrane (Schelider & Schuel, USA) by wet blotting method during 2h at 4ºC in transfer buffer (25 mM Tris, 192 mM Glicina, Metanol 20% v/v, pH 8,3) using Mini-protean II system (Bio-Rad, USA).

The proteins were visualised by the following immunostaining protocol:

1. Blocking. The membranes were incubated in blocking solution [5% (w/v) non-fat dry milk with 0.05% (v/v) Tween 20], for 1 h at room temperature with orbital shaking.
2. Immunostaining. Following three washes of 5 minutes with TBST [25 mM Tris/HCl (pH 7.5)/0.15 M NaCl/0.1% (v/v) Tween 20], blots were incubated with embryonic antibodies (table III 2.) in TTBS containing 5% BSA overnight at 4ºC or 1h at room temperature. Thereafter, the blots were washed again with TBST and further incubated with the coresponding secondary antibody (table III 2.) conjugated to horseradish peroxidase (Santa Cruz) for 1h at room temperature.
3. Detection. Finally, blots were washed with TBST and detection was carried out using the chemiluminescent luminol reagent developed by using the LumiGLOl® reagent as specified by the manufacturer (Cell Signaling Technologies) and susequently detected by CCD camera.

Digital images created were stored as tif documents. Alternativelly, a sensitive sheet of photographic film was placed against the membrane, and exposure to the light from the reaction created an image of the antibodies bound to the blot. The films were scaned using PrestoPage manager para EPSON, and stored as digital TIF documents.

4. Quantification. The intensity of the bands was measured by densitometry using the GeneGenius system and the GeneTools analysis software (Syngene).

2.5.2. Immunoblot analysis of the level of glutationilation and oxidation of nuclear proteins.

Preparation of nuclear protein lysate for western blotting

3T3 cells were subjected to nuclear protein extraction, following the instructions of the Nuclear Extract Kit (Active Motif North America).

The efficiency of nuclear extraction was determined by measuring the relative activity of a cytosolic enzyme, lactate dehydrogenase, in nuclei and in whole cell. Nuclear lactate deshydrogenase activity was less than 1.2 % of the total cellular activity. Nuclear lysates obtained were used for determination of protein oxidation and protein glutathionation.

Determination of nuclear protein oxidation

To measure the level of nuclear protein oxidation nuclear lysates were derivatised, and the western blotting was performed according to the recommendation of the manufacturer. The level of nuclear protein oxidation was determined by the Oxy Blot protein Oxidation Detection Kit (Chemicon International) which detects carbonylated proteins.

The oxidative modification of the proteins by the action of free radicals and other reactive oxidative species, e.g. hydroxynonenal, occur both in pathological and physiological processes. As a consequence of these modifications, carbonyl groups are introduced in the chains of amino acids in a specific manner.

Carbonyl groups are derivatized to 2,4-dinitrophenilhydrazone (DNP-hydrazone) by its reaction with 2,4-dinitrophenilhidrazine (DNPH). The derivatized samples are separated by electrophoresis in a acrilamide gel followed by western blotting and immunodetection protocols as described previously.

Determination of nuclear protein glutathiolation

Nuclear lysates were obtained as described previously in the absence of reductive agents .

Western blotting. 40 µg of samples was loaded and electrophoresis procedure was performed as usual. Addition of any reducing agents was avoided. Membrane was blocked in 5% BSA in TBST for 1h at room temperature, and probed against the anti-glutathione antibody at the dilution 1:1000 over night at 4ºC, and secondary antibody at 1:10 000 for 1h at room temperature.

- Embryonic antibody: IgG2a monoclonal mouse antibody against glutathione-protein complexes, Virogen, product number: 101-A-250.
- Secondary antibody: goat anti-Mouse IgG, Calbiochem (401215) conjugated to horseradish peroxidase

Detection procedure was performed using Amersham RPN 2106 ECL Western Blotting Detection Reagent.

Table III. 2. Description of antibodies used in western blotting procedures

PRIMARY ANTIBODY	APPROXIMATE MOLECULAR WEIGHT (KD)	ANTIGEN	HOST/type	DILUTION USED	MANU-FACTURER	SECUNDARY ANTIBODY	DILUTION USED	MANU-FACTURER
Anti-ID2	15/17	ID2	Rabbit polydonal	1:1000/ 1:750	Santa cruz Sc-489	Anti-rabbit IgG antibody	1:2000 1:4000	Cell Signalling Technologies
Anti-p107	107	P107	Rabbit polydonal	1:1000	Santa cruz	Anti-rabbit IgG antibody	1:2000	Cell Signalling Technologies
Anti-Bcl-2	26/28	Bcl-2	Rabbit polydonal	1:1000	Santa cruz Sc-7382	Anti-rabbit IgG antibody	1:1000	Cell Signalling Technologies
Anti-GCS	73	GCS	Rabbit polydonal	1:750	Neomarkers	Anti-rabbit IgG antibody	1:2000	Cell Signalling Technologies
Anti-PCNA	36	PCNA	Mouse monoclonal	1:750	Santa cruz Sc-56	Anti-mouse IgG antibody	1:7500	Calbiochem
Anti-DNP		Carbonyl groups-protein oxidation	Rabbit polydonal	1:150	Chemicon international	Anti-rabbit IgG antibody	1:300	Chemicon international
Anti-GSH		Glutathione-protein complexes	Mouse monoclonal	1:1000	Virogen	Anti-mouse	1:7500	Calbiochem
Anti alpha-tubulin	55	Tubulin	Mouse monoclonal	1:1000	Santa cruz Sc-8035	Anti-mouse	1:7500	Calbiochem

2.6. FLOW CITOMETRY STUDIES

In this work flow citometry was used for cell cycle study, and apoptosis detection. Fluorochromes were excited with an argon laser tuned at 488 nm. Forward-angle and right-angle light scattering were measured. Samples were acquired for 11000-15000 individual cells.

2.6.1. Cell cycle

Cell cycle phases were determined using the fluorescent DNA dye propidium iodide (PI) (final concentration, 5µg/mL) at 630 nm fluorescence emission. The specific union between PI and DNA allows the quantification of the DNA content per cell, and thus the estimation of the proliferative activity of the cell population, apoptosis level and the portion of the dead cells (debris).

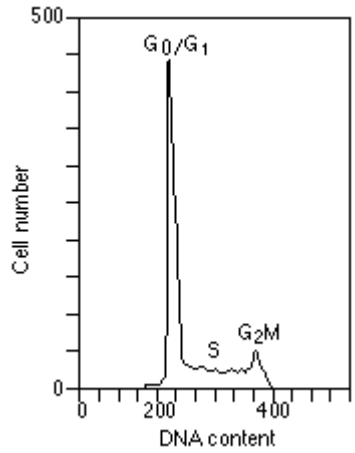

Figure XX. Typical DNA content histogram defining the phases of cell cycle

Sample preparation

1. Collect the cell culture medium to the test tube (on ice) and wash the cells twice with PBS, collecting it to the same test tube (any floating cells are collected this way)
2. Add trypsine to the cells (1ml for 25cm^2 flask) and incubate at 37ºC, 5% CO2 until the cells detach.

Maintain on ice:

3. Collect the detached cells with the ice cold PBS to the same test tube. Be sure to collect all the cells.
4. Centrifuge at 425g for 6 minutes at 4ºC.
5. Eliminate the supernatant and resuspend the pellet in 1ml of PBS.
6. Count the cells. Cell counts of each sample were obtained using a conventional Neu-bauer chamber and optical inverted microscope.
7. Put the aliquot with 1x106 cells in the tube for flow citometry.
8. Centrifuge again at 425g for 6 minutes at 4ºC.
9. Eliminate the supernatant.
10. Fix the cells in ice cold ethanol vortexing gently while adding 2ml of ethanol drop by drop to 1x10^6 cells.
11. Allow the sample to rest at –20ºC, at least over night before the staining and flow cytometry analysis.

Staining procedure

1. Warm the PBS to room temperature.

2. Centrifuge the samples in ethanol at 425g for 6 min at room temperature.

3. Eliminate ethanol carefully and resuspend each sample in 1ml of PBS.

4. Centrifuge the samples again at 425g for 6 min at room temperature.

5. While centrifuging prepare the staining solution for all the samples to be analysed, 1 ml/1X10^6 cells

- 50 μl propidium iodide ($[1\ mg/ml]_{stock}$),
- 25 μl RNAsa ($[1\ mg/ml]_{stock}$),
- 50 μl 10% IGEPAL (NP 40),
- 875 μl of pre-warmed PBS

6. Eliminate the supernatant and resuspend the pellet in 1 ml of staining solution per 1X10^6 cells

7. Incubate for 1h in the dark at room temperature, or 24h at 2-4ºC, before flow citometry analysis of the samples.

Flow citometry analysis of the DNA content in the monolayer cell cultures. Modified protocol used for embryonic neural culture.

Prepare hypotonic propidium solution:

Sodium citrate-5H2O: 100 mg

Triton X-100: 100 μl

Propidium iodide: 5 mg

H2O bi-distilled: 100 ml

Maintain in the fridge isolated from the light. Add RNAse on the day at the amount of 25 μl per ml of cell nuclei suspension.

Protocol

1. Collect the cell culture medium containing floating cells carefully to avoid detaching of the cells in monolayer and put it to the test tube.
2. Add 2 ml (for 30cm^2 Petri dish) of the hypotonic solution to the attached cells and maintain on ice.
3. Centrifuge the floating cells at 900 rpm, for 3 minutes at 25ºC
4. Eliminate the supernatant and resuspend the pellet in 500 μl of hypotonic solution. Add this cell suspension to the monolayer prepared for the incubation.
5. Incubate at 4ºC for 12-24h, making sure that the plates are maintained perfectly horizontal.
6. Resuspend with the Pasteur pipette the nuclei liberated by the hypotonic solution.
7. Filter through the nylon mash (diameter 35-60 μm).
8. Analyze by the flow citometry immediately

2.6.2. Detection of the apoptosis by flow citometry

In this work the percentage of apoptotic cells in cell population was detected by two different approaches:

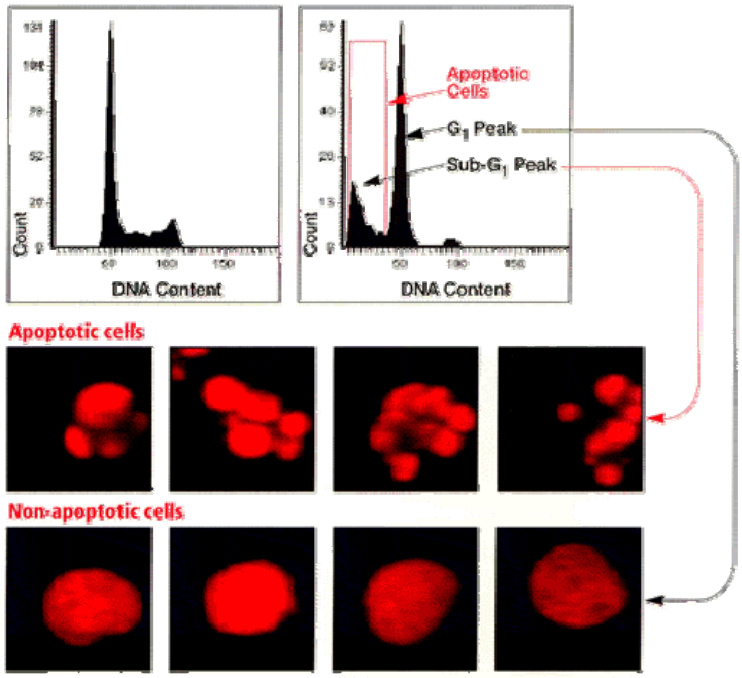

Figure III 1. Schematics of apoptosis detection by DNA content. Adapted from www.compucyte.com.

- presence of fragmented DNA defined by the subG1 fraction in DNA content histogram obtained by the propidium iodide staining (Fig. III 1.)

- double staining with annexin V, Alexa Fluor ® 488 conjugate (Molecular probes) that has a high affinity for phosphatidyl-serine exposed on the surface of apoptotic cells

and PI. The cells are considered apoptotic if they were annexin V positive and PI negative. (Fig. III 2.)

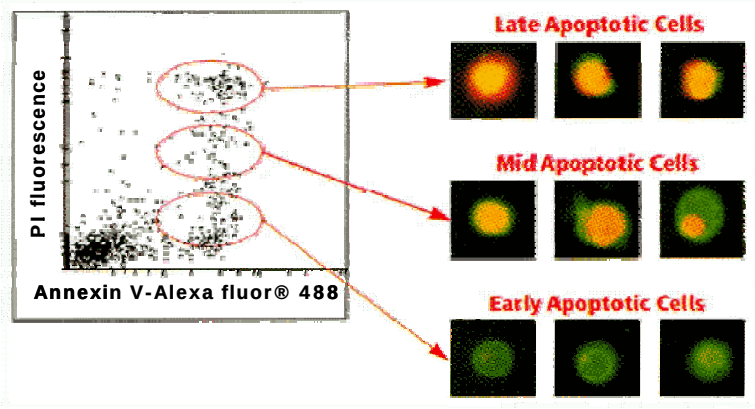

Figure III 2. Schematics of apoptosis measurement by Annexin V/PI staining. Adapted from www.compucyte.com

Protocol

1. The cell culture medium and PBS used to wash the cells were pulled together to a test tube to collect the floating cells. Following trypsinization, cells were centrifuged as described before, resuspended in annexin-binding buffer (AB, 10mM HEPES, 140mM NaCl, and 2,5mM $CaCl_2$, pH 7,4) and counted.

2. The suspension containing 100000 cells in 100 µl of AB was loaded with 4 µl of annexin V and incubated for 10min at room temperature in the dark

3. 10 µl of PI (1mg/ml) was added to cells and incubated for another 5 minutes under the same conditions. Finalized the

incubation period, 400 µl of AB per sample was added and immediately analyzed.

4. Flow citometry was used to analyze 11000 cells/per sample, and it was possible to discriminate between 4 groups of cells (table III.3.)

CELL STATUS	FLUOROCROME INTENSITY	
	ANNEXIN V	PI
ALIVE	LOW	LOW
NECROTIC/ DEBRIS	LOW	HIGH
EARLY APOPTOSIS	HIGH	LOW
LATE APOPTOSIS	HIGH	HIGH

Table III.3. Apoptosis detection by double staining with annexin v and PI

2.7. CONFOCAL MICROSCOPY

The principle of confocal imaging invented by Marvin Minsky, and patented in 1957, is employed in all modern confocal microscopes. This technique enables visualization deep within both living and fixed cells and tissues.

In a conventional fluorescence microscope, the entire specimen is exposed to light from a light source. This way, all parts of the specimen throughout the optical path will be excited and the fluorescence from whole sample will be detected by a photodetector or a camera. In confocal microscopy, the illumination is achieved by scanning one or

more focused beams of light, usually from a laser, across the specimen. The basic key to the confocal approach is the use of spatial filtering techniques to eliminate out-of-focus light or glare in specimens whose thickness exceeds the immediate plane of focus. Confocal microscopy offers the ability to control depth of field, elimination or reduction of background information away from the focal plane (that leads to image degradation), and the capability to collect serial of high-resolution images, termed optical sections. These images are produced in sequence through relatively thick sections or whole-mount specimens. Based on the optical section as the basic image unit, data can be collected from fixed and stained specimens in single, double, triple, or multiple-wavelength illumination modes, and the images collected with the various illumination and labeling strategies will be in register with each other. The design of temperature controlled chambers with the CO_2 suplementation and humidity control makes possible live cell imaging and long time-lapse sequences. Digital image processing methods applied to sequences of images allow obtaining of z-series (used in this work), and subsequent reconstruction of three-dimensional representation of specimens, as well as the time-sequence presentation of 3D data as four-dimensional imaging.

2.7.1. Visualisation of the GSH compartmentalization by confocal microscopy

3T3 fibroblasts and MCF7 cells were maintained in culture as described previously and plated in $2cm^2$ LAB-TEK II chambered cover glass (Nunc) for 5 days, 72h, 48h, 24h, 12h and 6h before the experiment, so cells in all phases of the cell cycle were dyed and analysed on the same day. Triple staining was performed: 2µg/ml propidium iodide (PI) (Sigma) to identify dead cells, 2µg/ml Hoechst (Sigma) to localize nuclei and 5µM CellTracker green 5-chloromethylfluorescein diacetate (CMFDA) (Molecular probes), to detect GSH (specificity 95%). When indicated, mitochondria were stained with MitoTracker Red 580. Cells were first stained with 5µM CMFDA in cell culture medium for 30 min., at 37ºC and 5% CO2. After washing with pre-warmed cell culture medium, cells were left to rest for 30 min at 37ºC and 5% CO_2, in cell culture medium or, alternatively, were loaded with 250 nM MitoTracker Red 580 (Molecular Probes). In the last 5 min of incubation 2 µg/ml Hoechst and 2 µg/ml PI were added. After incubation with the fluorochromes, staining solution was replaced with fresh pre-warmed cell culture medium and cells were analysed.

The excitation wavelengths for fluorochromes were 488 nm for CMFDA, 543 nm for IP, 364 nm for Hoechst and 543 nm for MitoTracker Red 580. The emission aperture for fluorescence detection were 510-540 nm for CMFDA, 585-

715 nm for PI, 380-485 for Hoechst and 575-650 nm for MitoTracker Red.

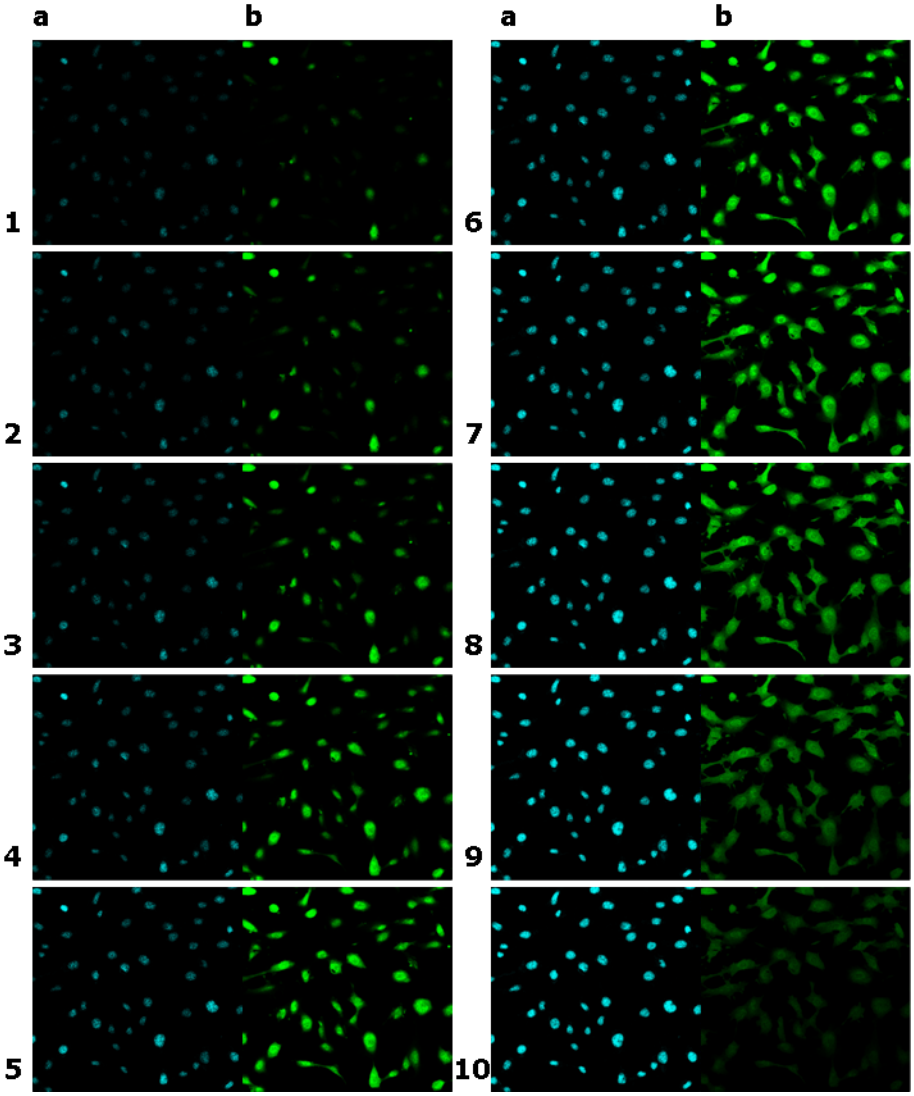

Figure III 3. **An example of microscopic confocal analysis of the intracellular distribution of GSH**. Triple staining was performed on living 3T3 fibroblasts: Hoechst 33342 to localize nuclei (blue fluorescence, a), CMFDA to mark GSH, (green fluorescence, b) and PI to exclude dead cells (results not shown). Cells were maintained in the chamber provided with 5% CO2 at 37 °C. A representative Z axes series is shown. Each panel represents one step in the Z-section series obtained beginning from the nuclear apex (1) and progressing downward in 1 ± 0.2-µm increments.

Z-section series obtained beginning from nuclear apex and progressing down in 1±0.2µm increments (at least 10 planes) were converted to maximum projection images to avoid subjectivity in the choice of plane to be analyzed (Fig. III 3.).

The distributions of green CMFDA fluorescence (GSH levels) and blue Hoechst fluorescence (nuclei localisation) were analysed by profile and by area as follows.

Fluorescence profile analysis. A cross section line of 200±20µm was drawn through a cell field to compare the intensity and distribution of Hoechst (DNA) and CMFDA (GSH) fluorescence (Fig. III 4.).

Fluorescence area analysis. Perimeters were drawn around the nucleus (according to the area marked with Hoechst) and around the entire cell excluding nucleus area (according to transmission image obtained by light microscopy) (Fig. III 5.).

Nucleus/cytoplasm ratio for GSH in every cell analysed was established by dividing the mean of green CMFDA fluorescence of nuclear area by the mean of CMFDA fluorescence in cytoplasmic area. We calculated the nucleus/cytoplasm ratio (n/c) using CMFDA fluorescence in 3 separate experiments (100 cells per condition).

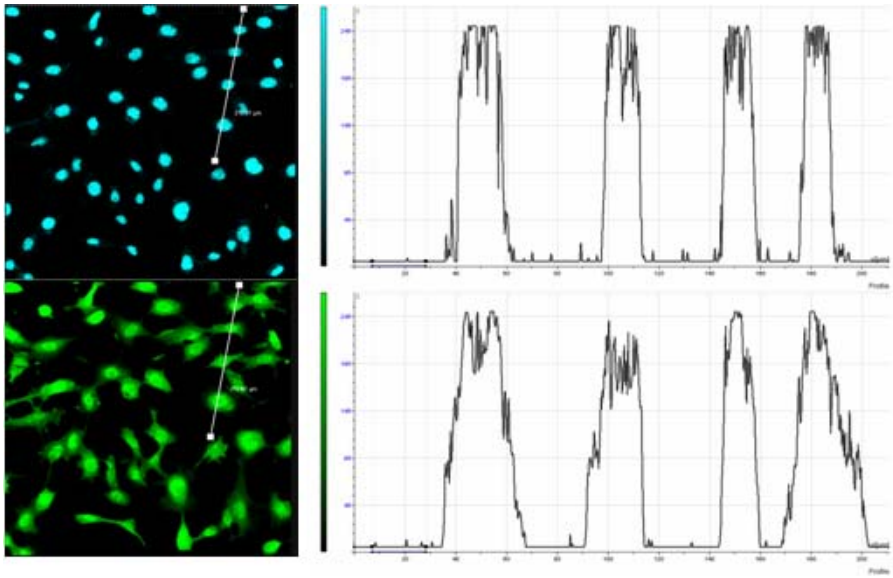

Figure III 4. Fluorescence profile analysis. An example of the analysis of the fluorescence distribution by obtaining the profile of its intensity along the cross section line.

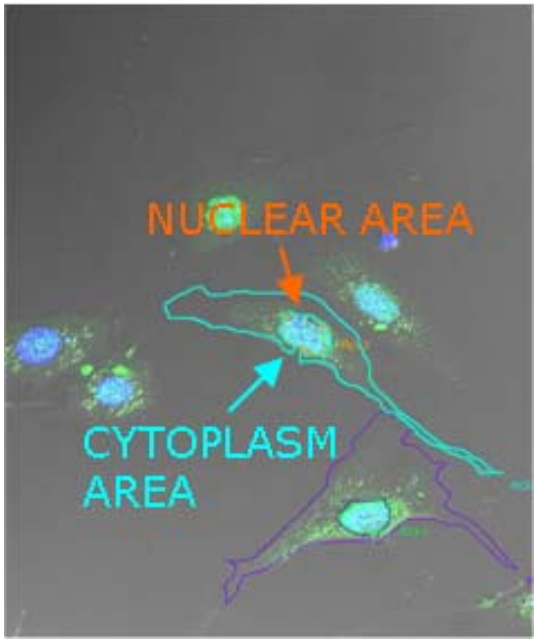

Figure III 5. Fluorescence area analysis. The perimeters were drown to define the nuclei stained blue by Hoechst 33342 (green and orange lines) and cytoplasmic area according to the transmission image (blue and turquoise lines)

2.8. ATP depletion by mitochondrial uncoupling agent. The determination of the ATP level.

3T3 fibroblasts were plated as usual and incubated for 30 min-2h with freshly prepared 20μM FCCP (p-trifluoromethoxy carbonyl cyanide phenyl hydrazone, Sigma), loaded with CMFDA, PI and Hoechst and analyzed by confocal microscopy as described before.

The determination of the ATP level

1. Wash the cells with cold PBS

2. Add 2% PCA and collect with a cell scraper to an eppendorf.

3. Centrifuge 10 min at 15000 rpm

3. Collect the supernatant measuring the volume of the acid sample (Va). Use the pellet for the protein concentration determination, as described for glutathione determination.

4. Neutralize with the KOH using ≈ 20μl of the indicator. Measure the volume of the neutralized sample (Vn).

5. Prepare control and the sample for the ATP determination:

Control: 1ml Coctail+1ml H_2O

Sample: 1ml cocktail+ 0,9ml H_2O+0,1ml sample

Coctail: TRIS 0,1M pH 8 (10ml), $MgCl_2$ 0,1M (1ml), NADP 1% (1ml), glucose 0,01M (1ml), G_6PDH (0,1ml)

6. Measure the absorbance at 340 nm

7. Add 10 µl of the hexokinase prepared in $SO_4(NH_4)_2$ (450 µl of $SO_4(NH_4)_2$ and 50 µl of hexokinase).

8. Measure the absorbance at 340nm at the final point of the reaction

9. Calculate the ATP level in µmols/ml using the formula:

$$\frac{\Delta OD * 2,01}{6,22} * \frac{1}{0,1} * \frac{Vn}{Va} = ATPlevel$$

2.9. GSH depletion by diethyl maleate (DEM) and butionine sulfoximine (BSO)

Cells were plated as usual and after attaching to the plate (3-6h) the GSH was depleted. Our model of differential GSH depletion included 3T3 fibroblasts treated with:

- 100 mM diethylmaleate (DEM) that depletes all cellular thiols in entire cell, including nuclear GSH

- 100mM DEM and 1mM GSH ester that enters the cell and protects it efficiently from GSH depletion induced by DEM
- 10mM BSO that prevents the GSH synthesis in 24h affecting mostly cytosolic GSH

GSH distribution was studied by fluorescence determination of its CMFDA conjugate using confocal microscopy and cell cycle by flow cytometry.

2.10. Statistical analysis of the results

The results presented in this thesis are expresed as a mean value ± standard deviation, with the number of experiments (n) indicated. If the normality of the data was confirmed, by Shapiro-Wilk test, for the comparison of two groups of the data student t test was used, while when comparing 3 and more groups ANOVA was applied. When statistical differences were observed, the Tuckey contrast was used. When the data did not follow the normal distribution, the mean values were compared with a non parametric test Kruskal-Wallis. The absence of the difference between mean values was considered the null hypothesis, and it was rejected when $\alpha \leq 0{,}05$. When the statistical significance was confirmed, Mann-Witney test U was performed, and values of $p<0{,}05$ were accepted as significant.

3. Bibliography

1. Borras, C., et al., *Glutathione regulates telomerase activity in 3T3 fibroblasts.* J Biol Chem, 2004. **279**(33): p. 34332-5.
2. Hoetelmans, R.W., et al., *The role of various Bcl-2 domains in the anti-proliferative effect and modulation of cellular glutathione levels: a prominent role for the BH4 domain.* Cell Prolif, 2003. **36**(1): p. 35-44.
3. Vahrmeijer, A.L., et al., *Development of resistance to glutathione depletion-induced cell death in CC531 colon carcinoma cells: association with increased expression of Bcl-2.* Biochem Pharmacol, 2000. **59**(12): p. 1557-62.
4. Voehringer, D.W., et al., *Bcl-2 expression causes redistribution of glutathione to the nucleus.* Proc Natl Acad Sci U S A, 1998. **95**(6): p. 2956-60.
5. Valles, S.L., et al., *Oestradiol or genistein rescues neurons from amyloid beta-induced cell death by inhibiting activation of p38.* Aging Cell, 2008. **7**(1): p. 112-8.
6. Reed, D.J., et al., *High-performance liquid chromatography analysis of nanomole levels of glutathione, glutathione disulfide, and related thiols and disulfides.* Anal Biochem, 1980. **106**(1): p. 55-62.
7. Asensi, M., et al., *A high-performance liquid chromatography method for measurement of oxidized glutathione in biological samples.* Anal Biochem, 1994. **217**(2): p. 323-8.

IV RESULTS

IV RESULTS

I THE RELATIONSHIP BETWEEN GLUTATHIONE LEVELS AND TELOMERASE ACTIVITY, AND ITS CONSEQUENCES ON CELL PROLIFERATION, A UNIVERSAL PHENOMENON.

II NUCLEAR DISTRIBUTION OF GLUTATHIONE AND CELL CYCLE

III THE DEPLETION OF NUCLEAR GLUTATHIONE AND THE CELL CYCLE

IV SEARCHING FOR THE MECHANISM TO EXPLAIN THE NUCLEAR COMPARTMENTALIZATION OF GLUTATHIONE

I THE RELATIONSHIP BETWEEN GLUTATHIONE LEVELS AND TELOMERASE ACTIVITY, AND ITS CONSEQUENCES ON CELL PROLIFERATION, A UNIVERSAL PHENOMENON.

1. The peak of GSH precedes the exponential phase of cell growth.
2. GSH as a driving force of cell cycle progression.
3. The peak of GSH coincides with the peak of telomerase activity in three proliferation models
4. Three different models of cell growth

II NUCLEAR DISTRIBUTION OF GLUTATHIONE AND CELL CYCLE

1. The election of the methodology
2. The cellular distribution of GSH along the cell cycle in three models of proliferation
3. The comprehensive analysis of the nuclear compartmentalization of GSH in 3T3 fibroblasts

III THE DEPLETION OF NUCLEAR GLUTATHIONE AND THE CELL CYCLE

1. Design and characterization of the model of nuclear GSH depletion
2. Depletion of nuclear GSH impairs cell growth

3. Alterations of the cell cycle were induced by depletion of the nuclear but not the cytoplasmic GSH

IV SEARCHING FOR THE MECHANISM TO EXPLAIN THE NUCLEAR COMPARTIMENTALIZATION OF GLUTATHIONE

1. The implication of the active transport or nuclear GSH synthesis *de novo* were not confirmed in our model
2. Bcl-2 as a potential mediator of the nuclear GSH compartmentalization
3. The importance of Bcl-2 in nuclear compartmentalization of GSH and its consequences on the proliferation activity. Study in MCF7 cells that over express Bcl-2.

I THE RELATIONSHIP BETWEEN GSH LEVELS AND TELOMERASE ACTIVITY, AND ITS CONSEQUENCES ON CELL PROLIFERATION, A UNIVERSAL PHENOMENON.

1. The peak of GSH precedes the exponential phase of cell growth.

1.1 The study of the GSH level during the cell growth in 3T3 fibroblasts.

1.2 The study of the GSH level during the cell growth in MCF7 cells.

1.3 The study of the GSH level during the cell growth in embryonic neural culture.

2. GSH as a driving force of cell cycle progression.

2.1 Flow cytometry study of DNA content in 3T3 fibroblasts
2.2 Flow cytometry study of DNA content in MCF7 cells
2.3 Flow cytometry study of DNA content in embryonic neural culture
2.4 The expression of proliferation related proteins, Id2 and PCNA, as indicators of the exponential phase of cell growth in 3T3 fibroblasts

2.5 The expression of proliferation related proteins, Id2 and PCNA, as indicators of the exponential phase of cell growth in MCF7 cells

2.6 The expression of proliferation related proteins, Id2 and PCNA, as indicators of the exponential phase of cell growth in embryonic neural culture

3. The peak of GSH coincides with the peak of telomerase activity in three proliferation models

3.1 The relationship between GSH level and telomerase activity during the growth of 3T3 fibroblasts.

3.2 The relationship between GSH level and telomerase activity during the growth of MCF7 cells.

3.3 The relationship between GSH level and telomerase activity during the growth of embryonic neural culture.

4. Three different models of cell growth

4.1 The rhythm of cell growth is diverse in 3T3 fibroblasts, cancer cells and embryonic neural culture.

4.2 The intensity of cell growth corresponds to the level of GSH

4.3 The profiles of telomerase activity along the cell cycle match the variation in GSH level

4.4 The GSH level correlates with the level of DNA synthesis in the three models of cell proliferation, but not with the percentage of cells in G2/M phase

4.5 The end time point and the cell death is different in the three cell lines.

I THE RELATIONSHIP BETWEEN GSH LEVELS AND TELOMERASE ACTIVITY, AND ITS CONSEQUENCES ON CELL PROLIFERATION, A UNIVERSAL PHENOMENON.

Previous research published by our group (1) for the first time associated the total cellular GSH level with the telomerase activity, offering the possible explanation of the effect of the former on the cell cycle progression. That study was entirely performed on 3T3 fibroblasts.

The first objective of the present thesis was to investigate and evaluate the mentioned phenomenon in two cellular models of different proliferative activity:

1. MCF7 cells, highly proliferating human mammary adenocarcinoma

2. Embryonic neural culture (ENC) characterised by two phases:

- non differentiated and proliferating until 4^{th} day of culture
- differentiated and very low proliferating, present from the 5^{th} day.

1. The peak of GSH precedes the exponential phase of cell growth.

1.1 The study of the GSH level during the cell growth in 3T3 fibroblasts.

The GSH level was high at the beginning of culture and reached its maximal value at 24h (81,52±19 nmols/mg prot.) when the exponential phase of the growth curve begun (Fig. 1).

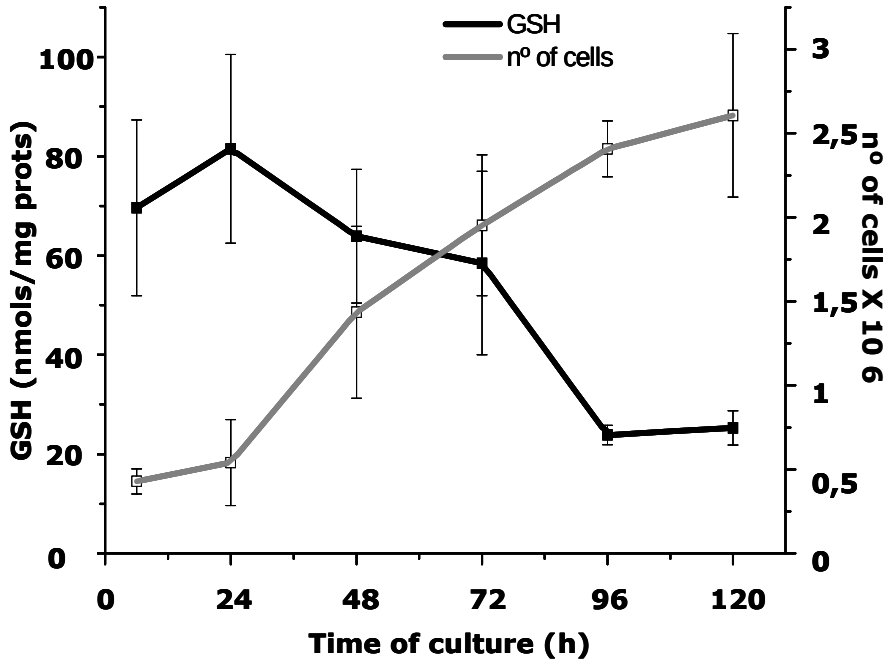

Figure 1. **GSH level and cell growth in 3T3 fibroblasts during cell culture.** The left Y axis shows the level of GSH along the cell culture and the right Y axis displays the cell number. The cells were plated as usual and counted at represented time points. The total cellular concentration of GSH was determined spectrophotometrically as described in "Materials and Methods". Data are represented as the mean ± SD of 6-10 different experiments.

1.2 The study of the GSH level during the cell growth in MCF7 cells.

In MCF7 cells (Fig. 2), our observations were similar: in the first 48h of culture the values of GSH were very high, with the extreme value at 18h, and then decreased progressively. The cell culture grew slowly but steadily, and at 24h we could already observe an important increase in cell number ($p \leq 0,05$ vs. 18h). However, the striking growth in this culture was observed after 48h. The cancer cells show no contact inhibition, and they continued to grow, still duplicating the population between 4^{th} to 7^{th} day of culture (2,033±0,133 and 4,336±0,127 X 10^6 cells, respectively).

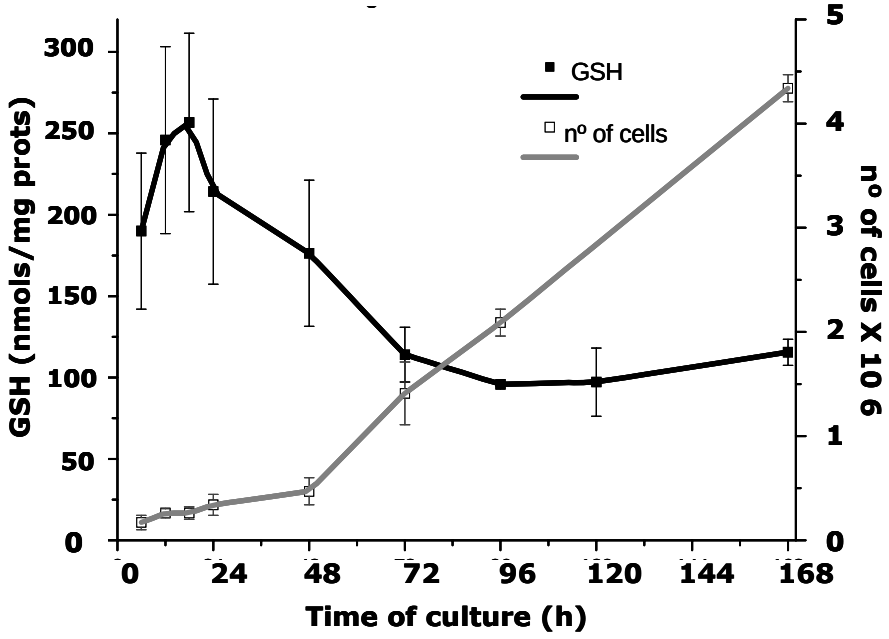

Figure 2. **GSH level and cell growth in MCF7 cells during cell culture.** The left Y axis shows the level of GSH along the cell culture and the right Y axis displays the cell number. The cells were plated as usual and counted at represented time points. The total cellular concentration of GSH was determined spectrophotometrically as described in "Materials and Methods". Data are represented as the mean ± SD of 6-10 different experiments.

The levels of GSH are lower than at the beginning of the culture, but still above the maximal value observed in 3T3 fibroblasts (95,77±0,96 nmols/mg prot.).

1.3 The study of the GSH level during the cell growth in embryonic neural culture.

Embryonic neural culture (ENC) (Fig. 3) is studied as a two phase model in coherence with the development of the rat neural system.

When isolated from the brains of rat foetuses at 14th day of gestation, this culture contained highly proliferating undifferentiated cells. The cell number increased rapidly and, as in 3T3 fibroblasts and MCF7 cells, the growth was preceded by an important increase in GSH level ($p \leq 0,01$ 24h vs. 6h), which maintained high plateau values until 72h (no significant difference at this time points).

An important change of the culture was at 96h, when the cytosine arabinoside was added to inhibit further glial growth (indicated with an arrow in the graph). Proliferating cells were eliminated from the plate and remaining culture contained mostly differentiated neurons. The remarkable fall of the cell number at 5 days of culture reflected the dying off of the glial cells. The cell number is maintained until the 7th day and then started to decline slowly towards the end of the culture. Although the level of GSH was maintained almost unchanged for several days (no significant difference

starting from 72h), the decrease in GSH observed in this phase of culture was significant comparing to the maximum reached in the proliferating phase ($p \leq 0,05$ 48h vs. 7 days of culture).

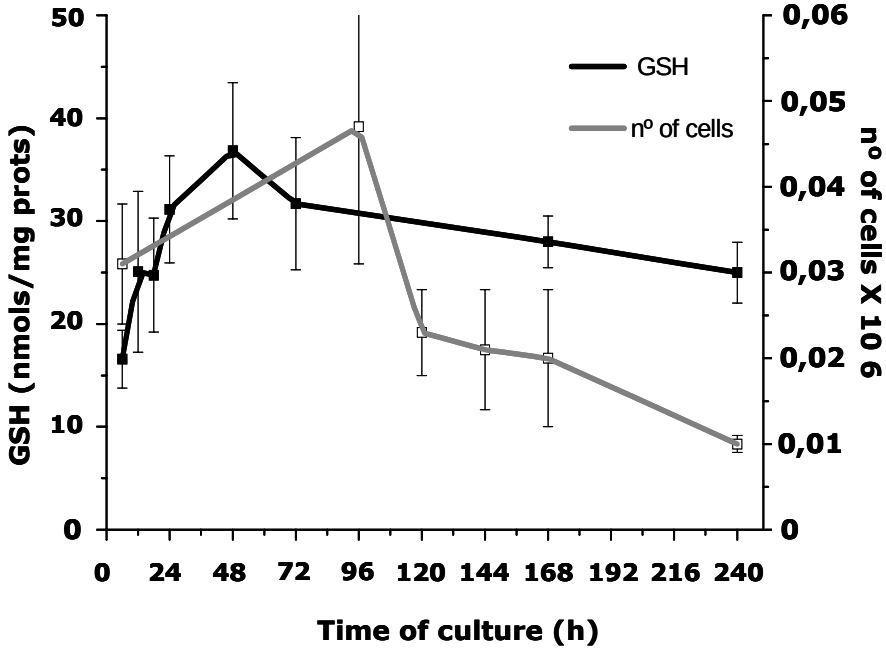

Figure 3. **GSH level and cell growth in embrionary neuronal culture (ENC).** The left Y axis shows the level of GSH along the cell culture and the right Y axis displays the cell number. The cells were plated as usual and counted at represented time points. The total cellular concentration of GSH was determined spectrophotometrically as described in "Materials and Methods". Data are represented as the mean ± SD of 3-5 different experiments.

2. GSH as a driving force of cell cycle progression.

2.1 Flow cytometry study of DNA content in 3T3 fibroblasts

The cell cycle study in 3T3 fibroblasts (Fig. 4A) proved that at 24h after plating, when GSH was at maximal level, the percentage of cells at the S+G2/M phase increased significantly ($p \leq 0,05$ VS. 6h) and remained elevated until 72h. Afterwards, the GSH level decreased progressively, until 5 days after plating ($p \leq 0,0001$ vs. 24, 48 and 72h). Consequently, at 72 h or later, cell growth slowed, and 5 days after plating most of the cells were in the G_0/G_1 phase (results not shown) and the culture was 100% confluent. Thorough analysis of the cell cycle data, shows that cell division (G2/M) (Fig. 4B) peaked at 24h and started to decrease slowly ($p \leq 0,001$ vs. 72h). However, the percentage of cells in the phase of DNA synthesis (S), after the striking boost at 24h ($p \leq 0,0001$ vs. 6h) continued to increase until 48h ($p \leq 0,05$ vs. 24h) and then quickly fell by half (Fig. 4C).

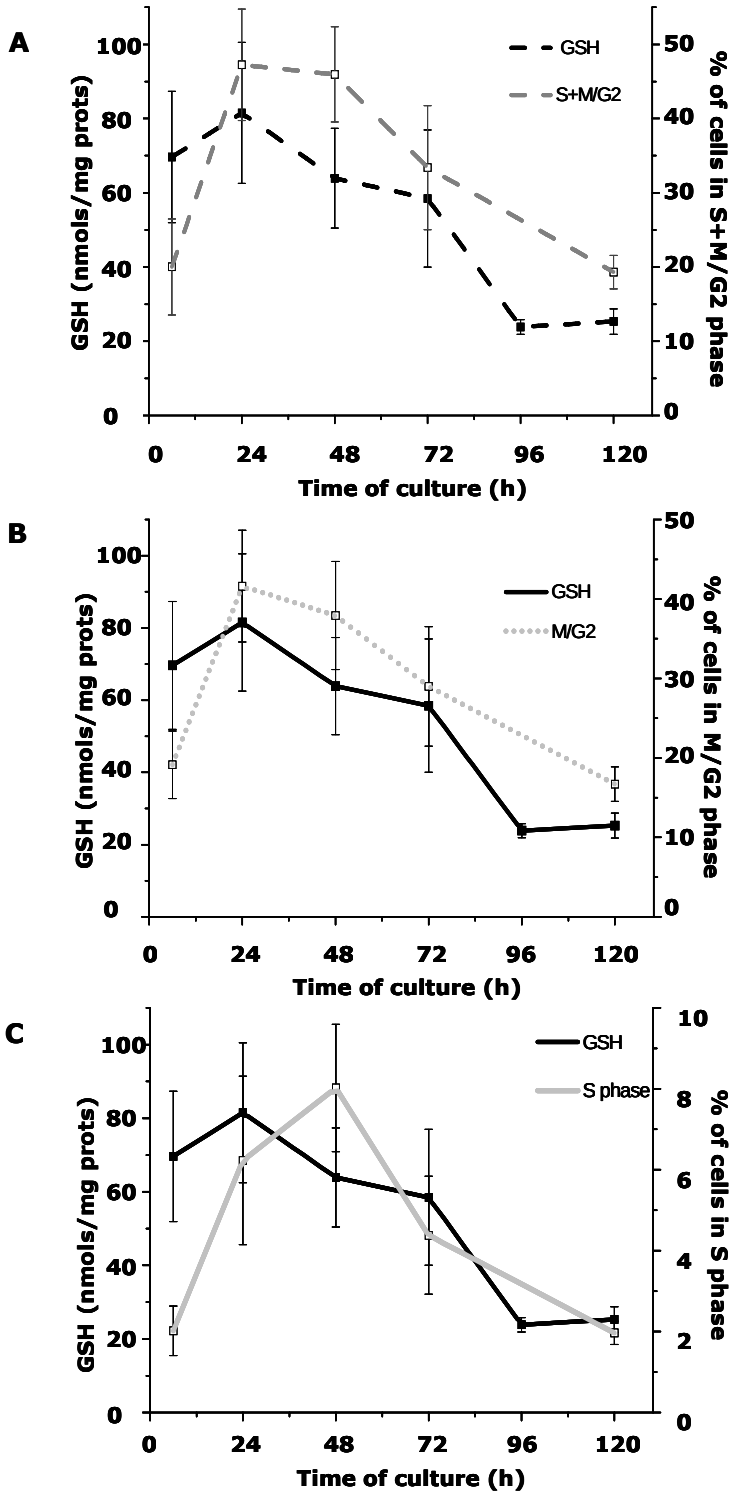

Figure 4. GSH level and cell proliferation in 3T3 fibroblasts during cell culture. The percentage of cells in the phase of DNA synthesis (S)

(figure A), in mitosis and G2 phase of the cell cycle (M/G2) (figure B), and the percentage of cells actively proliferating (S+M/G2) (Figure C) is shown on the right y axis. The level of GSH along the cell culture is represent at left y axis. Data are expressed as the mean ± SD of 6-10 different experiments.

2.2 Flow cytometry study of DNA content in MCF7 cells

In our cancer cell model, MCF7 cells, as well as in 3T3 fibroblasts, high levels of GSH preceded the maximum of cell proliferation.

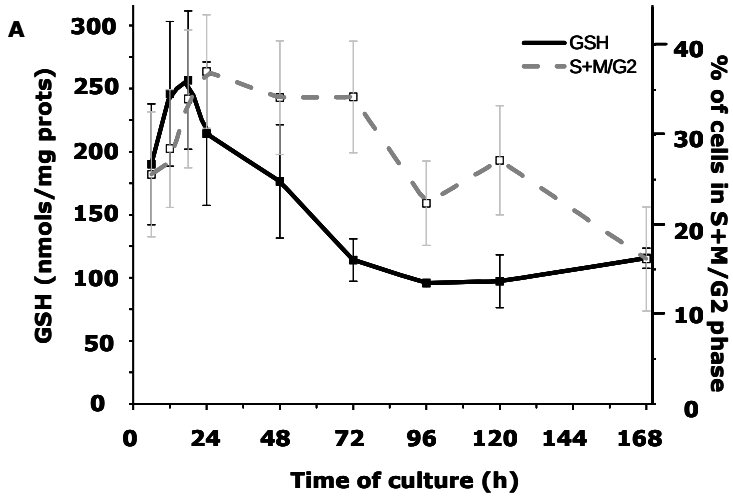

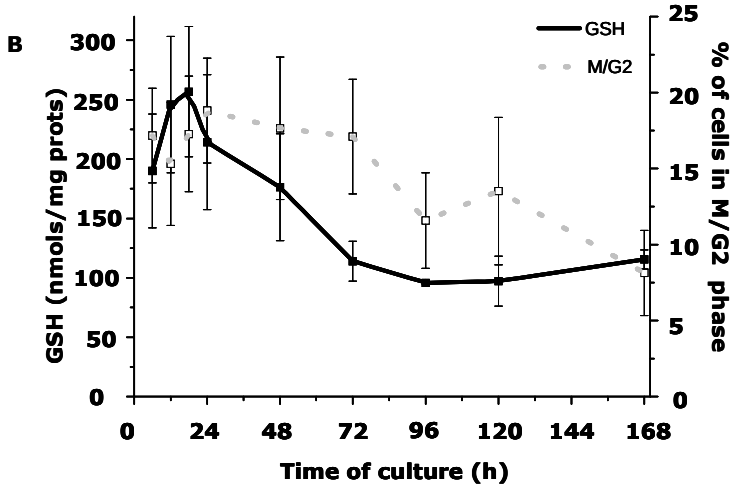

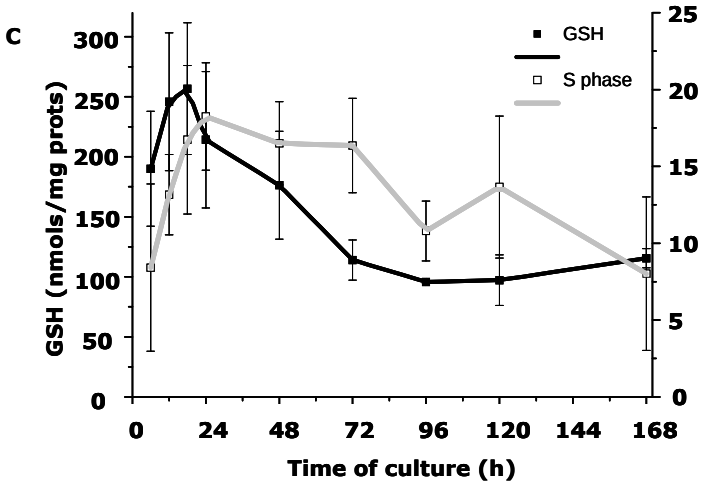

Figure 5. GSH level and cell proliferation in MCF7 cells during cell culture. The percentage of cells in the phase of DNA synthesis (S) (figure A), in mitosis and G2 phase of the cell cycle (M/G2) (figure B), and the percentage of cells actively proliferating (S+M/G2) (Figure C) is shown on the right y axis. The level of GSH along the cell culture is represent at left y axis. Data are expressed as the mean ± SD of 6-10 different experiments.

The exponential phase of cell growth, defined by the high percentage of cells in S (Fig. 5C) and G2/M (Fig. 5B) phase of cell cycle, was extended in MCF7 cells to several days. The peak is reached at 24h of culture and the level is preserved without significant fluctuations until the 4th day of culture, when the decline of proliferation coincided with the decrease in GSH level.

2.3 Flow cytometry study of DNA content in embryonic neural culture

As expected, during the first 4 days of neural culture, when the GSH level is increased, the percentage of cells in S and G2/M phase was also high.

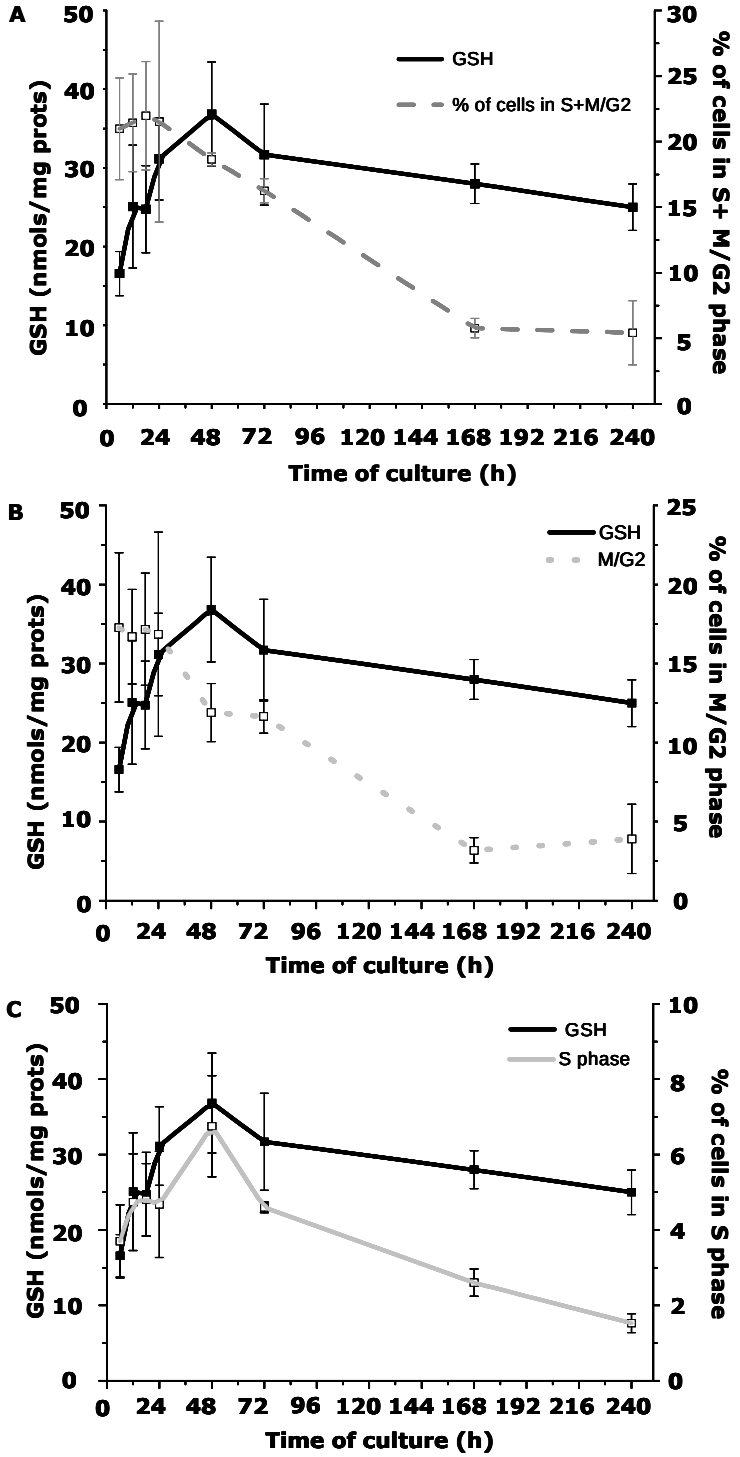

Figure 6. **GSH level and cell proliferation in embrionary neuronal culture.** The percentage of cells in the phase of DNA synthesis (S)

(figure A), in mitosis and G2 phase of the cell cycle (M/G2) (figure B), and the percentage of cells actively proliferating (S+M/G2) (Figure C) is shown on the right Y axis. The level of GSH along the cell culture is represent at left Y axis. Data are expressed as the mean ± SD of 3-5 different experiments.

Interestingly, the peak of GSH was posterior to the time point with the maximal number of dividing cells (Fig. 6B), but it overlapped with the highest percentage of the cells in S phase (Fig. 6C). In the second stage of the culture, at 7 and 10 days, although the GSH level shows no remarkable fall, the proliferation was almost absent; less than 5 % of the cells were dividing and less than 3% were in S phase.

2.4 The expression of proliferation related proteins, Id2 and PCNA, as indicators of the exponential phase of cell growth in 3T3 fibroblasts

To ensure that most cells at 24 and 48 h in culture were in the S/M+G_2 phase of the cell cycle, we studied Id2 and PCNA expression patterns during cell growth (Fig. 7A-F). These proteins are over expressed when cell division is active. Indeed, consistent with the evidence derived from flow cytometry, the expression of these proteins was high at 24 and 48h of culture in 3T3 fibroblasts (7A,B) and subsequently decreased towards the end of culture.

2.5 The expression of proliferation related proteins, Id2 and PCNA, as indicators of the exponential phase of cell growth in MCF7 cells

In MCF7 cells, the increase in Id2 was initiated as early as at 12h, and remained high throughout the culture (Fig. 7C), while the important increase in PCNA was observed at 48-72h (Fig. 7D).

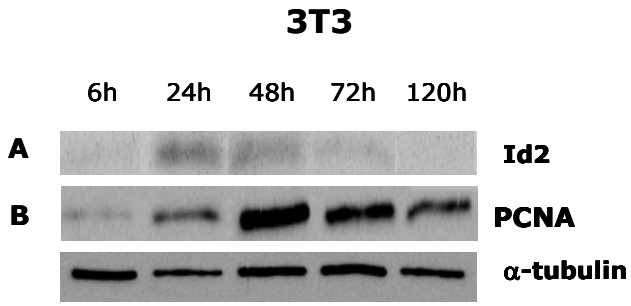

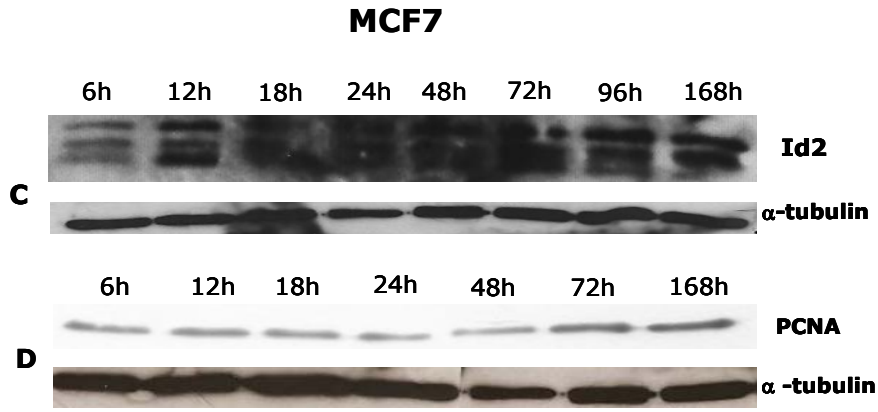

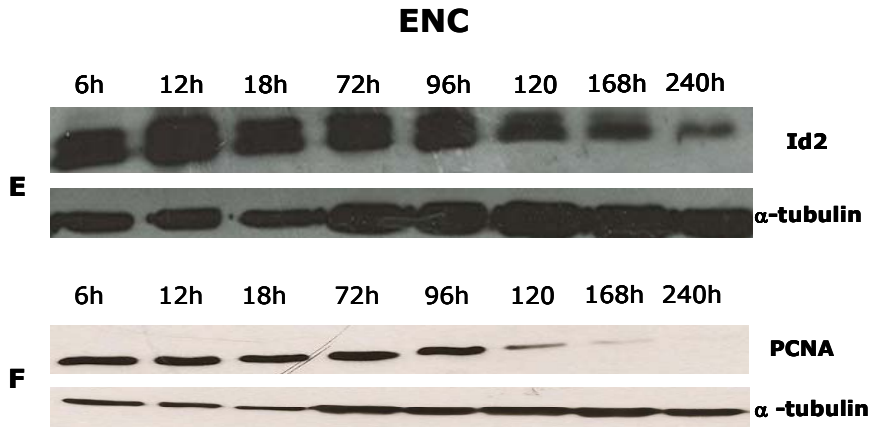

Figure 7. **Changes of Id2 and PCNA protein expression during cell culture.** Upper panels, Western blot analysis of Id2 in 3T3 fibroblasts, MCF7 cells and embrionary neuronal culture (ENC). Lower panels, Western blot analysis of PCNA expression along the cell cycle of mentioned cell lines. Representative results from at least 3 experiments are shown.

2.6 The expression of proliferation related proteins, Id2 and PCNA, as indicators of the exponential phase of cell growth in embryonic neural culture

The proliferating phase of neural culture, as expected, was characterized by high expression of both proteins. The deficiency of proliferation in the second phase of cell culture was confirmed by the considerable decrease in the expression of Id2 and PCNA at 5 and 7 days of culture, respectively, while at 10 days the level of both proteins was beyond detection (Fig. 7E, F).

3. The peak of GSH coincides with the peak of telomerase activity in the three proliferation models

3.1 The relationship between GSH level and telomerase activity during the growth of 3T3 fibroblasts.

The peak of telomerase activity (TA) overlapped with the maximal GSH value in the cell culture of 3T3 fibroblasts (1) (Fig. 8A). The TA at its maximal value, at 24h, was 3 times higher comparing to the beginning of the culture (6h) (Fig. 8B), and then decreased rapidly and continuously until the last time point.

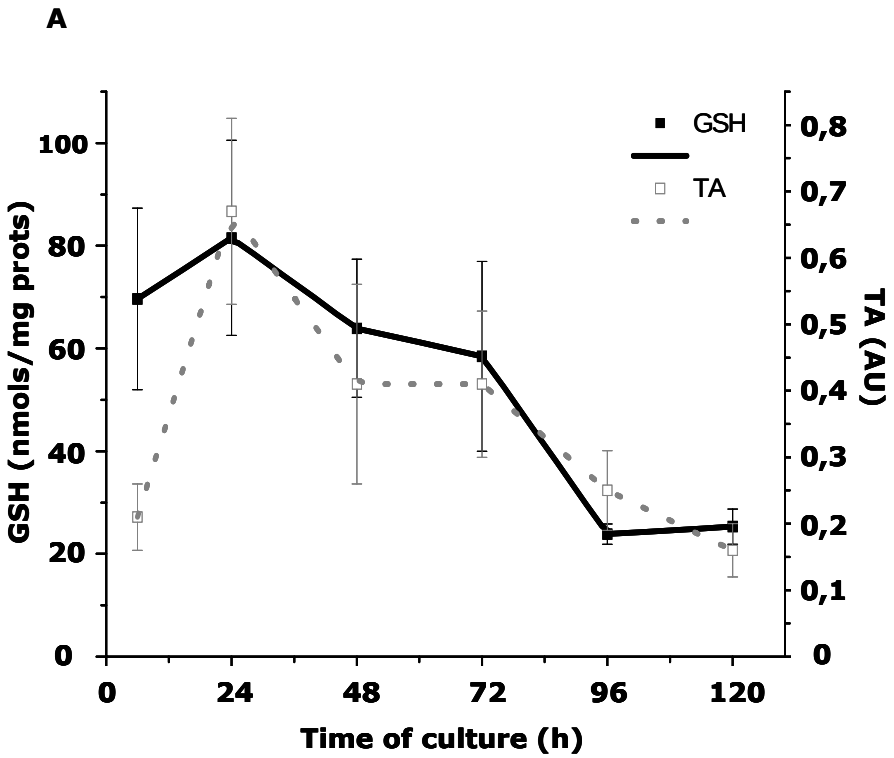

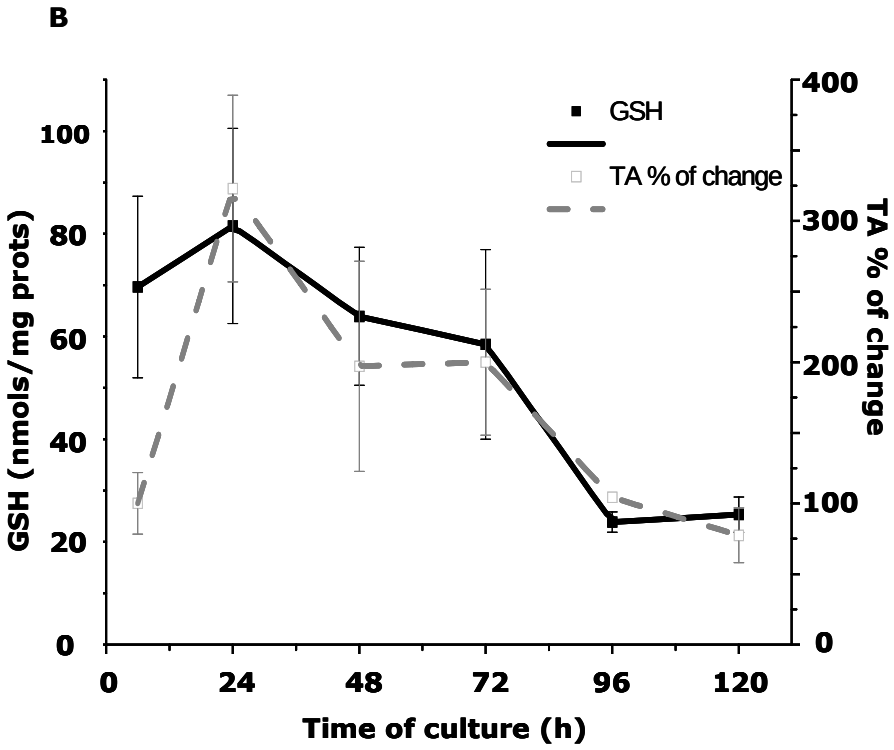

Figure 8. **GSH level and relative telomerase activity (TA) in 3T3 fibroblasts during cell culture.** The GSH level, presented at left Y axis, was measured as described previously and relative telomerase activity, at right Y axis, was estimated by TRAP reaction as explained in "Materials and Methods". Data are expressed as the mean ± SD of 6-10 different experiments (panel A) and as a % of change normalized by the starting point of culture (6h) (panel B).

3.2 The relationship between GSH level and telomerase activity during the growth of MCF7 cells.

In MCF7 cells we observed the same occurrence; the high level of GSH was accompanied by the plateau of elevated TA (Fig. 9A), and the profile of TA resembled that of GSH. The maximal TA increment was more than 200% (Fig. 9B), and the decrease was gradual until the end of culture.

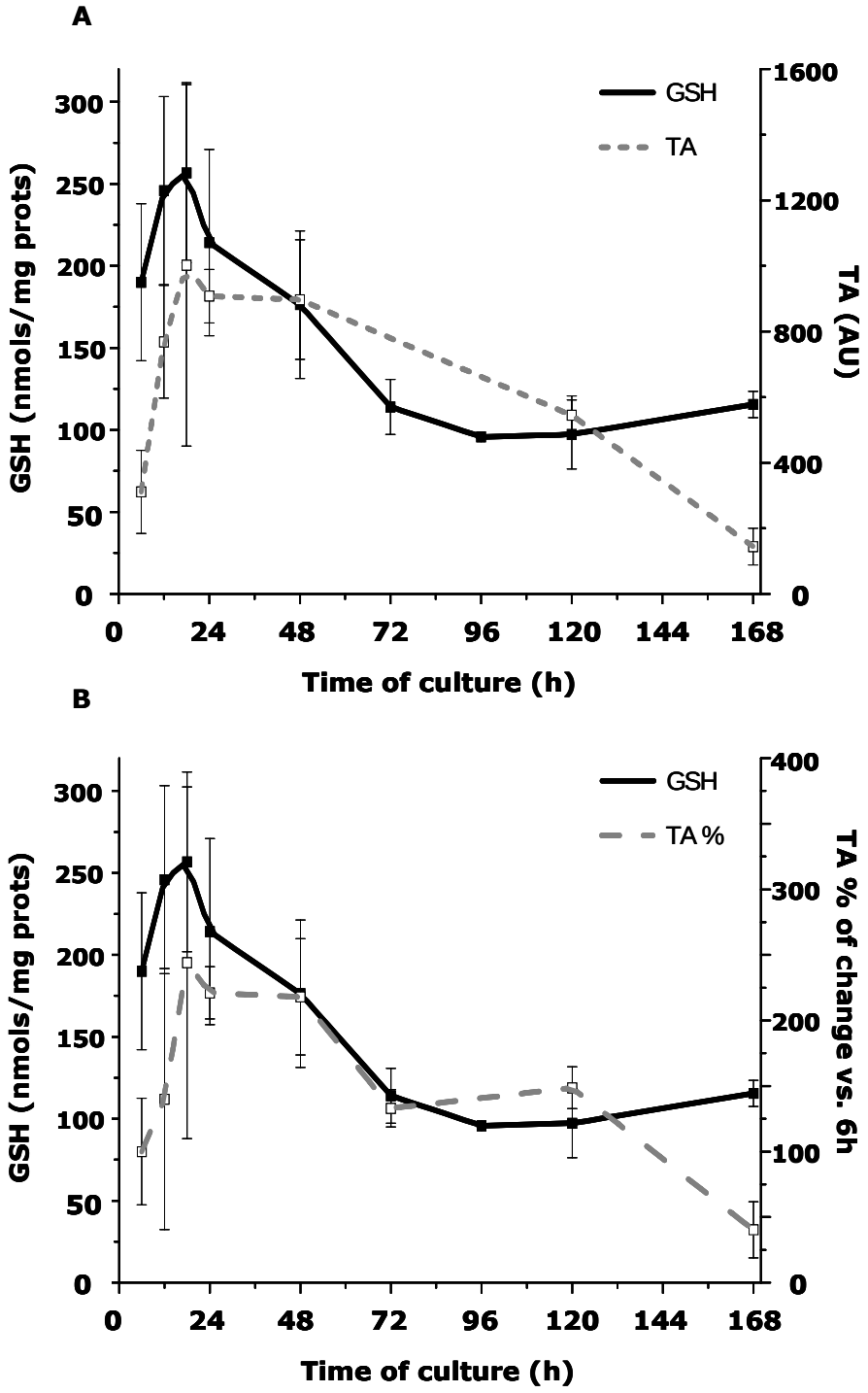

Figure 9. **GSH level and relative telomerase activity (TA) in MCF7 cells during cell culture.** The GSH level, presented at left Y axis, was

measured as described previously and relative telomerase activity, at right Y axis, was estimated by TRAP reaction as explained in "Materials and Methods". Data are expressed as the mean ± SD of 6-10 different experiments (panel A) and as a % of change normalized by the starting point of culture (6h) (panel B).

3.3 The relationship between GSH level and telomerase activity during the growth of embryonic neural culture.

In the proliferating phase of neural culture the peak of GSH matched the maximum of TA, while in differentiated culture the steady decrease of GSH was followed by more noticeable decline of TA (Fig. 10A). The changes of TA along the culture are less prominent than when other two cell

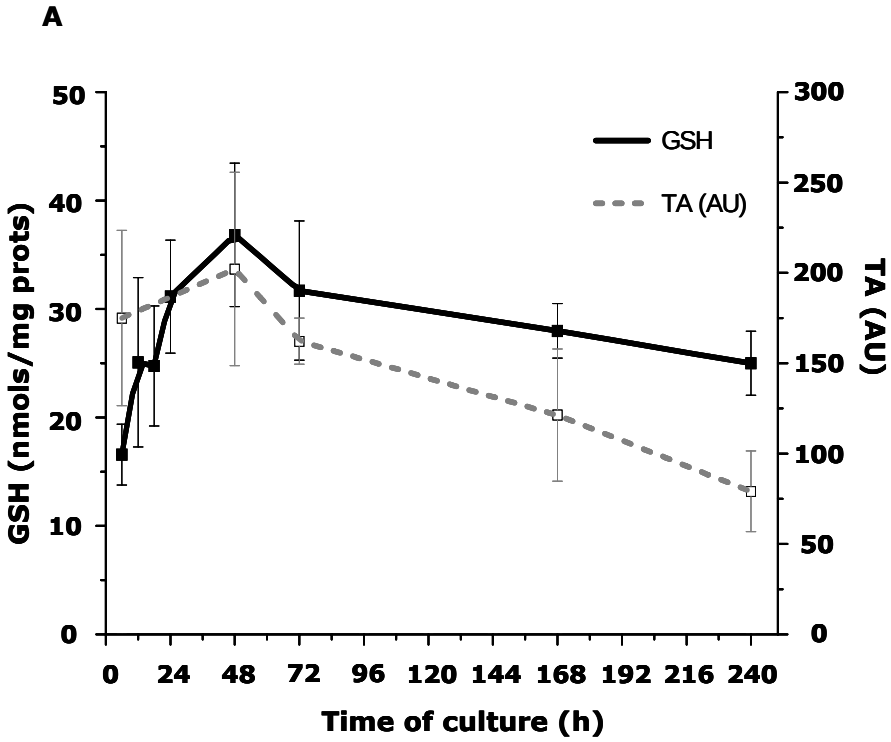

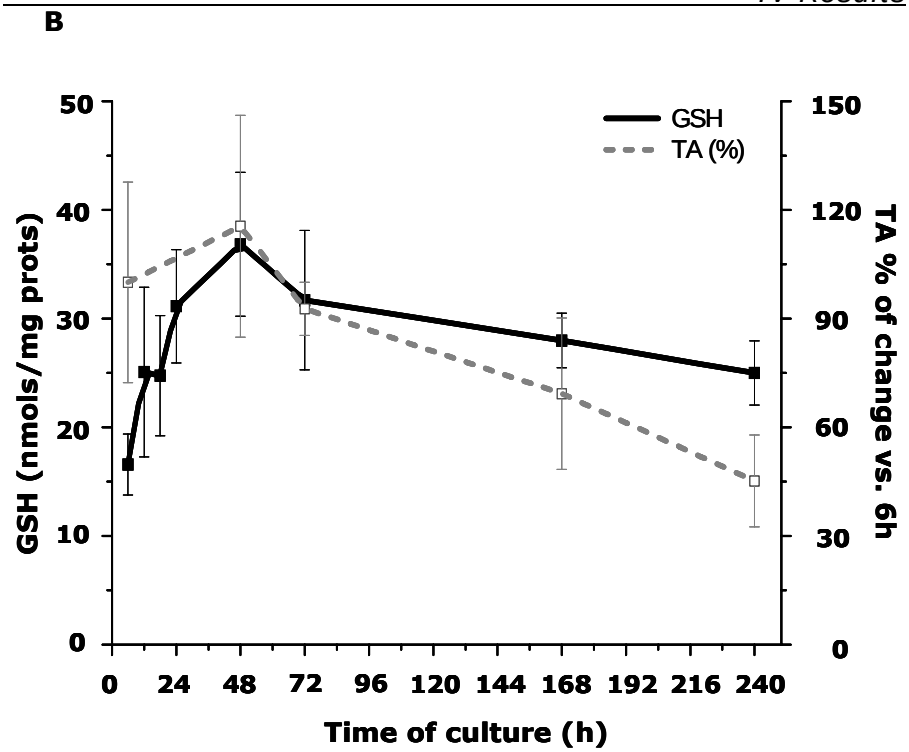

Figure 10. **GSH level and relative telomerase activity (TA) in embrionary neural culture.** The GSH level, presented at left Y axis, was measured as described previously and relative telomerase activity, at right Y axis, was estimated by TRAP reaction as explained in "Materials and Methods". Data are expressed as the mean ± SD of 3-5 different experiments (panel A) and as a % of change normalized by the starting point of culture (6h) (panel B).

types were considered; the maximal increase is of less than 20% (Fig. 10B).

4. Three different models of cell growth

4.1 The rhythm of cell growth is diverse in 3T3 fibroblasts, cancer cells and embryonic neural culture.

Figure 11 displays the differences in proliferation curves between the three cellular models under study in the present thesis.

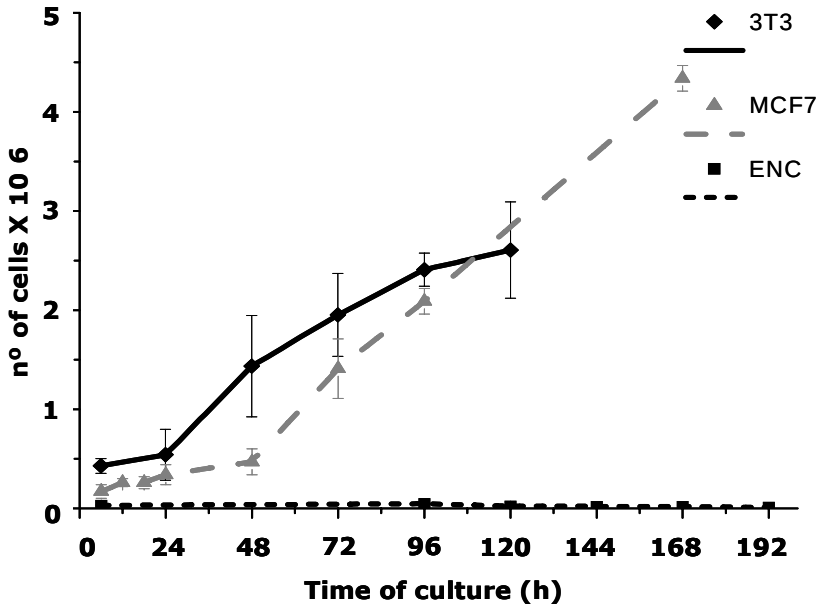

Figure 11. **The comparative population curves in different cell lines**. Cells were cultivated and plated as described in "Materials and Methods" and counted at established time points. Demonstrated results are the mean ± SD of at 3-10 experiments.

3T3 fibroblasts demonstrated different cell growth profile comparing to MCF7 cells. Cancer cells had later proliferation onset, but their exponential phase of cell growth was elongated and more intense. Probably due to the deficiency of contact inhibition, these cells continued to divide days after 3T3 fibroblasts have reached confluence and consequently entered quiescence. The total cell number of MCF cells on the plate, at the final time point, was almost twice as high as in the case of 3T3 fibroblasts. Embryonic neural culture showed certain proliferating activity limited to the first 4 days of culture (see Fig. 6). Afterwards, the proliferation was almost absent and the vast majority of the cells on the plate were differentiated in to neurons.

4.2 The intensity of cell growth corresponds to the level of GSH

Figure 12 demonstrate the results of the comparison of the GSH levels in the three models of cell proliferation.

In MCF7 cells, the peak of GSH was prior (at 18h) to the peak of 3T3 fibroblasts (24h of culture) and the value was three times higher (256,75±54,80 and 81,52±19 nmols/mg prot., respectively). When the ENC is concerned, the GSH values were higher while the cells were proliferating, until 96h of culture, then after, when the culture contained mainly differentiated cells.

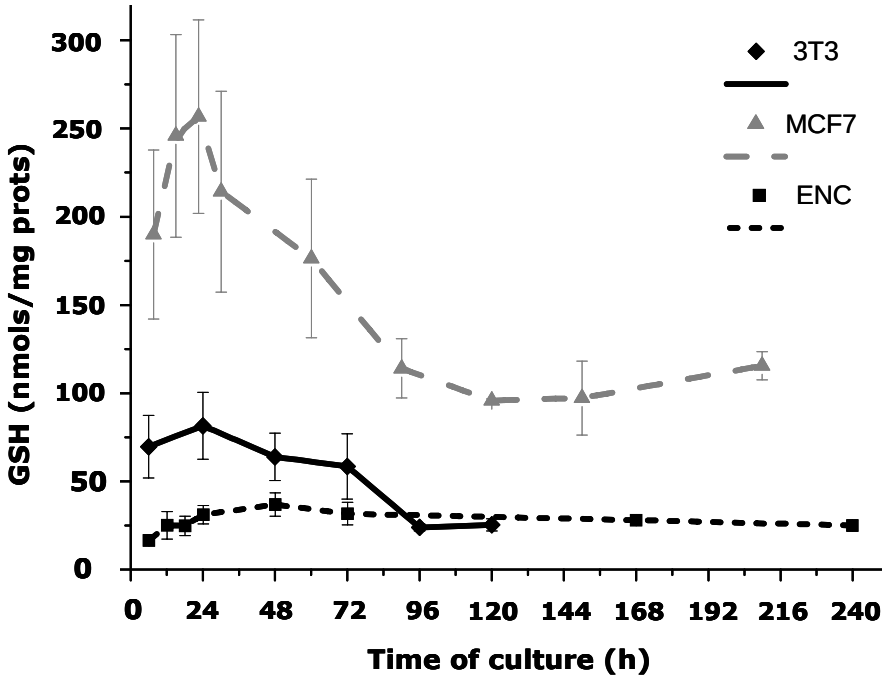

Figure 12 . **The comparison of GSH levels along the cell culture in diferent cell lines.** The total cellular concentration of GSH was determined spectrophotometrically as described in "Materials and Methods". Data are represented as the mean ± SD of 3-10 different experiments.

Beginning from the 7th day the level of GSH was very low (28,6±8,64 nmols/mg prot.) and without perceptible fluctuations until the end of the culture.

4.3 The profiles of telomerase activity along the cell cycle match the variation in GSH level

In MCF7 cells and 3T3 fibroblasts the changes in TA along the cell cycle were extraordinary (Fig. 13).

As described before, in 3T3 fibroblasts a striking augmentation of TA activity was accompanied by the increase of GSH, and the maximal values of both parameters concurred at 24h after plating. Likewise, in MCF7 cells, the level of TA doubled in the first 18h of culture, and this increase corresponded to the peak of GSH.

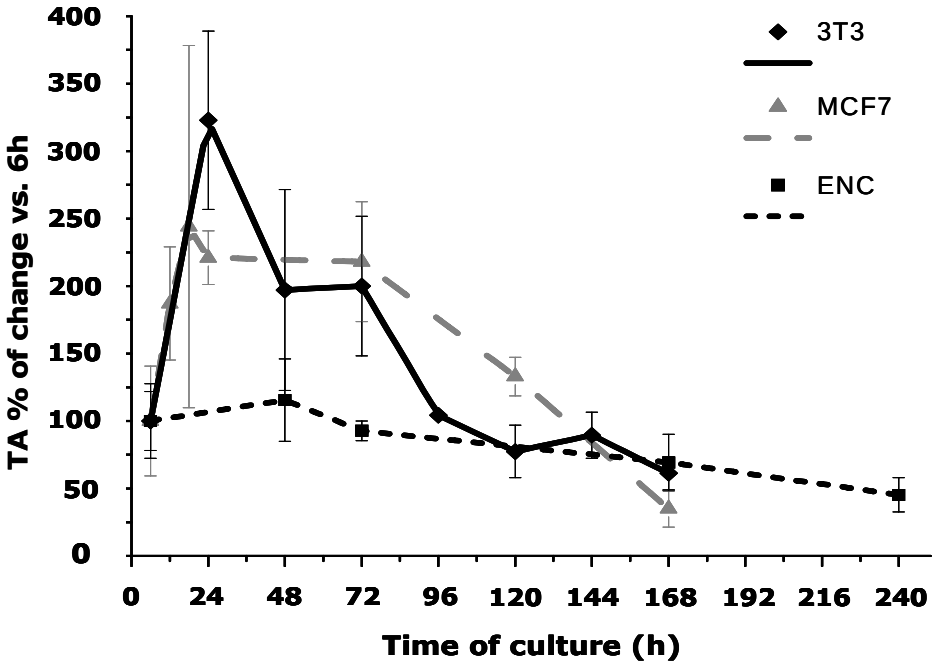

Figure 13. **The comparative rhythm of relative telomerase activity (TA) in different cell lines.** TA was estimated by TRAP

reaction as explained in "Materials and Methods". Data are normalized by the starting point of culture (6h) and expressed in the % of change as mean ± SD (n=3-5).

Interestingly, the augment in TA in MCF7 cells was less prominent than in 3T3 fibroblasts, but it endured longer. Embryonic neural culture showed more subtle increment, two days after plating it increased only 15%.

4.4 The GSH level correlates with the level of DNA synthesis in the three models of cell proliferation, but not with the percentage of cells in G2/M phase

The study of the cell cycle by flow cytometry allowed us to develop the comparative analysis of the intensity of

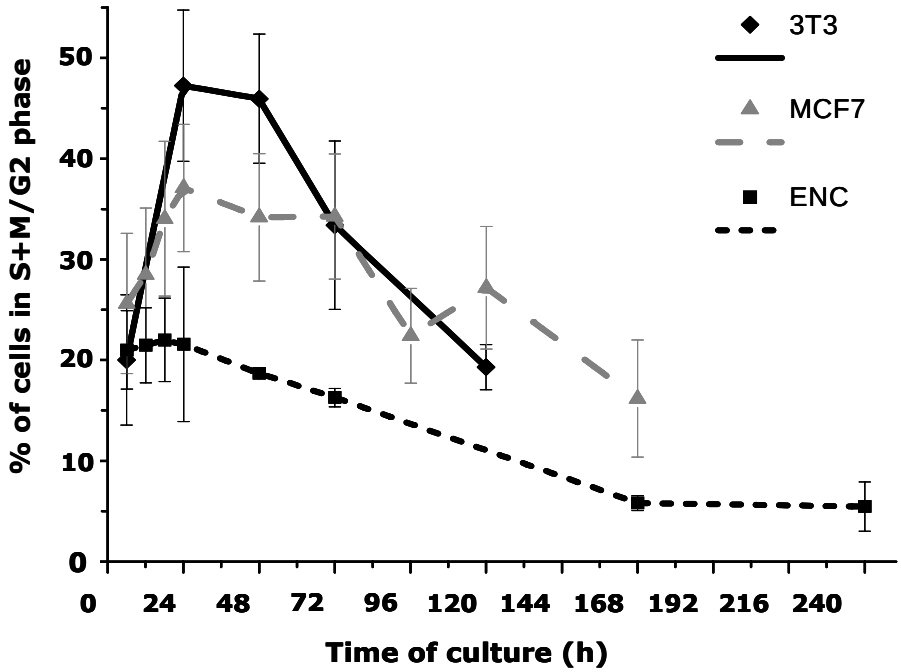

Figure 14. The comparative levels of the cell proliferating activity along the cell culture in different cell lines. The percentage of actively dividing cells is obtained as a sum of S+M/G2. Data are expressed as the mean ± SD of 3-10 different experiments.

cell proliferation (percentages of the cells in the phases S and G2/M) and its possible correlation with GSH levels in three cellular models along the cell cycle.

Surprisingly, the levels of cellular proliferating activity, defined by the sum of the cells in S+G2/M phases, demonstrated to be higher in 3T3 fibroblasts than in MCF7 cells (Fig. 14), although in MCF7 cells the higher values were sustained for longer time. Consequently, no clear correlation between S+G2/M phase and GSH levels could be demonstrated in our three models (Fig. 15).

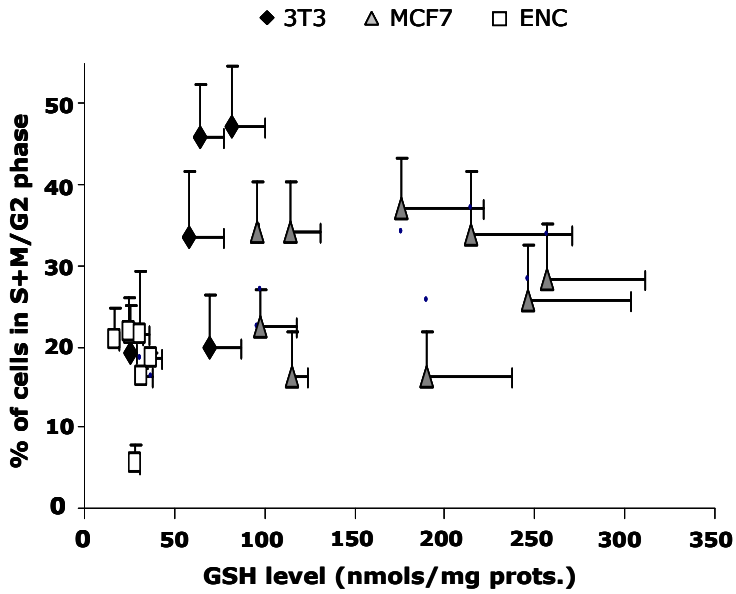

Figure 15. The correlation of the levels of cell proliferation and GSH levels along the cell cycle in different cell lines. The percentage of actively dividing cells is obtained as a sum of S+M/G2. GSH measurement was performed by spectrophotometry. Data are expressed as the mean ± SD of 3-10 different experiments.

Separate analysis of the G2/M phase of cell cycle showed analogous pattern and the absence of the correlation with GSH levels (Fig. 16. and Fig.17).

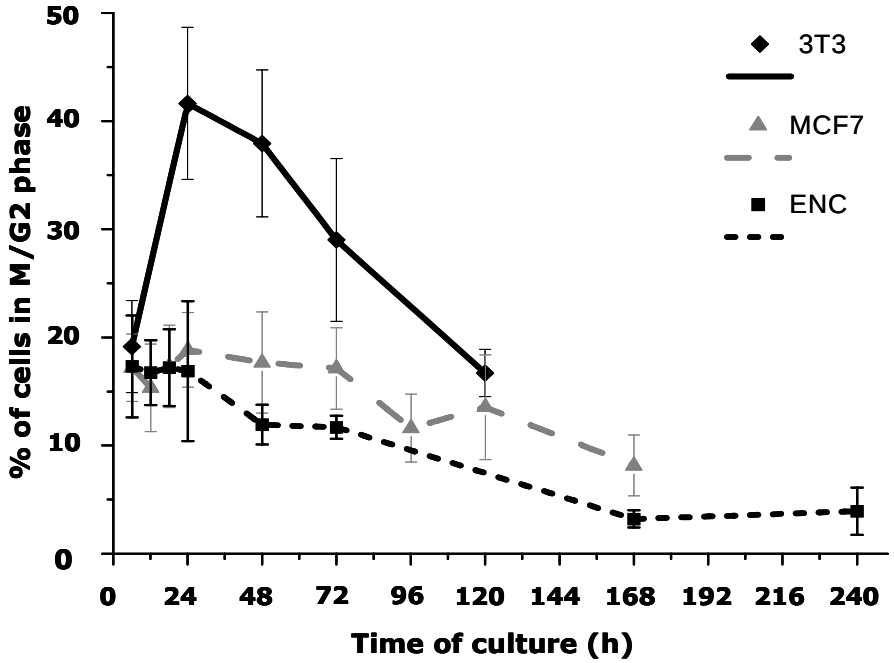

Figure 16. The comparative levels of the cell division along the cell cycle in different cell lines. The percentage of dividing cells (M/G2) was estimated by the flow cytometry analysis of the DNA content. Data are expressed as the mean ± SD of 3-10 different experiments.

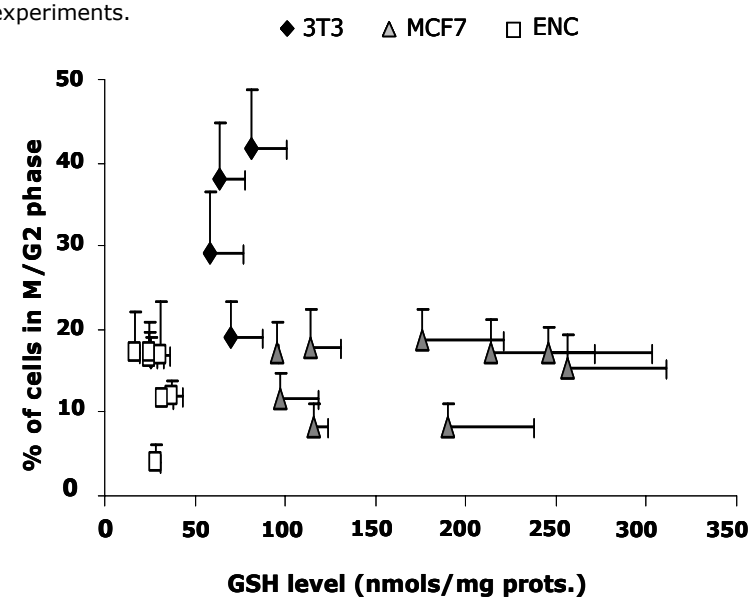

Figure 17. **The correlation of the levels of cell division and GSH levels along the cell cycle in different cell lines**. The percentage of cells in the M/G2 phase was estimated by the flow cytometry analysis of the DNA content. GSH measurement was performed by spectrophotometry. Data are expressed as the mean ± SD of 3-10 different experiments.

On the contrary, the analysis of the phase of DNA synthesis revealed considerable differences (Fig. 18, 19).

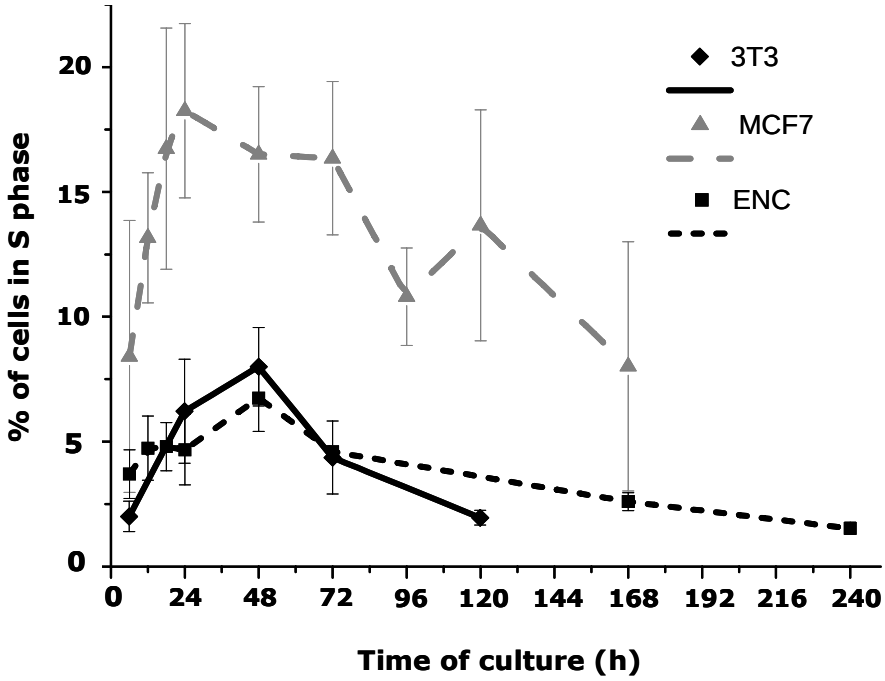

Figure 18. The comparative levels of DNA synthesis along the cell cycle in different cell lines. The percentage of cells in the phase of DNA synthesis (S) was estimated by the flow cytometry analysis of the DNA content. Data are expressed as the mean ± SD of 3-10 different experiments.

The neural culture was characterized by the low percentage of the cells in S phase and low level of GSH, while the extremely high GSH level of MCF7 cells was accompanied by high level of DNA synthesis. 3T3 cells showed medium levels both of GSH and of the quantity of cells synthesizing DNA.

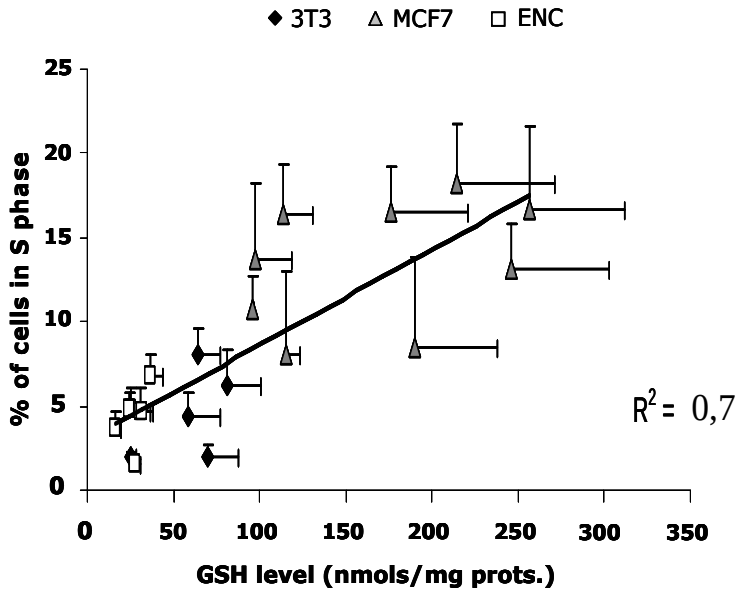

Figure 19. **The correlation of the levels of DNA synthesis and GSH levels along the cell cycle in different cell lines.** The percentage of cells in the phase of DNA synthesis (S) was estimated by the flow cytometry analysis of the DNA content. GSH measurement was performed by spectrophotometry. Data are expressed as the mean ± SD of 3-10 different experiments.

Based on this data, we conclude that there was a strong correlation (R^2=0,7) of GSH levels and DNA synthesis in the comparative study of the three cellular models

4.5 The end time point and the cell death is different in three cultures

The 3T3 fibroblasts were studied until reaching 100% confluence, which was at 5 days of culture. The longer maintenance of the cells in the plate would result in high

percentage of dead cells, due to the contact inhibition of cell growth.

MCF7 cells were cultivated up to 7 days of culture, and at this time point, were still dividing. Continuation of the cultivation would require the refreshing of the medium, which was avoided due to the possible consequences on the parameters under analysis.

Embryonic neuronal culture was maintained until 16th day (results not shown) with considerable variations in the percentage of cell death between experiments. In our study we have included neurons only until 10th day when the quality of culture was still highly reproducible.

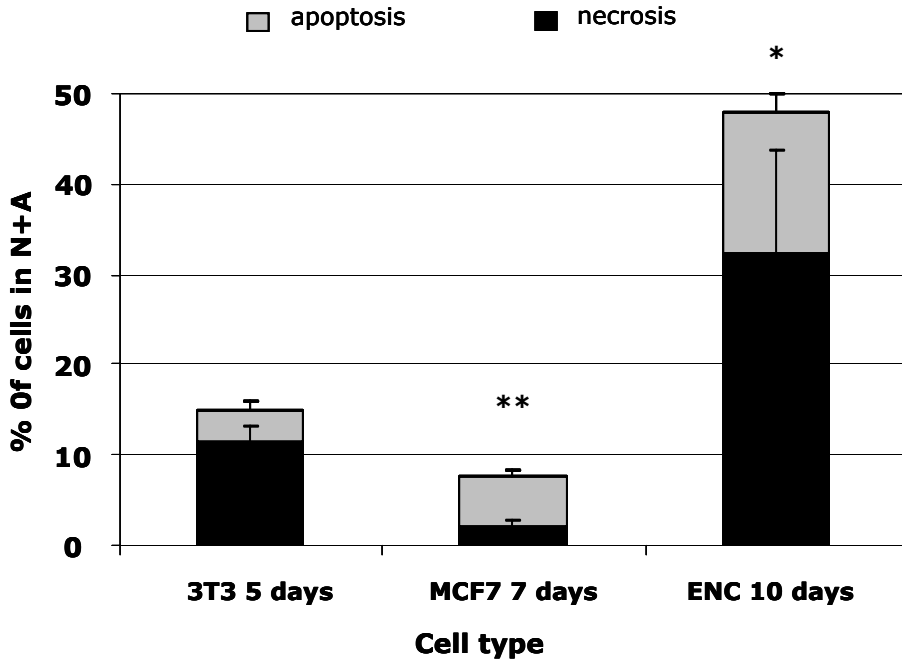

Figure 20. **The cell death at the final time point of the cell culture.** The percentage of necrotic and apoptotic cells was estimated by the flow cytometry analysis of the DNA content. Data are expressed as the mean ± SD of 3-10 different experiments. **P≤0,01 and *P≤0,05 derives from t student analysis of the statistical differences between 3T3 and MCF7 cells and 3T3 and ECN, respectively.

Figure 20 shows the level of cell death at the final time point of the culture. The MCF7 cells at 7 days of culture were still proliferating and the level of cell death was extremely low. 3T3 fibroblasts had reached confluence and as they are contact inhibited, some dead cells could be found in the culture. Embryonic neuronal culture at advanced time point had a higher death rate due to the sensibility to the cultivation conditions.

In conclusion, the comparative study of the GSH level and its effect on the cell growth parameters in three models of distinct proliferating activity proved the universality of the observations displayed previously only for 3T3 fibroblasts: the peak of GSH precedes the exponential phase of cell growth and coincides with the maximal value of telomerase activity. The dependence of the telomerase activity on the GSH level drove us to study the possible correlation between the DNA synthesis and GSH in our model, and it appears that there is direct correlation between the GSH level of the cell population and the percentage of the cells in the S phase.

These findings motivated the second goal in our research: to study the importance of the nuclear compartmentalization of GSH in the cell cycle progression.

1. Borras, C., Esteve, J. M., Vina, J. R., Sastre, J., Vina, J., and Pallardo, F. V. (2004) Glutathione regulates telomerase activity in 3T3 fibroblasts. *J Biol Chem* 279, 34332-34335

II NUCLEAR DISTRIBUTION OF GSH AND CELL CYCLE

1. The election of the methodology

2. The cellular distribution of GSH along the cell cycle in three models of proliferation

2.1 The GSH distribution in 3T3 fibroblasts.

2.2 The GSH distribution in MCF7 cells.

2.3 The GSH distribution in embryonic neural culture.

3. The comprehensive analysis of the nuclear compartmentalization of GSH in 3T3 fibroblasts

3.1 The GSH is increased in the nucleus when cells proliferate, and the level is equal to cytoplasmatic at confluence.

3.2 The quantification of nuclear GSH compartmentalization.

3.3 The study of the oxidative status of nuclear proteins

3.3.1. Oxidation of nuclear proteins

3.3.2. Glutathiolation of nuclear proteins

3.4 Resolving the limitations of the technique.

3.4.1 Variations in the relative cellular and nuclear surface along the cell cycle.

3.4.2 The interference of the mitochondrial pool of GSH

II NUCLEAR DISTRIBUTION OF GSH AND CELL CYCLE

In view of the results demonstrated previously, we planted a question whether nuclear compartmentalization of GSH might have a role in the evolution of the cell cycle during the early phases of cell culture.

1. The election of the methodology

Preliminary experiments that were based on classical cell fractionation protocols produced unsatisfactory results. The nuclear isolation and subsequent determination of total glutathione content (GT) and the level of oxidised glutathione (GSSG), by H.P.L.C. technique described in "Materials and Methods", revealed not only the substantial loss of GT level with repeated washings (Fig. 21 A), but its oxidation as well (Fig. 21 B).

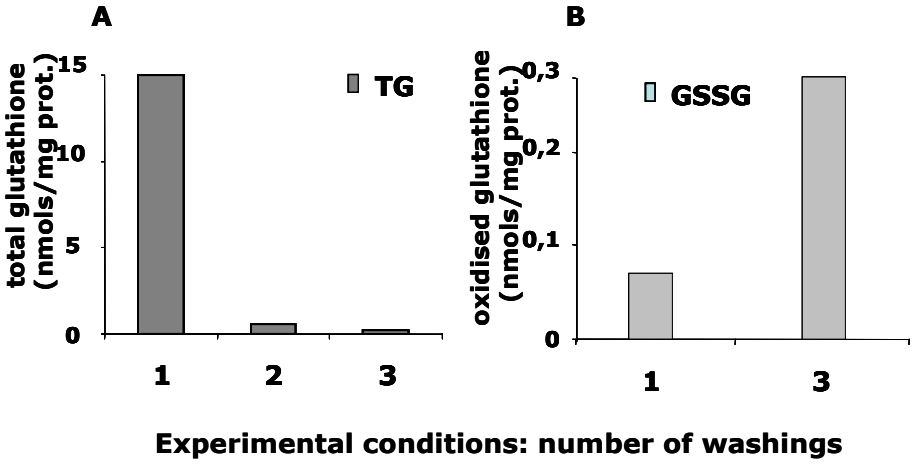

Figure 21. Determination of the nuclear glutathione level by fractionation technique. Total glutathione level (GT) (A) and oxidised glutathione level (GSSG) (B) in nmols/mg proteins were determined in isolated nuclei by HPLC as described in Materials and methods.

Therefore, in this study, a fluorescent confocal microscopy was the approach of choice. This non invasive technique enables the analysis of the living cells, under normal cell cultivation conditions (37ºC, 5% CO_2) using vital cellular dyes.

2. There is detectable nuclear compartmentalization of GSH in early phase of cell culture in three proliferating models

The cell cycle-dependent GSH distribution was studied in 3T3 fibroblasts, MCF7 cells and embryonic neural culture, at three time points: the beginning of culture (6h after plating), while proliferating (24h after plating) and at the final point of culture (5 days for 3T3, 7 days for MCF7 and 10 days when using ENC). The representative experiments are shown on the figure 22, 23 and 24, respectively. Cellular glutathione distribution is defined by the *green* CMFDA fluorescence, shown on the panels **a**. The *blue* staining of the nuclei with Hoechst 33342 is shown on the panels **b**, and transmission image is presented on the panels **c**.

We perceive that the highest green fluorescence co-localized with blue fluorescence of nuclei at 6h and 24h in all three cultures. To support this observation we quantified the intensity of blue and green fluorescence by drawing the cross section line (shown in red at panels a) throughout the cell field. Panels **d** show that the nuclei blue staining (*blue peaks* in the graph) co-localized with the green glutathione

staining (*green peaks* in the graph) at the beginning of the culture.

2.1 The GSH distribution in 3T3 fibroblasts.

The maximum correlation of blue/green fluorescence (Fig. 22A and 22B) and highest intensity of green fluorescence, i.e. GSH level, was observed at 24 h, in accordance with biochemical analysis (Fig. 1).

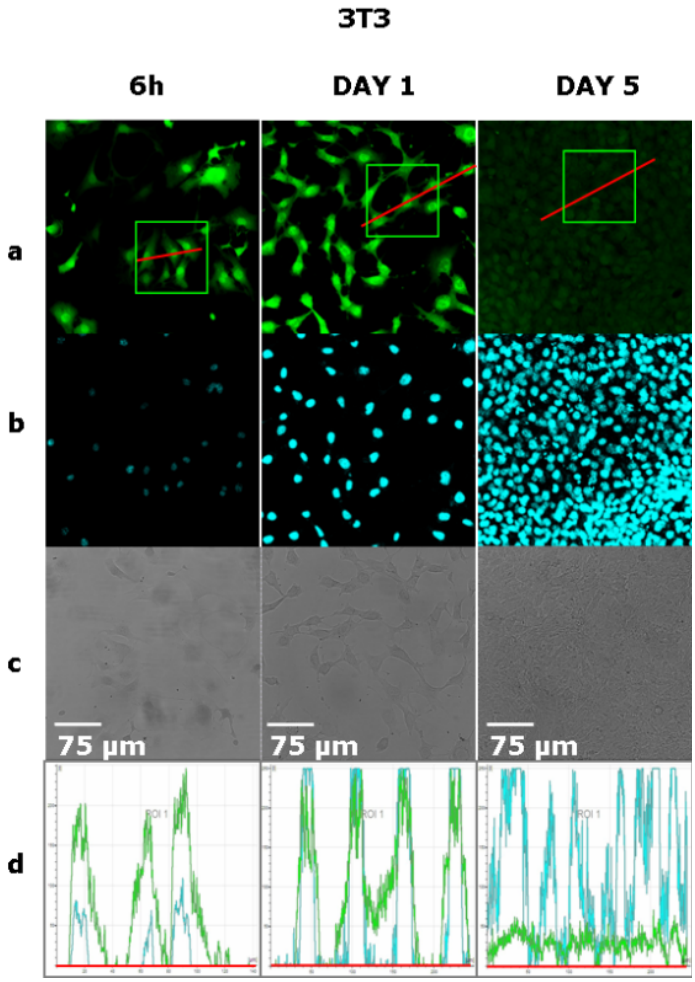

Figure 22 A. Microscopic confocal analysis of the nuclear compartimentation of GSH in 3T3 fibroblasts.

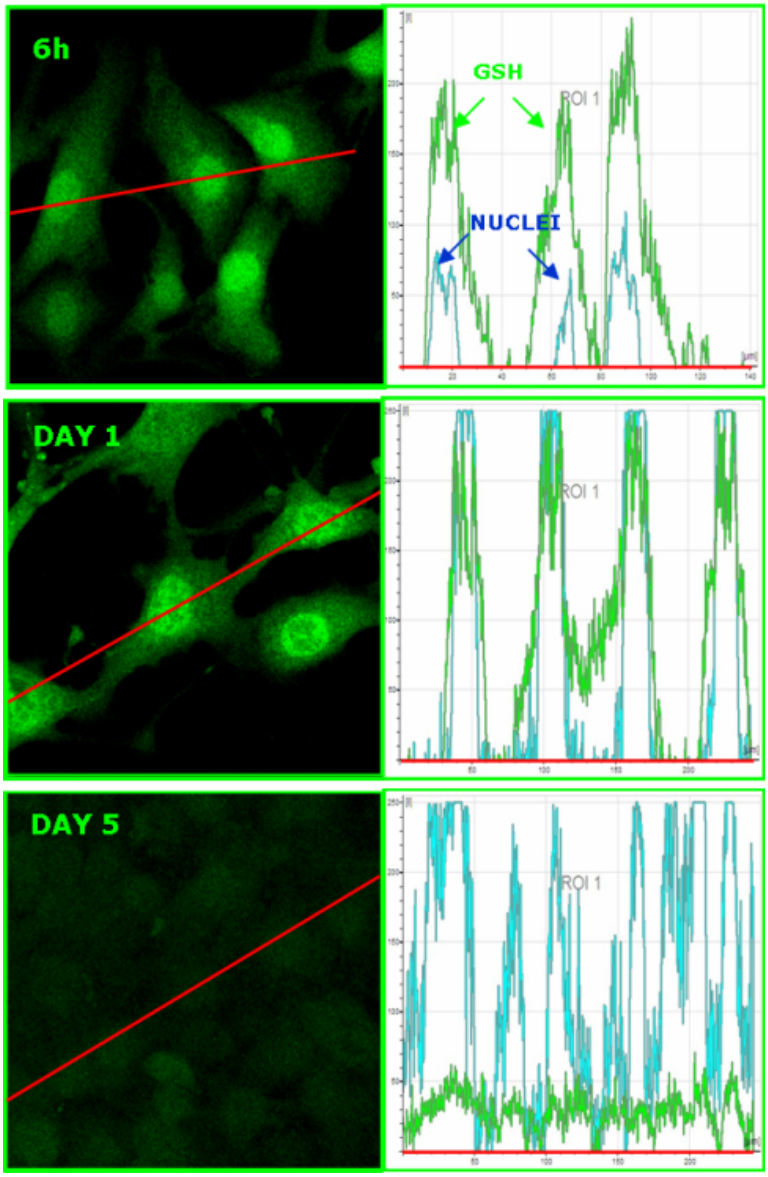

Figure 22 B. Microscopic confocal analysis of the nuclear compartimentation of GSH in 3T3 fibroblasts. Amplified detail.

Figure 22. Microscopic confocal analysis of the nuclear compartimentation of GSH in 3T3 fibroblasts. 3T3 fibroblasts (22 A and 22B), were studied at the beginning of culture (6h), during cell growth (24h) and at the end of culture (at 5 days). Triple staining was performed on living cells: Hoechst 33342 to localize nuclei (blue fluorescence, a), CMFDA to mark GSH, (green fluorescence, b), and PI to exclude dead cells (results not shown) and cells were maintained in the chamber provided with 5% CO2 at 37 °C. Histograms (panel d) show the level (axis y) of CMFDA

and Hoechst fluorescence (green and blue line, respectively) along the "red" line (axis X) used as quantification tool (shown on panel a) which allows the study of the blue/green fluorescence co localization. Panel c shows the images obtained by light microscopy. A representative Z axes series of at least 3 experiments are shown on figure 22 A, and the amplified details (1:4) are displayed in figure 22B.

At 5 days in culture, when the cells are confluent, the green staining was of lower intensity and homogeneous across the plate.

2.2 The GSH distribution in MCF7 cells.

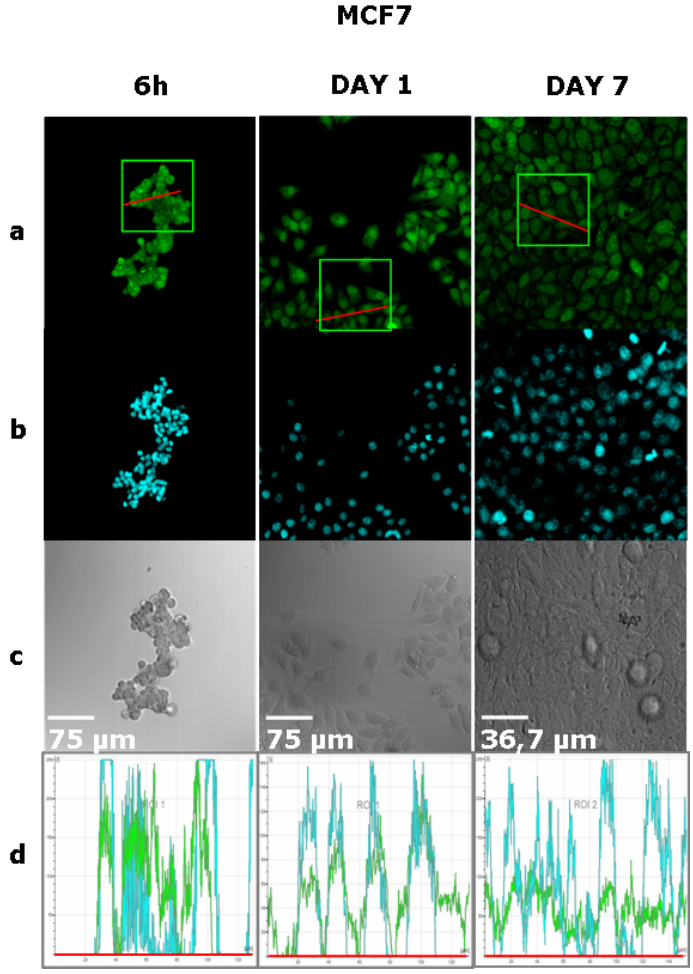

Figure 23A. Microscopic confocal analysis of the nuclear compartimentation of GSH in MCF7 cells.

MCF7

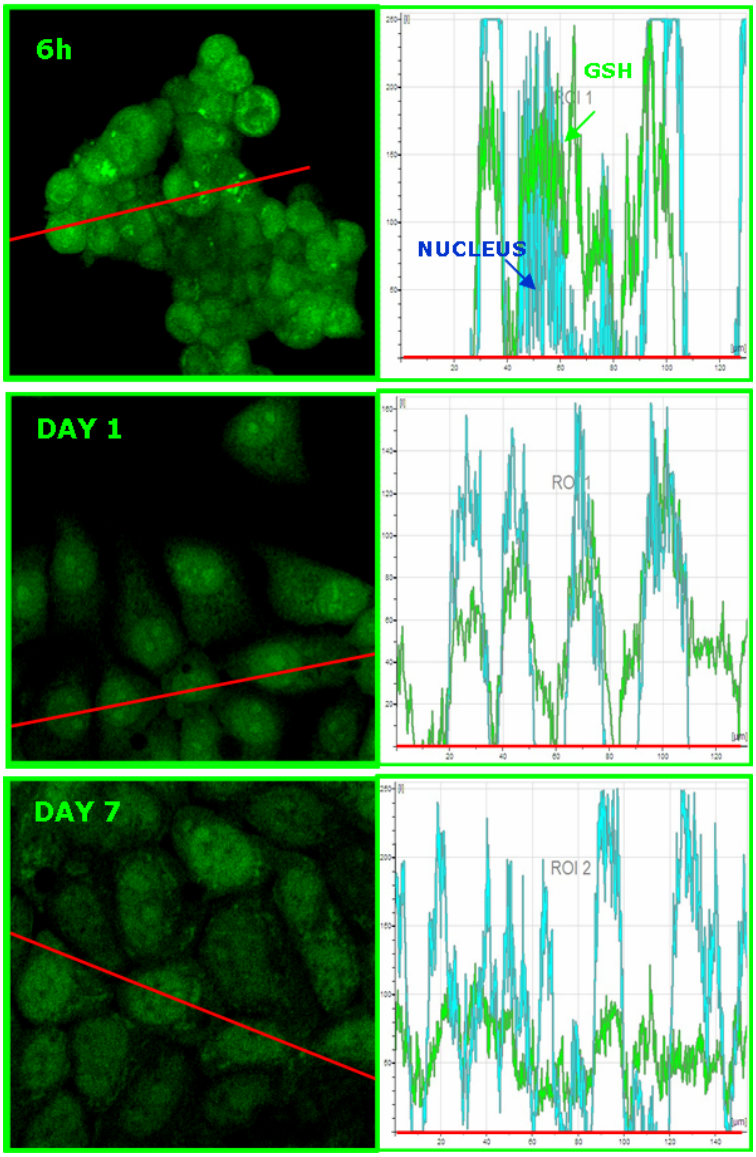

Figure 23 B. Microscopic confocal analysis of the nuclear compartimentation of GSH in MCF7 cells. Amplified detail.

Figure 23. Microscopic confocal analysis of the nuclear compartimentation of GSH in MCF7 cells. MCF7 cells were studied at the beginning of culture (6h), during cell growth (24h) and at the end of culture (at 7days). Triple staining was performed on living cells: Hoechst 33342 to localize nuclei (blue fluorescence, a), CMFDA to mark GSH, (green fluorescence, b), and PI to exclude dead cells (results not shown) and cells were maintained in the chamber provided with 5% CO2 at 37 °C.

Histograms (panel d) show the level (axis y) of CMFDA and Hoechst fluorescence (green and blue line, respectively) along the "red" line (axis X) used as quantification tool (shown on panel a) which allows the study of the blue/green fluorescence co localization. Panel c shows the images obtained by light microscopy. A representative Z axes series of at least 3 experiments are shown on figures 23 A, and the amplified details (1:4) are displayed in figure 23B.

2.3 The GSH distribution in embryonic neural culture.

In the proliferative phase of embryonic neural culture, at 24h, it was possible to detect the cells with nuclear GSH

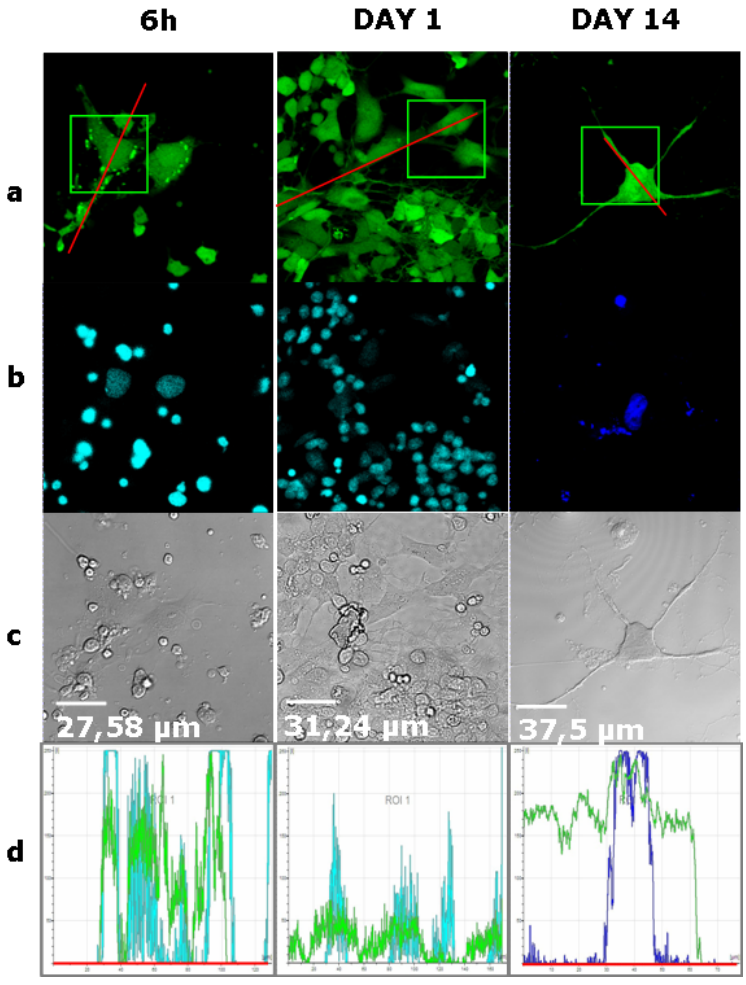

Figure 24A. Microscopic confocal analysis of the nuclear compartimentation of GSH in embrionary neuronal culture.

localization (Fig. 24A, panel **a**) although the nuclear compartmentalization in these cells was not of the same level as in other two models.

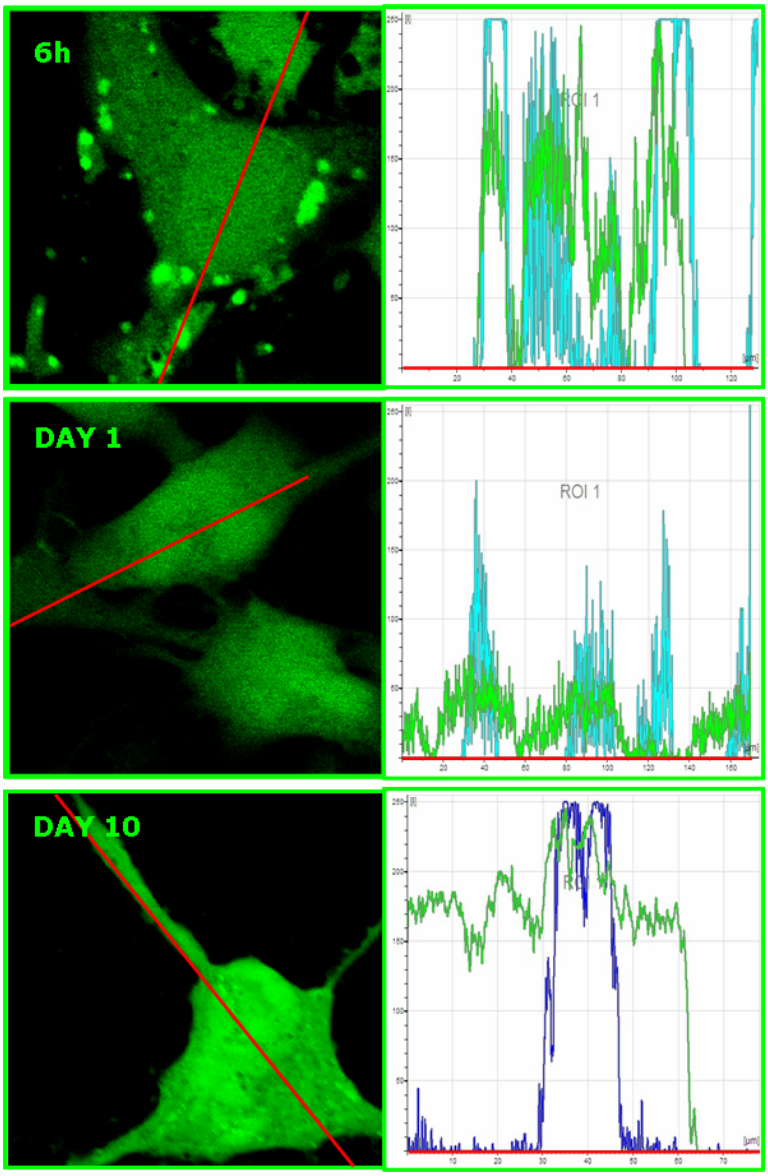

Figure 24B. Microscopic confocal analysis of the nuclear compartimentation of GSH in 3T3 fibroblasts. Amplified detail.

Figure 24. Microscopic confocal analysis of the nuclear compartimentation of GSH in embrionary neuronal culture. Embrionary culture of neurons (ENC) were studied at the beginning of

culture (6h), during cell growth (24h) and at the end of culture (10 days). Triple staining was performed on living cells: Hoechst 33342 to localize nuclei (blue fluorescence, a), CMFDA to mark GSH, (green fluorescence, b), and PI to exclude dead cells (results not shown) and cells were maintained in the chamber provided with 5% CO2 at 37 °C. Histograms (panel d) show the level (axis y) of CMFDA and Hoechst fluorescence (green and blue line, respectively) along the "red" line (axis X) used as quantification tool (shown on panel a) which allows the study of the blue/green fluorescence co localization. Panel c shows the images obtained by light microscopy. A representative Z axes series of at least 3 experiments are shown on figures 24 A, and the amplified details (1:4) are displayed in figure 24B.

On the contrary, in advanced state of culture differentiation towards neurons, the cellular distribution of GSH was more homogeneous (24 B).

Apparently, while cells are actively proliferating and entering the exponential phase of cell growth (24h of culture), the GSH level is high and its nuclear compartmentalization could be observed. When cells are proliferating more slowly, like MCF7 cells at 7 days of culture, or almost not at all, in the case of neuronal culture, the GSH level is lower and its distribution is uniform across the cell.

3. The comprehensive analysis of the nuclear compartmentalization of GSH in 3T3 fibroblasts

For a more extensive analysis of this phenomenon we have focused our attention on 3T3 fibroblasts.

3.1 The GSH level is increased in the nucleus when cells proliferate, and equal to cytoplasmatic at confluence.

The result of detailed confocal microscopy analysis of the GSH distribution along the cell cycle is shown in the Fig. 25. Six hours after plating, few cells could be seen on the plate. The *blue* staining of the nuclei with Hoechst 33342 is shown in panel **b**, and *green* (glutathione) staining is shown in *panel* ***c***. Magnified detail of glutathione staining (panel **d**) shows that the highest fluorescence is located in the nucleus. A white cross section line (best shown on panel **d**) was drawn throughout the cell field. Panel **e** displays the fluorescence level and distribution along the line. The nuclei blue staining (*blue peaks* in the graph) co-localizes with the green glutathione staining (*green peaks* in the graph) at the beginning of the culture. At 12 and 24 h of culture, cells continued to populate the plate. Cellular glutathione (CMFDA green fluorescence intensity) was maximal at 24 h. Analysis of the blue/green fluorescence (Fig. 25 b and d, respectively) distribution and intensity showed a maximum correlation of blue/green fluorescence at 24 h. When cells were confluent after 72 h or 5 days in culture, no correlation among the

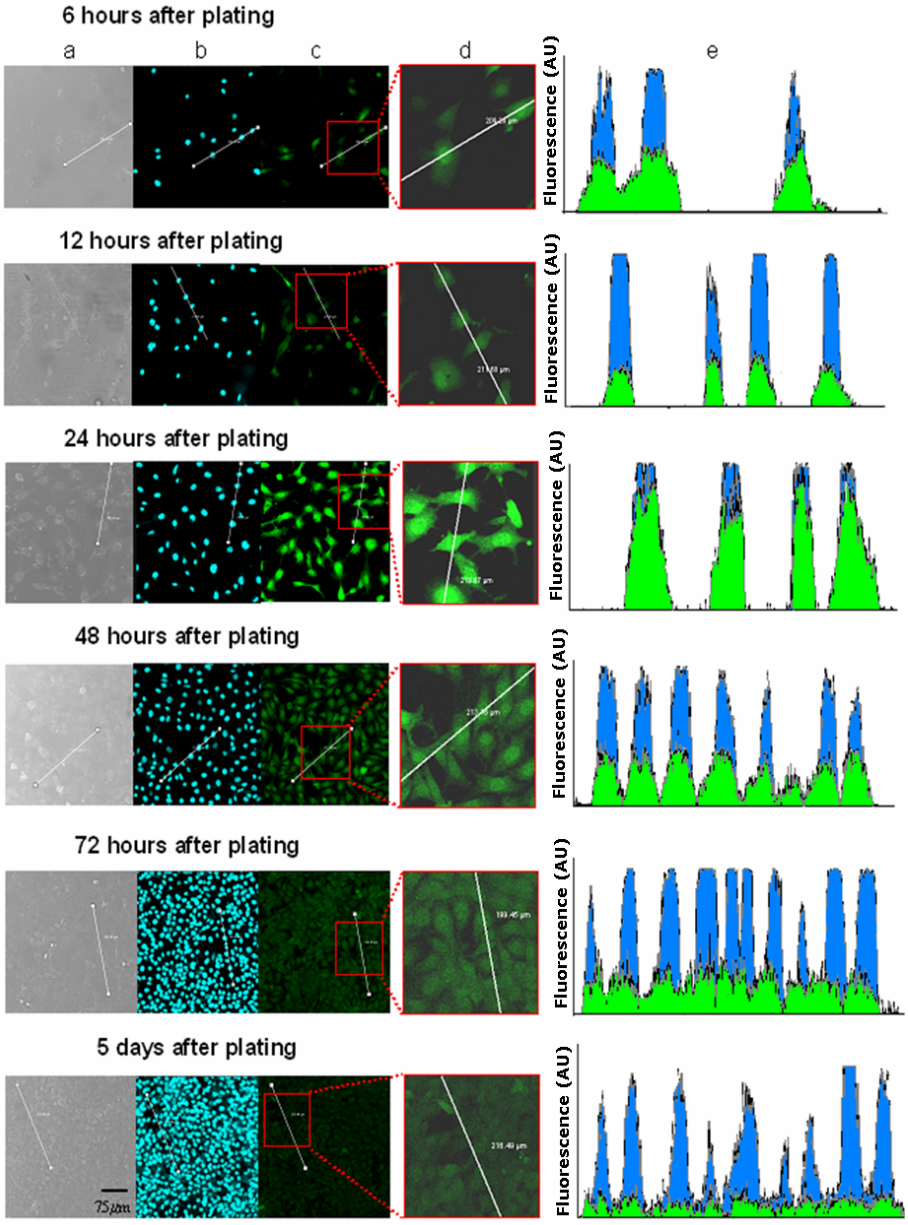

Figure 25. Confocal microscopic images of 3T3 fibroblasts during cell growth. Cells were plated in chamber slides 5 days, 72 h, 48 h, 24 h, 12 h, and 6 h before the experiment and were stained and analyzed the same day. Triple staining was performed on living cells: Hoechst 33342 to localize nuclei, CMFDA to mark GSH, and PI to exclude dead cells. During microscopic confocal analysis, cells were maintained in the chamber provided with 5% CO2 at 37 °C. Images veré taken by light microscopy (*a*) and confocal microscopy, as described in "Materials and Methods" to capture blue fluorescence of nuclei (*b*) and by green fluorescence, which marks GSH (*c*), and red fluorescence of dead cells (results not shown). Maximum

projection images were analyzed by profile of fluorescence, where a cross-section *white line* of 200 ± 20 μm was drawn through a cell field (best shown in amplified detail on the *d panels*) to compare distribution of green CMFDA fluorescence (levels of GSH) along the line (*green area under the curves* in the *e panels*) with blue Hoechst fluorescence (nuclei localization) (*blue* area *under the curves* in the *e panels*). *a.u.*, arbitrary units.

peaks of green and blue fluorescence could be found.

The increase over culture time in total cellular staining for CMFDA correlated with the peak of glutathione concentration (81,52 ± 19 nmols/mg prot.) determined spectrophotometrically (see Fig. 1). As expected, green (GSH) fluorescence clearly decreased at 72 h and 5 days in culture when cell culture reached confluence, cell-to-cell growth inhibition took place, and as a consequence the cell population entered quiescence (70–80% G_0/G_1). At these stages no significant difference could be seen between the nucleus and cytoplasm, and there was a homogenous green (CMFDA) pattern on the plates. Thus, when cells started to grow, GSH was located mainly in the cell nucleus. However, when cell growth slowed, GSH distribution was homogenous throughout the cell.

3.2. The quantification of nuclear GSH compartmentalization.

The capacity of the cell to concentrate GSH in the nucleus was estimated calculating the nuclear/cytoplasmic ratio, after measuring the levels of CMFDA fluorescence of the nuclear and cytoplasmatic area in ~100 cells one by one in each experiment. The results in Fig. 26 show a distribution

pattern where the maximal nuclear/cytoplasmic ratio (4.2 ± 0.8) was found very early after plating (6 h). Although a high nuclear/cytoplasmic ratio for GSH was maintained during cell growth, as the culture progressed, a steady decrease in the nucleus/cytoplasm ratio was present. Once the cells reached confluence and most of them were in the G_0/G_1 phase, the nuclear/cytoplasmic ratio for GSH was homogeneous, and no difference could be seen between the nucleus and the cytoplasm.

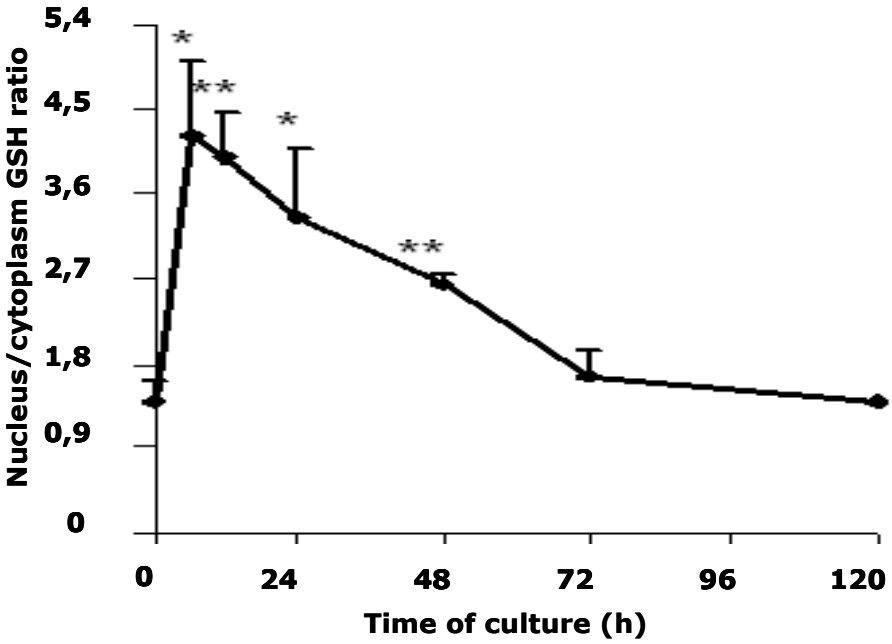

Figure 26. Nucleus/cytoplasm GSH ratio obtained by confocal microscopy. Analysis of the cellular distribution of GSH. Cells were plated and stained and images obtained as described previously. To quantify the changes in GSH distribution in cells along the cell cycle, cells were analyzed by area (as described in Materials and methods). The nucleus/cytoplasm ratio for GSH in every cell analyzed was established by dividing the mean of green CMFDA fluorescence of the nucleus area by the mean of CMFDA fluorescence in the cytoplasm area. Results are mean ± S.D. for three independent experiments, where 100 cells in at least five different fields were analyzed.

3.3 The study of the oxidative status of nuclear proteins

To elucidate the possible consequences of the high glutathione concentration in the nucleus in early phases of cell proliferation, we have studied the level of oxidation and glutathiolation of nuclear proteins.

3.3.1. Oxidation of nuclear proteins

Consequent with the finding that nuclear GSH is high during the early phases of cell cycle and low when cells are confluent, nuclear oxidized proteins levels are higher during

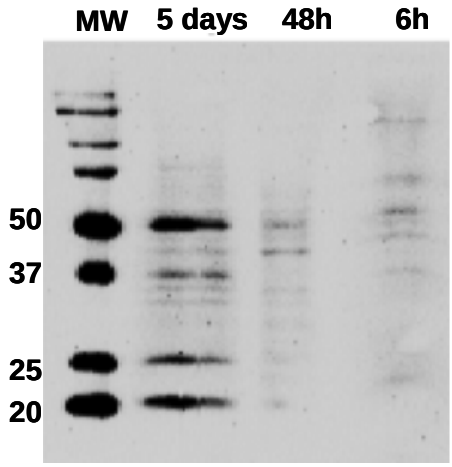

Figure 27. Oxidized nuclear proteins during cell growth. 3T3 cells were subjected to nuclear protein extraction, for the determination of protein oxidation. The level of nuclear protein oxidation was determined by detecting the carbonylation level with the Oxy Blot protein oxidation detection Kit (Chemicon International). Samples were lysed and derivatized, and Western blotting was performed according to the recommendation of the manufacturer.

cell cycle arrest than 6 h after culture (Fig. 27)

3.3.2. Glutathiolation of nuclear proteins

Western blot analysis of nuclear extracts showed the differences in the glutathiolation of nuclear proteins (Fig. 28); it was higher at 6 h after culture, when nuclear compartmentalization reached its maximum. As expected, when cells reached confluence and nuclear/cytoplasmic distribution was homogeneous, glutathiolation of nuclear proteins decreases.

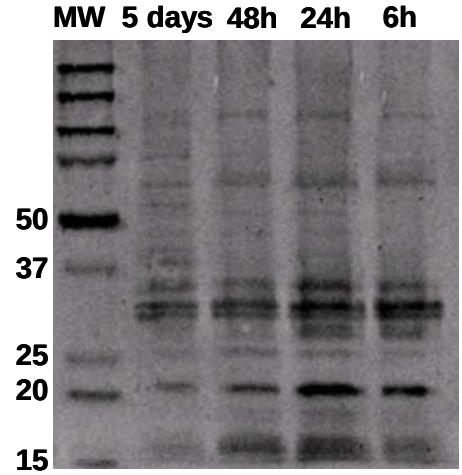

Figure 28. Glutathiolated nuclear proteins during cell growth. Nuclear lysates of 3T3 cells were obtained in the absence of reductive agents. Western blotting procedure was performed as described in "Materials and Methods" and the membrane was probed against anti-glutathione antibody (1:1000) (Virogen) at 4 °C overnight.

3.4 Resolving the limitations of the technique.

3.4.1 Variations in the relative cellular and nuclear surface along the cell cycle.

The confidence of this analysis was questioned by the possibility that the difference in the mean fluorescence ratio

could be the consequence of the changes in the cellular and cell compartments areas along the cell cycle. Figure 29.A demonstrate that during proliferation, the cellular and nuclear area is bigger than when cells are confluent, so the high mean fluorescence of the nuclei at the beginning of the culture is not due to underestimation of the nuclear surface.

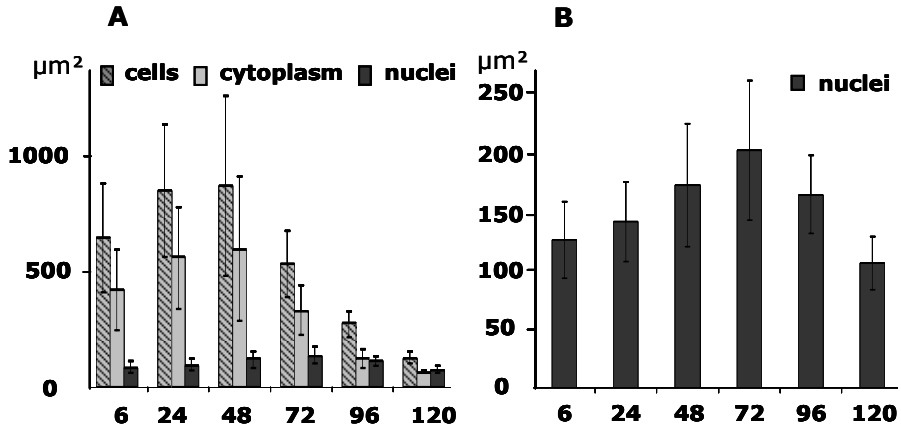

Figure 29. Analysis of the changes in cell compartments areas along the cell cycle. Cells were plated and stained and images obtained as described previously. The area was measured by drawing perimeters around the nucleus (A,B), cytoplasm excluding nucleus and whole cell (A) (as described in Materials and methods). Results are mean ± S.D. for three independent experiments, where 100 cells in at least five different fields were analyzed.

3.4.2 The interference of the mitochondrial pool of GSH

The mitochondria represent an important pool of GSH and their localization in the upper nuclear area at the apex of the cell could be mistaken for the nuclear fluorescence.

To ensure that it is not mitochondrial GSH that was responsible for the areas of high CMFDA fluorescence we incubated fibroblasts with Hoechst to stain genomic DNA (in

blue), CMFDA for GSH (*green*), and MitoTracker for mitochondrial staining (*red*) (Fig. 30). A selection of images obtained along the *z* axis starting from the cell apex is shown in Fig. 30 (a representative experiment of three).

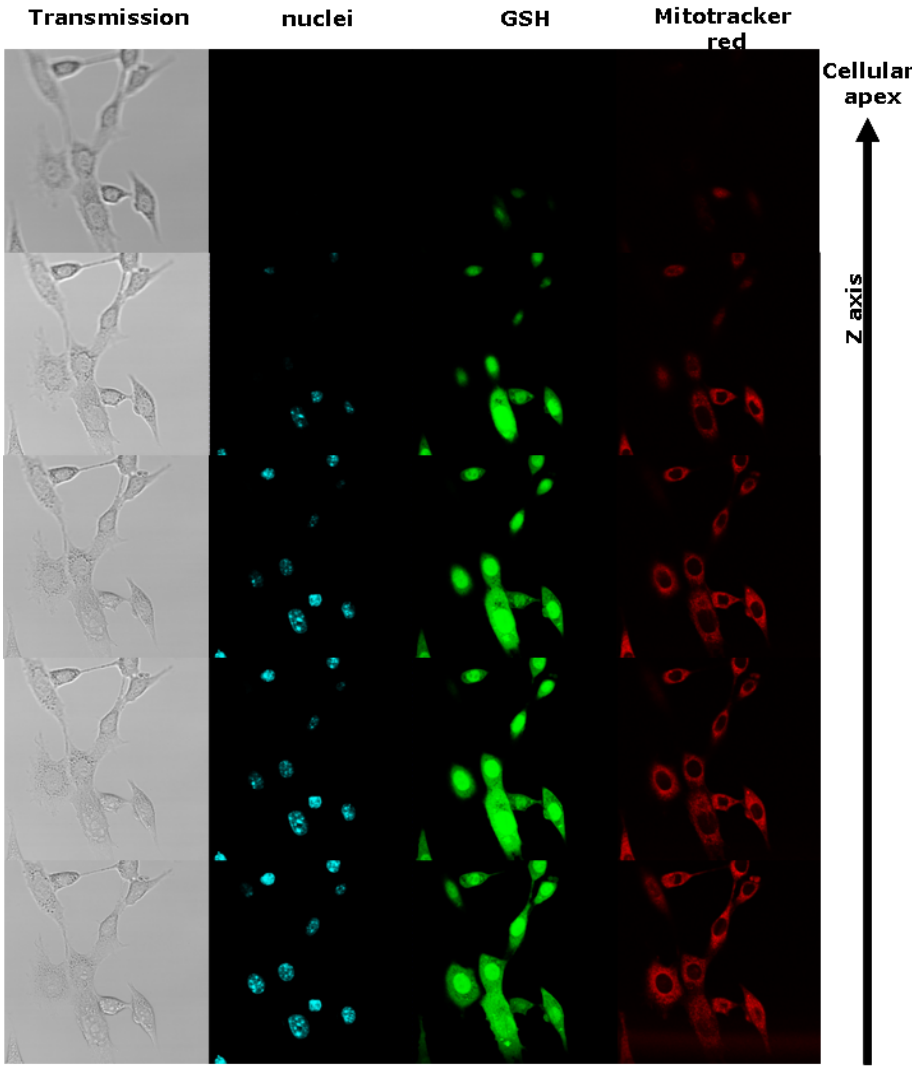

Figure 30. Cellular distribution of GSH and mitochondria in 3T3 fibroblasts after 24 h in culture. Cells were grown and stained and images obtained as described in "Materials and Methods". Blue fluorescence of nuclei dyed by Hoechst, green fluorescence of CMFDA that marks GSH, and fluorescence of MitoTracker Red 580 that stains mitochondria were captured by confocal microscopy. Each panel shows the Z-section series.

obtained beginning from the nuclear apex and progressing downward in 1 ± 0.2-µm increments.

The nuclear shape is clearly visible as is the presence of GSH in the nucleus. Mitochondrial distribution was perinuclear, as expected.

In conclusion, we have shown that cells need a reduced nuclear environment provided by glutathione to proliferate (see Fig. 31). Indeed, the nucleus/cytoplasm ratio was high several hours after plating.

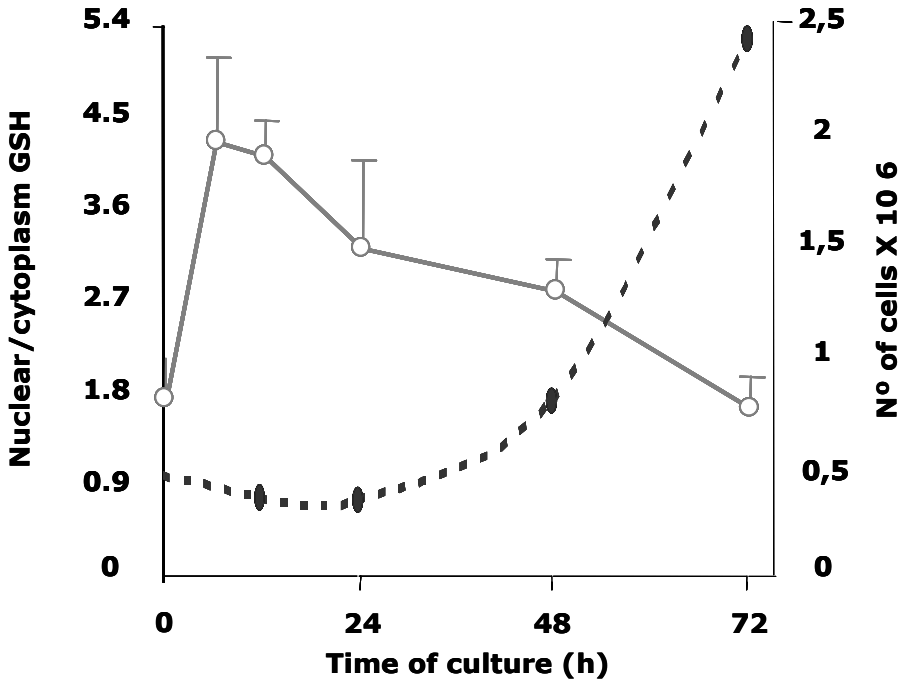

Figure 31. Correlation between nuclear GSH distribution and cell growth. The number of cells x106 is shown on the right y axis. The nucleus/cytoplasm GSH ratio is shown on the left y axis. Data are expressed as the mean ± SD of ten different experiments.

Thus, glutathione translocates to the nucleus before exponential cell growth. When cells reached confluence, at 3 and 5 days after plating, GSH distribution was similar in both cell compartments, nucleus and cytoplasm.

III THE DEPLETION OF NUCLEAR GSH AND THE CELL CYCLE

1. Design and characterization of the model of nuclear GSH depletion

1.1 DEM and BSO have different effect on the level of GSH and rhythm of its fluctuations during cell culture

1.2 DEM but not BSO causes the depletion of nuclear glutathione

1.3 Quantification of the nuclear GSH levels after the depletion with DEM and BSO

2. Depletion of nuclear GSH impairs cell growth

2.1 The rhythm of cell growth change with the nuclear GSH depletion (Fig. 35)

2.2 The difference in cell number along the cell cycle is not due to the induction of cell death

3. Alterations of the cell cycle were induced by depletion of the nuclear but not the cytoplasmic GSH

3.1 Flow cytometry analysis of the consequences of the nuclear GSH depletion

3.2. The effect of nuclear GSH depletion on the cell proliferation markers

III THE DEPLETION OF NUCLEAR GSH AND THE CELL CYCLE

1. Design and characterization of the model of the nuclear GSH depletion

To confirm the importance of nuclear GSH in the onset of cell proliferation we have designed a model based on the different effects of two depleating agents: diethyl maleate (DEM) and buthionine sulfoximine (BSO) on the cellular GSH level and distribution. DEM causes direct and instantaneous GSH depletion that affects all cell compartments. In contrast, BSO induces irreversible inhibition of gamma-glutamylcystein synthetase, thus gradually decreasing GSH level. Moreover, it has been demonstrated that nuclear GSH pool remains intact in the treatment with BSO.

This model allowed us to explore the differential effects of GSH depletion depending on the cell compartment affected.

1.1 DEM and BSO produce different consequences on the level of GSH and rhythm of its fluctuations during cell culture

The Fig. 32. shows the intensity of the GSH depletion and the rhythm of changes in GSH level in the four experimental groups included in our model. A clear decrease of GSH levels was observed in the cells treated with DEM at 6h of culture, while the similar decrease induced by BSO treatment did not

occur until 24h of culture (7,28 y 8,10 nmoles/mg prot., respectively, no significant difference).

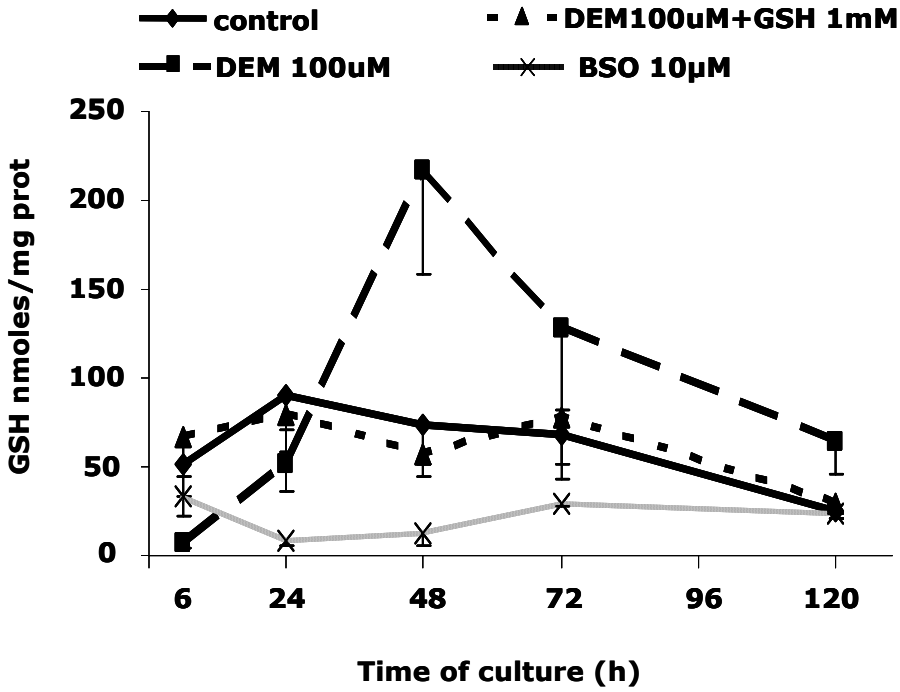

P significance

	6h	24h	48h	72h	5 days
C vs DEM	**0,000**	**0,018**	**0,036**	**0,035**	**0,016**
C vs DEM+GSHe	0,358	0,478	0,087	0,485	0,243
DEM vs DEM+GSHe	**0,001**	**0,070**	**0,018**	0,115	**0,037**
C vs BSO	**0,053**	**0,000**	**0,001**	**0,000**	0,549
DEM vs BSO	**0,003**	**0,000**	**0,007**	**0,001**	**0,011**
DEM 6h vs BSO 24h	0,613				

Figure 32. The time course analysis of the GSH level after depletion with DEM and BSO. The cells were plated as described previously and after attaching 100µM DEM, or 10mM BSO, or 100µM DEM+1mM GSH were added. The total cellular concentration of GSH was determined spectrophotometrically as described in "Materials and Methods". The results are presented as mean ± SD of at least five different experiments. The table of p significance derives from double ANOVA test followed by t student.

The level of GSH in the cells treated with BSO increased slowly and steadily, but was maintained significantly inferior to other experimental groups, until 5 days of culture when the difference was not significant any longer (except vs. DEM)

On the contrary, the level of GSH in the DEM treated cells rapidly increased; at 24h was already higher than in the case of BSO but still did not reach the level of control (51,96 nmoles/mg prots. comparing to 90,64, respectively, $p \leq 0,018$).

At 48h a rebound effect was observed, which to a lesser extent persisted until 72h, and declined significantly at 5 days of culture.

The cells simultaneously treated both with DEM and GSH ester, displayed similar pattern to the control, with the peak at 24h. Therefore, the effect of GSH depletion by DEM was completely compensated by the simultaneous addition of GSH ester.

1.2 DEM but not BSO causes the depletion of nuclear glutathione

Following the determination of the total cellular GSH level we studied the distribution of cellular GSH between the cytoplasm and the nucleus of the cells. As could be seen in Fig 33. untreated fibroblasts during 24 hours in culture showed that GSH (CMFDA staining-green fluorescence) was mainly distributed in the cell nucleus since it co-localizes with the DNA distribution (Hoechst-blue fluorescence).

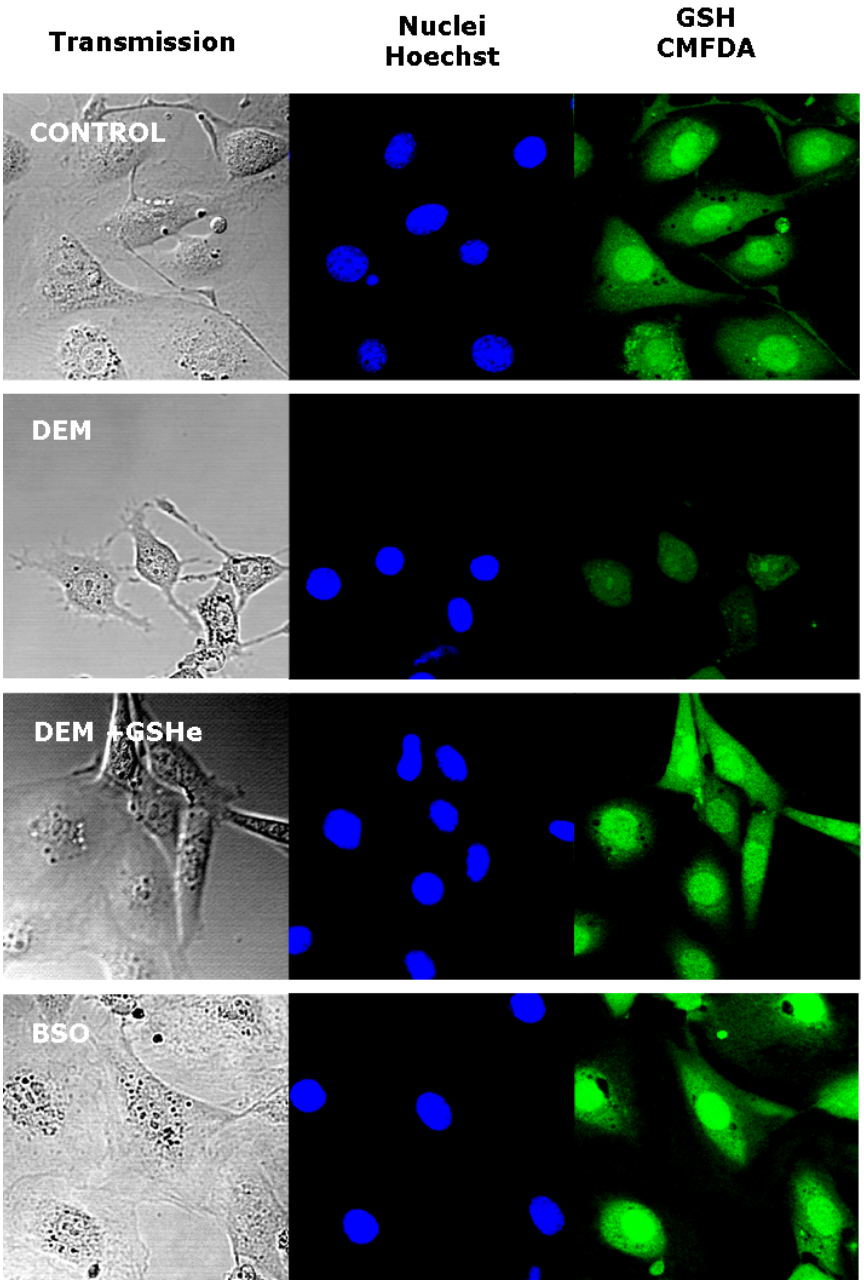

Figure 33. The confocal microscopy analysis of the GSH distribution after its depletion with DEM and BSO. The cells were plated as described previously and after attaching, 100μM DEM, or 10mM BSO, or 100μM DEM+1mM GSH were added. At 24h after plating the cells were stained as described in Materials and Methods and observed by confocal microscopy. Z series of at least 8 planes were obtained and maximum projection images were created and analysed. The representative experiment is presented.

However, cells incubated with 100 µM DEM showed clearly lower GSH level and more uniform GSH distribution within the cells. Surprisingly, the GSH depleting agent BSO was unable to change the distribution of cellular GSH, showing a cellular glutathione pattern different that the one shown in the DEM-treated cells. GSH was high in the nucleus and low in the cytoplasm, like in the control group.

Thus, each GSH-depleting agent induced different responses in the distribution of cellular GSH when fibroblasts were proliferating. As expected, co-incubating the cells with 100 µM DEM and 1mM GSHe showed similar glutathione distribution as untreated cells.

1.3 Quantification of the nuclear GSH levels after the depletion with DEM and BSO

Measurement of the fluorescence emission in the nuclear area (Fig. 34) showed that GSH levels in the nucleus of DEM treated cells was significantly lower than in the other groups of cells studied, including the BSO treated fibroblasts. BSO caused no effect on the nuclear GSH level, and the simultaneous administration of GSH ester completely abolished the effect of DEM.

In conclusion, the DEM treatment depletes GSH in the whole cell, while BSO shows no effect on the nuclear GSH.

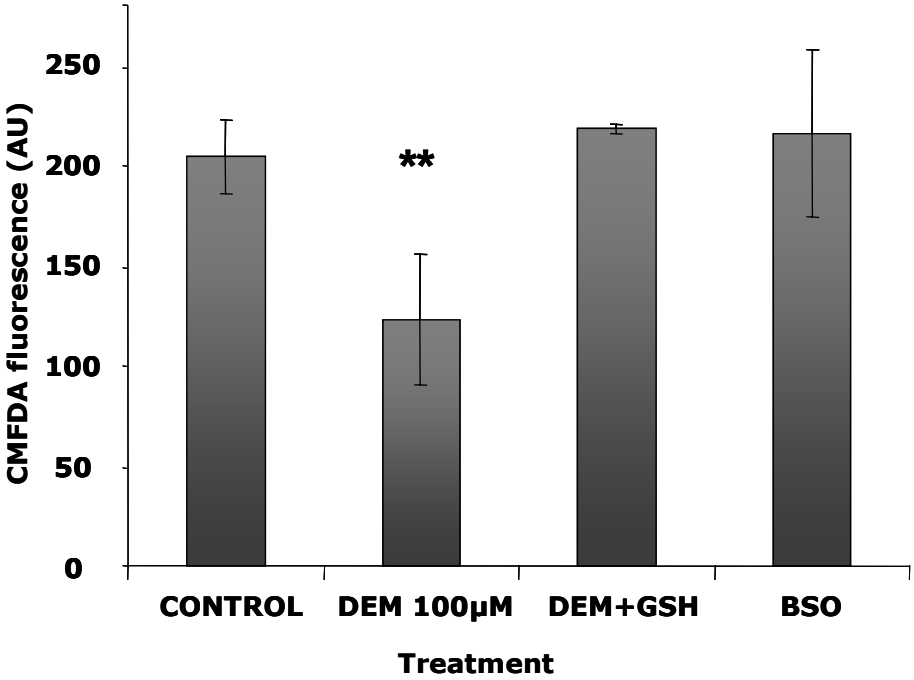

Figure 34. The effect of the depletion with DEM and BSO on nuclear GSH in 3T3 fibroblasts 24h in culture. The maximum projection images (as presented in the fig 33) were analysed by area, as described in "Materials and Methods". The results presented are mean ± SD values from at least 4 different experiments (50-80 cells per experiment) and the statistical significance is expressed as: ** $p < 0.01$ versus control value.

Following the characterization of the model, we proceeded to the study of the possible consequences of nuclear GSH depletion on cell proliferation.

2. Depletion of nuclear GSH impairs cell growth

2.1 The rhythm of cell growth change with the nuclear GSH depletion (Fig. 35)

Control 3T3 fibroblasts grew slowly during the first 24 hours in culture and reached exponential phase of cell

growth between 24 and 72 hours, when cells reached confluence and stopped growing; there were no significant difference in cell number comparing to the day 5.

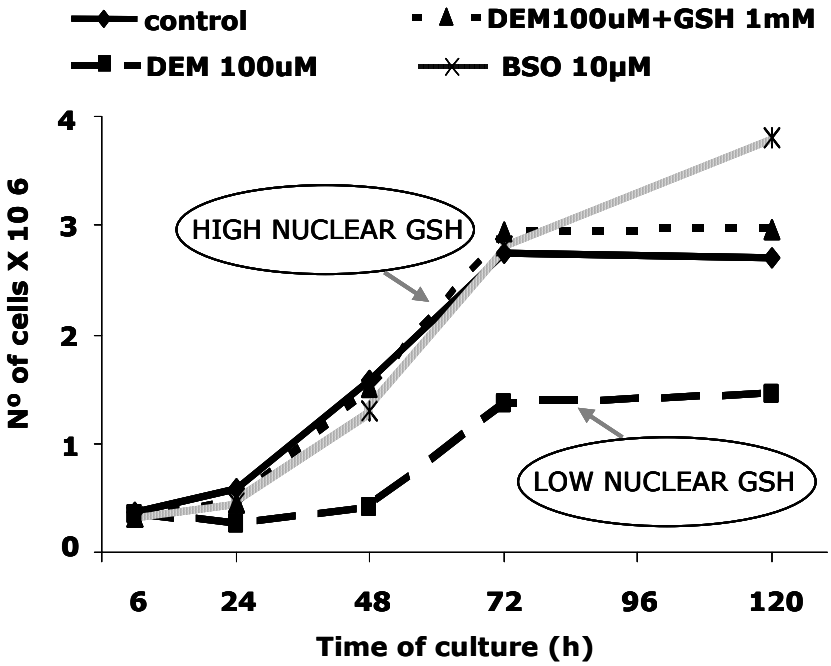

P significance

	6h	24h	48h	72h	5 days
C vs DEM	0,553	**0,000**	**0,000**	**0,000**	**0,001**
C vs DEM+GSHe	0,861	0,275	0,751	0,611	0,759
DEM vs DEM+GSHe	0,830	**0,000**	**0,000**	**0,001**	**0,001**
c vs BSO	0,543	0,050	0,163	0,868	0,129
DEM vs BSO	0,891	**0,001**	**0,000**	**0,000**	**0,030**

Figure 35. Nuclear GSH depletion (treatment with DEM) decreases the rate of cell growth in 3T3 fibroblasts. Cells were plated and treated as described previously, detached by trypsinization and counted. The proliferation curves are created on the bases of the mean results of at least 5 different experiments.

Fibroblasts incubated with 10 μM BSO exhibited a growth trend similar to controls, with a discrete delay detectable only at 24h, and even remained growing for a longer time than untreated cells (day 5 of culture). However, the cells treated with DEM 100 μM showed a very low growing profile. In the first 48h of culture, when the control group expands extremely, this cell population showed no increase: there was no significant difference in cell number from the beginning of culture until 48h later. The visible growth occurred between 48 and 72h and remained the same until 5 days of culture. The cell number was, at all time points, significantly lower ($p \leq 0{,}001$), and at the end of the culture this cell population hardly exceeded half of the control population ($1{,}46 \times 10^6$ and $2{,}71 \times 10^6$, respectively). When DEM-treated cells were co-incubated with 1mM glutathione ethyl ester (GSHe), in order to replenish GSH levels, cells grew at a similar rate to controls.

2.2 The difference in cell number along the cell cycle is not due to the induction of cell death

The different growing behaviour in the cells with depleted nuclear GSH was not due to an increased rate of cell death (Fig. 36). Indeed, the percentage of apoptotic and necrotic cells remained below 5% throughout the cell culture. Only during the fifth day in culture i.e. when control and DEM+GSHe treated cells reached confluence, an increase in

the number of dead cells was shown, but not in the DEM and BSO treated cells.

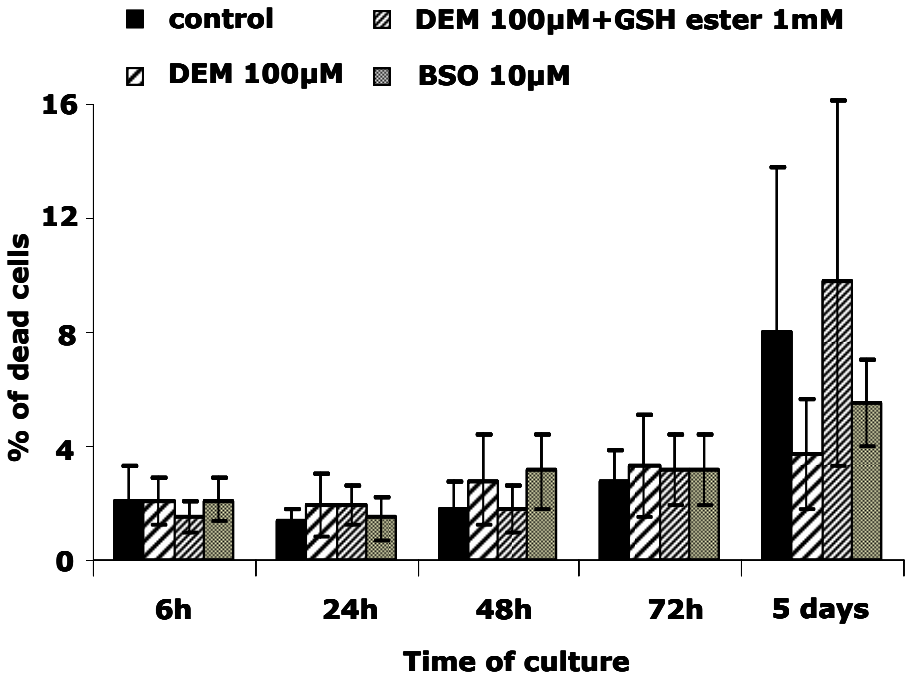

Figure 36. The effect of the GSH depletion on cell death in 3T3 fibroblasts. The sum of the percentage of apoptotic and necrotic cells along the proliferation curve of the 3T3 fibroblasts is shown. The cell death was studied by flow citometry analysis of the DNA content, and the results presented are mean±SD of at least five different experiments.

To summarize, the nuclear GSH depletion (with DEM) had severe consequences on the cell growth. On the contrary, when only the cytoplasmatic GSH was depleted (BSO) no marked differences were observed.

3. Alterations of the cell cycle were induced by the depletion of the nuclear but not the cytoplasmic GSH

3.1 Flow cytometry analysis of the consequences of the nuclear GSH depletion

Figure 37. shows the differences in the percentage of cells in the different phases of the cell cycle during the time of culture.

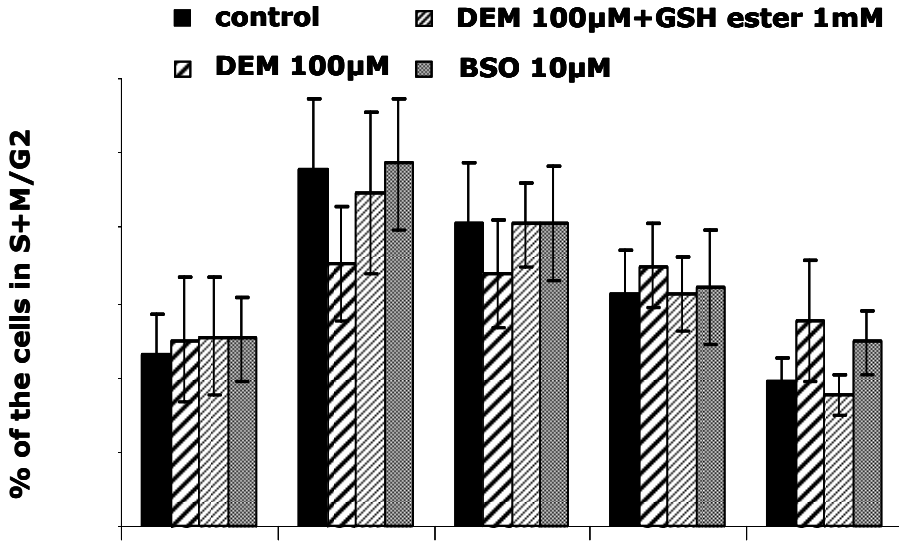

	6h	24h	48h	72h	5 days
C vs DEM	0,426	**0,001**	**0,018**	**0,057**	**0,012**
C vs DEM+GSH	0,556	0,439	0,942	0,934	0,319
DEM vs DEM+GSH	0,928	**0,041**	**0,026**	0,081	**0,005**
C vs BSO	0,416	0,786	0,958	0,657	0,295

Figure 37. The effect of the depletion of the nuclear GSH (treatment with DEM) on the cell cycle in 3T3 fibroblasts. Cells were plated and treated as described previously. The cell cycle was analysed by flow citometry detection of the changes in the DNA content, as described in Materials and Methods. The results correspond to mean±SD of at least 5 different experiments.

As expected, the percentage of cells in the phases S, M and G2 of the cell cycle was higher when cell were growing, i.e. at 24h (47,7±9,8%), 48h (40,7±8,2%) and 72 hours (30,9±6,2%) in culture. However, in those cells that were treated with DEM the percentage of cells in either proliferation phase S, or G2/M was lower (24-48 hours of culture) than in controls ($p \leq 0{,}001$, and $p \leq 0{,}018$, respectively). As expected BSO and DEM+GSHe treated cells showed results similar to control fibroblasts.

3.2. The effect of nuclear GSH depletion on the cell proliferation markers

In order to find a molecular explanation for the impairment of the cell cycle caused by the depletion of nuclear GSH levels with DEM, we studied the expression of the cell cycle-related protein Id-2.

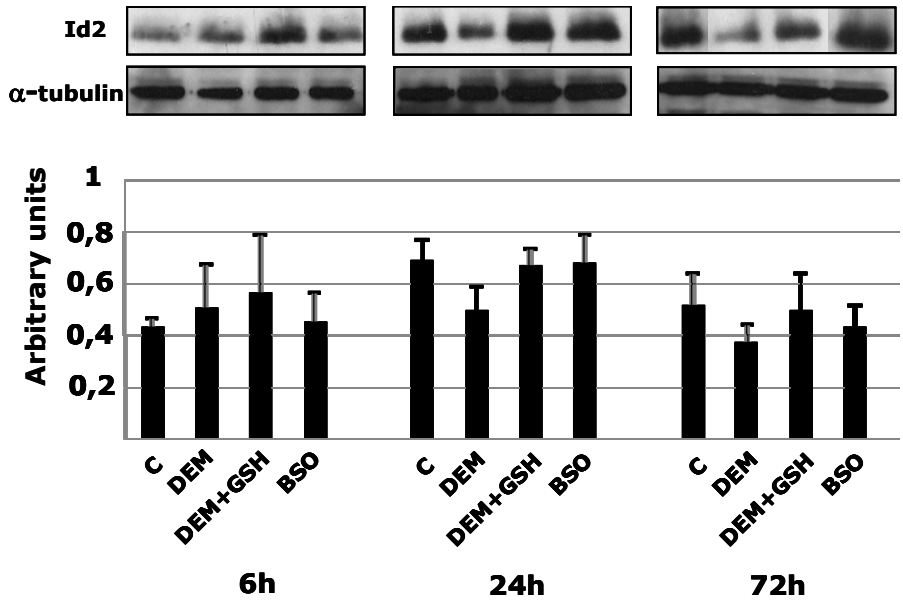

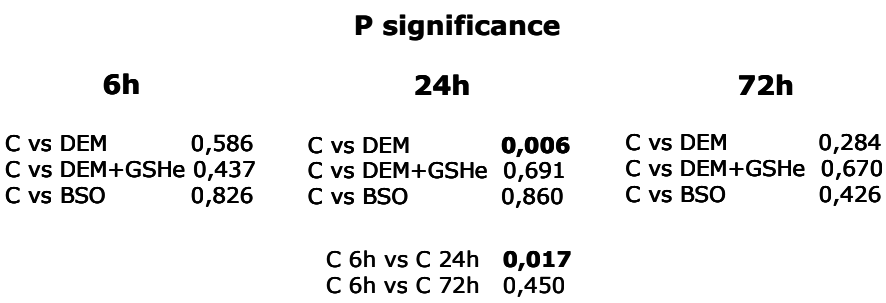

Figure 38. The expression of the cell proliferation marker, Id2, after the depletion of the nuclear GSH (treatment with DEM). At upper panel, Western blot analysis of Id2 in 3T3 fibroblasts at 6, 24, and 72h of culture is shown. Lower panel shows the Id2 content [Mean ± SD (n=4)] derived from densitometry.

Figure 38. shows that Id-2 expression, decreased in the DEM, but not in the BSO treated cells or in the DEM+GSHe treated cells.

Thus, depletion of nuclear, but not cytoplasmic glutathione levels is able to decrease Id-2 expression, impairing cell growth.

IV SEARCHING FOR THE MECHANISM TO EXPLAIN THE NUCLEAR COMPARTIMENTALIZATION OF GLUTATHIONE

1. The implication of the active transport or nuclear GSH synthesis *de novo* were not confirmed in our model

1.1 The depletion of ATP failed to prevent the nuclear GSH compartimentalization.

1.2 No evidence on the possible nuclear GSH synthesis could be discovered

2. Bcl-2 as a potential mediator of the nuclear GSH compartmentalization

2.1 The elevated nuclear presence of Bcl-2 concurred with the high GSH level in the nucleus in 3T3 fibroblasts.

3. The importance of Bcl-2 in nuclear compartmentalization of GSH and its consequences on the proliferation activity. Study in MCF7 cells that over express Bcl-2.

3.1 Bcl-2 induces a rapid increase in total cellular GSH level soon after cell plating

3.2 The Bcl-2 could be responsible for an early increase of nuclear GSH in MCF7 cells

3.3 Bcl2 causes augmentation in the maximal TA level which is delayed comparing to the peak of GSH level.

3.4 Bcl-2 had no significant consequences on cell proliferation in MCF7 cells

IV SEARCHING FOR THE MECHANISM TO EXPLAIN NUCLEAR COMPARTIMENTALIZATION OF GLUTATHIONE

One of the important questions that impose itself is the possible mechanism implicated in the nuclear compartmentalization of GSH.

1. The implication of the active transport or nuclear GSH synthesis *de novo* were not confirmed in our model

1.1 The depletion of ATP failed to prevent the nuclear GSH compartmentalization.

In order to elucidate the origin of the high nuclear GSH level we have considered that the tripeptide could enter the nucleus by an active, ATP dependent transport. We incubated 3T3 fibroblasts 24h in culture, when the nuclear compartmentalization is maximal, with FCCP, a mitochondrial uncoupling agent.

As shown in Fig. 39 A, 20μM FCCP decreased the ATP levels in treated cells to 40% of its control. Nevertheless, the results shown in Fig. 39 B imply that glutathione concentrates in the nucleus by an ATP-independent process, because the glutathione distribution was similar in both treated and untreated cells.

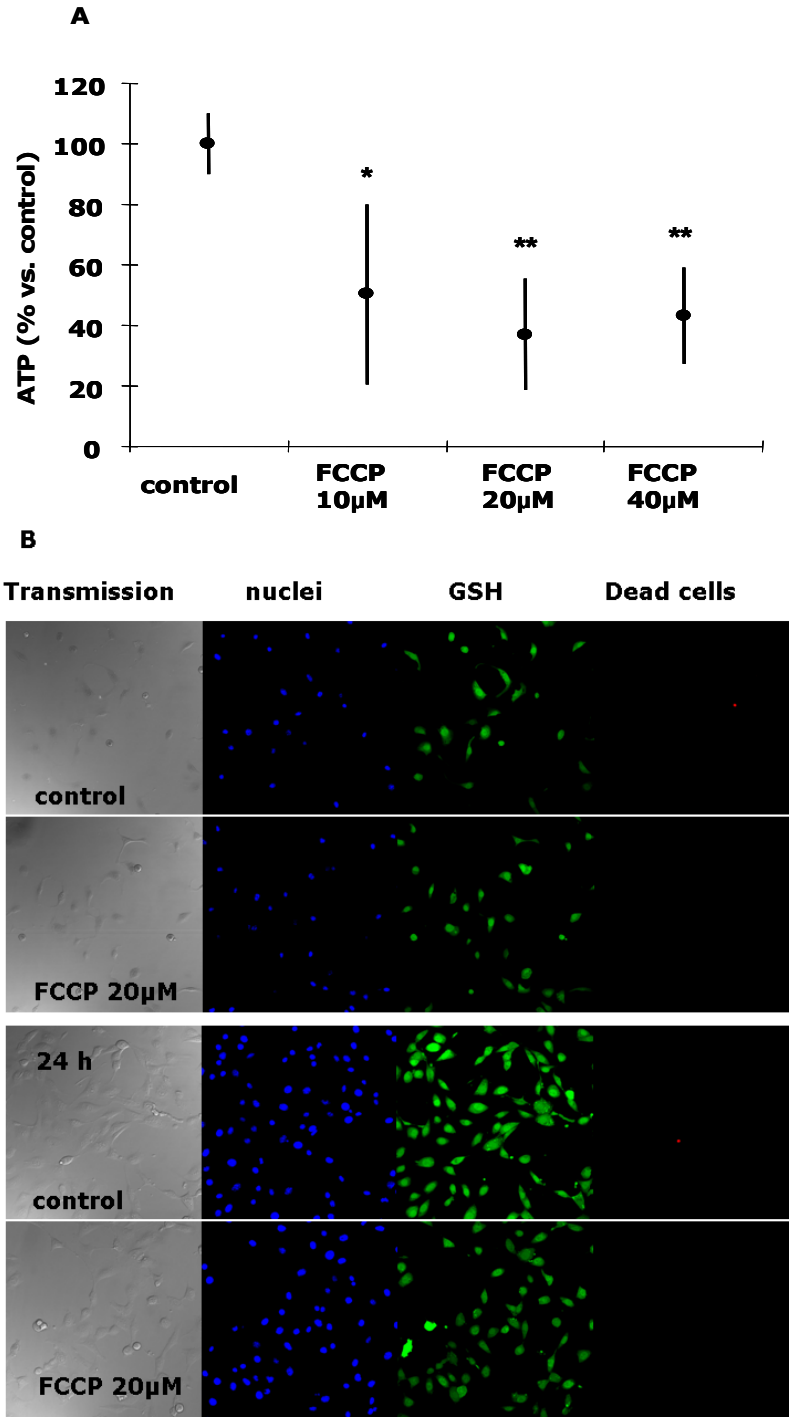

Figure 39. Glutathione distribution after ATP depletion. Cells were

incubated for 120 min with 10, 20 and 40 µM FCCP and the level of the ATP depletion is shown in the graph A. The results are presented as mean ± SD (n=3). The consequences of ATP depletion with 20 µM FCCP on GSH distribution are presented in the image B. *Blue* fluorescence of nuclei dyed by Hoechst, *green* fluorescence of CMFDA that marks GSH, and PI staining for dead cells were captured by confocal microscopy as described in "Materials and Methods".

1.2 No evidence on the possible nuclear GSH synthesis could be discovered

An additional possible explanation for the reported nuclear increase in GSH during the early phases of cell cycle would be the nuclear GSH synthesis. We studied the presence of the enzymes for GSH synthesis GCS and GSH synthetase. Fig. 40 shows a lack of expression of the rate-limiting enzyme GCS (1) in nuclear extracts, whereas samples from whole cells showed a marked expression.

Figure 40. Expression of glutamyl cysteine synthetase (GCS) in nuclear and cellular 3T3 fibroblasts extracts. 3T3 cells were subjected to nuclear protein extraction, and a Western blotting procedure was performed in nuclear lysates. The membrane was probed against anti-GCS antibody (1:750) (NeoMarkers, rabbit polyclonal antibody)

Thus, under our experimental conditions, the nuclear synthesis of GSH seems improbable.

2. Bcl-2 as a potential mediator of the nuclear GSH compartmentalization in 3T3 fibroblasts.

One of the proposed mechanisms of the entrance of GSH to the nucleus involves the transport mediated by Bcl-2, an anti-apoptotic protein whose over expression is shown to increase nuclear glutathione level (2)

2.1 The elevated nuclear presence of Bcl-2 concurred with the high GSH level in the nucleus in 3T3 fibroblasts.

The presence of Bcl-2 was studied in nuclear extracts of 3T3 fibroblasts 6, 24, 48h and 5 days in culture (Fig. 41). Interestingly, we have found it to express the highest levels in early phases of cell culture, at 6h and 24h, and decreases starting from 48h of culture.

Figure 41. Expression of Bcl-2 in nuclear extracts of 3T3 fibroblasts. 3T3 cells were subjected to nuclear protein extraction, and a Western blotting procedure was performed in nuclear lysates. The membrane was probed against anti-bcl2 antibody (1:1000) (rabbit polyclonal IgG, Santa Cruz Biotechnology)

Our result points to a correlation between the expression of Bcl-2 during the cell cycle and the distribution of cellular

GSH. When cells are dividing (6 and 24 h of culture), the presence of nuclear Bcl-2 is high, but it decreases later (48 h and 5 days of culture) when cell growth stops.

3. The importance of Bcl-2 in nuclear compartmentalization of GSH and its consequences on the proliferation activity. Study in MCF7 cells that over express Bcl-2.

In attempt to elucidate the possible implication of Bcl-2 in the nuclear compartimentalization of GSH we have used the cell line obtained by the stable transfection of MCF7 cell with the oncogen Bcl-2, "MCF7 Bcl-2" cells.

3.1 Bcl-2 induces a rapid increase in total cellular GSH level soon after cell plating

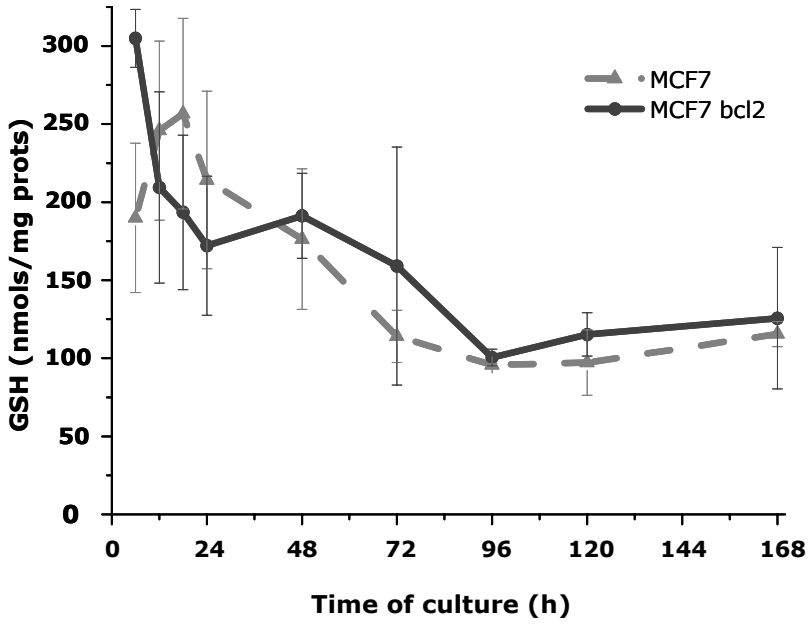

MCF7 wt vs. MCF7 bcl2

Time of culture	6	12	18	24	48	72	96	120
p	**0,001**	0,166	**0,015**	**0,045**	0,675	0,555	0,429	0,229

Figure 42. **The effect of bcl-2 on cellular GSH level in MCF7 cells.** The cells were plated as desribed above and the acid extracts were obtained as described in "Materials and Methods". The total cellular concentration of GSH was determined spectrophotometrically as described in "Materials and Methods". The results are presented as mean ± SD of at least five different experiments. The table of p significance derives from double ANOVA test followed by t student.

The MCF7 Bcl-2 cells had exceptionally high GSH value at 6h of culture (304,93±18,51 nmols/mg prot., p≤0,001 vs. MCF7) (Fig. 42). Afterwards, the level of GSH descended swiftly and at 18h of culture was already lower than in MCF7 cells (p≤0,05), which had their maximal GSH value at this time point. Total cellular GSH in MCF7 Bcl-2 cells continued to decline until 24h when it started to increase again. It stayed higher than in wild type MCF7 until the end of the culture, but the difference was not significant.

3.2 Bcl-2 could be responsible for an early increase of nuclear GSH in MCF7 cells

3.2.1 The confocal microscopy analysis of the nuclear compartmentalization of GSH.

The high level of total cellular and nuclear GSH (green CMFDA fluorescence) could be observed in both cells lines, particularly before 24h of culture (Fig. 43).

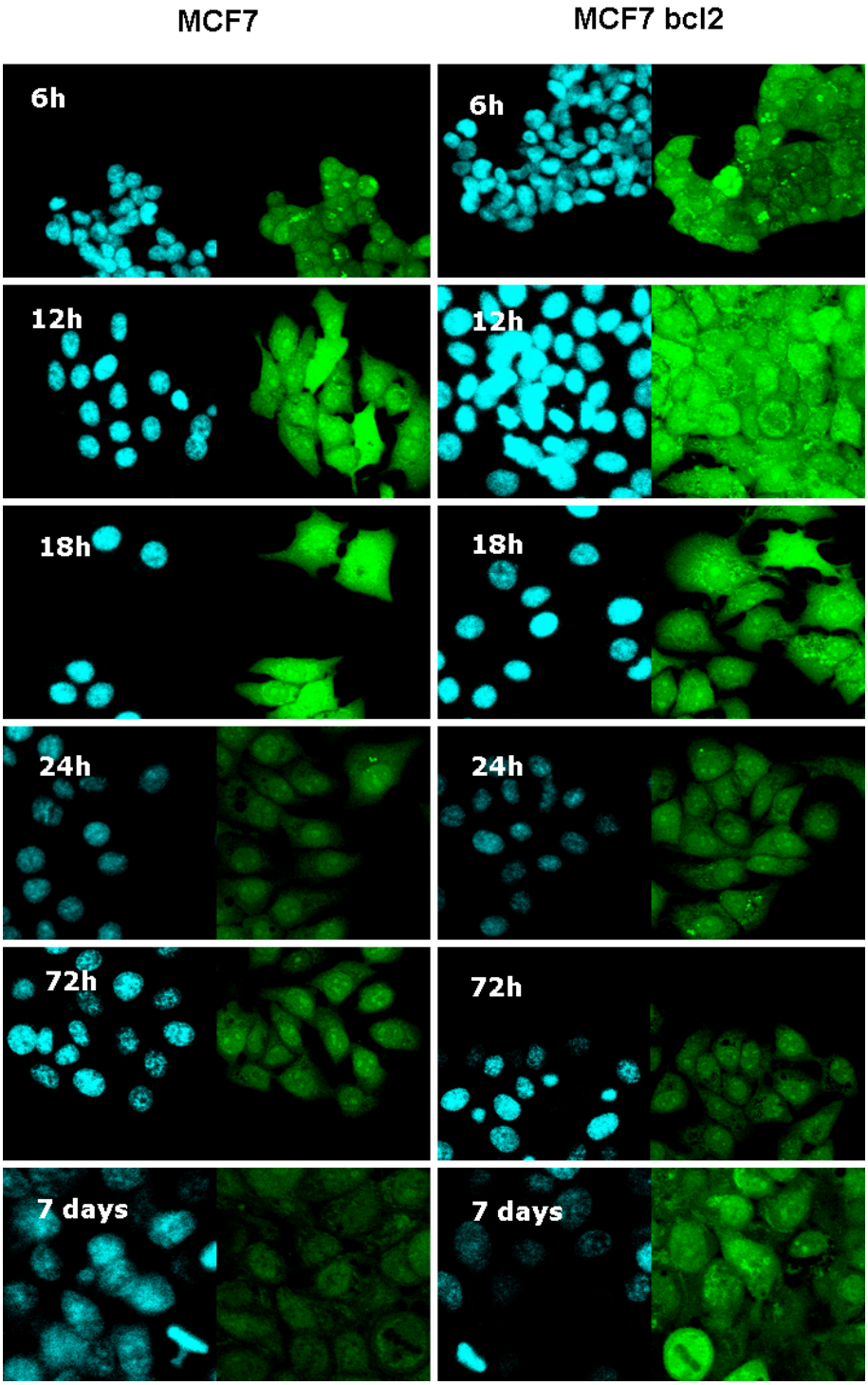

Figure 43. The confocal microscopy study of the effect of bcl-2 on the cellular distribution of GSH. MCF7 and MCF7 bcl2 cells were plated

7days, 72h, 24h, 18h, 12h, and 6h before the experiment as described in "Materials and Methods" and analyzed the same day. The staining was performed as described previously and the maximum projection images derive from 7-10 Z axis planes. The representative experiment is shown.

The nuclear compartmentalization of GSH became perceptible starting from 12h in culture in both cell lines. Although the level of the fluorescence decreased during the cell culture, in coherence with the decreased level of the total cellular GSH (obtained by biochemical analysis), the level of nuclear GSH compartmentalization seemed unchanged until 7 days in culture. Even in the advanced culture of cancer cells, some dividing cells with high GSH content and its nuclear localization could still be seen on the plate.

3.2.2 The quantification of the nuclear CMFDA fluorescence level in early phases of cell culture

At 12h of culture (Fig. 44) MCF7 Bcl-2 cells have reached the peak of nuclear GSH ($p \leq 0,01$ vs. 6h) and had significantly higher level of nuclear GSH than wild type ($p \leq 0,05$). On the contrary, at 18h of culture, the nuclear GSH level in transfected cells already decreases, although not significantly, while MCF7 cells reach their maximal nuclear GSH value.

The quantification of the nuclear levels of CMFDA fluorescence showed that Bcl-2 might cause the early increase of nuclear GSH level in MCF7 cells.

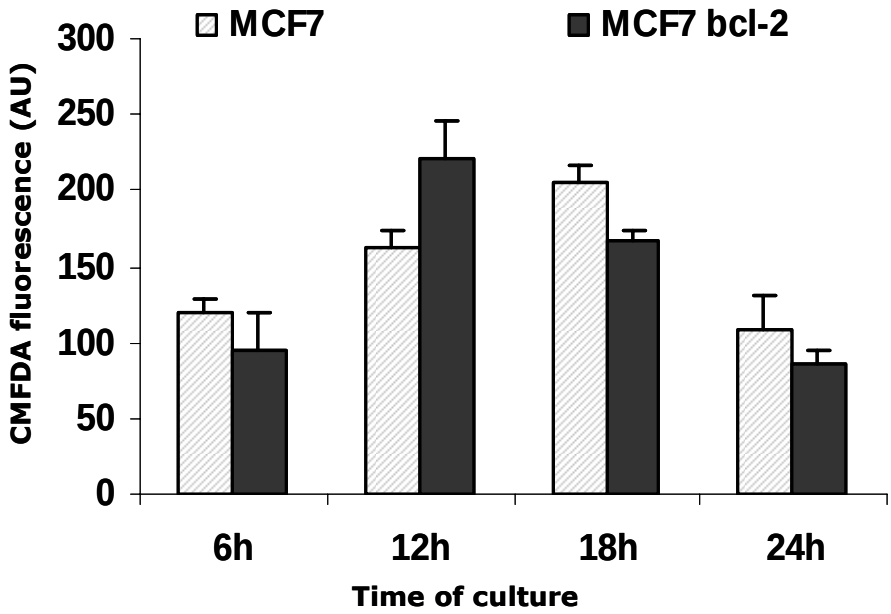

WT vs bcl2	6h	12h	18h	24h
p	0,21	**0,05**	**0,02**	0,22
MCF7	6 vs. 12h	12h vs. 18h	18h vs. 24h	
p	**0,006**	**0,012**	**0,006**	
MCF7 bcl2	6 vs. 12h	12h vs. 18h	18h vs. 24h	
p	**0,004**	0,068	**0,000**	

Figure 44. The effect of bcl-2 on nuclear GSH level in MCF7 cells The maximum projection images (as presented in the fig) were analysed by area, as described in "Materials and Methods". The results presented are mean values ± SD from 2 different experiments (200-500 cells per experiment). The table of p significance derives from double ANOVA test followed by t student.

3.3 Bcl2 causes augmentation in the maximal TA level which is delayed comparing to the peak of GSH level.

As previously shown (Fig. 9), the peak of telomerase activity of MCF7 cells was at 18h and it coincided with the peak of GSH. In MCF7 Bcl-2 cells, the peak of TA was at 12h-6h earlier comparing to the MCF7 cells (Fig. 45). Moreover, the increase comparing to 6h was four fold, and the level was more than double of the maximal TA level observed in MCF7 cells ($p \leq 0,05$ vs. MCF7 cells, and vs. 6h).

However, maximal TA did not coincide with the peak of GSH; it was 6h delayed with respect to the maximal GSH value.

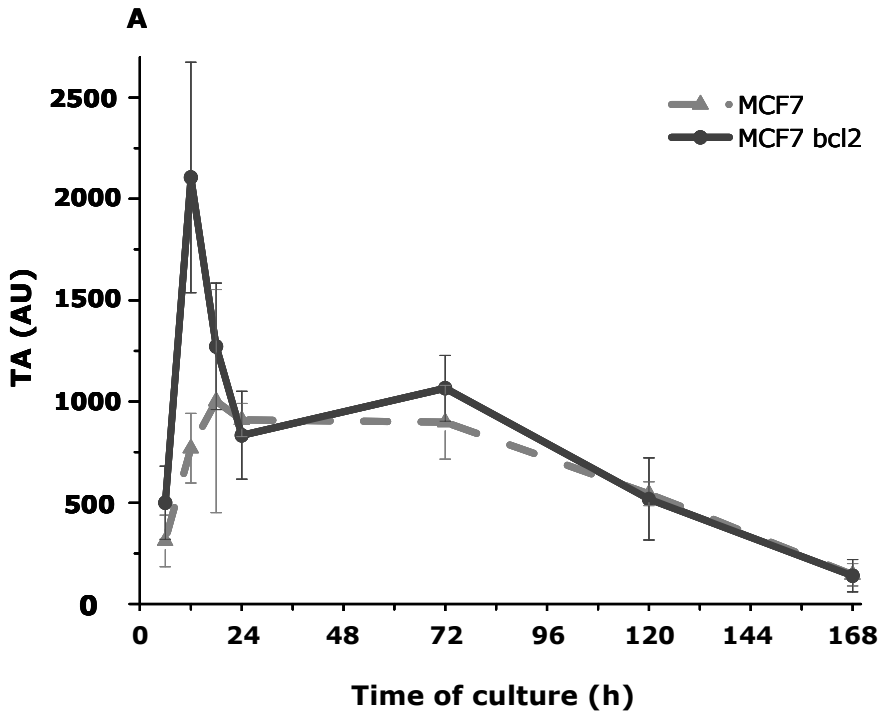

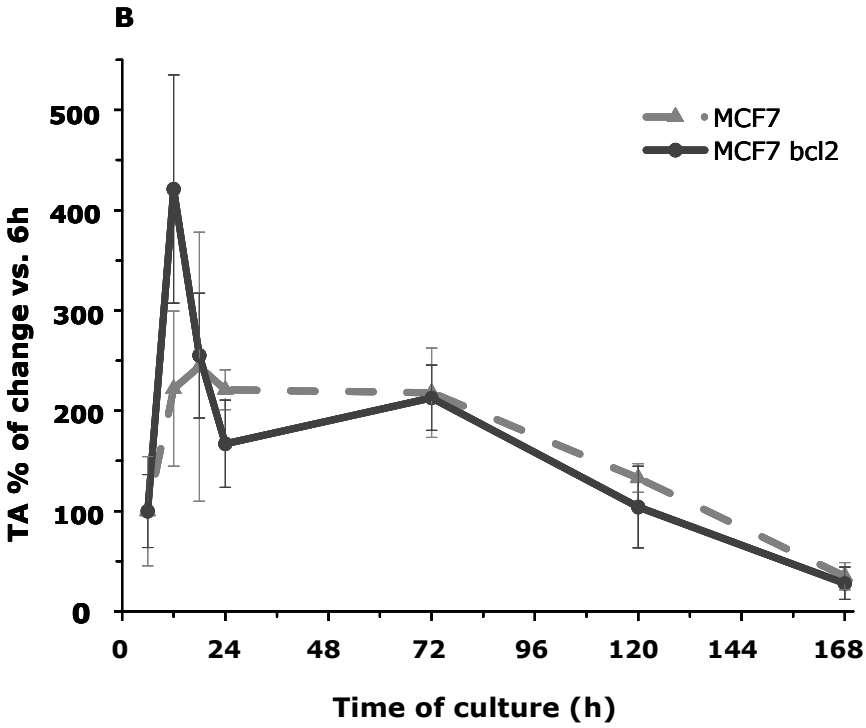

Figure 45. The effect of bcl-2 on telomerase activity in MCF7 cells. The cells were plated, the samples obtained and the relative telomerase activity was measured by TRAP as described in "Materials and Methods". The results are presented as mean ± SD of at least three different experiments (A) and as the % of change of TA along the cell cycle normalized by the value at the beginning of culture (6h) (B).

3.4 Bcl-2 had no significant consequences on cell proliferation in MCF7 cells

The flow cytometry analysis of the DNA content showed no differences between MCF7 and MCF7 Bcl-2 cells (Fig. 46).

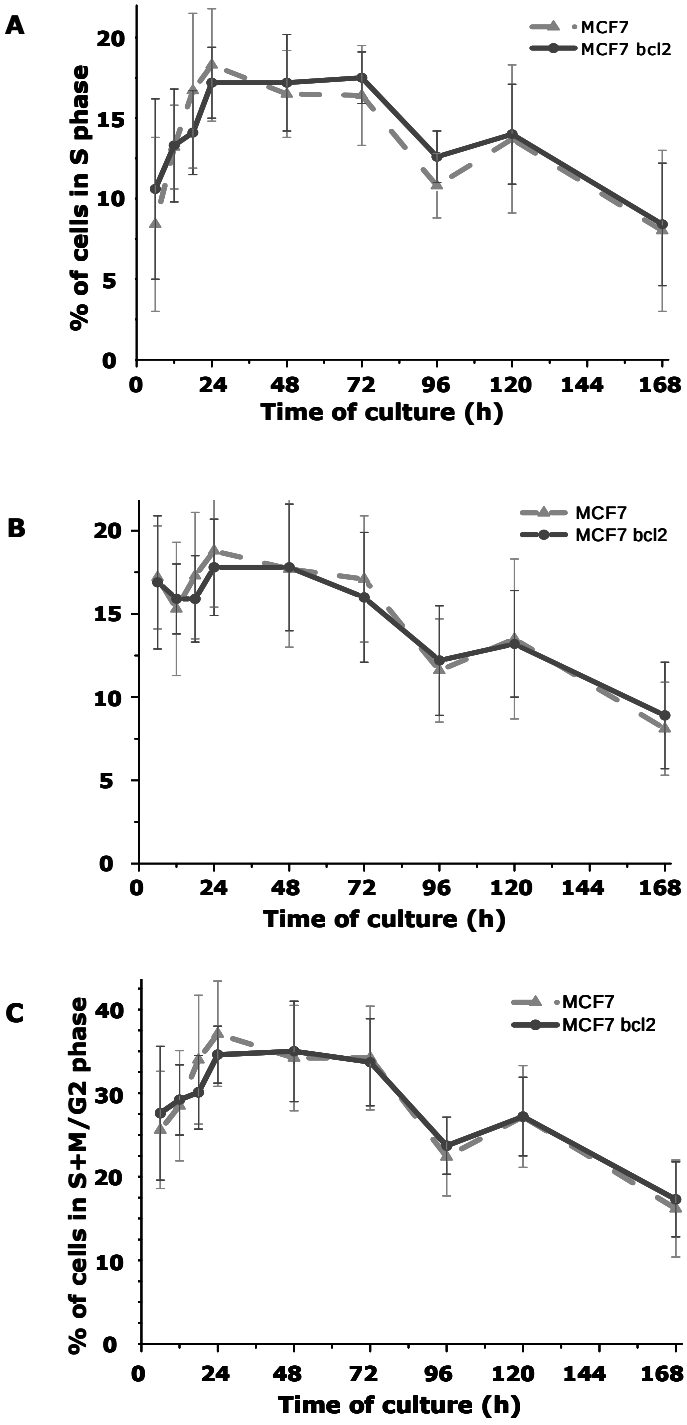

Figure 46. The effect of the bcl-2 on the cell proliferation in MCF7 cells. Cells were plated as described and the flow cytometry analysis of the

DNA content was performed as explained in "Materials and Methods". The results of cell cycle analysis for DNA synthesis (A), M+G2 phase (B), and total cell proliferation activity (S+M/G2) (C) are demonstrated as mean ± SD of at least 5 different experiments.

The percentage of cells in S phase was higher in transfected cells at 6h of culture and again starting from 48h of culture. These fluctuations are coherent with the changes in GSH level along the cell cycle (Fig. 42), but the differences are not statistically significant.

The study of the expression of cell proliferation marker, PCNA, confirmed the extended length of exponential growth phase of MCF7 cells (high expression 24-72h), but lacked to show any significant differences caused by Bcl-2 (Fig. 47)

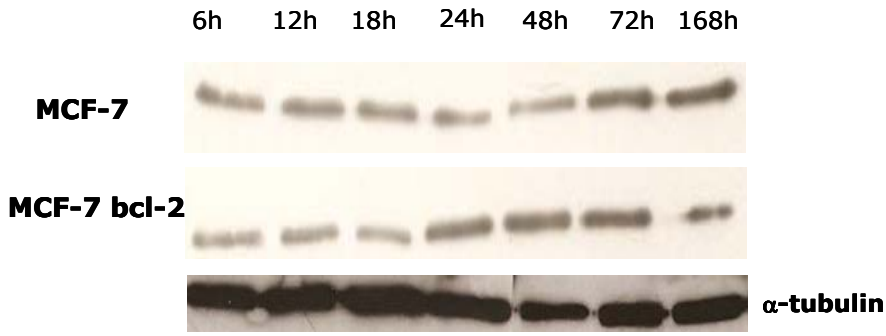

Figure 47. The effect of the bcl-2 on the expression of the cell proliferation marker, PCNA, along the cell cycle in MCF7 cells. The representative experiment (n=3) is shown.

In conclusion, the peak of telomerase activity (Fig. 45) coincides with the peak of nuclear GSH level (Fig. 44) in both cell types. Bcl-2 seemed to cause the early increase of total cellular GSH level, nuclear GSH level and telomerase activity (Fig. 42, 44 and 45, respectively). These values, although extremely high, did not persist and seemed to have no apparent consequences on the cell growth (Fig. 46).

4. Bibliography

1. Lu, S. C. (1999) Regulation of hepatic glutathione synthesis: current concepts and controversies. *Faseb J* 13, 1169-1183
2. Voehringer, D. W., McConkey, D. J., McDonnell, T. J., Brisbay, S., and Meyn, R. E. (1998) Bcl-2 expression causes redistribution of glutathione to the nucleus. *Proc Natl Acad Sci U S A* 95, 2956-2960

V DISCUSSION

V DISCUSSION

1. Overview of the results

The present thesis offers an insight in the importance of nuclear GSH in cell proliferation.

The research was performed in three different cellular models of diverse proliferating activity: immortalized mouse embryonic fibroblasts 3T3, mammary adenocarcinoma cell line MCF7 and primary embryonic neuralonal culture. The results presented here provide evidence that suggest that the relationship between GSH level and telomerase activity, previously described by our group for 3T3 fibroblasts is a common phenomenon in mammalian cells. Reduced glutathione emerged as a driving force of cell cycle progression; high level of GSH coincided with the peak of telomerase activity and preceded the exponential phase of cell growth in all three cell types analyzed. Moreover, the comparative studies of three distinct proliferating models revealed that the level of GSH corresponded to the intensity of the proliferation and clearly correlated with the level of DNA synthesis. This finding inspired the focus on the nuclear compartmentalization of GSH. Interestingly, nuclear localization of GSH was observed before the exponential phase of cell growth in all three cell types, while the GSH

distribution within the cell was uniform when the cells stopped proliferating. Comprehensive analysis of the nuclear GSH levels along the cell cycle, and the experiments with the depletion of nuclear GSH conducted in 3T3 fibroblasts, provided further evidence on crucial importance of nuclear GSH for the onset of cell proliferation. In the attempt to elucidate the possible mechanism of nuclear GSH compartmentalization, we have found no evidence either of active GSH transport or of its *de novo* synthesis in the nucleus. The implication of bcl2 in nuclear transport of GSH was evaluated in the study of MCF7 cells over-expressing this protein. In this model, bcl2 caused an early and striking increase of total cellular glutathione, nuclear GSH and telomerase activity; unexpectedly, these alterations induced no significant effect on cell proliferation.

In summary, our results reveal the importance of nuclear GSH compartmentalization in early phases of cell proliferation. This study suggests that the control of the cell cycle progression from G1 to S phase is dependent on elevated nuclear GSH levels and originates from its influence on telomerase activity and DNA synthesis.

2. The concurrence of increased levels of total cellular glutathione and telomerase activity before the exponential phase of cell growth is a common feature in the three cell types studied.

2.1. The high level of total cellular glutathione precedes the exponential phase of the cell growth.

The comprehensive comparative study of the relationship between GSH and cell cycle progression in three different models of cell proliferation, presented in this thesis, gave the evidence of the importance of the high GSH levels before the beginning of the cell growth. The same pattern was observed in all three cell types, with minor differences.

In 3T3 fibroblasts the GSH level was high at the beginning of culture and reached its maximal value at 24h, just before the beginning of the exponential phase of the cell growth (Fig. 1), remaining decreased while the cells were approaching confluency. Our finding supports the study of Hutter et al [1] who demonstrated that actively dividing normal fibroblasts had a redox potential of -222mV, which gradually increased while the population was growing and reached maximal level of -188mV when cells were contact inhibited.

In our cancer cell model, MCF7 cells, GSH level reached the peak earlier (at 18h) comparing to 3T3 fibroblasts, and the increased levels were sustained for a

longer period of time. In accordance to this, the interval of intensive cell growth was also longer in MCF7 cells (Fig. 2), and, surprisingly, the beginning of the exponential phase was delayed comparing to 3T3 fibroblasts.

However, in the embryonic neural culture model, we could clearly distinguish two growth patterns: 1) the prominent cell growth in the beginning of the culture which corresponded to the period of the intensive development of rat neural system (14-18th day of gestation, see Materials and Methods) and 2) the interval after 96h of culture when the cell growth was absent since the proliferation of glial cells was prevented (cytosine arabinoside was added, as described in Materials and Methods) and the culture consisted of non-proliferating neurons. Equivalent to the other two cell lines, the intensive growth was preceded and accompanied by the high GSH level, while the differentiated neuronal culture that stopped growing had lower GSH level (Fig. 3).

Thus, our results reveal that, regardless of the cell type studied and the proliferating capacity of the cell culture, the GSH level is always elevated before the cell growth begins; it is maintained during the initiation of the proliferation and decreases together with the growth intensity.

Additionally, the comparative analysis of the intensity of cell growth in these three cell lines revealed important differences in the profiles of the proliferation curves in these

cell types (Fig. 11). 3T3 fibroblasts started growing exponentially at 24h, when the GSH concentration was also at its maximal level. The growth slowed later and the GSH level decreased gradually and the growth slowed as the culture progressed to confluence. MCF7 cells showed a striking increase in cell number starting from 48h, and continued to grow at the same pace until the final time point. This could explain the extremely high number of cells present at the plate, almost double comparing to 3T3 fibroblast.
Regarding embryonic neural culture, due to a very low cell number and growth rate the cell growth profile was complicated to compare on the same scale with other two cell types.

Interestingly, the comparison of the GSH level between three cell lines provides further information that suggests the importance of GSH in cell proliferation. The GSH concentration in MCF7 cells, despite its prompt decrease after 18h, and continuous and gradual decline during the exponential phase of the cell growth, was always higher than the maximal value determined for 3T3 fibroblasts (Fig. 12). In accordance with that, the comparison of the GSH level (Fig. 12) of this culture with 3T3 fibroblasts and MCF7 cells revealed the same pattern as the cell growth; the GSH concentration in embryonic neural culture is lower than in the other two cell types.

Hence, our results indicate that the level of cellular GSH in a particular cell line could define its proliferating capacity and its variations along the cell culture dictate the rhythm of cell proliferation.

This finding is particularly interesting if we consider the importance of aberrant proliferation in various human pathophysiological conditions. Cancer, neurodegenerative processes, atherosclerosis, aging, hyperplasia induced fibrotic responses and wound healing are, basically, altered proliferative events, and, interestingly, have been associated with the alterations in antioxidant pathways and redox regulation [2]. Our results point to reduced glutathione, a major intracellular antioxidant, as a central player and an indicator of the cellular proliferation state.

Our results, in general, are in accordance with the work of Hutter at al, who have studied the redox potential (E) in the normal and malignant cells along the cell cycle.

The E of normal cells fluctuates during the cell cycle; for the proliferation to start it has to decrease at least 30mV comparing to its level in the G_0 phase (where the cells are 100% confluent). On the contrary, in cancer cells, the E remains low throughout the complete cell cycle, even at a high cell density [1]. Our evaluation of the GSH levels along the cell cycle in different models indirectly confirms these findings (Fig. 12).

The work of Hutter et al. was further developed and completed by Hoffman et al.[3], who proposed recently a novel redox model of cell proliferation. They postulate the existence of a redox switch that helps regulate the proliferation within normal cells; its absence in cancer cells enables the bypass of the restriction point and leads to the loss of the control of cell cycle. The authors offer this model as a base to understand the aberrant cellular proliferation that leads to malignant transformation (Fig V 1.).

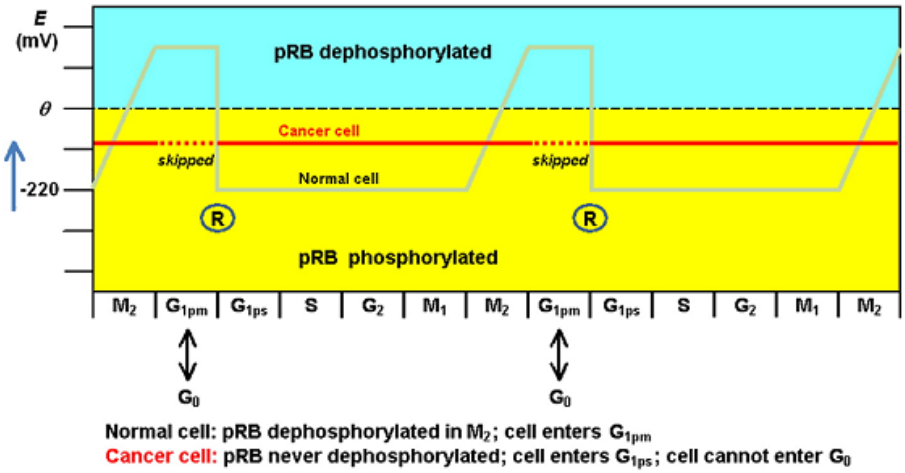

Hoffman A, Spetner LM, Burke M, 2008

According to "redox model of cell proliferation", in normal cells exist a threshold value (θ) of E≤ 207±11mV which initiates the phosphorylation of different regulatory proteins associated with different phases of the cell cycle and, consequently, cell proliferation. When E>θ cell enters G1/G0 phase. However, when cancer cells are concerned,

Hoffman does not take into account the fluctuations in the E level. In our hands, the increase in GSH level along the cell cycle (before the onset of the proliferation comparing to the GSH level at the final time point) is, indeed, less striking than in 3T3 fibroblasts; two-fold comparing to four-fold, respectively (Fig. 4 and 5, respectively). Moreover, the level of GSH in MCF7 cells is significantly higher than in 3T3 fibroblasts during the entire time of the culture (Fig. 12), so cancer cells are, indeed, in a permanent reduced state. Nevertheless, the exponential phase of the cell growth in MCF7 cells is somewhat delayed comparing to 3T3 fibroblasts.

The author hypothesizes, though, the existence of a reductive limit of -260mV which normal cell could not survive, but would not jeopardise cancer cell.

It was proposed previously that the proliferation occurs within the range of ROS levels, concentrations above or below this range could lead to growth arrest or cell death; hence ROS could act like a dual-edged sword [4]. Analogically, similar supposition could be made for glutathione: MCF7 cells at the beginning of culture are in extremely reduced state so it might be necessary for the GSH level to decrease to some point before the exponential growth could start. So, our results suggest that reductive limit for the proliferation onset could be present in cancer cells.

2.2. Cell cycle is governed by the level of GSH

The interdependence of the GSH level and cell growth intensity was further confirmed by the thorough analysis of the phases of the cell proliferation (Fig. 4, 5, and 6) and the expression of cell cycle regulatory proteins, such as Id2 and PCNA (Fig. 7).

In 3T3 fibroblasts maximal proliferative activity of the cells (S+G2/M), defined by the sum of the percentage of the cells in DNA synthesis (S) and the percentage of cells in G2 phase and mitosis, coincided with the peak of GSH. However, when these two phases were analysed separately, it appeared that the level of G2/M phase actually coincided with high values of GSH during 24-48h of culture, while the peak of S phase was delayed comparing to the peak of GSH Fig.4). On the other hand, in MCF7 cells, the peak of GSH preceded both S phase and G2/M phase maximum (Fig. 5). In contrast to 3T3 fibroblasts, the interval of high proliferation activity in these cells was prolonged, although the level of GSH continued to decrease gradually. It is not surprising if we bear in mind that the level of GSH in these cells was extremely high comparing to other two cell types at all time points of the cell culture.

In embryonic neural culture, considerable percentage of cells were in G2/M phase early in the culture, even before GSH level increased (Fig. 6). This culture originates from the cerebral cortex of the rat foetuses isolated at 14-15th day of

gestation; therefore an important number of dividing cells could already be present in the culture. DNA synthesis, like in other two cell types, was delayed until the GSH level had reached its maximal value. However, the increase of GSH level followed by the DNA synthesis could not have led to the proliferation onset because the latter was prevented by the addition of the cytosine arabinoside.

Furthermore, when proliferating cells i.e. astrocytes, were almost entirely absent in the culture of differentiated neurons, the GSH level was lower than in the mixed culture. This finding is in accordance with the redox switch theory (see above); the differentiated neurons are in G0 phase characterized by a less reduced state. E is significantly below the threshold value necessary for the new entrance to cell cycle and is maintained at the similar level until the dying off of the culture. Our results provide the support to previous reports that neurons in cultures prepared from the cortex contain less glutathione than astroglial cultures from cortex [5]. This is due to the inability of neurons to take up cystine and, therefore, rely on the presence of cysteine as substrate for glutathione synthesis which, again, is provided by astrocytes [6]. Nevertheless, the decrease in GSH level was not striking and in our hands a 10 days neuronal culture had total GSH concentration similar to the previously published (36,8±6,6 nmols/mg prot., vs. 40 nmols/mg prot., respectively) [7]. In accordance with the findings published by [8], GSH content was significantly higher in the G2/M

phase compared to G1, suggesting that the cells preparing for the cell division and undergoing mitosis are at a more reduced state compared to G1 phase. According to this study, S phase cells showed an intermediate redox state. Our findings not only supports this study, but also places in time the high levels of GSH in the cell culture before the prevalence of the cells that synthesise DNA. In conclusion, our work in three different models of cell proliferation provides further evidence in favour of the importance of the fluctuations of the cellular redox state in regulating the cell cycle. Whether the cell line was primary, immortalized or malignant, the high level of cellular GSH was essential before the onset of the exponential cell growth.

2.2.1. Glutathione controls the cell cycle regulatory proteins

2.2.1.1. Id2 as a redox sensitive protein.

The study of the expression of the Id2 along the cell cycle gave further support to this premise. The family of helix-loop-helix proteins denominated Id (inhibitor of DNA binding or inhibitor of differentiation) was demonstrated to be of considerable importance in the regulation of cell growth, differentiation and cancer in many mammalian tissues [9, 10]. Id2, in particular, was shown to disrupt antiproliferative effects of tumour suppressor proteins of the Rb family, thus allowing cell cycle progression [11]. Indeed, the pattern of the Id2 expression detected by Western

blotting (Fig. 7), confirmed the distribution of the phases of the cell proliferation detected by flow cytometry. Moreover, its level is comparable with the level of GSH: when and while GSH level is high the important expression of Id2 could be observed, at 24 and 48h in 3T3 fibroblasts, at 12, 18, and 24h in MCF7 cells and in the early embryonic neural culture. This observation is in the line with the proposed redox regulation of this protein [12]. In addition, the studies of liver regeneration, process that involves DNA synthesis and cell proliferation, gave further support to our findings. It was demonstrated that when the increase of GSH after partial hepatectomy was prevented, the liver regeneration was delayed and the total liver amount of the DNA was lower than in the control group [13]. Furthermore, an early increase in Id2 gene has been demonstrated as well as the contribution of Id2 in the control of hepatocyte priming through modulation of c-myc expression [14]. All these support our notion that Id2 could be an excellent candidate as a protein marker of the redox regulation of cell proliferation in our models.

2.2.1.2. PCNA as a possible redox sensor in the onset of DNA synthesis

PCNA, a proliferating cell nuclear antigen, is a central protein in both DNA replication and repair. It's a "sliding clamp" that localizes proteins, such as DNA polymerase, to DNA and thus enables the correct DNA replication. As

expected, this marker of DNA synthesis was up regulated at 48h in 3T3 fibroblasts, between 24-72h in MCF7 cells and before 96h of embryonic neural culture, when the % of cells in S phase was shown to be maximal also by flow cytometry. The time point characterized by the maximal GSH value precedes these intervals, which further confirms our premise that the reduced cellular environment is a prerequisite for the beginning of the DNA synthesis.

Replication of mammalian genome starts at thousands of origins, called replication foci, which contain PCNA and are activated at different times during S phase. The dynamics of replication foci is still a matter of debate; there are contradictory reports on the organization of the DNA replication sites in diverse cell types attributable to the differences in the technical approach [15, 16]. According to Dimitrova, SD and Berezney, R [17] there is no fundamental difference in the spatiotemporal organization of the DNA replication in primary, immortalized and malignant mammalian cells. On the contrary, Kennedy's group [16], observed different patterns of replication foci in primary versus immortalized cell lines, as well as their perinuclear localization in the contact-inhibited cells prior to cell cycle exit [18]. Another fundamental question was weather the replication foci are moving along the DNA in the process of the replication, or the DNA is spooling through fixed replication factories. It seems that the important body of evidence is accumulating supporting the fixed-replication-

site model [15, 19]. The replication machines bind to DNA, but they are also tethered to an underlying framework called nuclear matrix or skeleton [19]. Regardless of the discrepancies in their findings, all the authors call attention to the importance of the preserving nuclear architecture in order to guarantee the correct development of the process of DNA replication [15, 18, 19]. In addition, it has been shown that chromosome territory organization depends on association with the nuclear skeleton [19]. More than 20 years ago, Dijkwell et al. [20] postulated that the maintenance of the nuclear matrix, especially nuclear lamina, by preserving disulphide bonds depended on the level of nuclear thiols. In accordance to this work, Oleinick et al. [21] reported that DNA-protein cross links, present at basal level as normal associations of chromosomal loops with the nuclear matrix proteins, can be increased by ionising radiation and removal of intracellular glutathione, and decreased by hydroxyl radical scavengers. The importance of the GSH in cell proliferation could be extrapolated to the safeguarding of the nuclear architecture, providing in that way a proper milieu for the DNA replication. Our results could provide support to the hypothesis of Bellomo et al [22] that reduced nuclear glutathione may modulate the structural organization of chromatine. It is tempting to speculate that the high nuclear GSH level we observed before (late G1 phase) and at the onset of cell proliferation (S phase) could provide the redox environment

that stimulates chromatin decompaction by reducing disulfide bonds.

2.2.2. GSH is an indicator of cell proliferation potential

So, if the high level of GSH is crucial for the phase of proliferation to take place, the question whether the level of GSH defines the proliferation potential of the cell type imposes itself. The comparison of the three proliferation models yielded the most interesting results and provided further evidence in favour of our hypothesis.

In the comparative study of the interdependence of the GSH level and the cell proliferation intensity in the three cell types the highest correlation with the level of GSH was found for DNA synthesis (R^2=0,7) (Fig. 19), but not the cell division (G2/M) or total proliferation activity (S+G2/M) (Fig. 17 and Fig. 15, respectively).

Surprisingly, 3T3 fibroblasts had more cells in S+G2/M and G2/M phase of the cell cycle (Fig. 14. and Fig 16., respectively) than MCF7 cells and embryonic neural culture, although for shorter period of time. Nevertheless, at the final time point the number of MCF7 cells almost doubled the number of 3T3 fibroblasts. One possible explanation for this apparently contradictory finding we could trace in the very nature of malignant cells. According to Green, RD and Evan GI [23], cancer originates from a rare coincidence where at one cell at the same time arise deregulated cell proliferation

and suppressed apoptosis. This is just the case of MCF7 cells; the cell culture is highly desynchronised, and as a consequence, we can detect, at all time points, rather the significant proportion of cells in different phases of cell cycle than accumulation of the cells in one of the phases, as in 3T3 fibroblasts.

Our results showed the strong correlation between the level of DNA synthesis and GSH level indicates that high concentration of GSH is essential for this process. This result is not surprising knowing that the importance of GSH in the nucleotide synthesis has been demonstrated long since [24]. However, in an early work by Spyrou and Holmgren [25] it has been demonstrated that BSO, although it decreased glutathione level, did not affect the nucleotide synthesis. On the other hand, numerous papers demonstrate that the depletion of glutathione does induce growth arrest, in vivo as well as in vitro, and hampers DNA synthesis. Thus, the potential involvement of the GSH in the very process of the DNA replication prompted us to search for its further possible function in this process. One important parameter of cell proliferation, crucial for the correct and complete replication of the DNA, and possibly correlated with glutathione level is the telomerase activity.

2.3. The relationship between telomerase activity and the level of cellular glutathione controls the cell cycle progression

The increase of telomerase activity is associated with deregulated proliferation in human cancers [26] and is also present in highly proliferative germinal cells [27]. On the contrary, its decrease, which results in replicative senescence, was reported *in vitro* in growth arrested cells [27, 28], and *in vivo* in syndromes of premature aging, endothelial dysfunction and atherosclerosis [29]. Interestingly, oxidative stress has been implicated in all these pathological conditions [30]. In Warner's syndrome, characterised by adult premature aging, the significant alteration of GSSG/GSH ratio, as well as considerable DNA damage was demonstrated [31]. In Down's syndrome, which displays some features of accelerated senescence associated with telomere shortening [32], a prooxidant state with early onset has been demonstrated in vivo [33], as well as in several other aging-related genetic diseases [34]. All these reports point to an increasing interest in the possibility that oxidative stress could induce or accelerate the development of replicative senescence [35]. Furthermore, it was demonstrated in human vascular endothelial cells and in human skin keratinocytes that telomere shortening slows down when oxidative stress is suppressed by antioxidants, such as vitamin C [36, 37]. So, according to these studies,

telomerase activity could be stimulated or preserved by reduced environment.

In the context of our study, it was interesting to explore a possibility of redox control of telomerase activity by glutathione in the framework of cell cycle progression. Our group has previously described the connection between GSH level and telomerase activity in 3T3 fibroblasts [12]. Telomerase activity is regulated by the changes in glutathione redox potential at values comparable to those in vivo and changes in telomerase activity are modulated in coordination with changes in cell cycle proteins, particularly Id2. The rhythm of GSH fluctuations coincided with that of the telomerase activity (Fig. 8) and it was proposed that the control of the proliferation in 3T3 fibroblasts could be based on this relationship. Considering the importance of this finding and the possible implications it could have in various fields of cell biology, from cancer and development to the theory of aging, we have amplified the study to cancer cell line, MCF7 and embryonic neural culture.

It is interesting to find that, in the three different models of cell proliferation used in this study, the telomerase activity (TA) reaches its maximum at the same time point as total cellular GSH concentration and the fluctuations along the cell cycle are strikingly similar (Fig. 8., 9., 10.). In MCF7 cells the peak value of GSH and telomerase activity was considerably higher than in 3T3 fibroblasts and embryonic neural culture. Moreover, these values increased earlier and

were maintained elevated for longer period of time then in the case of 3T3 fibroblast where the increase was delayed and the peak value was easily distinguishable at 24h. In the embryonic neural culture, there was important telomerase activity before the peak of GSH was reached (attributable to the presence of the proliferating cells in the moment of the isolation of the primary culture, as discussed previously), and, as expected, it was declining steadily after the proliferating cells were eliminated from the plate.

This new results strongly confirmed the previous observations published by our group for immortalized cell line, 3T3 fibroblasts [12]. Even more, the fluctuations of telomerase activity resemble the fluctuation in cellular redox potential that, according to Hoffman et al (Fig. V 1) regulate the cell cycle progression. Variations in telomerase activity are more prominent in 3T3 fibroblasts than in MCF7 cells, and in embryonic neural culture telomerase activity seems relatively stable (Fig. III 13.) This further supports our premise that reduced glutathione level controls cell cycle progression by the regulation of telomerase activity.

On the contrary, in a recently published research by Perez-Rivero G et al [38] it has been asserted that it is telomerase deficiency that promotes the oxidative stress, due to reduced catalase activity, and not the other way around. This study was performed on cultured mouse embryonic fibroblasts (MEF) and renal cortex isolated from mice lacking telomerase activity and showing the signs of premature aging. On the other hand, it has been reported that the

mouse cells do not show senescence when cultured at a physiological oxygen concentration (3%). If mouse cells are grown at atmospheric oxygen concentration (20%), which provides an additional oxidative stress to the cells, cell growth slows after 12–15 population doublings, due to accumulated DNA damage [39, 40]; So, it is the oxygen sensitivity that could cause replicative senescence and not the opposite.

In addition, as Kurz DJ et al. [29] clearly demonstrates in human umbilical vein endothelial cells, glutathione-dependent redox homeostasis is a key factor in the preservation of telomere function, and mild chronic oxidative stress is at the root of the replicative senescence caused by the loss of telomere integrity. Their results are resumed in Fig V 2. The loss of catalase activity leads to accumulation of H2O2 and its translocation to the nucleus, where in subsequent Fenton reaction it induces telomere damage. This premise has a solid theoretical support; guanine rich composition of telomeres makes them several-fold more susceptible to oxidative stress mediated damage than non-telomeric DNA [41].

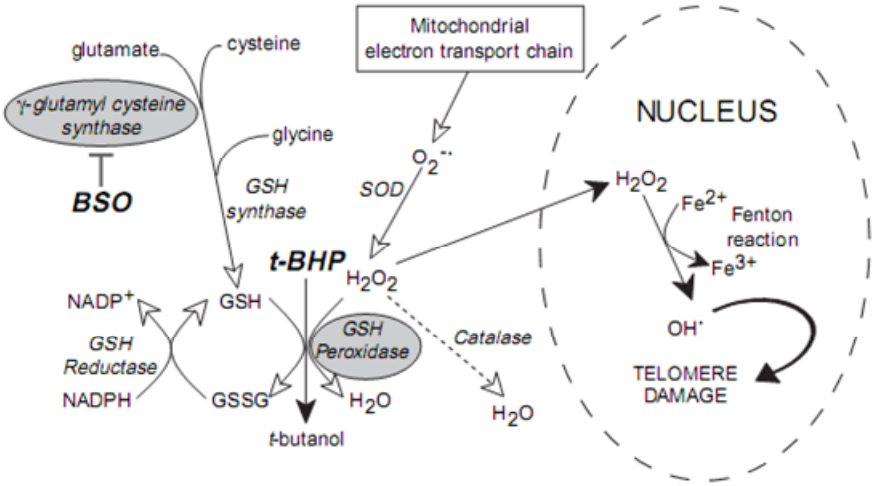

Kurz DJ, et al., 2004

In addition, a specific inhibitor of telomerase, 2- [3-(trifluoromethyl)phenyl]isothiazolin-3-one, reacts with a key cysteine residue which in order to guarantee telomerase activity must be kept reduced; dithiothreitol reverses this inhibition [42]. So, the high glutathione concentration could be important on the two levels: to preserve the telomere integrity by protecting it directly from oxidative damage, and/or to preserve the telomerase activity by maintaining the crucial cystein residue in reduced state. These findings indicate that the implication of glutathione in the control of telomerase activity might be considered as its new role in the DNA synthesis, further from previously described in the pentose phosphate pathway [24].

This finding is particularly significant, as it indicates that the telomerase activity is highly sensible to the cellular redox state, regardless of the cell type, its inherent proliferation capacity or the origin of the cells. It is a universal phenomenon which could have important implications in the study of various pathophysiological processes in which the importance of telomerase has been demonstrated, such as aging and cancer.

Furthermore, in a vigorously developing field of stem cell research one of the clear and recognized hazards of cell therapy is the subsequent development of cancer. Indeed, the epidemiological study in 926 patients that underwent a life-saving allogeneic hematopoietic stem cell transplantation (allo-HSCT) demonstrated an increased risk of development a second solid cancer [43]. Interestingly, the risk was significantly higher if the donor was a female. In the light of our study, this is of particular importance if we bear in mind that, on one side females have longer telomeres than males [44] and on the other have less oxidative stress [45]. In accordance to this, telomerase activity was proposed as a useful marker of non-differentiated, still pluripotent cells which, if accidentally implanted, could have malignant capacity [46]. It would be interesting to investigate if by modulation of glutathione these cells cold be eliminated, and thus, this threat could be avoided.

3. Nuclear compartmentalization of glutathione as an important feature of proliferating cell: reduce to replicate

The functional compartmentalization is an obvious characteristic of eukaryotic cell. The organelles, visible by light microscopy, are surrounded by membranes, which, although permitting communication, provide unique and defined environment in each one, which guarantee its accurate function. Probably the most remarkable examples of compartmentalization are oxidative phosphorilation in mitochondria, protein folding in endoplasmatic reticulum and, for the purpose of this study the most interesting of all, DNA synthesis.

It is interesting to note that, when the first two organelles are concerned, the dependence of their function on the correct GSH level has been thoroughly studied. The high intramitochondrial concentration of GSH is maintained by an active multicomponent transport system "pumping" glutathione from the cytosol into the matrix [47]. On the contrary, for the correct folding of proteins into a native structure by disulfide bond formation, the GSH level and the ratio GSH/GSSG in the endoplasmatic reticulum is maintained at extremely low level by the limited permeability of the vesicle membrane to GSH [48].

However, in the case of nuclear compartmentalization of glutathione the reports were scarce and contradictory over

the years. This could be attributed to two main factors: methodological difficulties in measuring nuclear glutathione content and the focus of the research generally limited to confluent cells.

3.1. Methodological challenge

Firstly, it is impossible to determine the nuclear concentration of GSH using standard cell fractionation and analytical techniques. This point was already addressed in an interesintg review by Soederdahl et al [49]). This approach in our hands also yielded unsatisfactory results (Fig. III 21).

In view of this knowledge we opted for confocal microscopy, the approach which, although providing the huge advantage of the possibility to analyse the nuclear glutathione of the living cells, is not without contradictions, previous reported. Mercury orange, monochloro bimane, and 5-chloromethylfluorescein diacetate (CMFDA) are the most commonly-used probes for GSH determination, but the results obtained by these methods are conflicting. Pioneer work by Bellomo et al. [22] using monochlorobimane-GSH conjugation demonstrated a 3:1 nucleus: cytoplasm ratio. However, a more recent report by Briviva et al. [50] argued that the high nuclear fluorescence was due to an influx of the fluorescent bimane-GSH adduct into the nucleus. In a different approach, Thomas et al. [51] used fractionation techniques and flow cytometry with mercury orange; this probe readily forms fluorescent adducts with GSH and other

non-protein sulphydryls (NPSH), but reacts much more slowly with protein sulphydryls. Contrary to previous reports, they found lower GSH levels in the nucleus than in the cytoplasm: the mean nucleus-cytoplasmic ratio was 0,57± 0,05. It was postulated the existence of a distinct pool of GSH in the nucleus since it was partially resistant to BSO depletion compared with the cytoplasm. More recently, Söderdahl et al. [49] showed the highest GSH staining in a perinuclear mitochondrial-rich compartment and low nuclear GSH staining using mercury orange and a specific GSH antibody. Finally, Voehringer et al. [52] using CMFDA which binds in 95% to GSH, showed that GSH was mainly distributed in the cytoplasm although Bcl-2 overexpression was able to increase nuclear GSH levels.

In recent years new methods have become available for measuring the nuclear redox state. These have been recently reviewed by Hansen, Go and Jones [53]. Two forms of the redox blot have been developed to separate nuclear proteins on the basis of different charge or mass oxidized. Other techniques include antibodies that only bind to the oxidized form of the protein [54], and mass spectrometry [55]. Alternatively, a redox-sensitive green fluorescent proteins (roGFP) have been designed with the hope to be used as an indicators of the nuclear redox. Although it is a promising step, so far no physiological oxidative treatment has been capable of triggering detectable changes in the excitation ratios of roGFP. Another method consisting in a Western blot technique which separates reduced and

oxidized Trx1 in nuclear fractions provide a new means to establish the redox state of the nucleus [56]. While this may be the way to evaluate nuclear redox state, measurement of nuclear GSH concentrations remains limited, and no methods are available to measure nuclear GSSG [54]. However, a substantial breakthrough seems to emerge in a very recent work of Tobias Dick's group, published in Nature Methods (may, 2008) [57]. Acording to this study, the Grx1-roGFP2 fusion protein allowed dynamic live imaging of the glutathione redox potential (E(GSH)) in different cellular compartments with high sensitivity and temporal resolution. The biosensor detected nanomolar changes in oxidized glutathione (GSSG) against a backdrop of millimolar reduced glutathione (GSH) on a scale of seconds to minutes. It facilitated the observation of redox changes associated with growth factor availability, cell density, mitochondrial depolarization, respiratory burst activity and immune receptor stimulation.

Our approach was based on determining of the cellular distribution of glutathione analyzing alive intact cells under the usual conditions of cultivation; at 37ºC, 5% CO2 and in cell culture medium. In order to study glutathione compartmentalization during cell growth, we used a triple staining (CMFDA-Hoescht-propidium iodide) or (CMFDA-Hoescht-mitotracker) and subsequent analysis by confocal microscopy [58].

3.2. The dynamic focus of the study

Most, if not all reports share the common insight in the nuclear GSH distribution in a static situation. Cells are usually studied under steady state conditions i.e. at confluence (G0/G1 phase). The nucleus changes dramatically during the different phases of the cell cycle. Therefore, studies designed to elucidate the nuclear compartmentalization of GSH should take into account the cell cycle physiology.

Indeed, if glutathione were necessary for the process of DNA synthesis and for regulating the telomerase activity and cell cycle proteins, as we believe, than it should be present in the nucleus in the key moments of cell proliferation.

Our study of cellular distribution of reduced glutathione in the three cell models before, during and after the exponential phase of cell growth provided evidence that contribute to our assumption (Fig III 22, 23, 24). The finding that, the high nuclear GSH level was detected in all three cell types at the beginning of culture, and while cells were actively proliferating, and, conversely, decreased significantly when the pace of the proliferation declined points to the role of nuclear glutathione in the onset of cell proliferation. In 3T3 fibroblasts, characterized by an early exponential phase of cell growth, and in the neural culture, which already contained proliferating cells (Fig. III4, and

III6, respectively), important nuclear compartimentalization of GSH was observed already at 6h of culture and it persisted at 24h. On the contrary, in MCF7 cells the maximal nuclear compartmentalization of GSH was delayed until 24h of culture, as well as the onset of exponential phase of cell growth (Fig. III5). The total cellular GSH was decreased at this time point, but the nuclear level of GSH was preserved.

In accordance with our premise, at the final time point, the nuclear compartmentalization of GSH is almost absent from the culture of 3T3 fibroblasts that have reached confluence (with less than 2% of the cells in S phase) and in differentiated neurons (with almost null proliferation activity). On the contrary, in the culture of MCF7 cells, that maintained the significant level of DNA synthesis until the 7th day of culture (Fig. III 18), the nuclear GSH compartmentalization was still detectable in some cells.
Moreover, the detailed study of the nuclear compartmentalization of GSH along the cell cycle performed in 3T3 fibroblasts showed that GSH co-localized with the nuclei at 6, 12, and 24 h after plating. However, when cells were confluent, at 3 and 5 days after plating, no differences between the nucleus and cytoplasm could be seen (Fig. III 25). The images obtained at 3 or 5 days in culture are similar to those reported previously by Soderdahl et al [49] using GSH antibody and mercury orange to study the GSH distribution in confluent A-549 cells. Thus, our results may

explain the apparent discrepancies in the GSH distribution. It is very important to take into account the moment of the cell cycle in which glutathione distribution is studied. We show here that cells that are preparing to divide have high nuclear GSH levels. Quiescent cells have similar (or even lower) GSH levels in the nucleus than the cytoplasm. The capacity of the cell to concentrate GSH in the nucleus was estimated by the nucleus/cytoplasm GSH ratio (Fig. III 26). It is high several hours after plating, and it is near one when cells are confluent. Thus, glutathione translocates to the nucleus before exponential cell growth which assures the reduced environment at the onset of cell proliferation.

Thus our results demonstrate that the cell nucleus suffers dramatic changes in its oxidative status and underscore the role of nuclear glutathione in the physiology of the cell cycle.

So, the presence of the high glutathione level in the nucleus appears to be a common characteristic of the cells that are preparing to divide whilst quiescent and differentiated cells have similar GSH levels in the nucleus and the cytoplasm. Our findings are in line with several other studies aimed to elucidate the fine redox regulatory mechanisms that lie behind the correct cell cycle progression. Conour et al, suggested that the reduction of the intracellular environment as cells progress from G1 to G2/M phase, as shown in our study, may protect genomic DNA from oxidative damage upon brakedown of the nuclear envelope [8]. Indeed, one of the assertions in support of this premise derives from the study of oxidative stress related to

genotoxicity, recently published by Green RM; oxidative DNA modifications displayed a negative linear correlation with nuclear GSH. This is of special importance considering the report of Menon et al [59] on the necessity of the oxidative event in early G1 phase to allow G1-S transition. Even more, it has recently been postulated that the restriction of DNA synthesis to the reductive phase of the cycle in yeast may be an evolutionarily important mechanism for reducing oxidative damage to DNA during replication [60], which implies the common mechanism of the DNA protection during S phase in all eukaryotes.

3.3. Modifications of nuclear proteins along the cell cycle

Various studies have demonstrated that the nucleus is more reduced than the cytosol (15mM GSH vs. 11 mM, respectively) [22, 61, 62]. An important number of nuclear proteins, including transcription factors, require a reduced environment to bind to DNA. More than 62 proteins are involved directly in transcription, nucleotide metabolism, (de)phosphorylation, or (de)ubiquitinylation, which are all essential processes for cell cycle progression [8]. For instance, it appears that, at the onset of cell proliferation in the early G1 phase, an increase of ROS in the cytoplasm is necessary for the initiation of the phosphorylation cascade mediated by epidermal growth factor (EGF) that, subsequently, activates DNA replication and the cell division

([63]). According to Jang and Surh [64] nuclear GSH may act as a transcriptional regulator of NF-κB, AP-1, and p53 by altering their nuclear redox state. The transcription factor NF-κB is an example of distinct redox-sensitive activation and DNA binding [53]; it is activated by various physiological stimuli known to produce ROS; on the contrary, to permit DNA binding, similar to Fos, Jun, and Nrf2, cysteine residue within DNA binding domain must be reduced. Both processes are guaranteed by the adequate redox state of the cytosolic and nuclear environment, respectively (Fig. V 3).

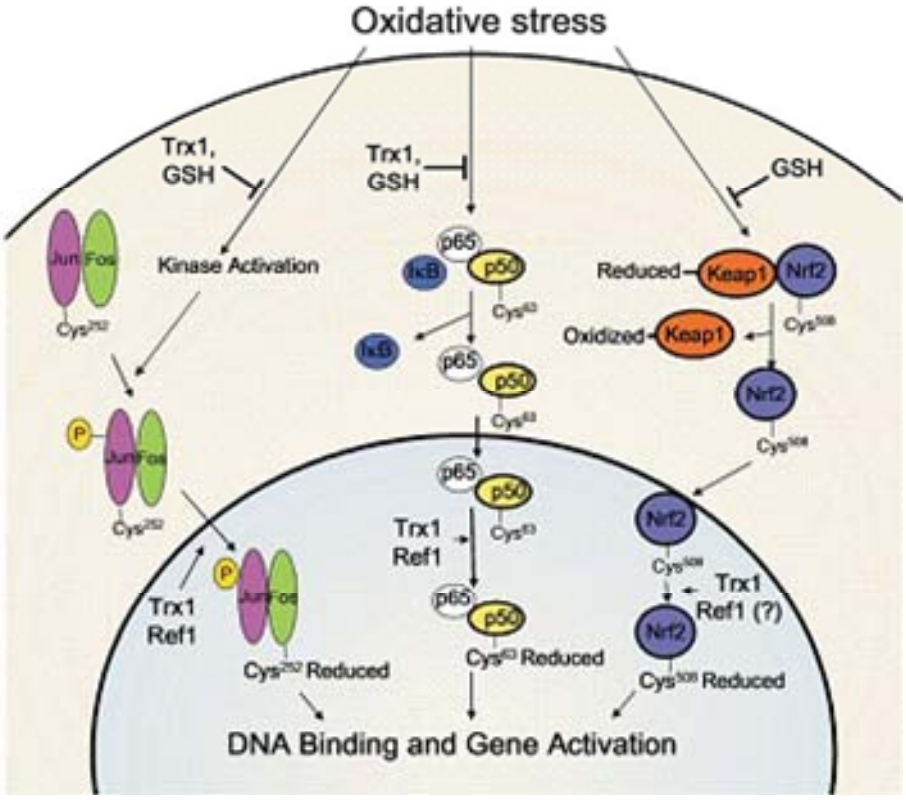

Hansen, JM, Go YM, Jones DP (2006)

Toledano *et al*. [65] found a redox-dependent shift of oxyR-DNA contacts along genomic DNA, suggesting a mechanism for differential promoter selection.

In addition, the reduced nuclear environment could protect oxidant sensitive proteins from oxidation [8] Fig. V 4.

Indeed, our study showed lower level of protein oxidation in nuclear extracts at 6 and 48h of culture, when the nuclear GSH was high, than at confluence, when the nuclear GSH level was lower and equal to cytoplasmic (Fig III 29.).

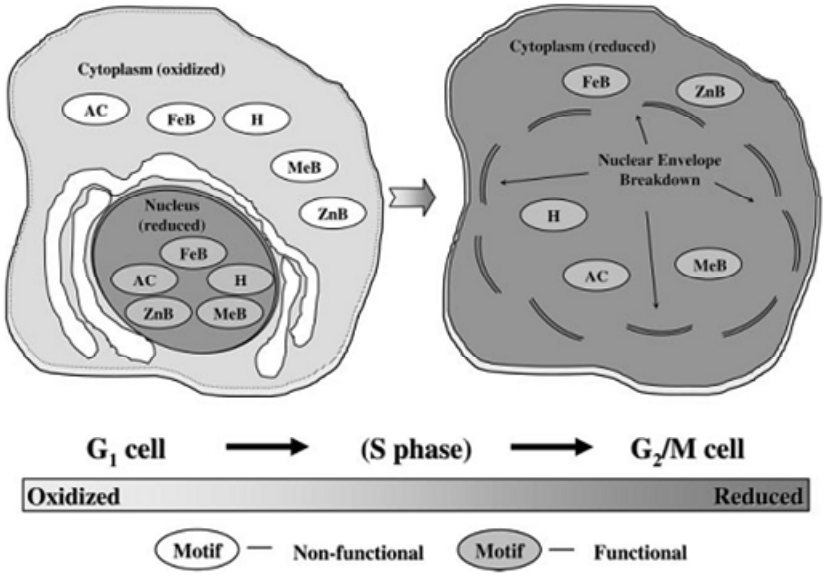

Conour et al., 2004

Interestingly, the nuclear proteins underwent stronger glutathiolation before and at the onset of cell proliferation than at quiescence (Fig III 30). It is not surprising if we bear in mind that high level of GSH in the nucleus could provide protection to the proteins against the oxidative threat coming from the cytoplasm at the early phase of cell proliferation, and that glutathiolation, as it is a reversible modification, could be just the way. On the other hand, based on the simplicity of the redox transition from thiol to disulfide and on the fact that the reversibility was energetically favourable, Cotgrave IA and Gerdes RG [66] more than 10 years ago have proposed glutathionilation as a posttranscriptional modification with the regulative finality. They state that it offers "a strong possibility for transducing "oxidative information" from intracellular oxidants via the GSH redox buffer to individual proteins containing "regulatory thiols". Also, recently, this posttranslational modification was proposed as a likely molecular mechanism for redox dependent signalling mediated by GSH [67]. Thus, high level of GSH in the nucleus, observed before and at the onset of cell proliferation, could provide the "GSH redox buffer" necessary for the progressing of oxidant stimulated mitogenesis.

It is encouraging to see that the findings of the present study have provided some support to the assumption that a dynamic intracellular redox environment directs the cell proliferation through redox sensitive cell cycle proteins.

4. The depletion of nuclear glutathione hampers the cell cycle progression

With the intention of providing further evidence of the importance of nuclear GSH in the initiation of cell proliferation, we have found ourselves in front of a challenge of depleting nuclear glutathione. A number of reports have focused on the consequences of the depletion of cellular glutathione levels on changes in cellular proliferation [51, 53]. However, all those reports were performed measuring cellular or total glutathione levels, but there is no information relating cellular proliferation with nuclear glutathione levels. A number of studies have indicated the existence of a nuclear GSH pool that resists depletion after exposure of cells to BSO (for a review see [51]). BSO treatment resulted in the concentration dependent depletion of cytoplasmic GSH, while the depletion of mitochondrial and nuclear pool of GSH required concentrations higher than 100 μM, which induced DNA damage [68]. Spyrou and Holmgren [25] showed that inhibition of glutathione synthesis by 0.1 mM BSO was able to decrease GSH synthesis after treatment for 12 hours, but GSH-depleted cells grew as well as control 3T6 cells with no decrease in DNA synthesis. Thus, incubation of cells with low concentration of BSO, although decreases glutathione levels, does not change cell

proliferation. On the other hand, Thomas *et al.* [51] showed that non toxic concentrations of N-ethyl maleimide or DEM decreased the GSH level in the nucleus and cytoplasm to a similar extent, whereas the nuclear pool of GSH was much more resistant to BSO depletion.

Based on this findings, we have designed a model to study the effects on the cell proliferation parameters caused by GSH depletion both in the nucleus and the cytoplasm, using 100μM DEM, comparing to the administration of 10 μM BSO when nuclear GSH level is preserved.

Results presented in Fig. III 32 show that inhibition of glutathione levels by BSO is delayed and last for a longer time than that induced by DEM; the rebound effect is obvious at 48 hours. The striking boost of GSH level following the administration of DEM has been observed previously in hepatocytes and attributed to a four- to five-fold increase in gamma glutamyl cysteinyl synthetase RNA levels [12]. Similarly, HepG2 cells exposed to DEM responded with the fourfold up-regulation of glutathione synthase [69]

The inhibition of glutathione synthesis by BSO induced a strong decrease in total GSH levels; however, as reported previously by various authors [51, 68, 70] nuclear GSH pool was preserved (Fig III 33). By contrast, depletion of glutathione levels by DEM induces a marked decrease in nuclear glutathione levels (Fig. III 34.).

The compartmentalization of glutathione depletion could explain the observed differences in the inhibition of cell

proliferation (Fig. III 35.). Indeed, our results show that inhibition of glutathione levels by DEM strongly impairs cell proliferation. This difference could be due to the fact that DEM decreases both nuclear and cytosolic glutathione levels in opposition to BSO, which only decreases cytosolic glutathione. It is worth mentioning that the impairment of cell proliferation could not be attributed to the alkylating properties of DEM, since the simultaneous administration of GSHe completely prevented it, nor to the toxicity of the treatment because the cell death was not significantly augmented (Fig III 36.).

In addition, we have observed the delay in the cell cycle progression caused by DEM, when both nuclear and cytoplasmic GSH was depleted, which is absent in the treatment with BSO when nuclear GSH pool was preserved (Fig. III 37). Interestingly, Esposito *et al*. [71] showed that direct administration of DEM on the nuclear extracts of COS7 cells induces cell cycle arrest. So, it is daring to speculate that, despite the depletion of cytoplasmic GSH with DEM could not be overlooked, the effect on the cell cycle progression could be attributed to the depletion of the nuclear GSH. Moreover, as Esposito shows, the depletion of nuclear GSH strongly induces a p53-independent accumulation of p21, which causes a cell cycle arrest. In our study, the expression of cell cycle regulatory protein, suggested previously to be under redox control, Id2, was

decreased when the level of nuclear GSH was depleted (Fig. III 38).

It has been known that cell proliferation is regulated by a variety of mechanisms working to allow the activation and repression of growth stimulatory genes, one of them being the transcription factors. Previous *in vitro* reports show that the activity of transcription factors is related to its redox environment. In addition, change in the redox potential could induce variations in the activity of those transcription factors. Alterations as small as $\pm$ 15 mV in the redox potential can result in transcription factor translocation and activation or deactivation, depending on the direction of the redox shift [1, 72, 73]

Recently Reddy *et al.* [74] have shown that Nrf2 deficiency leads to oxidative stress and DNA lesions, accompanied by impairment of cell-cycle progression, mainly G(2)/M-phase arrest. Both N-acetylcysteine and glutathione (GSH) supplementation ablated the DNA lesions and DNA damage-response pathways in Nrf2 (-/-) cells; however only GSH could rescue the impaired co-localization of mitosis-promoting factors and the growth arrest.

Our results demonstrate for the first time that it is nuclear GSH levels, and not total cellular glutathione levels, that specifically correlate with cellular proliferation. Glutathione is considered essential for survival in mammary cells and other eukaryotic cells, but not prokaryotic cells. However, although a number of important functions have been attributed to GSH, its outstanding role in nucleated,

but not in prokaryotic cells, remains unknown. Our results underscore the important role of nuclear glutathione in cell physiology and suggest that manipulation of nuclear GSH levels could be of paramount importance during development and cancer.

5. The occurrence of the glutathione in the nucleus; active transport, de novo synthesis, diffusion or something else.

How GSH enters the nucleus and how it is regulated during the different phases of the cell cycle is still a matter of debate. The regulation of such interactions is also unclear. According to Smith and colleagues [75], the possible biochemical mechanisms responsible for the turnover of nuclear GSH are the following: 1.GSH may be taken up from the cytoplasm into the nuclei either passively or through energy-dependent processes 2.GSH may be synthesized *de novo* in the nucleus by the enzymes glutamate cysteine ligase and GSH synthetase 3.GSH may function to transport γ-glu-cys-cys.

5.1. ATP dependent sequestration of the GSH to the nucleus

The role of ATP-dependent mechanisms in maintaining the nuclear/cytoplasmic GSH concentration in hepatocytes was demonstrated by Bellomo and co-workers [22]. After 20 min of incubation with the uncoupler protonophore CCCP the nuclear/cytoplasmic GSH gradient disappeared, but the total GSH content remain unchanged. This study was questioned by Briviba et al [50] because of the use of monochlorobimane (BmCl). Despite its high specificity for glutathione this fluorochrome was found to be of no value in the study of cellular GSH distribution; once GSH-BmCl conjugate is formed it demonstrates an increased tendency of nuclear compartmentalization. Indeed, in our study using CMFDA, we have not found an ATP-dependent mechanism of nuclear GSH compartmentalization in 3T3 fibroblasts (Fig. III 39.). Ho and Guenthner using nuclear fractions concluded that GSH is taken up by the nucleus by passive diffusion and no evidence for an ATP-dependent mechanism for GSH concentration was observed.

5.2. Nuclear synthesis of glutathione

Glutamate cysteine ligase (GCL) and GSH synthetase activities have been reported in nuclei, and a portion of 4-8% of cell GSH synthetic activity is considered capable of

maintaining nuclear GSH levels Ho and Guenthner. However, we could not find GCL expression in nuclei of 3T3 fibroblasts (Fig. III 40.)

In addition as previously reported bso, a specific inhibitor of gcl was unable of decreasing nuclear glutathione levels. Thus, at least under our experimental conditions, the possible "de novo" synthesis of nuclear glutathione seems improbable in 3t3 fibroblasts.

5.3. GSH enters nucleus via nuclear pores

The nuclear pore complex is the biochemical machinery that controls the molecular traffic across the nuclear envelope [76, 77]. Ions and small hydrophilic molecules, like glutathione, are considered to move by free and fast diffusion across the nuclear pore [78]; nevertheless ion gradients and transnuclear ATP-dependent membrane potential have also been reported [77]. In a series of creative experiments published in early 1990ies, Feldherr CM and Akin D [79, 80], shown that permeability of nuclear envelope and nuclear transport were higher in proliferating than in quiescent cells. Reported seven fold reduce in the nuclear transport capacity was induced by the alterations in the characteristics of the pores and not by the changes within the cytoplasm, specifically, the decrease in ATP concentration. One pore forming protein that has been

brought into the connection to nuclear glutathione content is Bcl-2. Voehringer and colleagues [52], showed that over-expression of Bcl-2 recruits GSH to the nucleus. The presence of this protein at the nuclear envelope was demonstrated [81] and the association with the nuclear pore complexes was suggested. Moreover, Zimmermann et al. [82] demonstrated that GSH binds to Bcl-2 in mitochondria, providing a molecular basis for its antioxidant function. Thus, Bcl-2 located in the mitochondrial membrane introduces GSH in the mitochondrial space. We have found that the presence of Bcl-2 in the nucleus is higher in proliferating than in quiescent 3T3 fibroblasts, i.e. it coincides with the high level of glutathione in the nucleus (Fig. III 41) as well as with the intense nuclear transport regulated by the nuclear pores.
Thus, we suggest that during the changes in the nuclear membrane that precede the cell division, nuclear Bcl-2 could facilitate the translocation of glutathione to the cell nucleus.

6. Contradictory effects of Bcl-2 over-expression on the proliferation of MCF7 cells.

Bcl-2 was first intracellular regulator of apoptosis to be discovered [83], and its function in the programmed cell death inspired over 20000 reports (medline entry). The implication of Bcl-2 in cellular proliferation emerged relatively soon afterwards; however, in this context it failed to show similar prominence being subject of fewer than 6000

reports. Interestingly, while the apoptotic prevention by Bcl-2 is unanimously documented, its effect on the cell cycle progression was a less elucidated issue. When expressed at high levels in cells derived from several cancers, Bcl-2 induced strong growth suppression in some but not in all of them [84]. Constitutive expression in HL60 cells showed no impact on the proliferation or spontaneous differentiation of these cells, but facilitated the latter when it was induced by specific agents [85]. In the non tumoral cell line, NIH 3T3 fibroblasts, it caused delay in response to serum stimulation [86]. It has also been shown that its anti-apoptotic function can be genetically separated from its inhibitory effect on cell proliferation: mutated tyrosine residue at the conserved BH4 domain did not interfere with apoptosis resistance of the cell while it did induce a faster cell cycle re-entering upon serum stimulation of quiescent cells [13]. On the other hand, the development of Bcl-2 knockout mice revealed the importance of this protein in regulation of cellular redox potential in the response to oxidative stress. Hockenbary at al showed that Bcl-2 was unable to block the generation of peroxides; however it did inhibit lipid peroxidation [13]. Therefore, the direct antioxidant protection provided by Bcl-2 occur downstream of mitochondria. Again, it was in the context of the process of apoptosis where this finding was profoundly studied: Kane et al [46] were the first to show that the capacity of Bcl-2 to suppress apoptosis depended on the concentration of cellular thiols, i.e. GSH, which was

always increased when the Bcl-2 was elevated. More studies followed supporting this premise demonstrating that the depletion of GSH restores apoptotic sensitivity to the cell over-expressing Bcl-2 [87]. Therefore, it was suggested that Bcl-2 modulated apoptotic sensitivity by means of high levels of GSH, downstream of its recognized detoxifying function (Paper bcl2 mcf7 ghs depletion cisplatin 2002-3). In 1999 Voehringer et al [52] demonstrated that the over-expression of Bcl-2 in HeLa cells, not only increased the total cellular glutathione level, but also induced its redistribution to the nucleus. The hypothesis emerged that the nuclear compartmentalization of GSH, facilitated by Bcl-2, provides the nuclear redox environment crucial for "fine-tuning" of transcriptional regulation [52]. This premise was encouraged by another line of studies revealing the Bcl-2 as a pore forming protein and a possible transporter regardless of the membrane it is localized on: mitochondrial, endoplasmatic reticulum, or nuclear membrane [52, 88, 89]. First reports on possible membrane transport function of Bcl-2 date from early 1990ies and involved the trafficking of proteins and Ca^{++} across the outer mitochondrial membrane, the endoplasmatic reticulum and nuclear envelope. It was suggested that proteins of this family could act as adaptor or docking proteins, capable of pulling other proteins out from the cytosol and/or as a channel proteins integrating into membranes [88]. Herrmann et al [89] proposed the role of Bcl-2 as a "gatekeeper" which selectively regulates nuclear localization of crucial transcription factors such as p53 and

NfkB. This model was further developed by the hypothesis of Voerhinger [52] (Figure V 5) on the nuclear transport of GSH dependent on Bcl-2 by an unidentified mechanism.

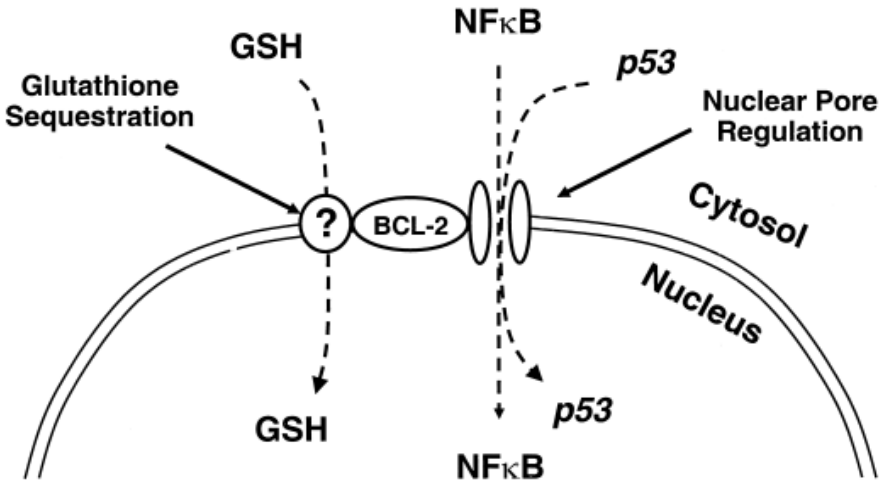

Voehringer DW, 1999

In the framework of our study it was of interest to investigate the possible effect of Bcl-2 on the proliferation parameters relative to the nuclear GSH level. For this endeavour we have compared the nuclear GSH level, telomerase activity and cell cycle progression in the milieu where only Bcl-2 expression was different. Apoptosis resistance and deregulated proliferation are two faces of the malignant transformation; the importance of understanding its mechanisms in order to design efficient anti cancer therapy, could not be underestimated. Therefore, in the

present work we gave preference to a cancer cell model overexpressing Bcl-2, MCF7 cells, over 3T3 fibroblasts. Nevertheless, our group is currently continuing this line of research using both 3T3 fibroblasts with the silenced Bcl-2 gene and its overexpressing counterpart.

Our results seem to be in concordance with numerous reports of the increase in GSH level caused by the overexpression of Bcl-2 (for a review see [52, 88]). Indeed, in contrast to MCF WT which showed the peak of GSH at 18h of culture, MCF7 bcl2 showed a striking and rapid increase of total cellular GSH 6h after plating, though followed by an immediate decline to a moderate value that was maintained till the end of culture (Fig III 42). In addition, the enhanced expression of Bcl-2 in the MCF7 cells, which includes the elevated presence at the nucleus, caused the increment in the levels of nuclear GSH (Fig III 43). This finding is in line with the results reported by Voehringer in HeLa cells and supports the hypothesis of the implication of nuclear Bcl-2 in GSH sequestration into the nucleus. However, this observation was limited to one time point; at 18h WT cells had more nuclear glutathione. This discrepancy could be explained by the changes in nuclear envelope and architecture during the cell cycle; Voehringer and coll. analysed the cellular GSH distribution at 48h of culture without the consideration of the cell cycle phase. Interestingly, the Bcl-2 caused the rapid increase in the level of GSH; however its nuclear sequestration was delayed. On

the contrary, the peak of nuclear GSH in MCF7 WT coincides with its maximal cellular level. Thus, if the elevated presence of Bcl-2 was not enough to provide the nucleus with more GSH although it was available, some other factor might be involved in the compartmentalization. One possible explanation could be that the relocalization of Bcl-2 from the cytoplasm to the nuclear envelope takes time, as previously described by Melan M and Sluder G [90]. On the other hand, strong intranuclear presence of Bcl-2 in interphase nuclei was shown in mammalian cells [91] and it was suggested that the intranuclear/perinuclear distribution of Bcl-2 was cell cycle dependent. So it is tempting to speculate that the presence of Bcl-2 at the nuclear envelope, as a request for its transport function, is related to the proliferative phase of the cell cycle. Indeed, our results in 3T3 fibroblasts confirm this premise: Bcl-2 is strongly present at the nucleus already at 6h (Fig III 41.) after plating and the entrance of the culture in the exponential phase of cell growth is advanced comparing to that of MCF7 cells (Fig. III 11).

We have found that, as well as GSH level, the level of telomerase activity augmented in MCF7 bcl2 cells. This result seemed to confirm previous findings of Mandal M and Kumar R [92] in HeLa cells and in DiFi cells: overexpresion of Bcl-2 was accompanied by elevated telomerase activity. On the other hand, these authors used subconfluent cell cultures for their analysis; although cancer cell lines do not show contact

inhibition induced growth arrest, it is expectable that their proliferating activity slows as they populate the plate, together with telomerase activity (Fig. 45), as shown in our model. Our culture could be considered "subconfluent" 5 days after plating; however, at this point we detected no significant differences in the TA between MCF7 Bcl-2 and WT cells. Although this report failed to provide any mechanistic explanation for the elevation of TA caused by Bcl-2, the proposed existence of the threshold level of telomerase activity in some cancer cells which could not be surpassed even though the Bcl-2 is elevated, is an interesting possibility. This might be the case in our cells, except in the interval before the proliferating phase, exactly when the difference in GSH level was striking. Moreover, in both cell types the maximal level of nuclear GSH concurred with the peak of telomerase activity; indeed, despite the extremely high cellular concentration of GSH in MCF7 Bcl-2 cells at 6h of culture the TA showed the increase when the nuclear compartmentalization of GSH occurred, i.e. 6h later. Therefore, according to our findings, telomerase activity is stimulated by the increase in nuclear GSH level, possibly caused by Bcl-2 relocation to the nuclear envelope.

6.1. The absence of the effect of Bcl-2 over-expression in MCF7 cells proliferation.

In the light of our findings, bcl2 induced an increase in GSH levels and is present in the nucleus of transfected cells but does not interfere with their proliferation.

6.1.1. Why MCF7 bcl2 cells show no proliferation decrease?

It has been shown previously that Bcl-2 over-expression was related to decreased proliferation of some cancer cell lines both in vitro and tumour growth in vivo [83, 86]. Unexpectedly, no significant consequences of Bcl-2 expression on the proliferation could be detected in our cell model. The work of Hoethelmans [93, 94] on the importance of various Bcl-2 domains in the influence of Bcl-2 on GSH level and proliferation activity could explain, at least in part, our findings.

According to this author, bcl2 is cleaved by caspase 3 at Asp 34 of the loop region, and by unidentified factor X at asp 64 (Fig V 6). First cleavage liberates 22kD Bcl-2ΔBH4 and inhibits the second one that produces 19kD Bcl-2 protein. Cells that were transfected with a Bcl-2 gene lacking BH4 domain showed an increase in GSH level and no decline in proliferation activity. Hoethelmans further argues that this

domain is crucial for the nuclear translocation of Bcl-2 and its impairment of cellular proliferation.

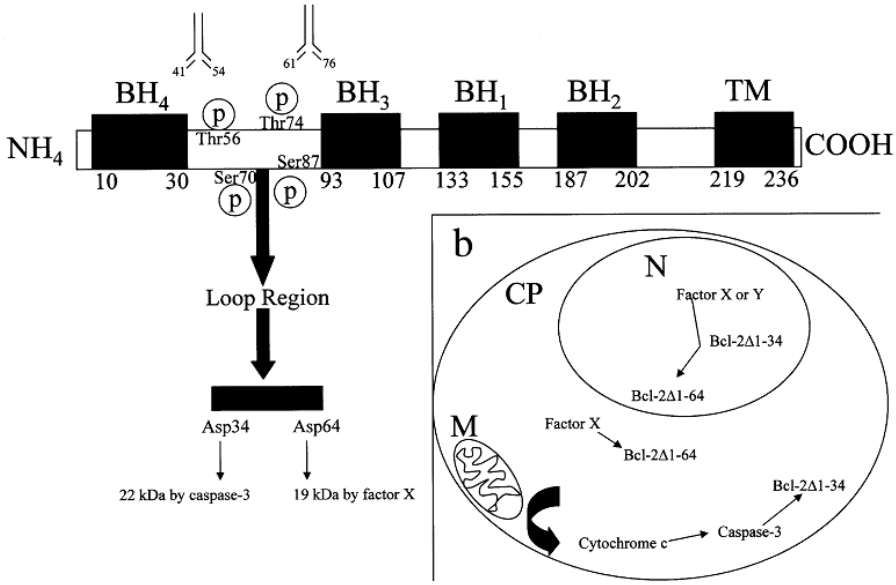

Hoetelmans RWM, Van de Velde CJH, Van Dierendonck JH, 2003

Conversely, the 19kD Bcl-2 is found in rapidly dividing nuclei, which suggests that ongoing cell proliferation requires cleavage of Bcl-2 into a 19kD fragment. In MCF7 cells caspase-3 is missing [95], therefore in this model, the 19kD bcl2 would prevail. Even more, authors speculated on the possible role of nuclear GSH in stimulating this type of cleavage: this would be another mechanism by which the nuclear presence of 19kD fragment would be favoured in our cell model.

In conclusion, despite of the increased expression of Bcl-2, proliferation would not be hampered in our cells because of the prevalence of 19kD Bcl-2 fragment caused by the absence of caspase 3 and increased nuclear GSH.

6.1.2 Why MCF7 bcl2 cells show no proliferation increase?

MCF7 Bcl-2 cells show the increase in total cellular GSH level and its nuclear compartmentalization and augmented telomerase activity; unexpectedly, they do not proliferate more then their WT counterpart.

This apparent paradox could be explained within the proposed model of the redox control of cell proliferation discussed previously (Fig V 1). To clarify the delay in the onset of exponential phase of cell growth in MCF7 cells, despite the presence of the high level of GSH, comparing to 3T3 fibroblasts where it coincides with the GSH maximum, we suggested the existence of the "reductive proliferation limit". This is a hypothetical hyper-reduced state when the cell, due to the extremely high GSH level, diminishes the ROS, even those necessary for the signalling in mitogen stimulation of cell proliferation. Thus, the cell proliferation is impaired due to the absence of the oxidative stimulus. In our model, MCF7 bcl2 cells accumulated GSH in the nucleus at 12h of culture, and MCF7 WT later, at 18h of culture, which is explained by the increased availability of GSH and

overexpression of Bcl-2. However, S+G2/M maximum is not reached until 24h of culture in both cell types, when the nuclear GSH level, and telomerase activity, decreased to a similar value. Thus, MCF7 WT have met the nuclear reductive limit, and further decrease of nuclear redox potential induced by over-expression of bcl2 confers no proliferative advantage.

7. Human pathologies possibly associated to nuclear glutathione.

A number of pathophysiological situations show the importance of nuclear GSH. Atzori et al. [96] showed variations in the amount and redox state of cellular thiols, particularly reduced glutathione, supporting a role for thiols in the regulation of growth and differentiation of human bronchial epithelial cells. In another example, depletion of nuclear GSH to 50-60% of initial values prior to irradiation (400 cGy) resulted in nuclear DNA fragmentation and apoptosis. These findings call attention to nuclear GSH as a determinant of intrinsic radiosensitivity of cells, suggesting that GSH plays a critical protective role in maintaining nuclear functional integrity [97].

Thalidomide produces human birth defects, mainly limb reduction malformations (phocomielia) [98]. A rat is proved to be thalidomide-resistant and rabbit thalidomide-

sensitive species; molecular base of this difference towards thalidomide treatment was studied in limb bud cells [99]. Confocal microscopy revealed that glutathione distribution (determined by CMFDA staining) was different in both cell types. Thalidomide induced cytosolic GSH depletion in both cell lines, however, nuclear GSH levels remained high in the rat thalidomide resistant cells but not in the rabbit thalidomide sensitive cells. Thus, it is tempting to speculate that a redox shift in the nucleus may result in the misregulation of interactions between transcription factors and DNA, causing defective growth and development. Interestingly, nowadays thalidomide is used in clinical practice as an inhibitor of angiogenesis and tumour growth.
Traditionally, GSH has been associated with increased resistance to radiation and xenobiotics [75, 97, 99-101]. Our study of the importance of the level of nuclear GSH compartmentalization for the onset of proliferation [12, 58] opens a series of new possible implications of nuclear GSH in human pathologies.

8. Suggested role of glutathione in the nucleus: an epigenetic perspective

Protection of the cellular integrity is the issue of maintaining the nuclear homeostasis. Hence, the importance of nuclear glutathione in the cellular defence from reactive

oxygen species (ROS) or xenobiotics should be comparable to the one of cytoplasm and mitochondria. Precisely, the production of glutathione has been biochemically linked to cofactors influencing epigenetic processes, because the biosynthesis of this molecule is directly related to the S-adenosylmethionine (SAM) pathway and SAM is the source of the methyl groups used for the methylation of DNA and histones [102].

Histone modifications are involved in regulating gene expression. The pattern of histone posttranslational modifications (PTMs) has prompted the "histone code hypotesis", which suggested that PTMs might affect the structure of chromatin or modify distinct binding regions of transcriptional factors [103, 104]. Chromatin can be divided into two distinct states: euchromatin, which is an unpacked permissive for transcription state and heterochromatin, characterized by having a repressive DNA conformation and structure. Furthermore, heterochromatin has two additional states: constitutive, generally silenced and facultative, which is silenced in some circumstances.

Well established in the literature, but relatively underappreciated, is the fact that most members of the histone H3 family contain one or more cysteine(s) (Cys110 in H3.1, H3.2 and H3.3 and one additional Cys96 in H3.1) in their protein core. This feature is a hallmark property of histone H3. The other histone proteins H2A, H2B and H4 do not have cysteine. As we have mentioned above, cysteine plays a specialized role in the function of proteins. The redox

behaviour–formation of disulfide bridges, sulphenic acid formation, glutathiolation, are all modifications associated with the alterations of redox environment [105]. Although the extent to which the nucleus contains an oxidizing or reducing environment is not well established, redox sensing mechanisms appear to play important roles in the nucleus. Hake and co-workers suggest the importance of clarifying the extension of H3 oxidation/reduction *in vivo* and understand the role of the Cys110 and Cys96, in the special case of H3.1, during the chromatin compactation process [106]. Furthermore, Hake proposes that histone H3 variants play a major role in cell differentiation and cell lineage restriction. With all these propositions Hake and co-workers proposed "the H3 barcode hypothesis". The unique cysteines in H3 variants might be important for nucleosomal and chromatin higher-order structures, through distinct intra- or inter-molecular disulphide bridges. Early studies developed by Allfrey et al. showed the distinct reactivity of H3 cysteines against sulfhydryl reagents in oxidative conditions. Cysteines were exposed in euchromatin regions and could form disulfide bonds with these reagents. In heterocromatin, cysteine residues did not react with the reagents, indicating that these cysteins are more buried [107]. In 1980, Lewis and Chiu showed that disulfide formation in Cys96 and 110 by sulfhydryl reagents destabilized the histone core [108]. Consequently, our finding that the pattern and level of glutathiolation of nuclear proteins change during the cell

cycle could confirm the possible implication of this modification in the control of chromatin structure dynamics [58].

How the H3 barcode and the histone code are connected or how different H3 variants become associated with distinct PTMs remains unresolved. A possible answer is that the distinct H3 isoforms, would control the precise folding of chromatin to make these fibers suitable substrates for the appropriate enzymes that introduce the PTMs. Another open question is how do the distinct H3 variants regulate the nucleosome stability? We propose that the glutathiolation of histone H3 cysteine residues could be a feasible answer to the regulation of chromatin conformation and compaction. Therefore, this modification would be a link in the regulation of all these phenomena.

If H3 glutathiolation occurs, do these changes take place during cell cycle? How could this modification affect the histone code (PTM's) and the histone H3 barcode during cell cycle?

Clearly, many questions remain unanswered, the regulation of the epigenetic process and its association with the gene expression during cell cycle or in the physiopathology of different diseases. Disruption of the balance of epigenetic networks can cause several major pathologies, including cancer, syndromes involving chromosomal instabilities, and mental retardation [109].

Thus, new approaches on the regulation of the epigenetic forces that control the package and un-package of

nuclear DNA during the different phases of the cell cycle could be envisaged. The information provided in the present thesis suggests an important role of nuclear glutathione as a key regulator of cell proliferation.

9. Bibliography:

1. Hutter, D.E., B.G. Till, and J.J. Greene, *Redox state changes in density-dependent regulation of proliferation.* Exp Cell Res, 1997. **232**(2): p. 435-8.
2. Menon, S.G. and P.C. Goswami, *A redox cycle within the cell cycle: ring in the old with the new.* Oncogene, 2007. **26**(8): p. 1101-9.
3. Hoffman, A., L.M. Spetner, and M. Burke, *Ramifications of a redox switch within a normal cell: its absence in a cancer cell.* Free Radic Biol Med, 2008. **45**(3): p. 265-8.
4. Davies, K.J., *The broad spectrum of responses to oxidants in proliferating cells: a new paradigm for oxidative stress.* IUBMB Life, 1999. **48**(1): p. 41-7.
5. Langeveld, C.H., et al., *Presence of glutathione immunoreactivity in cultured neurones and astrocytes.* Neuroreport, 1996. **7**(11): p. 1833-6.
6. Sagara, J.I., K. Miura, and S. Bannai, *Maintenance of neuronal glutathione by glial cells.* J Neurochem, 1993. **61**(5): p. 1672-6.
7. Dringen, R., B. Pfeiffer, and B. Hamprecht, *Synthesis of the antioxidant glutathione in neurons: supply by astrocytes of CysGly as precursor for neuronal glutathione.* J Neurosci, 1999. **19**(2): p. 562-9.
8. Conour, J.E., W.V. Graham, and H.R. Gaskins, *A combined in vitro/bioinformatic investigation of redox regulatory*

mechanisms governing cell cycle progression. Physiol Genomics, 2004. **18**(2): p. 196-205.
9. Norton, J.D., *ID helix-loop-helix proteins in cell growth, differentiation and tumorigenesis.* J Cell Sci, 2000. **113 (Pt 22)**: p. 3897-905.
10. Yokota, Y. and S. Mori, *Role of Id family proteins in growth control.* J Cell Physiol, 2002. **190**(1): p. 21-8.
11. Lasorella, A., A. Iavarone, and M.A. Israel, *Id2 specifically alters regulation of the cell cycle by tumor suppressor proteins.* Mol Cell Biol, 1996. **16**(6): p. 2570-8.
12. Borras, C., et al., *Glutathione regulates telomerase activity in 3T3 fibroblasts.* J Biol Chem, 2004. **279**(33): p. 34332-5.
13. Huang, Z.Z., et al., *Mechanism and significance of increased glutathione level in human hepatocellular carcinoma and liver regeneration.* Faseb J, 2001. **15**(1): p. 19-21.
14. Rodriguez, J.L., et al., *Id2 leaves the chromatin of the E2F4-p130-controlled c-myc promoter during hepatocyte priming for liver regeneration.* Biochem J, 2006. **398**(3): p. 431-7.
15. Dimitrova, D.S. and D.M. Gilbert, *Temporally coordinated assembly and disassembly of replication factories in the absence of DNA synthesis.* Nat Cell Biol, 2000. **2**(10): p. 686-94.
16. Kennedy, B.K., et al., *Nuclear organization of DNA replication in primary mammalian cells.* Genes Dev, 2000. **14**(22): p. 2855-68.
17. Dimitrova, D.S. and R. Berezney, *The spatio-temporal organization of DNA replication sites is identical in primary, immortalized and transformed mammalian cells.* J Cell Sci, 2002. **115**(Pt 21): p. 4037-51.
18. Barbie, D.A., et al., *Nuclear reorganization of mammalian DNA synthesis prior to cell cycle exit.* Mol Cell Biol, 2004. **24**(2): p. 595-607.
19. Leonhardt, H., et al., *Dynamics of DNA replication factories in living cells.* J Cell Biol, 2000. **149**(2): p. 271-80.
20. Dijkwel, P.A. and P.W. Wenink, *Structural integrity of the nuclear matrix: differential effects of thiol agents and metal chelators.* J Cell Sci, 1986. **84**: p. 53-67.
21. Oleinick, N.L., et al., *The formation, identification, and significance of DNA-protein cross-links in mammalian cells.* Br J Cancer Suppl, 1987. **8**: p. 135-40.

22. Bellomo, G., G. Palladini, and M. Vairetti, *Intranuclear distribution, function and fate of glutathione and glutathione-S-conjugate in living rat hepatocytes studied by fluorescence microscopy.* Microsc Res Tech, 1997. **36**(4): p. 243-52.
23. Green, D.R. and G.I. Evan, *A matter of life and death.* Cancer Cell, 2002. **1**(1): p. 19-30.
24. Thelander, L. and P. Reichard, *Reduction of ribonucleotides.* Annu Rev Biochem, 1979. **48**: p. 133-58.
25. Spyrou, G. and A. Holmgren, *Deoxyribonucleoside triphosphate pools and growth of glutathione-depleted 3T6 mouse fibroblasts.* Biochem Biophys Res Commun, 1996. **220**(1): p. 42-6.
26. Kim, N.W., et al., *Specific association of human telomerase activity with immortal cells and cancer.* Science, 1994. **266**(5193): p. 2011-5.
27. Harley, C.B., A.B. Futcher, and C.W. Greider, *Telomeres shorten during ageing of human fibroblasts.* Nature, 1990. **345**(6274): p. 458-60.
28. Bodnar, A.G., et al., *Extension of life-span by introduction of telomerase into normal human cells.* Science, 1998. **279**(5349): p. 349-52.
29. Kurz, D.J., et al., *Chronic oxidative stress compromises telomere integrity and accelerates the onset of senescence in human endothelial cells.* J Cell Sci, 2004. **117**(Pt 11): p. 2417-26.
30. Finkel, T. and N.J. Holbrook, *Oxidants, oxidative stress and the biology of ageing.* Nature, 2000. **408**(6809): p. 239-47.
31. Pagano, G., et al., *In vivo prooxidant state in Werner syndrome (WS): results from three WS patients and two WS heterozygotes.* Free Radic Res, 2005. **39**(5): p. 529-33.
32. Vaziri, H., et al., *Loss of telomeric DNA during aging of normal and trisomy 21 human lymphocytes.* Am J Hum Genet, 1993. **52**(4): p. 661-7.
33. Pallardo, F.V., et al., *Multiple evidence for an early age pro-oxidant state in Down Syndrome patients.* Biogerontology, 2006. **7**(4): p. 211-20.
34. Lloret, A., et al., *Different patterns of in vivo pro-oxidant states in a set of cancer- or aging-related genetic diseases.* Free Radic Biol Med, 2008. **44**(4): p. 495-503.

35. Serrano, M. and M.A. Blasco, *Putting the stress on senescence.* Curr Opin Cell Biol, 2001. **13**(6): p. 748-53.
36. Furumoto, K., et al., *Age-dependent telomere shortening is slowed down by enrichment of intracellular vitamin C via suppression of oxidative stress.* Life Sci, 1998. **63**(11): p. 935-48.
37. Yokoo, S., et al., *Slow-down of age-dependent telomere shortening is executed in human skin keratinocytes by hormesis-like-effects of trace hydrogen peroxide or by anti-oxidative effects of pro-vitamin C in common concurrently with reduction of intracellular oxidative stress.* J Cell Biochem, 2004. **93**(3): p. 588-97.
38. Perez-Rivero, G., et al., *Telomerase deficiency promotes oxidative stress by reducing catalase activity.* Free Radic Biol Med, 2008.
39. Itahana, K., J. Campisi, and G.P. Dimri, *Mechanisms of cellular senescence in human and mouse cells.* Biogerontology, 2004. **5**(1): p. 1-10.
40. Parrinello, S., et al., *Oxygen sensitivity severely limits the replicative lifespan of murine fibroblasts.* Nat Cell Biol, 2003. **5**(8): p. 741-7.
41. Henle, E.S., et al., *Sequence-specific DNA cleavage by Fe2+-mediated fenton reactions has possible biological implications.* J Biol Chem, 1999. **274**(2): p. 962-71.
42. Hayakawa, N., et al., *Isothiazolone derivatives selectively inhibit telomerase from human and rat cancer cells in vitro.* Biochemistry, 1999. **38**(35): p. 11501-7.
43. Gallagher, G. and D.L. Forrest, *Second solid cancers after allogeneic hematopoietic stem cell transplantation.* Cancer, 2007. **109**(1): p. 84-92.
44. Canela, A., et al., *High-throughput telomere length quantification by FISH and its application to human population studies.* Proc Natl Acad Sci U S A, 2007. **104**(13): p. 5300-5.
45. Vina, J., et al., *Why females live longer than males: control of longevity by sex hormones.* Sci Aging Knowledge Environ, 2005. **2005**(23): p. pe17.
46. Ellerby, L.M., et al., *Shift of the cellular oxidation-reduction potential in neural cells expressing Bcl-2.* J Neurochem, 1996. **67**(3): p. 1259-67.

47. Martensson, J., J.C. Lai, and A. Meister, *High-affinity transport of glutathione is part of a multicomponent system essential for mitochondrial function.* Proc Natl Acad Sci U S A, 1990. **87**(18): p. 7185-9.
48. Hwang, C., A.J. Sinskey, and H.F. Lodish, *Oxidized redox state of glutathione in the endoplasmic reticulum.* Science, 1992. **257**(5076): p. 1496-502.
49. Soderdahl, T., et al., *Visualization of the compartmentalization of glutathione and protein-glutathione mixed disulfides in cultured cells.* Faseb J, 2003. **17**(1): p. 124-6.
50. Briviba, K., et al., *Distribution of the monochlorobimane-glutathione conjugate between nucleus and cytosol in isolated hepatocytes.* Biochem J, 1993. **294 (Pt 3)**: p. 631-3.
51. Thomas, M., T. Nicklee, and D.W. Hedley, *Differential effects of depleting agents on cytoplasmic and nuclear non-protein sulphydryls: a fluorescence image cytometry study.* Br J Cancer, 1995. **72**(1): p. 45-50.
52. Voehringer, D.W., et al., *Bcl-2 expression causes redistribution of glutathione to the nucleus.* Proc Natl Acad Sci U S A, 1998. **95**(6): p. 2956-60.
53. Hansen, J.M., Y.M. Go, and D.P. Jones, *Nuclear and mitochondrial compartmentalization of oxidative stress and redox signaling.* Annu Rev Pharmacol Toxicol, 2006. **46**: p. 215-34.
54. McKernan, T.B., E.B. Woods, and L.H. Lash, *Uptake of glutathione by renal cortical mitochondria.* Arch Biochem Biophys, 1991. **288**(2): p. 653-63.
55. Kim, J.R., et al., *Oxidation of thioredoxin reductase in HeLa cells stimulated with tumor necrosis factor-alpha.* FEBS Lett, 2004. **567**(2-3): p. 189-96.
56. Watson, W.H. and D.P. Jones, *Oxidation of nuclear thioredoxin during oxidative stress.* FEBS Lett, 2003. **543**(1-3): p. 144-7.
57. Gutscher, M., et al., *Real-time imaging of the intracellular glutathione redox potential.* Nat Methods, 2008. **5**(6): p. 553-9.
58. Markovic, J., et al., *Glutathione is recruited into the nucleus in early phases of cell proliferation.* J Biol Chem, 2007. **282**(28): p. 20416-24.

59. Menon, S.G., et al., *Redox regulation of the G1 to S phase transition in the mouse embryo fibroblast cell cycle.* Cancer Res, 2003. **63**(9): p. 2109-17.
60. Klevecz, R.R., et al., *A genomewide oscillation in transcription gates DNA replication and cell cycle.* Proc Natl Acad Sci U S A, 2004. **101**(5): p. 1200-5.
61. Schafer, F.Q. and G.R. Buettner, *Redox environment of the cell as viewed through the redox state of the glutathione disulfide/glutathione couple.* Free Radic Biol Med, 2001. **30**(11): p. 1191-212.
62. Soboll, S., et al., *The content of glutathione and glutathione S-transferases and the glutathione peroxidase activity in rat liver nuclei determined by a non-aqueous technique of cell fractionation.* Biochem J, 1995. **311 (Pt 3)**: p. 889-94.
63. Carpenter, G. and S. Cohen, *Epidermal growth factor.* J Biol Chem, 1990. **265**(14): p. 7709-12.
64. Jang, J.H. and Y.J. Surh, *Potentiation of cellular antioxidant capacity by Bcl-2: implications for its antiapoptotic function.* Biochem Pharmacol, 2003. **66**(8): p. 1371-9.
65. Spector, D., J. Labarre, and M.B. Toledano, *A genetic investigation of the essential role of glutathione: mutations in the proline biosynthesis pathway are the only suppressors of glutathione auxotrophy in yeast.* J Biol Chem, 2001. **276**(10): p. 7011-6.
66. Cotgreave, I.A. and R.G. Gerdes, *Recent trends in glutathione biochemistry--glutathione-protein interactions: a molecular link between oxidative stress and cell proliferation?* Biochem Biophys Res Commun, 1998. **242**(1): p. 1-9.
67. Fratelli, M., et al., *Gene expression profiling reveals a signaling role of glutathione in redox regulation.* Proc Natl Acad Sci U S A, 2005. **102**(39): p. 13998-4003.
68. Green, R.M., et al., *Subcellular compartmentalization of glutathione: correlations with parameters of oxidative stress related to genotoxicity.* Mutagenesis, 2006. **21**(6): p. 383-90.
69. Casey, W., et al., *Transcriptional and physiological responses of HepG2 cells exposed to diethyl maleate: time course analysis.* Physiol Genomics, 2002. **8**(2): p. 115-22.
70. Britten, R.A., et al., *The relationship between nuclear glutathione levels and resistance to melphalan in human*

ovarian tumour cells. Biochem Pharmacol, 1991. **41**(4): p. 647-9.
71. Esposito, F., T. Russo, and F. Cimino, *Generation of prooxidant conditions in intact cells to induce modifications of cell cycle regulatory proteins.* Methods Enzymol, 2002. **352**: p. 258-68.
72. Sen, C.K. and L. Packer, *Antioxidant and redox regulation of gene transcription.* Faseb J, 1996. **10**(7): p. 709-20.
73. Sun, Y. and L.W. Oberley, *Redox regulation of transcriptional activators.* Free Radic Biol Med, 1996. **21**(3): p. 335-48.
74. Reddy, N.M., et al., *Genetic disruption of the Nrf2 compromises cell-cycle progression by impairing GSH-induced redox signaling.* Oncogene, 2008.
75. Smith, C.V., et al., *Compartmentalization of glutathione: implications for the study of toxicity and disease.* Toxicol Appl Pharmacol, 1996. **140**(1): p. 1-12.
76. Feldherr, C.M. and D. Akin, *EM visualization of nucleocytoplasmic transport processes.* Electron Microsc Rev, 1990. **3**(1): p. 73-86.
77. Nigg, E.A., *Nucleocytoplasmic transport: signals, mechanisms and regulation.* Nature, 1997. **386**(6627): p. 779-87.
78. Ribbeck, K. and D. Gorlich, *Kinetic analysis of translocation through nuclear pore complexes.* Embo J, 2001. **20**(6): p. 1320-30.
79. Feldherr, C.M. and D. Akin, *The permeability of the nuclear envelope in dividing and nondividing cell cultures.* J Cell Biol, 1990. **111**(1): p. 1-8.
80. Feldherr, C.M. and D. Akin, *Regulation of nuclear transport in proliferating and quiescent cells.* Exp Cell Res, 1993. **205**(1): p. 179-86.
81. Krajewski, S., et al., *Investigation of the subcellular distribution of the Bcl-2 oncoprotein: residence in the nuclear envelope, endoplasmic reticulum, and outer mitochondrial membranes.* Cancer Res, 1993. **53**(19): p. 4701-14.
82. Zimmermann, A.K., et al., *Glutathione binding to the Bcl-2 homology-3 domain groove: a molecular basis for Bcl-2 antioxidant function at mitochondria.* J Biol Chem, 2007. **282**(40): p. 29296-304.

83. Vaux, D.L., S. Cory, and J.M. Adams, *Bcl-2 gene promotes haemopoietic cell survival and cooperates with c-myc to immortalize pre-B cells.* Nature, 1988. **335**(6189): p. 440-2.
84. el-Deiry, W.S., et al., *WAF1/CIP1 is induced in p53-mediated G1 arrest and apoptosis.* Cancer Res, 1994. **54**(5): p. 1169-74.
85. Vairo, G., K.M. Innes, and J.M. Adams, *Bcl-2 has a cell cycle inhibitory function separable from its enhancement of cell survival.* Oncogene, 1996. **13**(7): p. 1511-9.
86. O'Reilly, L.A., D.C. Huang, and A. Strasser, *The cell death inhibitor Bcl-2 and its homologues influence control of cell cycle entry.* Embo J, 1996. **15**(24): p. 6979-90.
87. Mirkovic, N., et al., *Resistance to radiation-induced apoptosis in Bcl-2-expressing cells is reversed by depleting cellular thiols.* Oncogene, 1997. **15**(12): p. 1461-70.
88. Reed, D.J., et al., *High-performance liquid chromatography analysis of nanomole levels of glutathione, glutathione disulfide, and related thiols and disulfides.* Anal Biochem, 1980. **106**(1): p. 55-62.
89. Herrmann, J.L., E. Bruckheimer, and T.J. McDonnell, *Cell death signal transduction and Bcl-2 function.* Biochem Soc Trans, 1996. **24**(4): p. 1059-65.
90. Melan, M.A. and G. Sluder, *Redistribution and differential extraction of soluble proteins in permeabilized cultured cells. Implications for immunofluorescence microscopy.* J Cell Sci, 1992. **101 (Pt 4)**: p. 731-43.
91. Vahrmeijer, A.L., et al., *Development of resistance to glutathione depletion-induced cell death in CC531 colon carcinoma cells: association with increased expression of Bcl-2.* Biochem Pharmacol, 2000. **59**(12): p. 1557-62.
92. Mandal, M. and R. Kumar, *Bcl-2 modulates telomerase activity.* J Biol Chem, 1997. **272**(22): p. 14183-7.
93. Hoetelmans, R.W., et al., *The role of various Bcl-2 domains in the anti-proliferative effect and modulation of cellular glutathione levels: a prominent role for the BH4 domain.* Cell Prolif, 2003. **36**(1): p. 35-44.
94. Hoetelmans, R.W., C.J. Van de Velde, and J.H. Van Dierendonck, *The presence of 19-kDa Bcl-2 in dividing cells.* Cell Prolif, 2003. **36**(6): p. 293-306.

95. Janicke, R.U., et al., *Caspase-3 is required for DNA fragmentation and morphological changes associated with apoptosis.* J Biol Chem, 1998. **273**(16): p. 9357-60.
96. Atzori, L., et al., *Growth-associated modifications of low-molecular-weight thiols and protein sulfhydryls in human bronchial fibroblasts.* J Cell Physiol, 1990. **143**(1): p. 165-71.
97. Morales, A., et al., *Oxidative damage of mitochondrial and nuclear DNA induced by ionizing radiation in human hepatoblastoma cells.* Int J Radiat Oncol Biol Phys, 1998. **42**(1): p. 191-203.
98. Mellin, G.W. and M. Katzenstein, *The saga of thalidomide. Neuropathy to embryopathy, with case reports of congenital anomalies.* N Engl J Med, 1962. **267**: p. 1238-44 concl.
99. Hansen, J.M., et al., *Thalidomide modulates nuclear redox status and preferentially depletes glutathione in rabbit limb versus rat limb.* J Pharmacol Exp Ther, 2002. **300**(3): p. 768-76.
100. Biaglow, J.E., et al., *The role of thiols in cellular response to radiation and drugs.* Radiat Res, 1983. **95**(3): p. 437-55.
101. Jevtovic-Todorovic, V. and T.M. Guenthner, *Depletion of a discrete nuclear glutathione pool by oxidative stress, but not by buthionine sulfoximine. Correlation with enhanced alkylating agent cytotoxicity to human melanoma cells in vitro.* Biochem Pharmacol, 1992. **44**(7): p. 1383-93.
102. Hitchler, M.J. and F.E. Domann, *An epigenetic perspective on the free radical theory of development.* Free Radic Biol Med, 2007. **43**(7): p. 1023-36.
103. Fischle, W., Y. Wang, and C.D. Allis, *Binary switches and modification cassettes in histone biology and beyond.* Nature, 2003. **425**(6957): p. 475-9.
104. Fischle, W., et al., *Regulation of HP1-chromatin binding by histone H3 methylation and phosphorylation.* Nature, 2005. **438**(7071): p. 1116-22.
105. Netto, L.E., et al., *Reactive cysteine in proteins: protein folding, antioxidant defense, redox signaling and more.* Comp Biochem Physiol C Toxicol Pharmacol, 2007. **146**(1-2): p. 180-93.
106. Hake, S.B. and C.D. Allis, *Histone H3 variants and their potential role in indexing mammalian genomes: the "H3*

barcode hypothesis". Proc Natl Acad Sci U S A, 2006. **103**(17): p. 6428-35.

107. Prior, C.P., et al., *Reversible changes in nucleosome structure and histone H3 accessibility in transcriptionally active and inactive states of rDNA chromatin.* Cell, 1983. **34**(3): p. 1033-42.
108. Lewis, P.N. and S.S. Chiu, *Effect of histone H3 sulfhydryl modifications on histone-histone interactions and nucleosome formation and structure.* Eur J Biochem, 1980. **109**(2): p. 369-76.
109. Egger, G., et al., *Epigenetics in human disease and prospects for epigenetic therapy.* Nature, 2004. **429**(6990): p. 457-63.

VI CONCLUSIONS

VI CONCLUSIONS

1. The level of cellular glutathione in the particular cell line could define its proliferating capacity. Its variations along the cell culture dictate the rhythm of cell proliferation, possibly by the modulation of redox sensitive cell cycle regulatory proteins

2. The telomerase activity is highly sensible to the cellular redox state, regardless of the cell type, its inherent proliferation capacity or the origin of the cells. The dependence of the cell cycle progression on the level of glutathione could be attributed, at least in part, to its modulation of telomerase activity

3. The nuclear compartmentalization of glutathione is a prerequisite for the onset of the exponential phase of the cell growth. The redox state of nuclear proteins, defined by the glutathiolation and oxidation, varies significantly with the cell proliferation activity.

4. The depletion of nuclear glutathione severely impairs the cell cycle progression

5. During the changes in the nuclear membrane that precede the cell division, nuclear Bcl-2 could facilitate the translocation of glutathione to the cell nucleus. The overexpression of bcl-2 induced an early increase of the total glutathione level, telomerase activity and nuclear GSH compartmentalization.

VII RESUMEN DE LOS RESULTADOS Y DISCUSIÓN

1. Introducción

El glutatión reducido (GSH) es uno de los antioxidantes endógenos más importantes en las células. Por su propiedad de mantener estado redox (tioles/disúlfidos) de la célula, ocupa un lugar central en el control de muchos procesos celulares. Es imprescindible en la síntesis de proteínas (1), juega un papel crucial en la defensa celular frente a estrés oxidativo y xenobioticos (2) y en la regulación de la muerte celular programada (3) y el ciclo celular (4). Esa gran diversidad de procesos vitales dependientes del glutatión y realizados en diferentes orgánulos de la célula implica la necesidad de su compartimentación y existencia de mecanismos que controlarían su concentración y garantizarían el ambiente adecuado en cada compartimiento. Integridad celular se defiende en el núcleo, en su "software" - el acido desoxiribonucleico (ADN) que controla los procesos celulares atreves de la regulación de la expresión génica. El papel protector del glutatión sobre el ADN (5), y su implicación en numerosos procesos que tienen lugar en el núcleo, sobre todo la síntesis de ADN (6) y en el mantenimiento de organización del matriz nuclear (7) han sido claramente demostrados. Sin embargo, sobre la concentración del glutatión en el núcleo y su regulación se sabe relativamente poco. Eso se debe a dos factores principales. El primero es metodológico: es imposible determinar la concentración del GSH nuclear usando clásicos métodos de fraccionamiento celular (para la revisión ver

Söderdahl *et al*. (8)). El segundo factor es el enfoque: el GSH nuclear se estudiaba, por lo general, en las células confluentes (en la fase G0/G1) lo que se aproxima a la situación in situ, es decir, en el tejido las células están diferenciadas, han salido del ciclo celular, y confluentes. El núcleo cambia dramáticamente durante las diferentes fases del ciclo celular, por lo tanto los estudios de la compartimentación nuclear del GSH tienen que tener en cuenta esta dinámica celular.

El objetivo de la presente tesis es investigar la importancia del nivel de GSH y su distribución celular, especialmente la compartimentación nuclear, en la proliferación celular y posibles mecanismos involucrados en el control del dicho fenómeno.

2. Resultados

Hemos estudiado los cambios en la compartimentación nuclear de GSH en diferentes fases del ciclo celular. 24h después de la siembra, los fibroblastos 3T3 empiezan a crecer exponencialmente (Fig. 1); a las 24 y 48h después de la siembra el porcentaje de las células en la fase S+M/G2 aumenta significativamente (41% y 35%, respectivamente). A las 72h y mas tarde, crecimiento celular es menos intenso y a los 6 días en cultivo células llegan a confluencia, caracterizada por la mayoría de las células (81%) en la fase G0/G1.

La concentración del GSH celular total era máxima a las 24h de cultivo (20 nmoles/10^6 célula) (Fig. 2A), cuando un alto

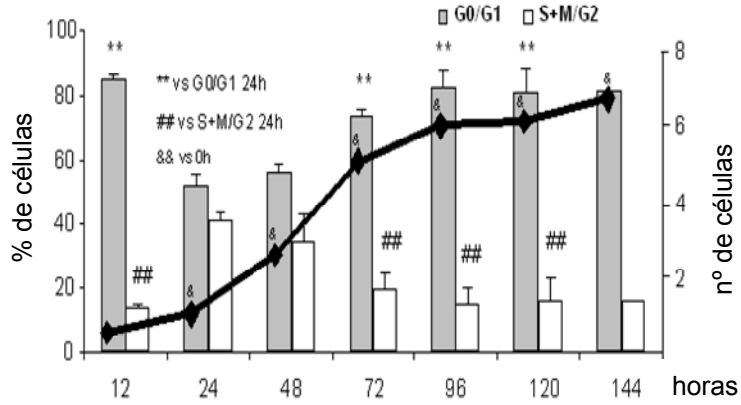

Figura 1. Curva de crecimiento y proliferación celular en los fibroblastos 3T3

porcentaje de células (41%) estaba a punto de entrar en mitosis o ya en la división celular. Sin embargo, cuando las células llegaron a confluencia (día 6) y mayoría de las células eran quiescentes, la concentración de GSH tenia un nivel bajo (11 nmoles/10^6 células).

A

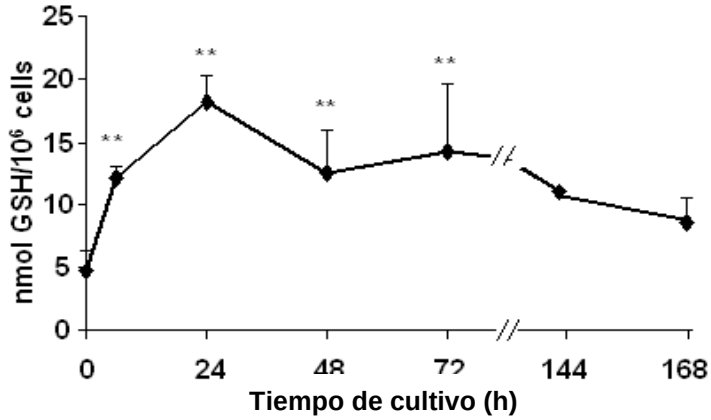

Figura 2a. Concentración total del GSH en el cultivo de los fibroblastos 3T3

Hemos determinado el ratio GSH/GSSG en las células a lo largo del ciclo celular y encontramos que no cambiaba significativamente (Fig. 2B).

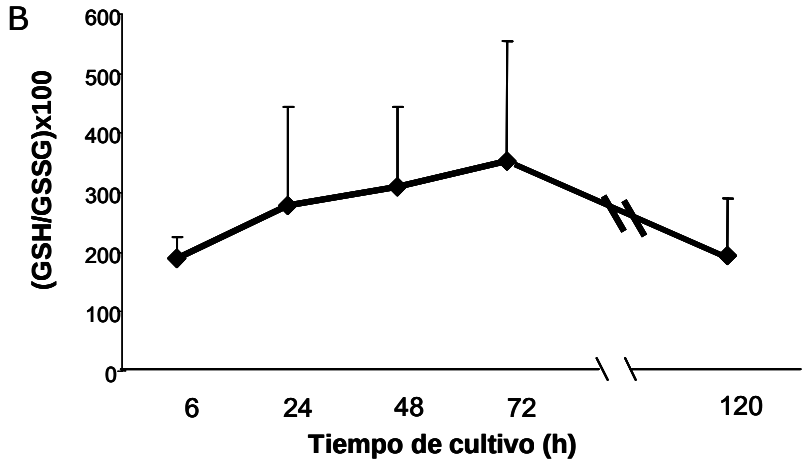

Figura 2b. El ratio de GSH/GSSG celular en el crecimiento de los fibroblastos 3T3

A la luz de estos resultados, nos planteamos si la compartimentación nuclear del GSH podría tener un papel en la progresión del ciclo celular durante las fases tempranas del cultivo celular. Figura 3. muestra la distribución celular del GSH dependiente del ciclo celular en los fibroblastos 3T3. Seis horas después de la siembra, se ven pocas células en la placa (Fig. 3ª y 3b). Los núcleos teñidos en azul con el Hoechst 33342 aparecen en el panel b y la distribución del glutatión definida por la fluorescencia verde del CMFDA se ve en el panel c. Un detalle (aumentado) representado en el panel d facilita la visualización de la compartimentación nuclear del glutatión. La línea blanca que se observa en las fotos es la herramienta de cuantificación del software (que apoya el microscopio confocal) que permite la medición del

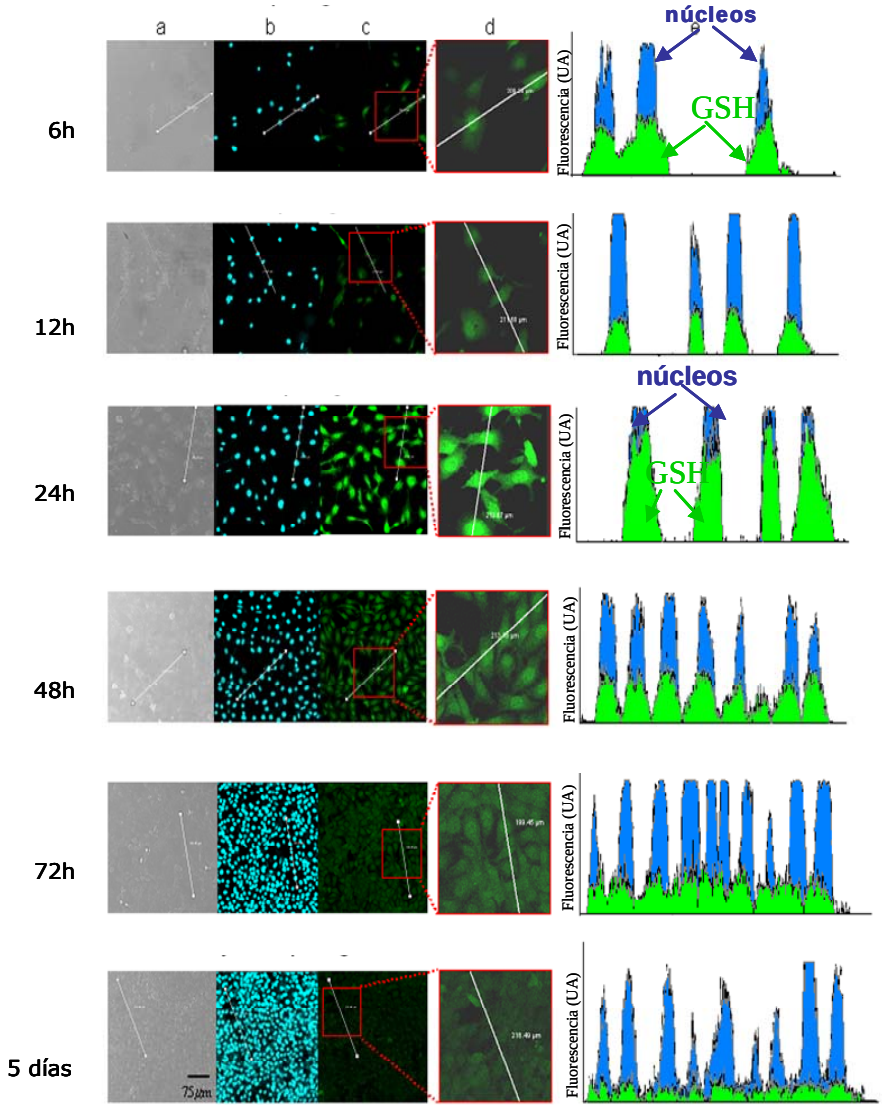

Figura 3. Distribución intercelular del GSH en los fibroblastos 3T3

nivel de fluorescencia. Los histogramas en el panel e son producto de la comparación de los niveles de fluorescencia verde, que nos da la distribución del GSH y la fluorescencia azul, que nos da la localización de los núcleos. Los picos

azules coinciden con los verdes al principio del cultivo, existe una importante compartimentación nuclear del GSH. A las 12 y 24h la población celular sigue creciendo. El GSH celular (intensidad de la fluorescencia verde) era máximo a las 24h. El análisis de la intensidad y la distribución de la fluorescencia azul/verde (Fig. 3b y 3d, respectivamente) muestra máxima correlación a las 24h. Cuando las células llegaron a confluencia, a las 72h y 6 días en cultivo, los picos de GSH ya no coincidían con los núcleos celulares.

La variación en los niveles de GSH a lo largo del ciclo celular definida por espectrofotometría (Fig. 2a) coincide con la variación del nivel total de fluorescencia verde en la población celular (Fig. 3c). Como se esperaba, la fluorescencia verde del GSH baja claramente a las 72h y 5 días en cultivo, cuando las células llegan a la confluencia, ocurre inhibición por contacto y como consecuencia, la población celular entra en la quiescencia (70-80% de células en la fase G0/G1). En esta fase, no se observaba diferencia en la fluorescencia verde entre el núcleo y el citoplasma de las células: la distribución del GSH era homogénea en la población celular.

Por lo tanto, cuando las células empiezan a crecer, el GSH estaba localizado predominantemente en el núcleo de las células. Sin embargo, cuando el crecimiento celular se ha disminuido, la distribución celular del GSH era homogénea.

La capacidad de la célula de concentrar el GSH en el núcleo se ha estimado midiendo el ratio núcleo/citoplasma de la fluorescencia verde de CMFDA. Se han comparado los

niveles de la fluorescencia verde proveniente del área nuclear definida con el teñido azul de Hoechst y el área celular visualizada por contraste de fases (panel 3a), célula por célula, en 100 células por cada experimento y condición. Los resultados en la figura 4 muestran un patrón de distribución donde el ratio máximo de núcleo/citoplasma (4.2 ± 0.8) se alcanza muy temprano después de la siembra (a las 6h). Aunque el alto nivel del ratio núcleo/citoplasma se haya mantenido durante el crecimiento exponencial de la población celular, se observaba una persistente caída en la compartimentación nuclear del GSH a o largo de la progresión del ciclo celular.

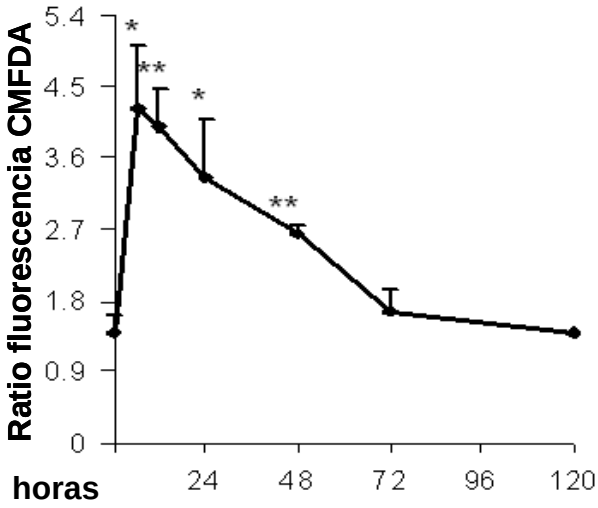

Figura 4. El ratio nuclear/citoplasmático del GSH en el crecimiento de los fibroblastos 3T3

Una vez las células llegaron a la confluencia, la mayoría en la fase G0/G1, el ratio núcleo/citoplasma era cercano a uno, es decir, la distribución celular del GSH era homogenea.

Para confirmar las fases del ciclo celular obtenidas en base al análisis del contenido de ADN (fluorescencia de ioduro de propidio) por citometria de flujo, hemos estudiado los patrones de expresión de la proteína Id2 y p107. Estas proteínas se sobreexpresan cuando se activan la proliferación y división celular. Los resultados en la figura 5. muestran la marcada expresión de estas proteínas a las 24 y 48h de cultivo, que baja significativamente a partir de las 72h.

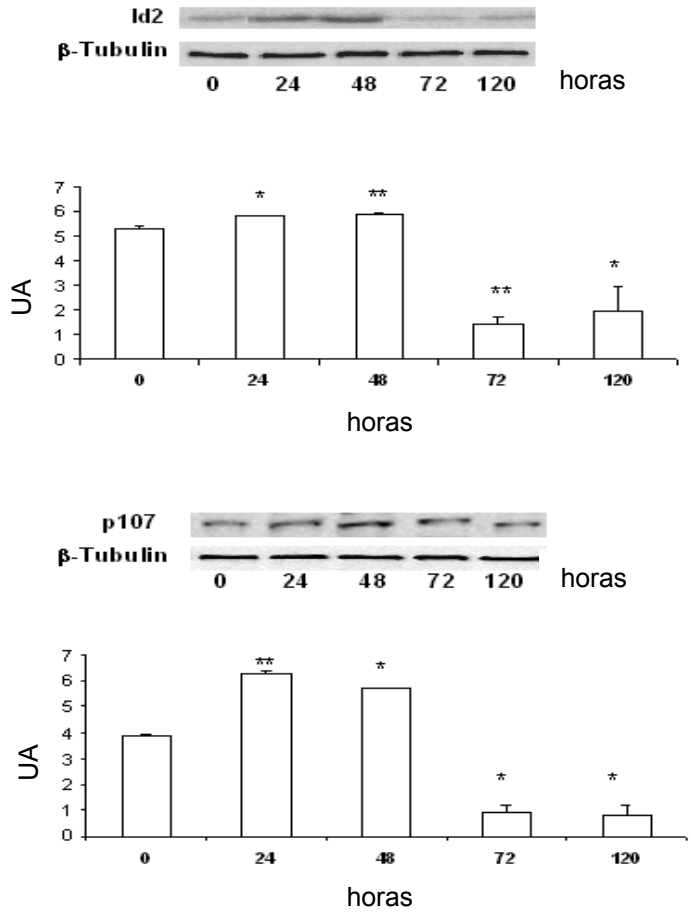

Figura 5. Expresión de las proteínas del ciclo celular

Las áreas de alta fluorescencia del CMFDA no provenían del GSH mitocondrial. Lo demostramos en los experimentos de triple teñido en los que marcamos el ADN celular con Hoechst (en azul), el GSH con CMFDA (en verde) y las mitocondrias con MitoTracker (en rojo).

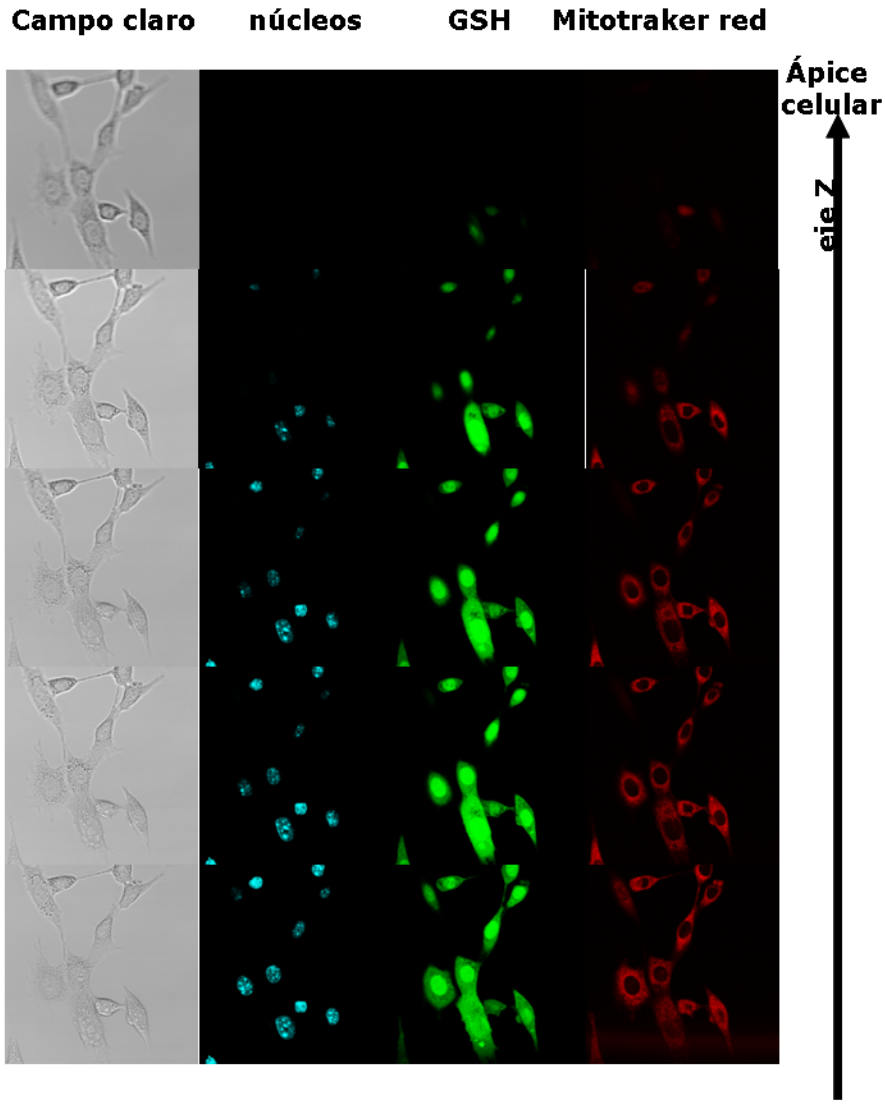

Figura 6.- Fibroblastos 3T3 24h en cultivo. Estudio de la distribución intercelular del GSH y mitocondrias

En la figura 6. está representada una serie de imágenes obtenida a lo largo del eje Z, desde el ápice celular hasta el fondo. La forma de los núcleos se ve claramente y se muestra de nuevo que coincide con el máximo brillo de la fluorescencia verde del CMFDA en el centro de la célula. La distribución mitocondrial era periférica.

Intentamos, también, elucidar los mecanismos incluidos en la compartimentación del GSH; dado que no esta muy claro si el GSH se mueve entre el citoplasma y el núcleo por difusión o hay un transporte activo y un transportador dependiente del ATP.

En los fibroblastos 3T3 24h en cultivo, en el momento de máxima compartimentación nuclear del GSH, usamos un desacoplante mitocondrial FCCP 20μM para disminuir la síntesis de ATP y estudiamos el efecto producido en la compartimentación del GSH.

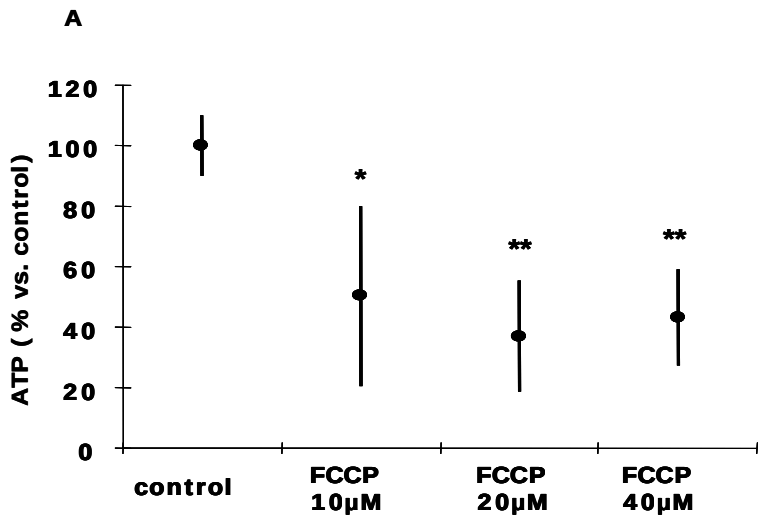

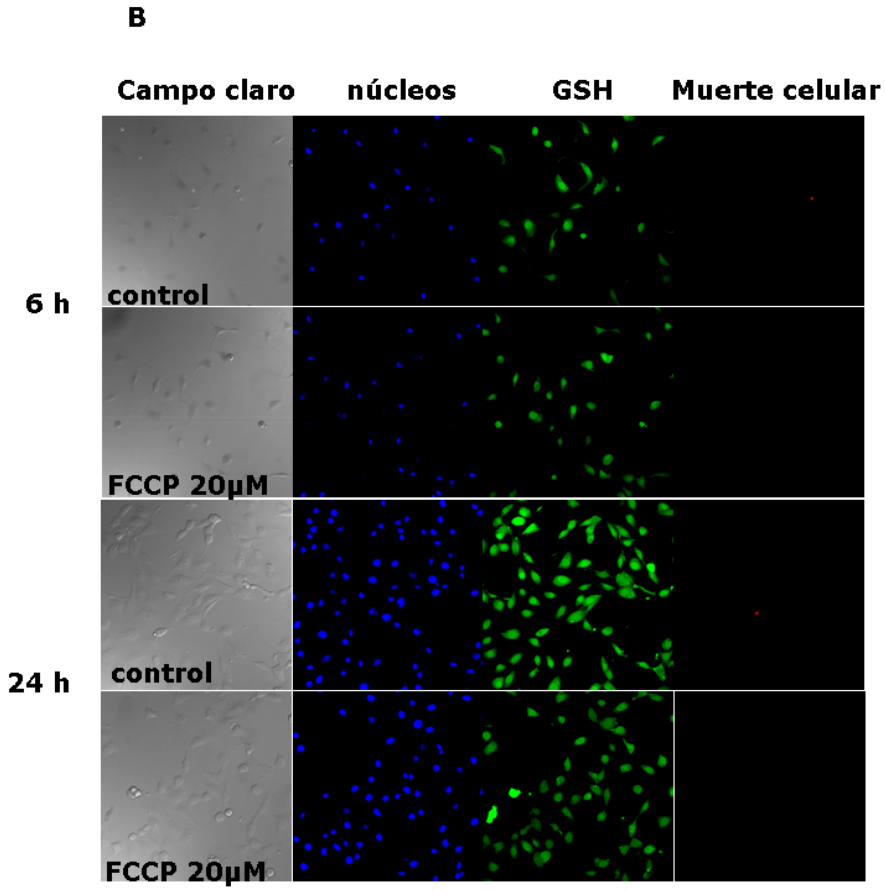

Figura 7. Distribución de GSH después de la depleción de ATP con FCCP

Los niveles de ATP, determinados bioquímicamente, en las células tratadas bajaron un 40% respecto de su control. Sin embargo, por microscopía confocal no se han observado cambios en la distribución celular del GSH; su compartimentación nuclear y mitocondrial no ha sido afectada por la depleción del ATP.

Los resultados presentados en la fig.7 sugieren que la concentración del GSH en el núcleo no depende del ATP,

porque la distribución era similar en las células tratadas con FCCP y las células control.

Una posible explicación para el aumento de la concentración del GSH en el núcleo antes de la proliferación celular podría ser su síntesis *de novo*. Estudiamos la presencia de una enzima imprescindible para la síntesis de GSH, la glutatión cistein sintetasa (GCS) en los extractos nucleares. Fig. 8A muestra la ausencia de la expresión de la enzima GCS en los extractos nucleares, mientras se observa su clara presencia en el extracto celular. Por lo tanto, bajo nuestras condiciones experimentales, la síntesis nuclear del GSH no parece probable.

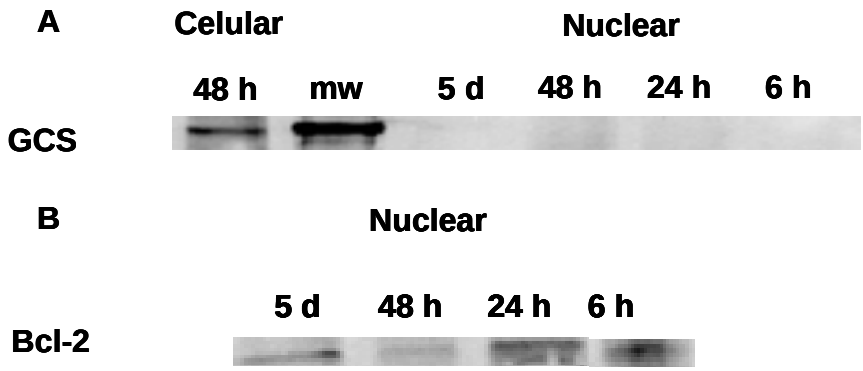

Figura 8. Expresión de la γ-glutamylcysteine sintetasa y Bcl-2 en los fibroblastos 3T3

Uno de los mecanismos sugeridos por los cuales el GSH podría entrar en el núcleo era el transporte mediado por la bcl-2, una proteína anti-apoptotica cuya sobreexpresión aumenta el glutatión nuclear (9).

A lo largo de la curva de proliferación de los fibroblastos 3T3 estudiamos la distribución nuclear del bcl-2 mediante la

técnica de Western blotting en los extractos nucleares de las células 6, 24, 48, 72h y 5 días en cultivo.

La distribución celular del bcl-2 variaba con la fase del ciclo celular. La máxima presencia del bcl-2 en el núcleo se encuentra a las 6h y 24h de cultivo, antes de la proliferación, y baja a partir de las 48h de cultivo.

Para elucidar las posibles consecuencias de la alta concentración de GSH en el núcleo, estudiamos el nivel de oxidación y la glutatiónilación en las proteínas nucleares. En la figura 9. se observa un aumento en la oxidación de las proteínas nucleares, en las fases tardías del cultivo celular, cuando el bajo nivel del crecimiento esta acompañado por un nivel del GSH nuclear bajo. A las 6h de cultivo, cuando el ratio del GSH núcleo/citoplasma es máximo, hay muchas menos proteínas oxidadas en el núcleo.

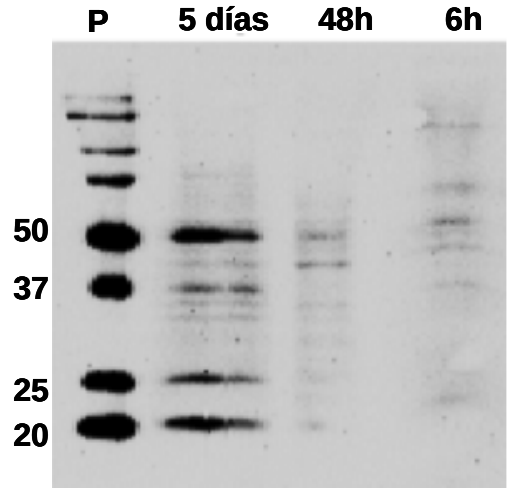

Figura 9. El nivel de oxidación de las proteínas nucleares en los fibroblastos 3T3

El estudio por Western blotting de la glutatiónilacion de las proteínas nucleares muestra diferencias relacionadas con el nivel de la compartimentación nuclear del GSH y la proliferación (Fig.10). A las 6h del cultivo había más glutatiónilación de las proteínas nucleares que cuando las células llegaron a la confluencia y la distribución del GSH era homogénea.

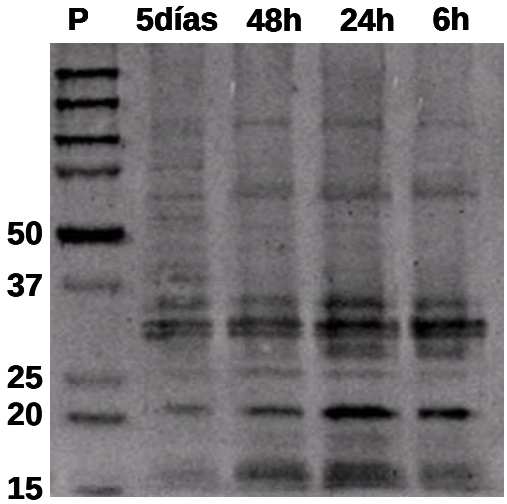

Figura 10. Glutationilación de las proteínas nucleares en los fibroblastos 3T3

Para confirmar la importancia del GSH nuclear en la transición de las células de la fase G1 a la fase S y M/G2 del ciclo celular, usamos un modelo diferencial que se fundamentaba en la depleción del GSH: con dietilmaleato (DEM), que afecta a todos los tioles por toda la célula y con BSO que previene la síntesis del GSH pero no afecta el pool nuclear. Incluimos un grupo control en el que los efectos de la depleción con DEM se compensaban con la administración simultanea del GSH ester. Estudiamos los efectos

diferenciales en la proliferación dependiendo del compartimiento celular afectado por la depleción del GSH.

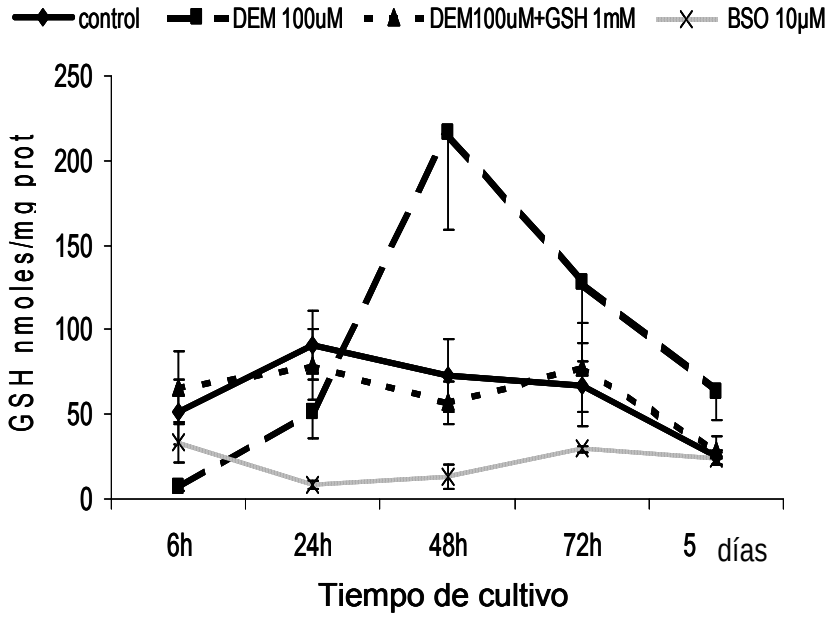

Figura 12. Depleción del GSH en el cultivo de los fibroblastos 3T3. Concentración celular

La figura 12. muestra el grado de depleción y ritmo de cambios de los niveles de GSH total celular en los 4 grupos experimentales de nuestro modelo. Se observa una clara bajada del nivel del GSH en las células tratadas con DEM, ya a las 6h de cultivo, mientras el tratamiento con BSO tenia un retraso de unas 24h para bajar el GSH a un nivel parecido (7,28 y 8,10 nmoles/mg prot., respectivamente). El nivel de GSH en las células tratadas con BSO subía lentamente pero en general se mantiene significativamente mas bajo comparando con otros grupos experimentales, hasta los 5

días de cultivo cuando la diferencia ya no es estadísticamente significativa, excepto en el caso de DEM. El nivel de GSH en las células tratadas con DEM subía rápidamente; a las 24h era más alto que en las células tratadas con BSO pero todavía no llegaba al nivel del control (51,96 nmoles/mg prots. comparado con 90,64, respectivamente, $p \leq 0,001$). A las 48h se observa un efecto rebote, previamente demostrado en diferentes tipos celulares, que en menor medida persiste a las 72h para caer significativamente a los 5 días del cultivo. Las células tratadas simultáneamente con DEM y GSH ester muestran el mismo patrón que el control, con el pico a las 24h, y la diferencia en los niveles de GSH a lo largo del ciclo celular entre estos dos grupos nunca llega a ser significativa.

Estudios de la distribución del GSH por microscopia confocal en nuestro modelo, 24h en cultivo, muestran una clara compartimentación nuclear en las células control que con el tratamiento con DEM disminuye significativamente (Fig. 13). Sin embargo, el BSO no era capaz de afectar la distribución del GSH, el pool nuclear del GSH se ha conservado en estas células y el patrón era bastante parecido al del control.

La cuantificación del nivel de la fluorescencia verde del CMFDA como la medida del nivel de GSH apoya esta observación (Fig.14). Los niveles de GSH nuclear en las células tratadas con DEM son significativamente más bajos que en otros grupos experimentales. El BSO no ha causado la depleción del GSH nuclear y la administración simultanea del GSH ester suprime completamente el efecto del DEM,

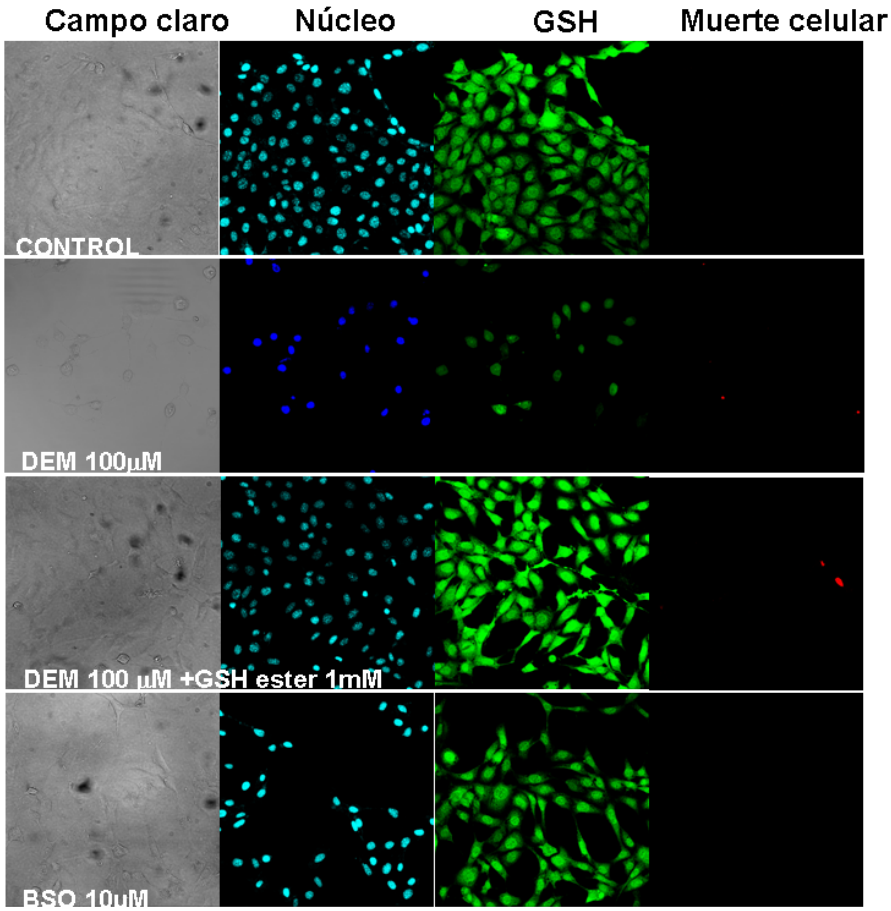

Figura 13. Depleción del GSH y su compartimentación intercelular en los fibroblastos 3T3 24h en cultivo

siendo el nivel de GSH en el núcleo similar al control. Por lo tanto, el DEM depleciona el GSH en toda la célula, tanto en el núcleo como en el citoplasma, mientras el BSO no muestra efecto sobre el GSH nuclear.

Las consecuencias en la proliferación celular de la depleción del GSH nuclear y celular (DEM) comparadas con las observadas por la depleción del GSH citoplasmático mientras

el nuclear se mantiene (BSO) han sido objeto de nuestro estudio.

La figura 15. muestra el ritmo de crecimiento celular en 4 grupos experimentales. Como habíamos demostrado anteriormente, los fibroblastos 3T3 crecen despacio en las primeras horas de cultivo, para llegar al crecimiento exponencial entre 24-48h después de la siembra. A las 72h llegan a la confluencia y el crecimiento se para. Los fibroblastos incubados con BSO muestran un perfil de crecimiento similar al de control, con un pequeño retraso a las 24h ($p \leq 0,05$), y continúan creciendo hasta los 5 días de cultivo.

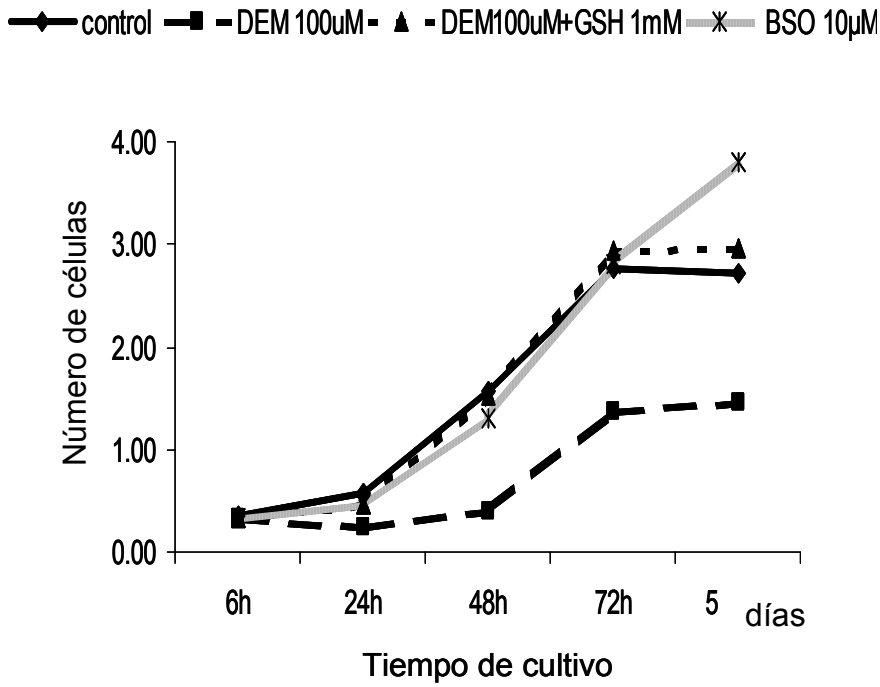

Figura 15. El efecto de la depleción del GSH nuclear en el crecimiento de los fibroblastos 3T3

Sin embargo, los fibroblastos tratados con DEM se caracterizan por un patrón de crecimiento muy diferente. En las primeras 48h de cultivo, la población celular casi no aumenta: no existe diferencia significativa entre el número de células a las 6h y 2 días después. El crecimiento importante de estas células ocurre entre 48 y 72h y se mantiene en el mismo nivel hasta los 5 días de cultivo. El numero de células es en todo momento significativamente mas bajo que en el control ($p \leq 0{,}001$) y al final del cultivo había casi dos veces menos células en este grupo que en el control ($1{,}46 \times 10^6$ y $2{,}71 \times 10^6$, respectivamente). Las células tratadas simultáneamente con DEM y GSH ester crecían al mismo ritmo que las células control. Consecuentemente, la depleción del GSH nuclear afectaba gravemente el crecimiento del cultivo celular, sin embargo, cuando solo el GSH citoplasmático estaba deplecionado no había diferencias marcadas en el ritmo de crecimiento de las células 3T3.

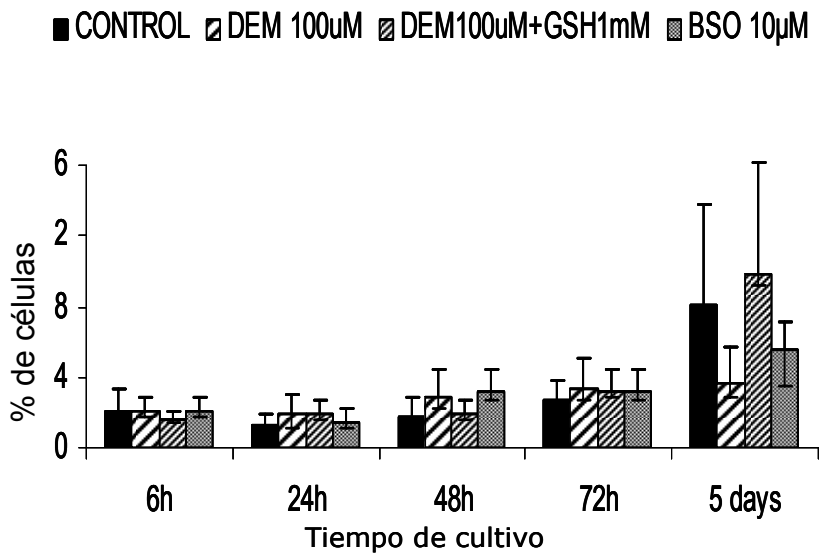

Figura 16. El efecto de la depleción del GSH nuclear en la muerte celular en los fibroblastos 3T3

La muerte celular se mantuvo por debajo del 5% a lo largo del ciclo (Fig. 16), para subir a los 5 días en los grupos control y BSO debido a la muerte celular inducida por la confluencia completa de las células e inhibición por contacto. En ningún momento se encontró un aumento importante en el grupo tratado con DEM, por lo tanto la diferencia en el numero de células en este grupo comparado con los demás no se debería a la muerte celular sino a un retraso en el crecimiento de la población celular.

El estudio del ciclo celular de los 4 grupos experimentales, presentado en la figura 17, nos proporciona las pruebas de esta suposición. En el grupo control el porcentaje de células en las fases que definen la proliferación celular, S - síntesis de ADN y M/G2-división celular, es alto entre las 24 y 72h de cultivo (47,7±9,8% a las 24h).

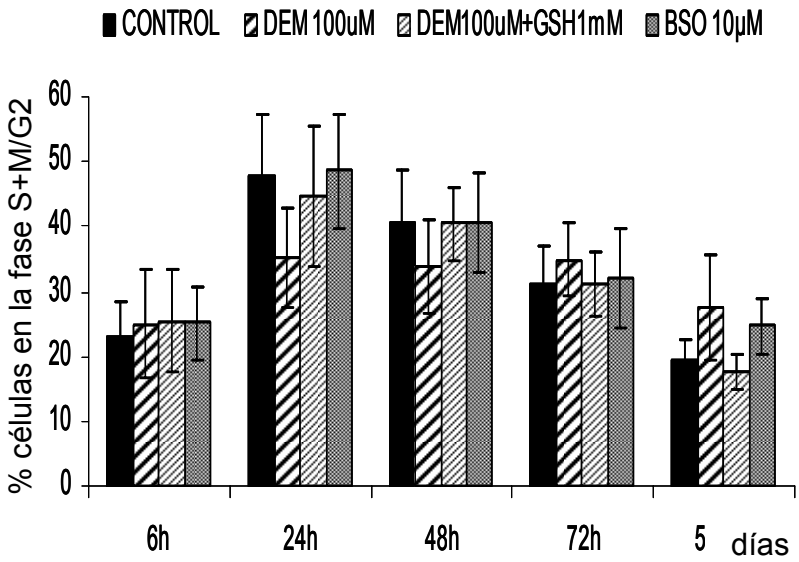

Figura 17. El efecto de la depleción del GSH nuclear en el ciclo celular.

Antes y después de esta fase exponencial de crecimiento, a las 6h y 5 días de cultivo, respectivamente, la mayoría de las células esta en la fase G0/G1. Sin embargo, las células tratadas con DEM se mantienen en la fase G0/G1 hasta después de 48h, y el porcentaje de células en la fase S+M/G2 se mantiene bajo (35,1±7,8%) a lo largo del experimento. Como era de esperar, las células tratadas con BSO y con el DEM y GSH ester simultáneamente, muestran niveles de proliferación similares al control. La confirmación de estos resultados la encontramos en el estudio de la expresión de las proteínas relacionadas con la proliferación celular, concretamente el Id2.

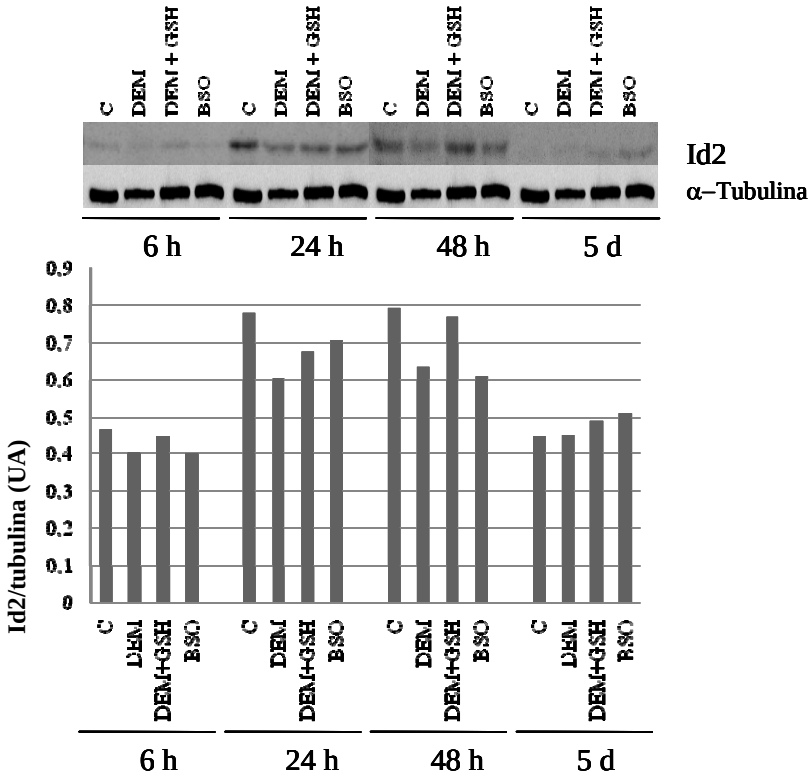

Figura 18. Expresión de las proteínas del ciclo celular después de la depleción del GSH nuclear

La Figura 18. presenta los resultados de un experimento representativo que indican una disminución de la expresión de esta proteína, comparando con el control, en las células tratadas con DEM, pero esto no ocurre con BSO ni con la combinación del DEM y GSH ester. El nivel de expresión de esta proteína solo se iguala al control a los 5 días, donde las células control son confluentes y ya no proliferan más. De esta manera hemos vuelto a demostrar que la depleción del GSH nuclear induce una disminución de la proliferación celular.

En la continuación de nuestro trabajo nos ha interesado evaluar la universalidad de nuestra hipótesis sobre la importancia del nivel de GSH y su compartimentación nuclear para la proliferación celular. Hemos elegido dos tipos celulares provenientes de diferentes especies y con un nivel de proliferación muy distinto. Las células de cancer MCF7 provienen de un adenocarcinoma mamario de una mujer caucasiana de 67 años. Es una línea celular establecida que se caracteriza por un nivel de proliferación muy alto. Por otro lado, el cultivo embrionario de neuronas de rata, nos ha ofrecido la posibilidad de realizar un estudio comparativo considerando estas células como un control negativo. La figura 19. muestra diferentes ritmos de proliferación de estos 3 tipos celulares. Los fibroblastos 3T3 muestran el perfil de crecimiento celular, analizado previamente, distinto a las células MCF7. Las células de cáncer de mama empiezan a crecer mas tarde que los fibroblastos pero tiene una fase exponencial de

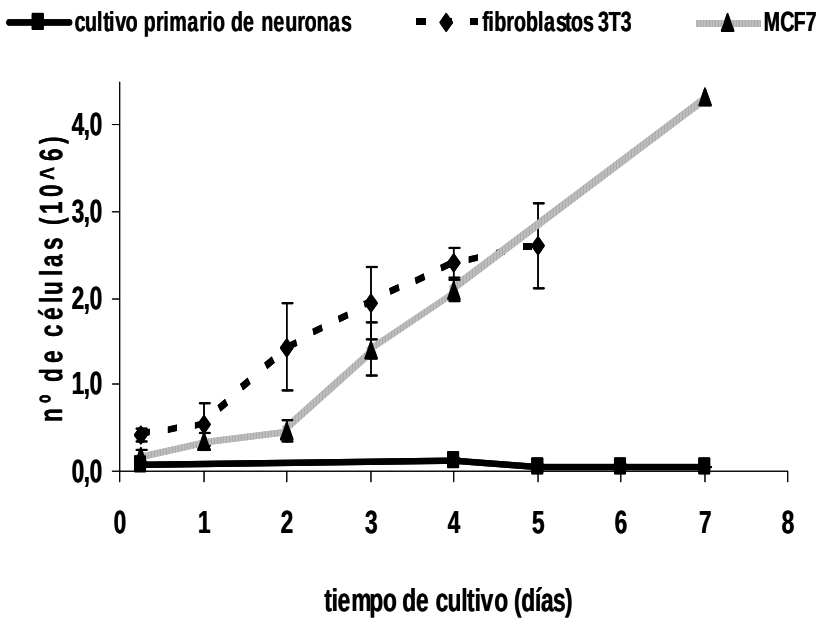

FIGURA 19. Curvas de proliferación comparativas de diferentes tipos celulares

crecimiento mas larga y mas intensa que las 3T3. Dado que no muestran la inhibición por contacto, después de 7 días de cultivo esta población celular seguía creciendo. El cultivo embrionario de rata muestra cierta actividad proliferativa con un suave aumento hacia el cuarto día de cultivo. En este periodo en el cultivo están presentes las células que originaran diferentes tipos celulares del sistema nervioso. A partir del cuarto día de cultivo se añade el citosin para eliminar las células que proliferaban, con lo cual en la placa se mantenían solo las células que se diferenciarían en neuronas (con un máximo de 3% de astrocitos restantes) (10), caracterizadas por un nivel de proliferación extremadamente bajo.

El estudio comparativo del nivel de GSH a lo largo del ciclo celular es acorde con las observaciones previamente expuestas para los fibroblastos 3T3. En las células de cáncer de mama, MCF7, el pico de GSH es anterior, a las 18h, comparado con los fibroblastos 3T3 (24h de cultivo), y el valor máximo es 3 veces mas alto (256,75±54,80 y 80,22±22,80 nmoles/mg prot, respectivamente). Por el contrario, las neuronas no muestran un pico claro del nivel de GSH, aunque se puede observar una meseta con el nivel mas alto de GSH en primeros 4 días durante la "fase proliferativa" del cultivo. A partir del séptimo día de cultivo primario de neuronas se percibe un nivel de GSH bajo y sin variaciones significativas (27,0±2,7 nmoles/mg prot) hasta 16 días cuando el cultivo empieza a morirse.

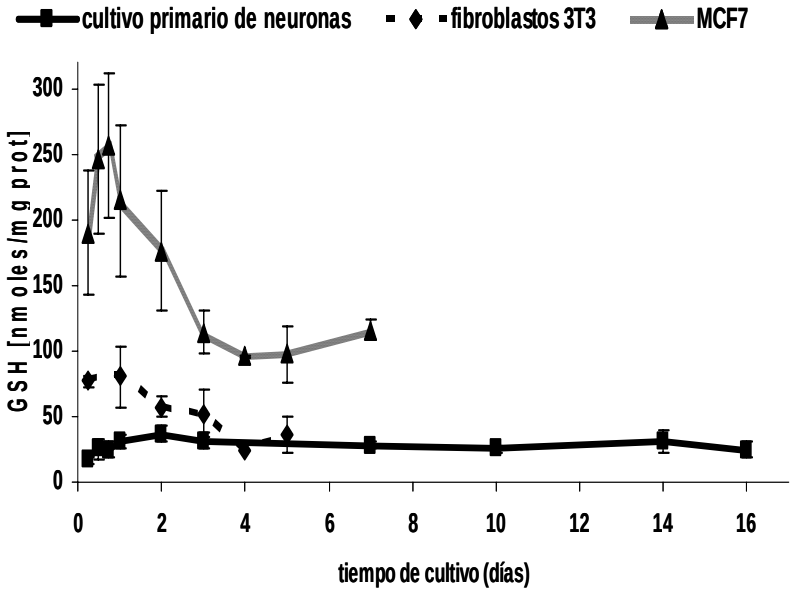

Figura 20. Comparación de los niveles de GSH celular total en diferentes tipos celulares

El análisis del ciclo celular por citometria de flujo nos ha permitido realizar un estudio de correlación entre el porcentaje de células en la fase de síntesis de ADN en una población celular y el nivel de GSH. Se ha mostrado que en la población de neuronas caracterizada por un nivel de GSH bajo hay muy pocas células que se encuentran en esta fase de ciclo celular, mientras una tasa alta de proliferación de las células de cáncer de mama esta acompañada por un nivel de GSH extremadamente alto. Las 3T3 tienen unos valores medios tanto en la proliferación como en el nivel de GSH celular.

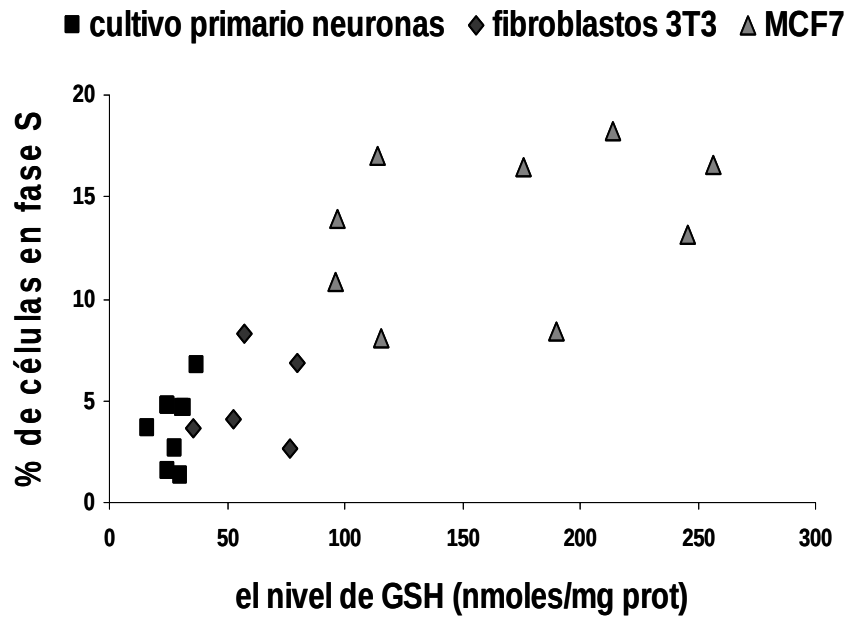

Figura 21. Correlación entre el nivel de GSH y la síntesis de ADN en diferentes tipos celulares

Otro parámetro relacionado con la actividad proliferativa de las células, estudiado previamente por

nuestro grupo en los fibroblastos 3T3 es la actividad de la telomerasa (4). El pico de GSH total celular coincide con el pico de la actividad de telomerasa a las 24h del cultivo y precede a la fase exponencial del crecimiento. El perfil de la actividad de la telomerasa a lo largo del ciclo celular en las células MCF7 y el cultivo primario de neuronas se ha manifestado coherente con lo que se ha mostrado previamente (4) para los fibroblastos 3T3 (Figura 22).

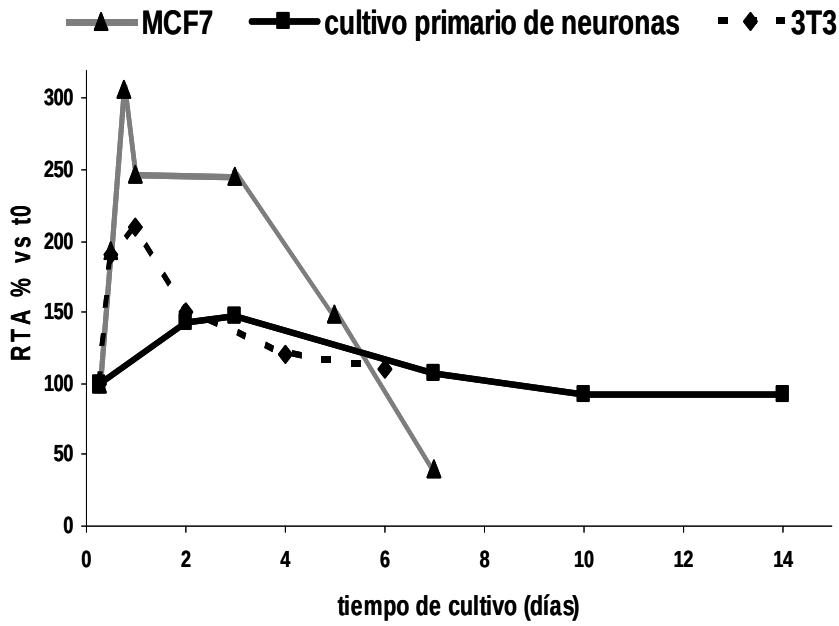

Figura 22. Cambios en el nivel de la actividad telomerasa a lo largo del ciclo celular.Estudio comparativo en diferentes líneas celulares.

Los cambios en la actividad de la telomerasa en las células MCF7 son extremos, en las primeros 18h se triplica, en los fibroblastos 3T3 llega solo a duplicarse a las 24h, mientras que en el cultivo primario de neuronas se observa

un incremento mucho mas sutil (46%) a los 3 días de cultivo. Los marcadores de la fase de proliferación del ciclo celular, id2 y PCNA (proliferating cell nuclear antigen) se han estudiado en los 3 tipos celulares. En las células MCF7 el PCNA aumenta a partir de las 72h, lo que marca el principio de la fase exponencial del crecimiento en estas células. En neuronas, el nivel de PCNA es alto en los primeros días de cultivo y disminuye considerablemente a los 7 días. Hacia los 16 días del cultivo sigue disminuyendo hasta niveles difícilmente detectables.

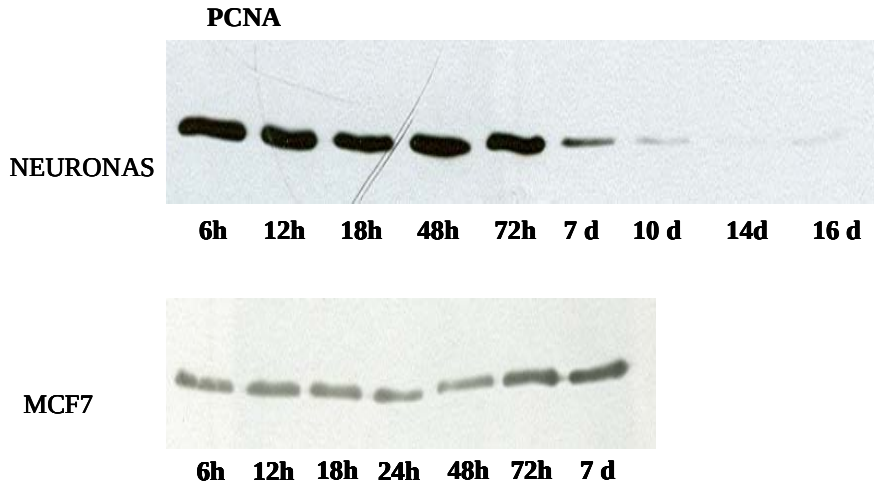

Figura 23. Estudio comparativo de la expresión de las proteínas relacionadas con la proliferación en diferentes tipos celulares

De la misma manera que en los fibroblastos 3T3 se ha estudiado la distribución celular del GSH a lo largo del ciclo celular (Fig. 24) en las células MCF7 (Fig. 24 A) y en el cultivo primario de neuronas (Fig. 24 B). En las células de

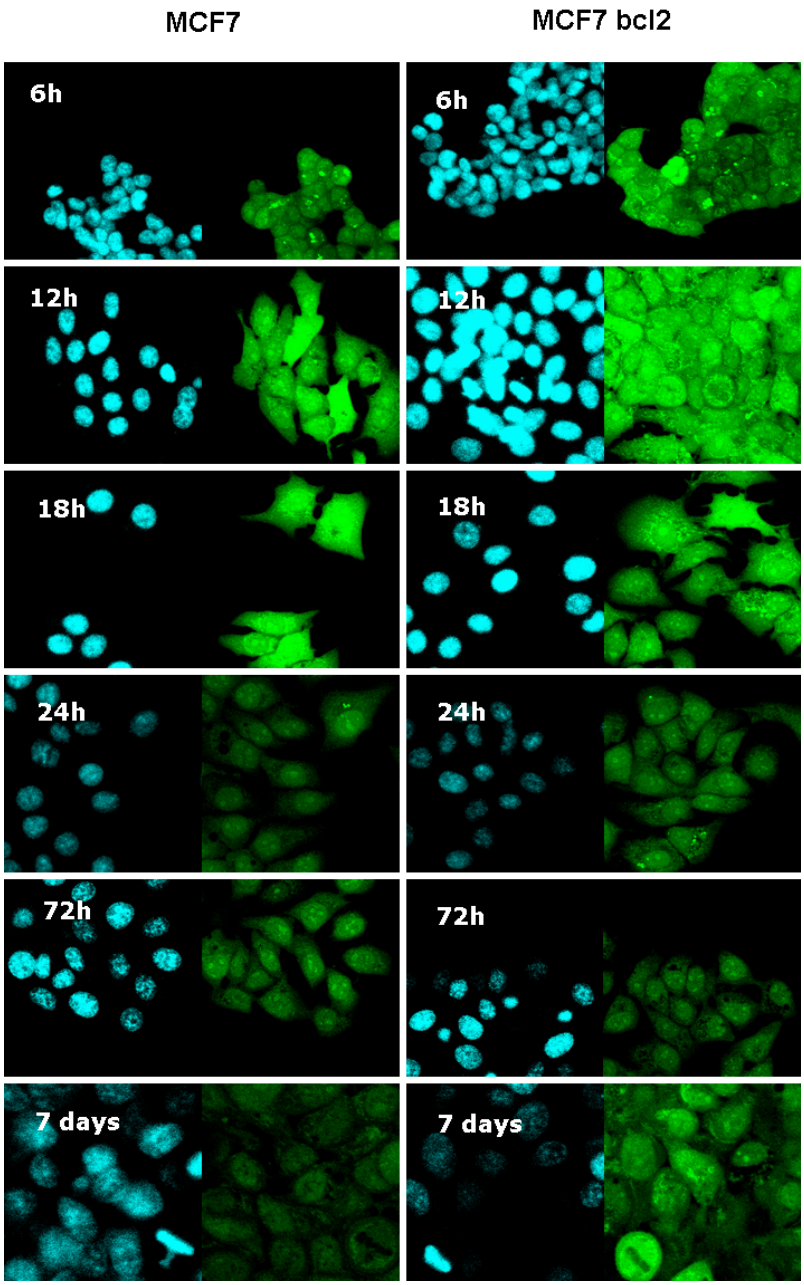

Figura 24. Compartimentación intercelular de GSH en la proliferación de las células

cáncer de mama se observa una marcada compartimentación nuclear del GSH a partir de las 24h de

cultivo y se mantiene, en algunas células, hasta los 7 días de cultivo. En la fase proliferativa del cultivo primario se pueden detectar algunas células con glutatión en el núcleo. Como era de esperar en el cultivo primario de neuronas, después del día 4 cuando en la placa quedan solo las células diferenciadas en neuronas, se observa una distribución homogénea del GSH.

3. Discusión

Los resultados presentados demuestran que en los fibroblastos 3T3 hay concentración del GSH en el núcleo en los primeros 24h del cultivo, justo antes de que se dispare el crecimiento celular. A las 72h y 5 días de cultivo cuando la actividad de la telomerasa y el nivel de GSH total disminuyen, las células llegan a la confluencia y entran en quiescencia, se aprecia una distribución uniforme.

Las imagines obtenidas a los 3 y 5 días de cultivo son similares a las publicados previamente por Söderdahl *et al.* (8). Es muy importante considerar el momento del ciclo celular a la hora de estudiar la distribución del GSH y su compartimentación nuclear. Nosotros mostramos que las células que se preparan para la división tienen niveles de GSH en el núcleo altos. Las células quiescentes se caracterizan por un nivel del GSH nuclear muy parecido al del citoplasma (Fig. 3).

La disponibilidad del GSH en los compartimentos celulares esta definida por un equilibrio complejo entre la utilización, el transporte, la síntesis, la glutationilación de las proteínas

y la reducción de GSSG. La regulación de estos procesos a nivel nuclear no esta clara. Según Smith et al. (11) posibles mecanismos bioquímicos involucrados en el recambio nuclear del GSH son:

1. GSH entra al núcleo desde el citoplasma de manera pasiva o mediante un proceso dependiente de la energía.
2. podría existir una síntesis nuclear de GSH mediante las enzimas γ-glutatmil cistein ligasa y GSH sintetasa.
3. GSH podría funcionar como trasportador del γ-Glu-Cys-Cys.

Ho and Guenthner (12), en su estudio en los núcleos aislados del hígado, concluyeron que el GSH entraba al núcleo por difusión pasiva y no mediante un proceso dependiente del ATP. Según esta investigación, alrededor del 4-8% de la actividad de las enzimas de síntesis de GSH se ha encontrado en el núcleo, manteniendo así los niveles nucleares del GSH.

En los fibroblastos 3T3 no encontramos la evidencia del trasporte activo del GSH (Fig. 7) ni detectamos la presencia de la γ-glutamil-cistein-sintetasa en el núcleo (Fig. 8A). Diferentes autores señalan la importancia del oncogen humano bcl-2 en el posible trasporte del GSH a través de la membrana nuclear. En varios estudios se demuestra que la sobreexpresión de dicho oncogen conlleva un aumento en la concentración del GSH en el núcleo (9, 13, 14). Por otro lado, se ha mostrado la relación entre el bcl-2 y los poros nucleares (15)

Por lo tanto, nosotros proponemos que durante los cambios en la membrana nuclear que preceden la división celular, el bcl-2 nuclear podría actuar como transportador selectivo de algunos compuestos, entre ellos glutatión, hacia el interior del núcleo celular.

Un gran número de situaciones patofisiológicas desvela la importancia del GSH nuclear. Atzori et al. (16), demuestran la importancia de la cantidad y el estado redox de los tioles celulares, especialmente el GSH, para la proliferación y diferenciación de las células bronquiales epiteliales en humanos. Por otro lado se revela la importancia del glutatión nuclear en la protección del ADN, el mantenimiento de la integridad funcional del núcleo y en la determinación de sensibilidad intrínseca de las células a la radiación (17). Hansen et al (18), sugieren que el cambio del estado redox del núcleo puede resultar en la desregulación de las interacciones entre el ADN y los factores de trascripción lo que puede llevar al trastornos en el crecimiento y desarrollo.

Un número importante de proteínas nucleares, incluyendo los factores de trascripción, requiere de un ambiente reducido para poder unirse al ADN. Según Jang y Surh (19), el GSH nuclear podría actuar como regulador de la trascripción controlada por NFkB, AP-1 y p53, alterando su estado redox en el núcleo.

La importancia del GSH nuclear para la transición de los fibroblastos 3T3 de la fase G1 a la fase S y M/G2 del ciclo celular ha sido investigada en estudios en un modelo diferencial de la depleción del GSH. Usando las propiedades

del DEM, que depleciona todos los tioles en toda la célula, y el BSO, que disminuye la síntesis de GSH y su concentración en citoplasma, pero no afecta el pool nuclear de GSH, pudimos confirmar que la depleción del GSH nuclear afectaba gravemente a la proliferación celular. Mientras el pool nuclear del GSH se mantenía, no se observaban cambios en la proliferación celular. Por lo tanto, el GSH nuclear es el que regula el crecimiento de la población celular y el ritmo del ciclo celular.

En nuestro modelo cancerígeno, así como en los fibroblastos 3T3, hemos demostrado nuevamente la importancia de la compartimentación nuclear del GSH en la preparación de las células para la fase exponencial de crecimiento.

En las células de cáncer de mama, MCF7, mediante microscopía confocal, observamos una importante compartimentación de GSH en el núcleo a partir de 24h de cultivo. En las células MCF7 este nivel máximo esta retrasado comparando con los fibroblastos 3T3, al igual que la fase exponencial de crecimiento: en los fibroblastos es entre las 24h y 48h de cultivo, mientras que en las MCF7 es entre las 48h y 72h de cultivo. La fase exponencial de crecimiento de las MCF7 era más larga y el número de células mayor.

El nivel del GSH celular total y la actividad de la telomerasa en las células MCF7 eran significativamente más altos y estaban adelantados comparando con los picos correspondientes en los fibroblastos 3T3 y el cultivo primario de neuronas.

Nuestros resultados muestran que el nivel de GSH, su compartimentación nuclear y la actividad de la telomerasa en las células MCF7 eran elevados justo antes de que se dispare su proliferación. En el caso del cultivo primario de neuronas, cuya tasa de proliferación es insignificante, los niveles del GSH y telomerasa eran muy bajos y estaban acompañados por una distribución homogénea del GSH en la célula.

En el trabajo de investigación aquí presentado se ha demostrado la gran importancia del nivel de GSH y su compartimentación nuclear para el inicio de la proliferación celular. El fenómeno parece universal, confirmado en cultivos celulares provenientes de diferentes especies y con distintos niveles de proliferación.

4. Bibliografía

1. Ochoa S. (1983) Arch Biochem Biophys. 223(2):325-49
2. Viña, J. (ed) (1990) *Glutathione: Metabolism and Physiological Function*, CRC Press, Boston)
3. Esteve, J. M., Mompó, J., García de la Asunción, J., Sastre, J., Boix, J., and Viña, J. R., Viña, J., and Pallardó, F. V. (1999) *FASEB J.* **13,** 1055-1064

4. Borras, C., Esteve, J. M., Vina, J. R., Sastre, J., Vina, J., and Pallardo, F. V. (2004) *J. Biol. Chem.* **279,** 34332-34335)
5. Biaglow, J. E., Varnes, M. E., Clark, E. P., and Epp, E. R. (1983) *Radiat. Res.* **95,** 437-455
6. Reichard, P., and Thelander, L. (1979) *Annu. Rev. Biochem.* **48,** 133-158
7. Peter A. Dijkwel and Paul W. Wenink (1986)J. Cell Sci. 84, 53-67
8. Söderdahl, T., Enoksson, M., Lundberg, M., Holmgren, A., Ottersen, O. P., Orrenius, S., Bolcsfoldi, G., and Cotgreave, I. A. (2003) *FASEB J.* **17,** 124-126
9. Voehringer, D. W., McConkey, D. J., McDonnell, T. J., Birsbay, S., and Meyn, R. E. (1998) *Proc. Natl. Acad. Sci. U. S. A.* **95,** 2956-2960)
10. Brewer G.J. (1997) J. Neurosci Methods 71, 143-155).
11. Smith, C. V., Jones, D. P., Guenthner, T. M., Lash, L. H., and Lauterburg, B. H. (1996) *Toxicol. Appl. Pharmacol.* **140,** 1-12)
12. Ho, Y. F., and Guenthner, T. M. (1994) *Toxicologist* **14,** 178
13. Ellerby, L. M., Ellerby, H. M., Park, S. M., Holleran, A. L., Murphy, A. N., Fiskum, G., Kane, D. J., Testa, M. P., Kayalar, C., and Bredesen, D. E. (1996) *J. Neurochem.* **67,** 1259-126,
14. Hoetelmans, R. W., Vahrmeijer, A. L., van Vlierberghe, R. L., Keijzer, R., van de Velde, C. J.,

Mulder, G. J., and Van Dierendonck, J. H. (2003) *Cell Prolif.* **36,** 35-44)

15. Krajewski, S., Tanaka, S., Takayama, S., Schibler, M. J., Fenton, W., and Reed, J. C. (1993) *Cancer Res.* **53,** 4701-4714).
16. Atzori, L., Dypbukt, J. M., Hybbinette, S. S., Moldeus, P., and Grafstrom, R. C. (1994) *Exp. Cell Res.* **211,** 115-120)
17. Morales, A., Miranda, M., Sanchez-Reyes, A., Biete, A., and Fernandez-Checa, J. C. (1998) *Int. J. Radiat. Oncol. Biol. Phys.* **42,** 191-203).
18. Hansen, J. M., Go, Y. M., and Jones, D. P. (2006) *Annu. Rev. Pharmacol. Toxicol.* **46,** 215-234
19. Jang, J. H., and Surh, Y. J. (2003) *Biochem. Pharmacol.* **66,** 1371-1379

VIII CONCLUSIONES

VIII CONCLUSIONES

1. El nivel de glutation celular en una línea celular puede determinar su capacidad proliferativa. La variación del nivel del glutation durante el cultivo celular impone el ritmo de la proliferación celular, posiblemente vía la modulación de las proteínas reguladoras del ciclo celular sensibles al estado redox.

2. La actividad de la telomerasa es altamente sensible al estado redox de la célula, independientemente del tipo celular, su inherente capacidad proliferativa o la especie de la que procede el cultivo celular. El vínculo entre la progresión del ciclo celular y el nivel de glutation se podría atribuir, por lo menos en parte, a la modulación de la actividad telomerasa.

3. La compartimentación nuclear del glutation es imprescindible en el principio de la fase exponencial del crecimiento celular. El estado redox de las proteínas nucleares, definido por su glutationilacion y oxidación,

varía significativamente con la actividad proliferativa de las células.

4. La depleción del glutation nuclear interfiere gravemente con la progresión del ciclo celular.

5. Durante los cambios en la membrana nuclear que preceden la división celular, el Bcl-2 nuclear podría facilitar la translocacion del glutation al núcleo. La sobre expresión del Bcl-2 induce el incremento del nivel del glutation celular, de la actividad telomerasa y de la compartimentación nuclear del GSH.